MCEER
EARTHQUAKE ENGINEERING TO EXTREME EVENTS

ISSN 1520-295X

Seismic Protection of Electrical Transformer Bushing Systems by Stiffening Techniques

by
Maria Koliou, Andre Filiatrault,
Andrei M. Reinhorn and Nicholas Oliveto

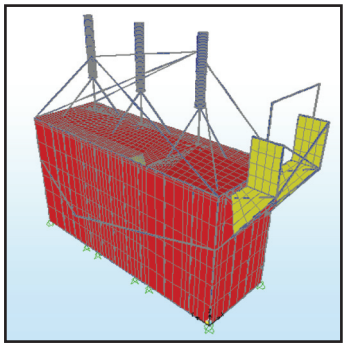

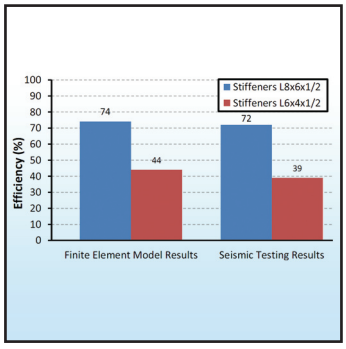

Technical Report MCEER-12-0002

June 1, 2012

This research was conducted at the University at Buffalo, State University of New York. It was sponsored by the Bonnevile Power Administration under Contract Number 00041295 and the California Energy Commission under Contract Number 500-07-037 (Subcontract TRP-08-03).

NOTICE

This report was prepared by the University at Buffalo, State University of New York as a result of research sponsored by the Bonneville Power Administration and the California Energy Commission. Neither MCEER, associates of MCEER, its sponsors, the University at Buffalo, State University of New York, nor any person acting on their behalf:

a. makes any warranty, express or implied, with respect to the use of any information, apparatus, method, or process disclosed in this report or that such use may not infringe upon privately owned rights; or

b. assumes any liabilities of whatsoever kind with respect to the use of, or the damage resulting from the use of, any information, apparatus, method, or process disclosed in this report.

Any opinions, findings, and conclusions or recommendations expressed in this publication are those of the author(s) and do not necessarily reflect the views of MCEER or its sponsors.

Seismic Protection of Electrical Transformer Bushing Systems by Stiffening Techniques

by

Maria Koliou,[1] Andre Filiatrault,[2] Andrei M. Reinhorn[3] and Nicholas Oliveto[1]

Publication Date: June 1, 2012
Submittal Date: January 20, 2012

Technical Report MCEER-12-0002

Bonneville Power Administration Contract Number 00041295
California Energy Commission Contract Number 500-07-037 (Subcontract TRP-08-03)

1 Graduate Research Assistant, Department of Civil, Structural and Environmental Engineering, University at Buffalo, State University of New York
2 Professor, Department of Civil, Structural and Environmental Engineering, University at Buffalo, State University of New York
3 Clifford C. Furnas Professor of Engineering, Department of Civil, Structural and Environmental Engineering, University at Buffalo, State University of New York

MCEER
University at Buffalo, State University of New York
133A Ketter Hall, Buffalo, NY 14260
Phone: (716) 645-3391; Fax (716) 645-3399
E-mail: *mceer@buffalo.edu*; WWW Site: *http://mceer.buffalo.edu*

Preface

MCEER is a national center of excellence dedicated to the discovery and development of new knowledge, tools and technologies that equip communities to become more disaster resilient in the face of earthquakes and other extreme events. MCEER accomplishes this through a system of multidisciplinary, multi-hazard research, in tandem with complimentary education and outreach initiatives.

Headquartered at the University at Buffalo, The State University of New York, MCEER was originally established by the National Science Foundation in 1986, as the first National Center for Earthquake Engineering Research (NCEER). In 1998, it became known as the Multidisciplinary Center for Earthquake Engineering Research (MCEER), from which the current name, MCEER, evolved.

Comprising a consortium of researchers and industry partners from numerous disciplines and institutions throughout the United States, MCEER's mission has expanded from its original focus on earthquake engineering to one which addresses the technical and socio-economic impacts of a variety of hazards, both natural and man-made, on critical infrastructure, facilities, and society.

The Center derives support from several Federal agencies, including the National Science Foundation, Federal Highway Administration, National Institute of Standards and Technology, Department of Homeland Security/Federal Emergency Management Agency, and the State of New York, other state governments, academic institutions, foreign governments and private industry.

The Bonneville Power Administration (BPA) and the California Energy Commission (CEC) are supporting a series of studies on the resilience of electric power substation equipment that focus on the following topics:

- Reducing Disruption of Power Systems in Earthquakes: Advanced Methods for Protecting Substation Equipment
- Analysis of the Seismic Performance of Transformer Bushings

It is envisioned that these studies will result in the development of cost effective seismic protective solutions for transformer–bushing systems and other electrical substation equipment considering inertial effects and dynamic interaction with conductors. Furthermore, new knowledge discovered about the bushing-transformer seismic interaction will be translated into a proposed revision of the IEEE 693 Standard. A series of MCEER reports will document the results of these studies.

In this report, the dynamic response of high voltage transformer bushing systems under seismic excitation was studied to evaluate possible methods to mitigate the seismic vulnerability and damage to "as installed" bushings. Finite element models of four different high voltage transformers were used to perform modal and linear dynamic time analyses to compare the response

of the bushing structures "as installed" on flexible transformer covers and on a rigid base, and to investigate the efficiency of several stiffening techniques used to ensure the integrity of the bushings during strong earthquakes. In addition, a two-stage experimental investigation, consisting of system identification testing and shake table testing, was conducted to verify the response trends identified by the numerical studies. The experimental and numerical results clearly show that the bushing structures "as installed" on flexible transformer covers are more vulnerable to seismic excitations compared to the ones mounted on a rigid base. Moreover, these studies showed that stiffening the transformer covers at the base of the bushings can be beneficial for their response against ground shaking. From the stiffening techniques investigated, incorporating flexural stiffeners on the cover plate of the transformer tank appears to be the most efficient approach.

ABSTRACT

In the past few decades, electrical substation equipment has shown vulnerable behavior under strong earthquakes, resulting in severe damage to electric power networks. High voltage bushings, which are designed to isolate and transmit electricity from a transformer to the high voltage lines, are the most critical as well as the most vulnerable components of the electrical substations. Rehabilitation of existing bushing structures and proper design of new ones could considerably reduce potential damage to them. Several experimental and numerical studies conducted to investigate the seismic performance of transformer bushing structures have shown that improved seismic performance may be achieved for bushings mounted on a rigid base compared to those mounted on actual transformer tanks ("as installed" conditions), which appear to be very flexible.

This reports investigates the seismic response of bushing structures both "as installed" on a flexible base and on a rigid base as well as attempts to identify feasible approaches of stiffening the base of the transformer bushings as a measure to mitigate their vulnerability under strong seismic excitation. Finite element models of four different high voltage transformers were used for performing modal and linear dynamic time history analyses in order to compare the response of the bushing structures "as installed" and on a rigid base as well as investigate the efficiency of several stiffening techniques to ensure the integrity of the bushings during strong earthquakes. In addition, a two stage experimental investigation, consisting of system identification testing and shake table testing, was conducted to verify the response trends identified by the numerical studies.

Both numerical and experimental studies clearly showed that the bushing structures "as installed" are very vulnerable to seismic excitation as well as very flexible compared to the ones mounted on a rigid base. Moreover, these studies showed that stiffening the base of the bushings can be beneficial for their response against ground shaking. From the stiffening techniques investigated, incorporating flexural stiffeners on the cover plate of the transformer tank appears to be the most efficient approach.

ACKNOWLEDGEMENTS

Financial support for the work presented in this report was provided by the Bonneville Power Administration and is gratefully appreciated. The authors would like to acknowledge Dr. Leon Kempner, Principal Structural Engineer at Bonneville Power Administration, for providing important technical information and recommendations, as well as Dr. Anshel Schiff, President at Precision Measurement Instruments, for serving as external advisor to this research project. Moreover, Mr. Konstantinos Oikonomou and Mr. Fahad Muhammad, Ph.D. Candidates in the Department of Civil, Structural and Environmental Engineering at the University at Buffalo, are greatly acknowledged for their considerable contribution during the analytical and experimental studies, respectively. The assistance of the personnel of the Structural Engineering and Earthquake Simulation Laboratory (SEESL) of the State University of New York at Buffalo with the execution of the testing is greatly appreciated.

TABLE OF CONTENTS

TABLE OF CONTENTS (CONT'D)

TABLE OF CONTENTS (CONT'D)

LIST OF ILLUSTRATIONS

LIST OF ILLUSTRATIONS (CONT'D)

LIST OF ILLUSTRATIONS (CONT'D)

LIST OF ILLUSTRATIONS (CONT'D)

LIST OF ILLUSTRATIONS (CONT'D)

LIST OF ILLUSTRATIONS (CONT'D)

LIST OF TABLES

LIST OF TABLES (CONT'D)

SECTION 1

INTRODUCTION

The electric power network is a vital component of everyday life in modern societies. Electrical substations are critical components of the electric power network that supplies power for industrial, business and residential use and they are susceptible to significant damage under strong seismic excitation. Rehabilitation of existing substations and proper design of new systems will reduce the possible post-earthquake effects/damage. In Figure 1-1 a typical electrical substation is presented.

Figure 1-1 Typical Electrical Substation (Ersoy et al., 2008)

1.1. Description of Electrical Substation Equipment

Electrical substation is called the subsidiary station which serves several functions starting with the protection of the transmission and distribution lines as well as the equipment within the substation by using sensors of abnormal system operating conditions that trigger devices which isolate these lines and equipment. Most of the substations operate as a means of transfer of power between different voltage levels by utilizing power transformers and as a means of

reconfiguration of the power network by opening transmission lines or partitioning multi-section busses (Schiff, 1999).

One of the most essential pieces of equipment in any electrical substation is the power transformer. The power transformer is a device, without any moving parts, which transfers the electric power from one circuit to another through inductively coupled conductors. The basic components of this device are the coils, steel core, oil, tank and bushings. A simplified cross section of a typical power transformer with its components is illustrated in Figure 1-2.

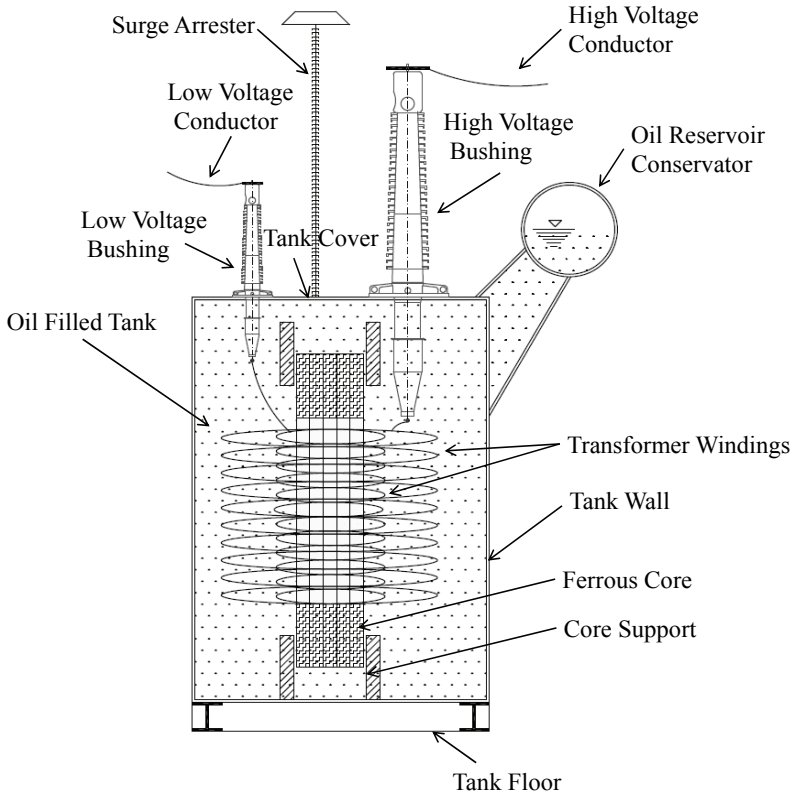

Figure 1-2 Simplified Cross Section of Typical High Voltage Power Transformer and its Components (Koliou et al., 2012)

The coils and core are enclosed in the steel tank in order to protect them from the elements of nature, vandalism and for safety purposes, while the oil is placed in the tank, over the coils and core, as a means of cooling (Pansini, 1999).

Bushings are insulated conductors providing electrical connections between high voltage lines and oil-filled transformers, and are typically mounted on the top of a transformer or on a turret attached to the transformer. They are mainly composed of a flange plate by which the bushing is

attached to the turret, porcelain units (above the flange plate) and a metallic dome at the top. In cross section, the bushing is composed of a central core that provides electrical connectivity, a condensor that wraps the core, perimeter annular porcelain units, and oil that fills the gaps between the condensor and the porcelain unit (Gilani et al., 2001). A typical porcelain 230 kV bushing with its components is presented in Figure 1-3.

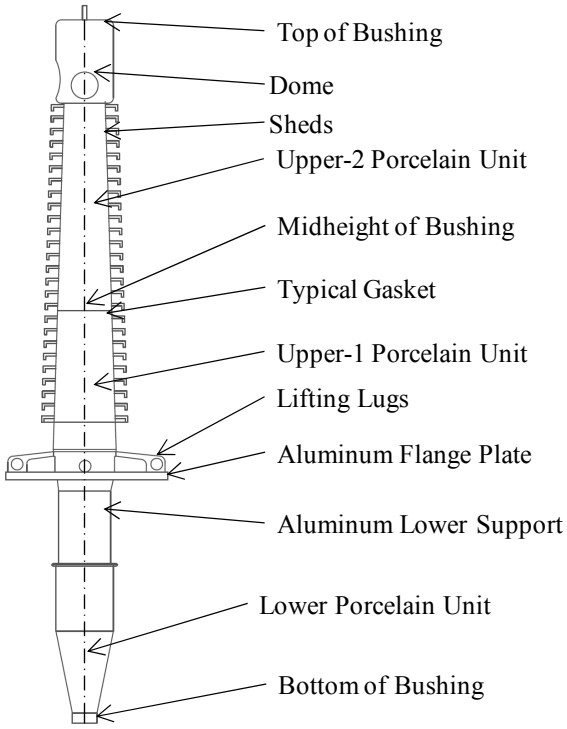

Figure 1-3 Typical Porcelain 230 kV Bushing with its Components (after Gilani et al., 2001)

1.2. Background on Seismic Vulnerability of Transformer Bushing Systems

In the past few decades, electrical substation equipment has demonstrated vulnerable behavior during several earthquakes worldwide, resulting in severe damage to the electric power networks. Characteristic examples of such events are the 1989 Loma Prieta (Villaverde et al., 2001) and 1994 Northridge (Schiff, 1997) earthquakes in United States, 1995 Kobe earthquake in Japan (Schiff, 1998), 1999 Chi-Chi earthquake in Taiwan (Schiff & Tang, 2000) and 1999 Izmit earthquake in Turkey (Tang, 2000).

The overall seismic performance of the substations and their equipment varies. It has been observed that the low voltage equipment (at or below 115kV) performs well when properly

anchored, while the performance of high voltage equipment (at or above 220kV) depends on the specific type of components and their installation practices (Schiff, 1999).

The most severe damage to electrical substation equipment can be categorized into damage to the power transformers and damage to the bushings. The observed failure types of power transformers are: (i) failure (overturning or shifting) of unrestrained transformer, (ii) anchorage failure, (iii) conservator failure, (iv) foundation failure, (v) damage to control boxes, (vi) oil leakage of radiators and (vii) failure of lightning arrestors (Ersoy et al, 2008; Schiff, 1999). The first two types of failure are the most common despite the fact that it is a simple procedure to fix the transformer base to the foundation either by anchor bolts or welds. Characteristic damage of foundation failure and overturned transformer in 1999 Izmit earthquake are shown in Figure 1-4 and Figure 1-5, respectively.

As for the bushing failures, it has been observed that the lack of slack in the connecting cable between the bushing and the connecting equipment results in fracture of the porcelain body, while oil leakages between the base flange of high voltage bushings and their upper porcelain body have occurred due to gasket failure. Note that the most vulnerable gasket is the one closest to the flange connecting the bushing to the transformer. Figure 1-6 presents the bushing failure at the gasket level, while bushing failures during the 1999 Chi-Chi earthquake are shown in Figure 1-7. Table 1-1 summarizes the damage observed during past earthquakes.

Table 1-1 Damage Observed during Historical Earthquake Events (Koliou et al., 2012)

Earthquake Event	Magnitude (M_w)	Observed Damage
Loma Prieta (1989), USA	6.9	Cracked porcelain bushings, anchorage failures & oil leakage
Northridge (1994), USA	6.7	Failure of bushings, anchorage, radiators, surge arrestors & conservators
Kobe (1995), Japan	6.9	Anchorage failure
Chi-Chi (1999), Taiwan	7.6	Transmission tower foundation damage & surge arrestors' damage
Izmit (1999), Turkey	7.4	Failures of transformer tanks & bushings due to unanchored transformers

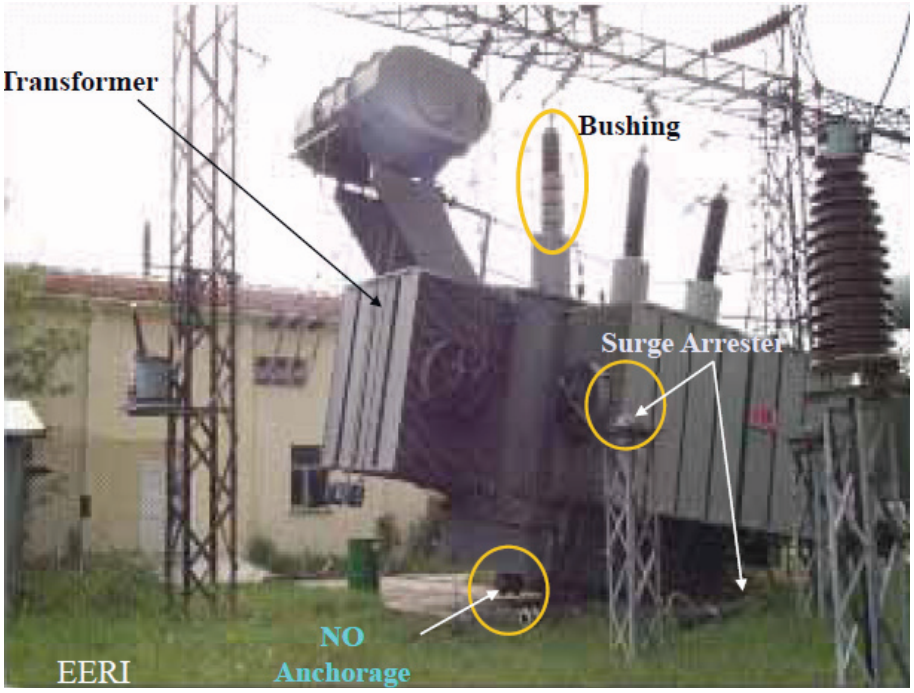

Figure 1-4 Damage to Transformer Foundation due to Lack of Anchorage, Izmit Turkey 1999 (Wang, 2008)

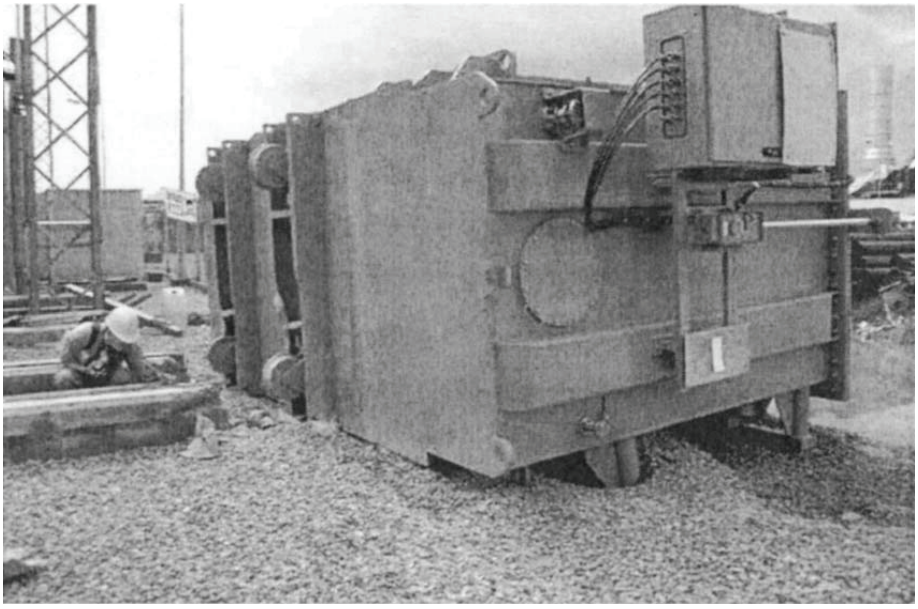

Figure 1-5 Transformer Turned Over, Izmit Turkey 1999 (Sezen & Whittaker, 2006)

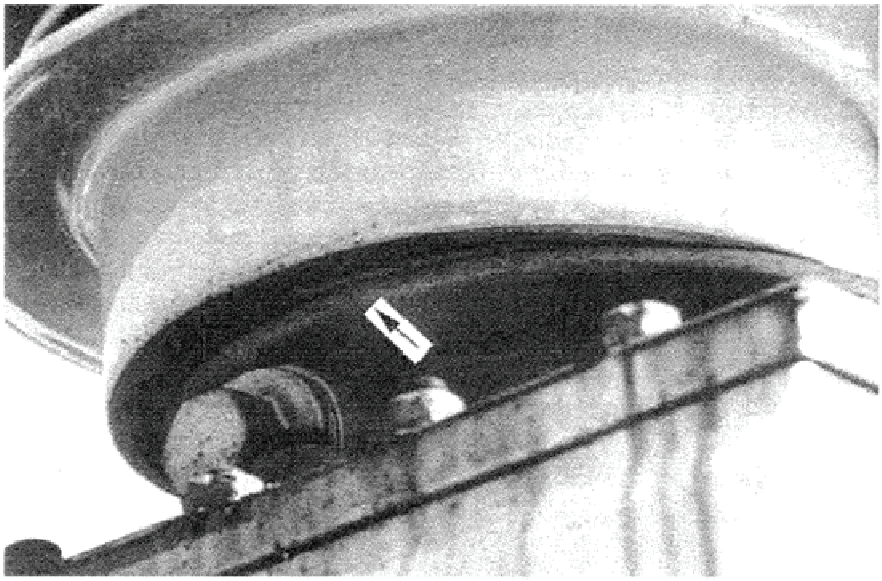

Figure 1-6 Bushing Failure at the Flange (Ersoy et al., 2008)

Figure 1-7 Bushing Failure, Taiwan 1999 (Wang, 2008)

1.3. Seismic Design Recommendations for Electrical Substation Equipment

In the United States, recommendations for the seismic design of substation buildings, structures and equipment located in moderate and high seismic areas are provided in the IEEE-693 Standard (IEEE, 2005). Although substation designers are not obligated to follow the guidelines

within this document, most of them have generally adopted the IEEE-693 Standard for the design of new electrical equipment.

The IEEE-693 Standard has established design response spectra of high and moderate seismic qualification level for analysis and testing of equipment as shown in Figure 1-8 and Figure 1-9, respectively. A damping ratio of 2% is recommended for the analysis of substation equipment.

According to IEEE-693 Standard, the substation equipment can be qualified by conducting static analysis, static coefficient analysis, response spectrum analysis or shake table testing depending on the type of the equipment and the voltage rating. The seismic qualification of high voltage bushing structures is conducted through shake table testing with the bushing mounted on a test fixture, simulating a rigid base. For this reason, the IEEE-693 Standard considers that the motion at the base of the bushing is equal to the ground motion multiplied by a frequency independent amplification factor of 2.

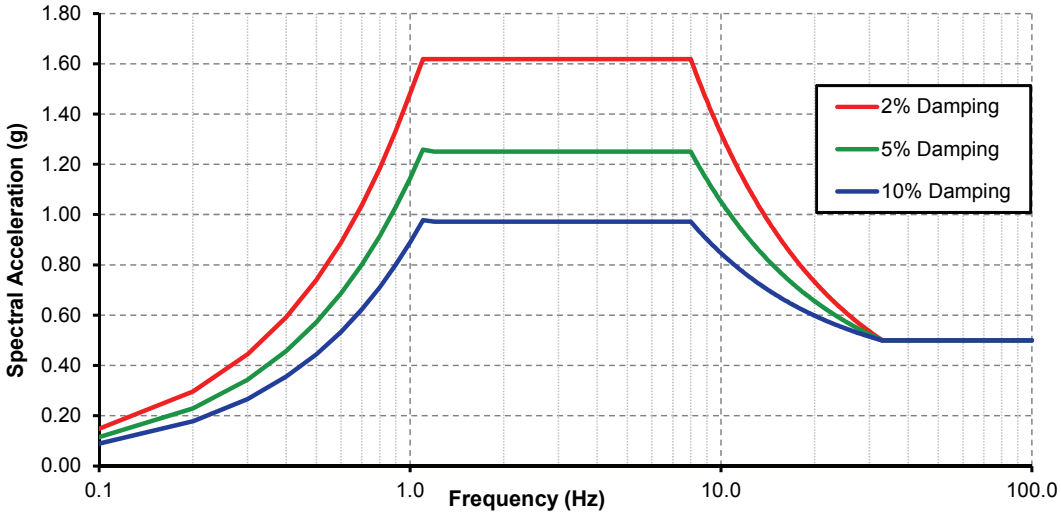

Figure 1-8 High Required Response Spectrum (after IEEE, 2005)

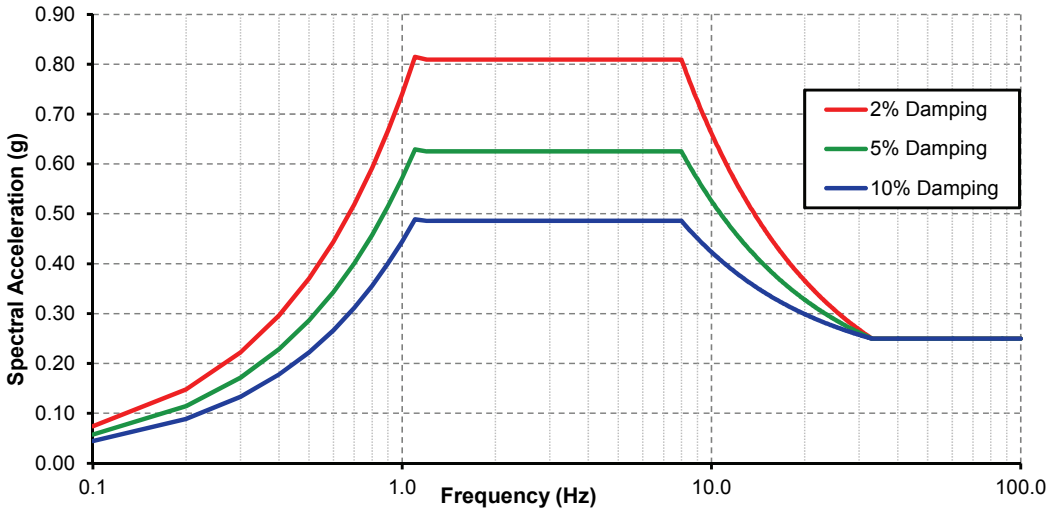

Figure 1-9 Moderate Required Response Spectrum (after IEEE, 2005)

1.4. Literature Review

Several experimental and numerical studies have been conducted during the past 15 years on the seismic performance evaluation and/or rehabilitation of transformer-bushing systems.

In 1997, Wilcoski & Smith (Wilcoski & Smith, 1997) developed a fragility testing procedure to define the vulnerability of bushing structures under earthquake and other transient motions by documenting the failure modes observed. During shake table tests of a 500kV bushing, which were conducted as part of this study, the bushing structure experienced oil leakage when the IEEE-693 spectrum was scaled to Peak Ground Acceleration (PGA) of 1g. The measured fundamental frequencies of the 500kV bushing varied within a range of 5.7Hz to 6.4Hz, while the damping ratio was reported to lie between 2.5% and 3% of critical.

Bellorini et al. (1998) performed seismic qualification tests as well as finite element analyses of a 230kV transformer-bushing system in order to evaluate the dynamic characteristics of both the power transformer and the bushing structure. During the experimental phase, which consisted of multi point random (MPR) excitation tests as well as forced vibration (FV) tests, the fundamental frequencies of the transformer tank and bushing structure were measured equal to 3.5Hz and 11Hz, respectively, while the damping ratio was estimated as 2% of critical. The experimental findings matched with good accuracy the numerical results. In this study, the amplification between the ground and the bushing flange as well as the ground and the bushing center of

gravity (CG) was investigated and compared to the IEC 61463 (International Electrotechnical Commotion "Bushing-Seismic Qualification" Standard).

Seismic qualification tests (per the IEEE-693 Provisions) of three different voltage rate bushings (196kV, 230kV and 550kV) were performed at the earthquake simulator at the Pacific Earthquake Engineering Research (PEER) Center at the University of California, Berkeley (Gilani et al., 1998; Gilani et al., 1999; Gilani et al., 2001; Whittaker et al., 2004). Two 196kV porcelain bushings mounted on a rigid support structure at an angle of 20 degrees were tested under earthquake motions of moderate and high seismicity level. Both bushing structures were qualified for the moderate level motions, and survived the high level motions with negligible damage. The measured fundamental frequencies of the bushings were between 14Hz and 16Hz, while the damping ratio was estimated to vary within a range of 2.5% to 4% of critical. Two identical 230kV porcelain bushings were tested using the same configuration as for the 196kV bushings (rigid frame structure) as well as a flexible support structure. For the rigid mounting conditions, the bushings were qualified for high level seismicity motions without any structural damage or oil leakage. Their fundamental frequencies were measured varying between 18Hz and 20Hz, while the damping ratio was computed to fluctuate between 2% to 3% of critical. As for the flexible support, the fundamental frequencies were between 5.5Hz and 7.5Hz, while the damping ratio varied within a range of 2% to 5% of critical. One of the bushings survived oil leakage and slip of the porcelain units during high level qualification shaking. Additionally, two different ring configurations around the gasket were used as a retrofit approach to prevent slippage and oil leakage during extreme ground shaking, which appeared to work efficiently for only one of the bushing structures. Finally, three 550kV porcelain bushings were tested using the rigid support structure as for the rest of the bushings. None of the bushings was qualified for moderate level earthquake motions, since they survived oil leakage as well as slippage of the upper porcelain unit over the gasket connection, exposing the gasket to significant residual displacement. Frequency of approximately 8Hz and damping ratio of 4% of critical were measured for all three bushings.

Villaverde et al. (2001) performed experimental and numerical studies to quantify the ground motion amplification at the bushing base due to the flexibility of the transformer tank and turrets. For these studies, typical 230kV and 500kV bushings were considered. According to the results

obtained by the testing, the frequencies of the bushing structures varied between 2.5Hz and 3.5Hz for the 500kV bushings and were approximately 4Hz for the 230kV ones. As for the damping ratios, they were within a range of 1.5% and 4% of critical for both 230kV and 500kV bushings. Three dimensional finite element models were developed to match the experimental findings and investigate the amplification factor between the ground and the bushing flange. For some analysis cases, the amplification factor was found to be almost double compared to the proposed value per IEEE-693 Standard.

Ersoy et al. (2001) investigated analytically and experimentally friction pendulum systems (FPS) as an approach of seismic rehabilitation and design of transformer-bushing systems in order to mitigate their seismic vulnerability. The effect of various parameters (i.e., on the bushing ground motion characteristics, peak ground acceleration, bi-axial motions, and bearing radius) on the seismic performance of typical transformer-bushing systems isolated with FPS bearings was investigated under one- and two-dimensional earthquake motions. Isolating the transformer tank using FPS appeared to be an effective approach since the inertia forces decreased considerably in the transformer-bushing system.

Implementation of base isolation systems as a means to reduce the seismic demand of the transformer-bushing systems was also investigated by Murota (2003). Experimental and numerical studies were performed for two types of isolation systems: (i) sliding bearing system and (ii) segmented high-damping rubber bearing system and were proven to be effective techniques for seismic protection of power transformers.

Ersoy and Saadeghvaziri (2004) identified and verified with numerical analysis of finite element models for three different transformer-bushing systems, the influence of the flexible tank top plate on the response of the bushing structure.

Filiatrault & Matt (2005, 2006) conducted numerical and experimental studies on the response of transformer-bushing systems during ground shaking, mainly aiming on investigating the amplification factor between the ground and the base of the bushing. Finite element analyses of four different transformer-bushing models (525kV, 230kV and two 500kV) were performed under an ensemble of 20 ground motions representative of the California region scaled to match the IEEE-693 high performance required spectrum. Note that analyses were performed

considering two different support conditions of the bushing: (i) rigid support and (ii) flexible support on the tank top plate. It was found that the amplification factor between the ground and the base of the bushing exceeded the factor of 2 proposed by the IEEE-693 Standard, especially for transformer-bushing systems with bushing's fundamental frequency close to the fundamental frequency of the transformer tank. The experimental investigation included uniaxial shake table tests of a 525kV transformer-bushing system conducted at the University of California, San Diego. The results of the tests confirmed the influence of the flexibility of the tank top plate on the dynamic properties of the bushing. As for the amplification factor, the numerically identified trends were verified experimentally since it was observed that four out of five ground motions considered for testing generated amplification factors larger than the IEEE-693 recommended value of 2.0. Additionally, as presented in Matt & Filiatrault (2004), two retrofit schemes were investigated numerically for a 230kV transformer in order to reduce the amplification that occurs between the ground and the bushing attachment point. More specifically, the first approach included double angle braces attached between the top of the turret and the top of the transformer tank, while the second scheme consisted of four bracing elements attached between the top of the transformer tank and the foundation in addition to the double angle braces (first bracing configuration). Despite the fact that both bracing configurations appeared to considerably reduce the amplification between the ground and the base of the bushing structure, the reduction was not large enough to meet the criteria of IEEE-693 Standard (value of 2.0).

Analytical investigation incorporating modeling variations and structural modifications of finite element models representing existing transformer-bushing structure was conducted by Oikonomou (2010). The main objective of this study was to identify the dynamic characteristics and important interactions between various components (of the transformer-bushing system) and the high voltage bushings. Detailed sensitivity analyses, which were conducted utilizing a three dimensional finite element model, consisted of three identical 196kV bushings mounted on tank top plate of a 230kV power transformer, clearly showed that the top (cover) plate of the transformer tank influences significantly the response of the high voltage bushings (Reinhorn et al., 2011).

The numerical and experimental studies conducted in the past 15 years have indicated a generally improved seismic response of high voltage bushings when mounted on a rigid base

compared to their actual performance in the field during real earthquakes. The reason for this discrepancy is that the high voltage bushings, "as installed" in the field, are mounted on the flexible plate of the transformer tank, while during the shake table tests (qualification testing) are mounted on a rigid base.

1.5. Research Objectives

The main objectives of this research were to investigate the seismic response of transformer bushing systems installed both on a rigid base and on the flexible plate of the transformer tanks ("as installed" conditions), as well as identify feasible approaches to stiffen the base of the "as installed" bushings in order to reduce the seismic demand and achieve an improved seismic response. The seismic demand of the transformer bushing systems may be reduced by isolating the transformer tank itself (global stiffening solution) as already reported in the literature (Ersoy et al., 2001; Murota, 2003; Matt & Filiatrault, 2004), however in this research, the local solution of stiffening the base of the bushing structure was investigated.

The approach of stiffening the bushing base to shift its fundamental frequency towards the rigid base conditions and reduce the seismically induced loading is conceptually presented in Figure 1-10. As shown in this figure , the fundamental frequency of the "as installed" high voltage bushings is in the green area, which includes the plateau of the response spectra, while by stiffening the bushing base, the fundamental frequency range moves towards the pink area, where the bushing receives less seismic forces. Note that the frequency ranges indicated in Figure 1-10 are based on the computed fundamental frequencies of transformer-bushing systems in Section 2. Several stiffening approaches were investigated in order to achieve a significantly improved response of the bushing structures and are presented in the following chapters.

This research was divided into three parts. The first part consisted of a series of numerical finite element analyses for different transformer models, while the second part focused on the experimental investigation of a typical transformer bushing system. In both parts, the response component of interest was the moments at the base of the high voltage bushings since the shear and axial force demand imposed during an earthquake is typically much lower than the bushing capacity. The third part focused on analytical derivations of simplified relations of evaluating the dynamic properties and forces of the transformer-bushing system mainly showing that the

flexibility of the transformer cover produces (i) a reduction of the fundamental frequency, (ii) additional motion at the bushing base and (iii) additional vertical vibration of the bushings.

Finite element numerical analyses were conducted for four different transformer models of various sizes and voltages. The first series of linear dynamic time-history analyses were performed in order to evaluate the dynamic properties of the bushings and compare the response of the bushing structure installed on a rigid base and "as installed". The second part of the numerical analyses focused on investigating the efficiency of several stiffening approaches in order to ensure the bushing structure integrity during strong earthquakes.

The results obtained from the finite element analyses were verified experimentally by a series of shake table tests performed in the Structural Engineering and Earthquake Simulation Laboratory (SEESL) at the University at Buffalo. A numerical model was also developed for the test configurations in order to predict the response of the bushing structure through modal and dynamic time history analyses.

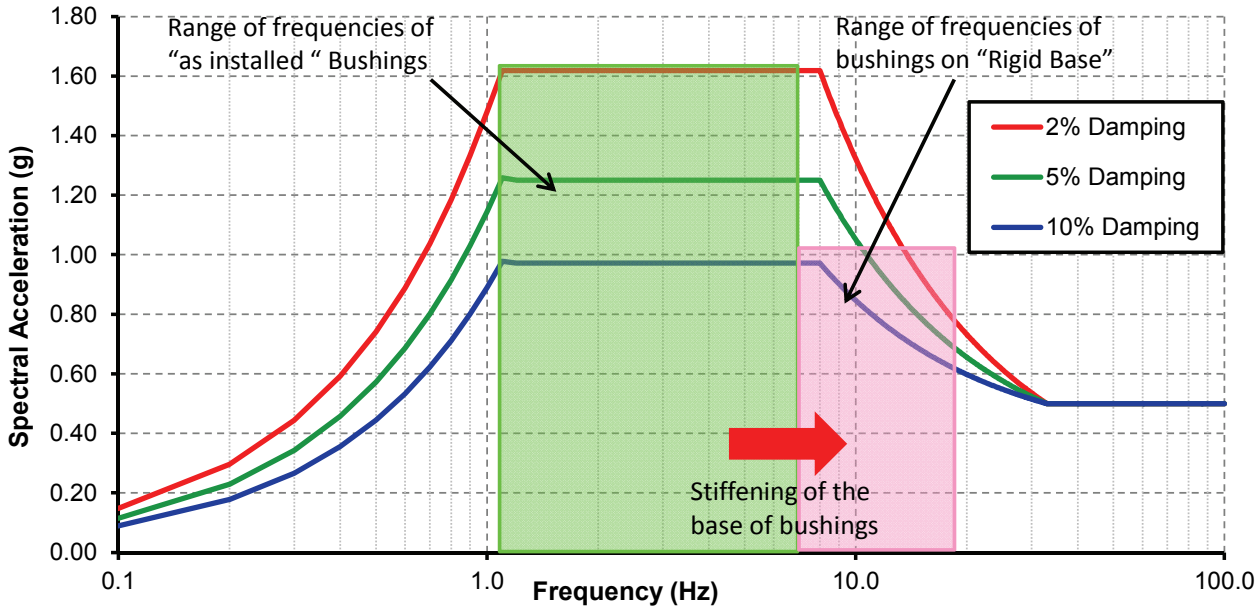

Figure 1-10 Influence of Stiffening the Base of the High Voltage Bushings on the IEEE-693 High Required Response Spectra (Koliou et al., 2012)

1.6. Report Organization

Following this introductory section, Section 2 presents the four finite elements models of the transformer bushing systems considered for numerical investigation. Moreover, this section deals with a preliminary investigation of the transformer bushings through modal and dynamic time history analyses. Section 3 refers to the proposed stiffening approaches that can be used in order to mitigate the seismic vulnerability of the bushing structures. The finite element models were modified and analyzed to determine the efficiency of each stiffening technique. Sections 4 and 5 present an experimental study aiming at the verification of the numerically identified trends. System identification testing of the bushing structure by a series of hammer tests and pull-back tests are described in Section 4, while Section 5 presents a series of shake table tests on the same bushing test structure. In Section 6, a comparison between the predicted numerical results and the experimental measurements is presented. Section 7 presents the analytically derived simplified methods of evaluating the dynamic properties of the transformer-bushing systems. Finally, Section 8 summarizes this study, along with the most important conclusions. Recommendations for future research are also included in this last section.

SECTION 2

NUMERICAL INVESTIGATION OF HIGH VOLTAGE TRANSFORMER-BUSHINGS SYSTEMS

2.1. Introduction

In this section, a numerical investigation on the seismic response of bushings mounted on transformer tank bases ("as installed") and on rigid bases is presented. Four different finite element models of transformer bushing systems were used for performing modal and linear dynamic time history analyses using the commercial structural analysis program *SAP2000 Advanced V.14.1.0* (Computers and Structures, 2009).

2.2. Description of Transformer Models Considered

Four different types of transformer bushing systems of various sizes, geometries and voltages, as shown in Figure 2-1, were considered for analysis in this research. Table 2-1 presents details on the dimensions and weight of each transformer model (Filiatrault & Matt, 2006; Oikonomou, 2010).

Each three dimensional finite element model was built in the commercial structural analysis program *SAP2000 Advanced V.14.1.0* (Computers and Structures, 2009). The transformer frames were modeled as shell elements with the appropriate thickness and mass allowing for in–plane deformation and out–of–plane bending, while the transformer tank was considered to be full of oil. Beam elements as well as appropriate shell elements were used for modeling the stiffeners attached to tank sides (Filiatrault & Matt, 2006). The high voltage bushings were mounted on the cover plate of the transformer tank and each bushing, which was modeled as multiple beam elements in series with the appropriate geometry, stiffness and mass, consisted of three parts.: (i) the upper part represented the actual high voltage bushing, (ii) the central part was a radial array of rigid elements connected to the turret, which represented the bushing flange and (iii) the lower part in the assembly was the turret, which was modeled as a polyhedron of the same number of surfaces as the number of the radial rigid elements. The radiators were represented by vertical elements of rectangular cross section, while the high voltage surge arrestors were modeled as

vertical beams with circular cross section (Oikonomou, 2010). The oil conservator of the 230kV Ferranti Packard transformer model, which was represented by a cylindrical tank made up of shell elements, considered to be full of oil and the oil was distributed uniformly on the walls as vertical loading. The tank was supported by two horizontal and two diagonal beams fixed to the tank wall (Oikonomou, 2010).

Finally, it has to be mentioned that the geometry, thickness and locations of all walls, plates and beams were obtained from manufacturer's structural drawings.

Table 2-1 Dimensions of Transformer Models Considered

Transformer Model	Dimensions (ft)			Weight** (kips)
	Length	Width	Height	
Westinghouse 525kV	8.8	9.9	22.8	463
Siemens 230kV	10.0	24.2	14.4	478
Siemens 500kV	10.8	26.0	16.8	673
Ferranti Packard 230kV	8.3	26.0	13.0	266

**Including oil

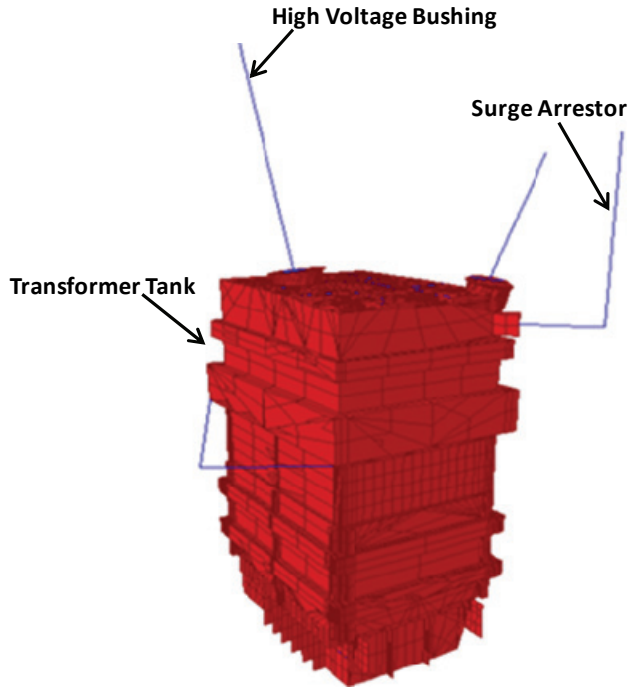

a. Westinghouse 525kV Transformer Model

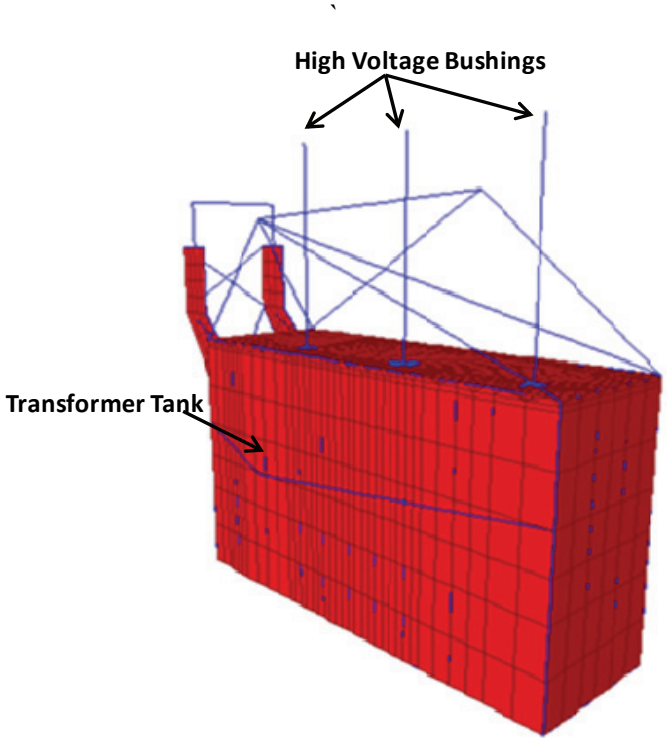

b. Siemens 230kV Transformer Model

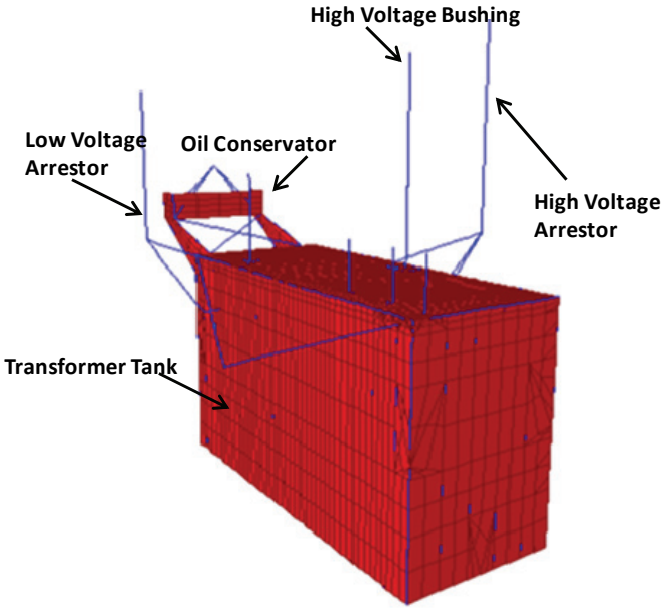

c. Siemens 500kV Transformer Model

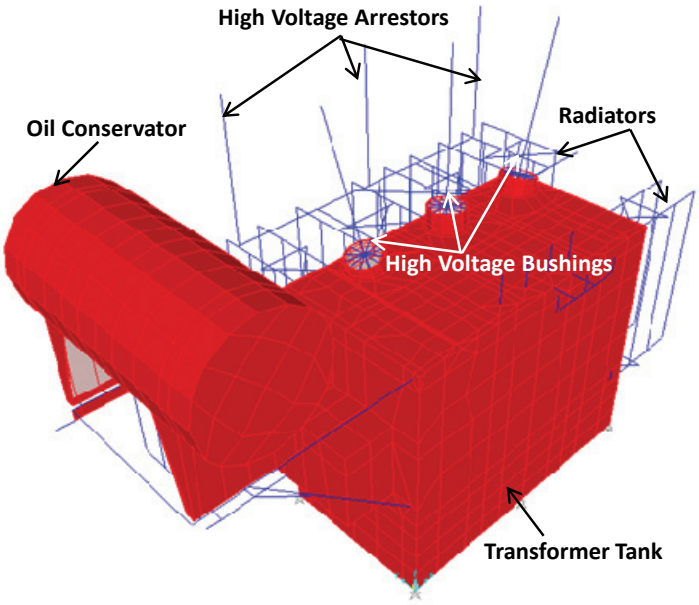

d. Ferranti Packard 230kV Transformer Model

Figure 2-1 Transformer Models Considered

2.3. Modal Analysis of High Voltage Transformer-Bushings Systems

2.3.1. Modal Analysis of High Voltage Bushings on a Rigid Base

In order to conduct the modal analysis of bushing systems installed on a rigid base, the dynamic properties of the transformer bushing models were modified. More specifically, two different procedures were followed to create a rigid base for the high voltage bushings. The first approach focused on the restraint of all the degrees of freedom of the initial model, except for those of the bushing, resulting in bushing on rigid foundations, while for the second approach all the elements of the initial model, except for the bushing, were deleted and the bushing itself is restrained at its base.

Note that in both procedures used to represent the rigid base the results of the modal analysis were identical. Moreover, the period obtained for the Ferranti Packard 230kV model was almost equal to the period computed for the Siemens 230kV model, as shown in Table 2-2, which indicates that the frequency of the 230kV bushing on a rigid base is independent of the manufacturer.

Table 2-2 Fundamental Periods and Natural Frequencies of High Voltage Bushings on a Rigid Base

Model Description	Period (sec)	Frequency (Hz)
Westinghouse 525kV Model – mode 1 –	0.108	9.27
Siemens 230kV Model – mode 1 –	0.059	16.85
Siemens 500kV Model – mode 1 –	0.114	8.75
Ferranti Packard 230kV Model – mode 1 –	0.060	16.80

2.3.2. Modal Analysis of High Voltage Bushings on a Transformer Tank ("as installed" conditions)

For each one of the transformer bushing models, a modal analysis was performed and the natural frequencies for all the modes were obtained. Note that for the Westinghouse 525kV, Siemens 230kV and Siemens 500kV transformers, the number of modes considered are greatly reduced due to the complexity of the finite element models (Filiatrault & Matt, 2006), while for the Ferranti Packard 230kV transformer model more than 200 modes were considered. At least 90% of the total mass participation was accounted for in the two principal directions of each model.

The frequency of each mode is presented in Table 2-3, Table 2-4 and Table 2-5 for the Westinghouse 525kV, Siemens 230kV and Siemens 500kV transformer, respectively, while the first 40 modes of the Ferranti Packard 230kV transformer are shown in Table 2-6. However, since the high voltage bushings were mainly investigated in this research, the deformation of the first mode of each bushing system is presented in Figure 2-2.

Table 2-3 Periods and Natural Frequencies of Westinghouse 525kV Transformer-Bushing Model

Mode	Mode Description	Period (sec)	Frequency (Hz)
1	Surger Arrestor (1st mode)	0.377	2.65
2	High Voltage Bushing (1st mode)	0.342	2.92
3	Surger Arrestor (2nd mode)	0.328	3.05
4	High Voltage Bushing (2nd mode)	0.292	3.42
5	Transformer Frame (1st mode Transverse)	0.119	8.38
6	Transformer Frame (1st mode Longitudinal)	0.088	11.37
7	High Voltage Bushing (3rd mode)	0.076	13.15
8	Surger Arrestor (3rd mode)	0.069	14.58
9	Surger Arrestor (4th mode)	0.065	15.31
10	Transformer Frame (Transverse 2nd mode)	0.049	20.16
11	Transformer Shell (1st mode Out of plane bending)	0.040	24.81
12	Transformer Frame (Longitudinal 2nd mode)	0.029	33.90
13	Transformer Frame Torsion (1st mode)	0.023	42.79
14	Transformer Shell (2nd mode Out of plane bending)	0.019	50.71

Table 2-4 Periods and Natural Frequencies of Siemens 230kV Transformer-Bushing Model

Mode	Mode Description	Period (sec)	Frequency (Hz)
1	High Voltage Bushings (1st mode)	0.109	9.14
2	High Voltage Bushings (2nd mode)	0.097	10.26
3	Transformer Frame (1st mode Transverse)	0.093	10.76
4	Transformer Frame & Bushings (2nd mode Transverse)	0.086	11.57
5	Oil Conservator Tank (1st mode Longitudinal)	0.083	12.03
6	High Voltage Bushings (3rd mode)	0.076	13.23
7	High Voltage Bushings (4th mode)	0.074	13.51
8	Transformer Frame (2nd mode Transverse)	0.059	16.88
9	Transformer Shell (1st mode Out of plane bending)	0.052	19.17
10	Transformer Frame (1st mode Longitudinal)	0.039	25.05
11	Transformer Frame (4th mode Transverse)	0.039	25.95
12	Transformer Shell (2nd mode Out of plane bending)	0.027	37.19
13	Transformer Frame (2nd mode Longitudinal)	0.026	37.89
14	Transformer Shell (3rd mode Out of plane bending)	0.024	41.32

Table 2-5 Periods and Natural Frequencies of Siemens 500kV Transformer-Bushing Model

Mode	Mode Description	Period (sec)	Frequency (Hz)
1	High Voltage Arrestor (1st mode)	0.369	2.71
2	High Voltage Arrestor (2nd mode)	0.340	2.94
3	High Voltage Bushing (1st mode Transverse)	0.292	3.42
4	Oil Conservator (1st mode)	0.158	6.35
5	Oil Conservator (2nd mode)	0.143	6.99
6	Low Voltage Arrestor (1st mode)	0.134	7.45
7	Low Voltage Arrestor (2nd mode)	0.123	8.13
8	High Voltage Bushing (2nd mode Longitudinal)	0.119	8.38
9	High Voltage Bushing (3rd mode)	0.118	8.44
10	Oil Conservator & Low Voltage Bushing (1st mode)	0.101	9.89
11	Transformer Frame (1st mode Transverse)	0.095	10.51
12	High Voltage Arrestor (3rd mode)	0.091	11.01
13	Low Voltage Bushing(1st mode)	0.080	12.46
14	Low Voltage Arrestor (3rd mode)	0.067	14.90
15	Transformer Frame (2nd mode Transverse)	0.063	15.84
16	Transformer Shell (1st mode Out of Plate Bending)	0.057	17.61
17	High Voltage & Low Voltage Bushings and Arrestors(4th mode)	0.050	19.85
18	Transformer Frame (1st mode Longitudinal)	0.048	20.85
19	Transformer Frame (2nd mode Longitudinal)	0.046	21.93
20	Transformer Frame (2nd mode Longitudinal)	0.044	22.73
21	Transformer Shell (2nd mode Out of Plate Bending)	0.035	28.73
22	Oil Conservator (2nd mode)	0.026	37.81
23	Transformer Shell (3rd Out of Plate Bending)	0.022	44.86
24	Transformer Shell and Oil Conservator (1st mode)	0.021	47.94

Table 2-6 Periods and Natural Frequencies of Ferranti Packard 230kV Transformer-Bushing Model (Oikonomou, 2010)

Mode	Mode Description	Period	Frequency (Hz)
1	High Voltage Arrestor Close to Conservator	0.596	1.68
2	High Voltage Arrestor Furthest to Conservator	0.595	1.68
3	Radiator	0.370	2.70
4	Conservator/Radiator	0.368	2.72
5	High Voltage Arrester Middle Unit	0.345	2.90
6	High Voltage Arrestor Support with Bushing	0.243	4.12
7	High Voltage Bushing Center unit	0.210	4.76
8	Radiator with High Voltage Bushing movement	0.192	5.20
9	Radiator with High Voltage Bushing movement	0.186	5.39
10	Radiator with High Voltage Bushing movement	0.183	5.46
11	High Voltage Bushings Outer Units	0.179	5.59
12	Radiator and Conservator with High Voltage Bushing	0.170	5.89
13	Radiator and Conservator with High Voltage Bushing	0.164	6.09
14	High Voltage Bushings Outer Units	0.159	6.30
15	High Voltage Bushings Outer Units	0.158	6.31
16	Larger Radiator	0.149	6.72
17	High Voltage Bushings large movement	0.142	7.05
18	Radiators	0.139	7.21
19	High Voltage Bushing Center Unit	0.131	7.64
20	High Voltage Bushing Center Unit	0.128	7.81
21	Radiators	0.124	8.08
22	Radiators	0.117	8.56
23	High Voltage Arrestor Support, Vertical movement	0.115	8.72
24	High Voltage Arrestor Support, Vertical movement	0.111	9.01
25	Radiator	0.102	9.79
26	Radiator	0.094	10.68
27	Radiator, Conservator, and Low Voltage Arrestor	0.090	11.07
28	Radiator and Conservator	0.087	11.55
29	Radiator	0.077	12.97
30	Low Voltage Arrestor Support	0.073	13.63
31	Radiator, Conservator, and Low Voltage Arrestor	0.069	14.40
32	Low Voltage Bushings and Arrestor Support	0.061	16.35
33	Low Voltage Bushings and Arrestor Support	0.056	17.80
34	Radiator, Conservator, and Low Voltage Arrestor	0.049	20.35
35	Transformer Tank	0.040	25.10
36	Transformer Tank, top plate vertical movement	0.035	28.35
37	Transformer Tank	0.033	29.96
38	Transformer Tank	0.018	54.51
39	Transformer Tank	0.018	55.74
40	Transformer Tank, vertical movement	0.017	60.39

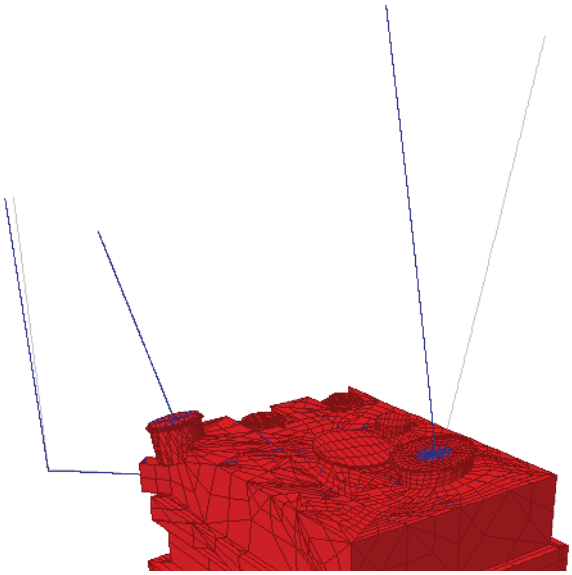

a. Westinghouse 525kV Transformer Model (1^{st} mode – Longitudinal)

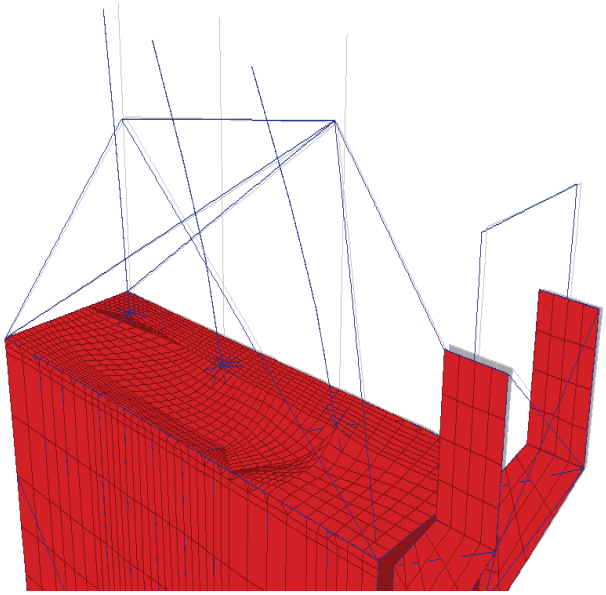

b. Siemens 230kV Transformer Model (1^{st} mode – Transverse)

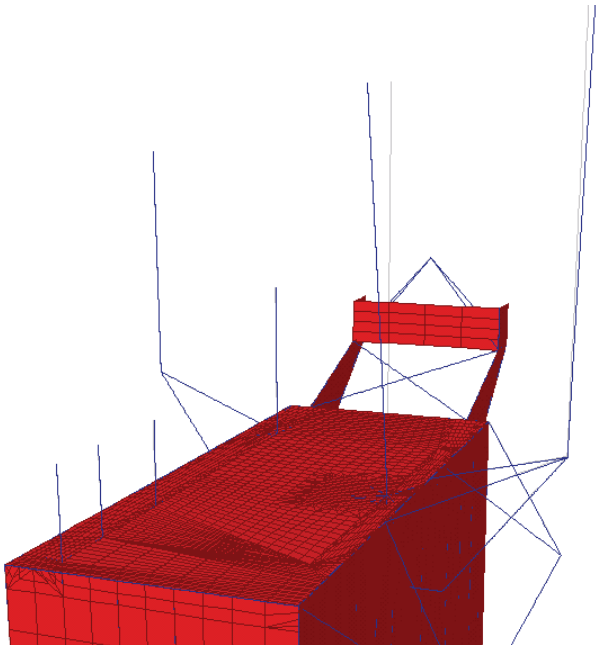

c. Siemens 500kV Transformer Model (1^{st} mode – Transverse)

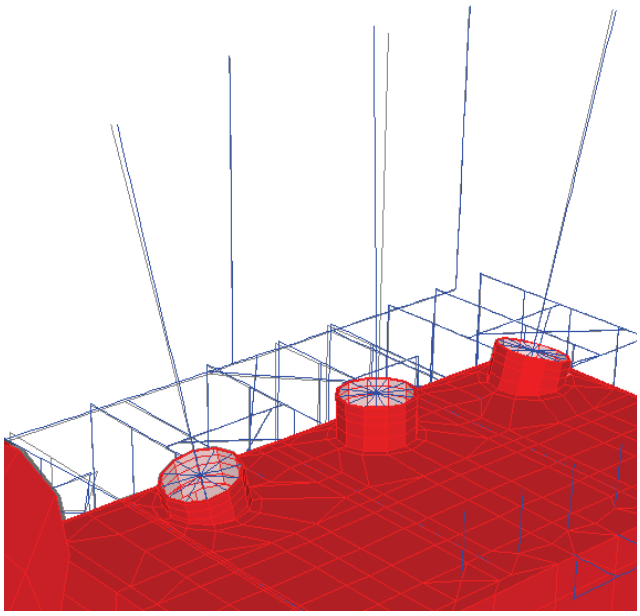

d. Ferranti Packard 230kV Transformer Model (1^{st} mode Transverse)

Figure 2-2 Deformed Shape of High Voltage Bushing Models

Comparing the results obtained from the modal analyses of bushings installed on transformer tanks ("as installed" conditions) and on a rigid base, it can be concluded that the transformer tanks are very flexible compared to the rigid base in all the four cases of the high voltage transformer- bushing models. The fundamental frequencies of bushings mounted on a rigid base are more than double of the ones mounted on the flexible tank top plate as shown in Table 2-7.

Table 2-7 Comparison of High Voltage Bushings on a Rigid Base and "As Installed"

Model Description	Support	Frequency (Hz)
Westinghouse 525kV Model – mode 1 –	"As installed"	2.92
	Rigid Base	9.27
Siemens 230kV Model – mode 1 –	"As installed"	9.14
	Rigid Base	16.85
Siemens 500kV Model – mode 1 –	"As installed"	3.42
	Rigid Base	8.75
Ferranti Packard 230kV Model – mode1 –	"As installed"	4.76
	Rigid Base	16.80

2.4. Dynamic Analysis of Transformer Bushings

2.4.1. Earthquake Ground Motions Considered

Two ground motion ensembles were selected for performing linear dynamic time history analyses of the transformer-bushing models. The first ensemble consisted of 20 ground motions recorded within the California region selected such that the location of the measurement was far enough from the fault rupture to be free of any near fault directivity pulses (Filiatrault & Matt, 2006). The second ensemble selected in this study was the un-normalized (original) motions of the FEMA P695 Far Field Ground Motion Set (FEMA P695, 2009), which contains 22 historical ground motions from all over the world with two horizontal components each, recorded at the same station. This ground motion ensemble is considered to be representative of the seismicity in the Western United States. Further information about the earthquake events is presented in Table 2-8 and Table 2-9 for ensemble 1 and ensemble 2, respectively.

Table 2-8 California Region Earthquake Ground Motion Ensemble – Ensemble 1 –

EQ. Index	Earthquake Event			Recording Station	PGA (g)
	Name	Year	M_w		
1	Superstition Hills	1987	6.7	Brawley	0.12
2	Superstition Hills	1987	6.7	El Centro Imp. Co. Cent	0.26
3	Superstition Hills	1987	6.7	Plaster City	0.19
4	Northridge	1994	6.7	Beverly Hills 14145 Mulhol	0.42
5	Northridge	1994	6.7	Canoga Park – Topanga Can	0.36
6	Northridge	1994	6.7	Glendale – Las Palmas	0.36
7	Northridge	1994	6.7	LA – Hollywood Stor FF#	0.23
8	Northridge	1994	6.7	LA – N Faring Rd	0.27
9	Northridge	1994	6.7	N. Hollywood – Coldwater Can	0.27
10	Northridge	1994	6.7	Sunland – Mt Gleason Ave	0.16
11	Loma Prieta	1989	6.9	Capitola	0.53
12	Loma Prieta	1989	6.9	Gilroy Array #3	0.56
13	Loma Prieta	1989	6.9	Gilroy Array #4	0.42
14	Loma Prieta	1989	6.9	Gilroy Array #7	0.23
15	Loma Prieta	1989	6.9	Hollister Diff. Array	0.28
16	Loma Prieta	1989	6.9	Saratoga – W Valley Coll.	0.33
17	Cape Mendocino	1992	7.1	Fortuna Fortuna Blvd#	0.12
18	Cape Mendocino	1992	7.1	Rio Dell Overpass – FF#	0.39
19	Landers	1992	7.3	Desert Hot Springs#	0.15
20	Landers	1992	7.3	Yermo Fire Station#	0.15

Table 2-9 FEMA P695 Earthquake Ground Motion Ensemble – Ensemble 2 –

EQ. Index	Earthquake Event				Recording Station	PGA(g)*
	Name		Year	M_w		
	EQ_ID.	Earthquake				
1	12011	Northridge	1994	6.7	Beverly Hills – Mulhol	0.52
2	12012	Northridge	1994	6.7	Canyon Country–WLC	0.48
3	12041	Duzce, Turkey	1999	7.1	Bolu	0.82
4	12052	Hector Mine	1999	7.1	Hector	0.34
5	12061	Imperial Valley	1979	6.5	Delta	0.35
6	12062	Imperial Valley	1979	6.5	El Centro Array#11	0.38
7	12071	Kobe, Japan	1995	6.9	Nishi – Akashi	0.51
8	12072	Kobe, Japan	1995	6.9	Shin – Osaka	0.24
9	12081	Kocaeli, Turkey	1999	7.5	Duzce	0.36
10	12082	Kocaeli, Turkey	1999	7.5	Arcelik	0.22
11	12091	Landers	1992	7.3	Yermo Fire Station	0.24
12	12092	Landers	1992	7.3	Coolwater	0.42
13	12101	Loma Prieta	1989	6.9	Capitola	0.53
14	12102	Loma Prieta	1989	6.9	Gilroy Array#3	0.56
15	12111	Manjil, Iran	1990	7.4	Abbar	0.51
16	12121	Superstition Hills	1987	6.5	El Centro Imp. Co.	0.36
17	12122	Superstition Hills	1987	6.5	Poe Road (temp)	0.45
18	12132	Cape Mendocino	1992	7.0	Rio Dell Overpass	0.55
19	12141	Chi-Chi, Taiwan	1999	7.6	CHY 101	0.44
20	12142	Chi-Chi, Taiwan	1999	7.6	TCU045	0.51
21	12151	San Fernando	1971	6.6	LA – Hollywood Stor.	0.21
22	12171	Friuli, Italy	1976	6.5	Tolmezzo	0.35

*Larger component

2.4.2. Scaling Procedure

The geometric mean spectrum of each ensemble was scaled to match the IEEE – 693, 2% damped, high required response spectrum in a range of frequencies between 2.0 and 30.0Hz. This range was selected since the fundamental frequencies of the bushing structures vary from 2.5Hz ("as installed") and 25Hz (rigid base) for the different types of bushings (Filiatrault & Matt, 2006; Fahad et al., 2010; Muhammad, 2012).

Despite being a popular measure in the investigation of ground motions, the median was rejected as a scaling parameter in this study, since it is not defined by an analytical mathematical equation. In fact, the *median* is described as the number separating the higher half of a sample/population from its lower half, and is computed by arranging all the values of that sample

in ascending/descending order and picking the middle one (or the arithmentic mean of the two middle ones). On the other hand, the *geometric mean*, which indicates the central tendency or typical value of a set of numbers, is a more appealing measure, since it is calculated by the following equality as:

$$S_{ageomean}(f) = \left(\prod_{i=1}^{N} S_{ai}(f) \right)^{1/N} \tag{2-1}$$

where $S_{ageomean}(f)$ is the geometric mean of the spectral acceleration at a number of prescribed frequencies and $S_{ai}(f)$ is the spectral acceleration at the prescribed frequencies.

The scaling of both ground motion ensembles was performed using the "*Weighted Scaling Procedure*". This method, which utilizes information on spectral acceleration at a number of frequencies, is more complex to apply but should, in principle, result in better matching of the target spectra.

The main target of this procedure was that each ensemble of ground motions *J* (*J=1* to *2*) must be scaled only in amplitude by a factor F_J in order to minimize the error between the scaled motion spectrum and the target IEEE - 693 spectrum at a number of prescribed frequencies. The error to minimize was obtained as a weighted average of the errors at the prescribed frequencies as:

$$E_J = \sum_k w_k \left(S_{IEEE}(f_k) - F_J S_{ageomean}(f_k) \right)^2 \tag{2-2}$$

where E_J is the weighted average of the errors at the prescribed frequencies, w_k is the weight factor considered at a number of prescribed frequencies, $S_{IEEE}(f_k)$ is the target IEEE - 693 spectrum at a number of prescribed frequencies, $S_{ageomean}(f)$ is the geometric mean of the spectral acceleration at a number of prescribed frequencies and F_J is the scale factor in amplitude.

In order to find a minimum of the error function in equation (2-2), its derivative with respect to F_J was set equal to zero. Furthermore, to confirm that the obtained solution represented a minimum (and not a maximum), the second derivative was calculated and was found to be positive. This means that the obtained solution represented the minimum error, which was found to be:

$$F_J = \frac{\sum w_k S_{IEEE}(f_k) S_{ageomean}(f_k)}{\sum w_k S^2_{ageomean}(f_k)} \tag{2-3}$$

where F_J is the scale factor in amplitude, w_k is the weight factor considered at a number of prescribed frequencies, $S_{IEEE}(f_k)$ is the target IEEE - 693 spectrum at a number of prescribed frequencies and $S_{ageomean}(f)$ is the geometric mean of the spectral acceleration at a number of prescribed frequencies.

Considering that F_J referred to the geometric mean of the J^{th} ensemble, from equation (2-3), it was straightforward to show that the scale factor for each ground motion separately could be assumed equal to F_J. The scale factor F_J was computed based on the procedure described above equal to *2.20* for ensemble 1 and *1.74* for ensemble 2. The scaling result of both ensembles using both the geometric mean and the median spectra is presented in Figure 2-3 and Figure 2-4 for ensemble 1 and ensemble 2, respectively.

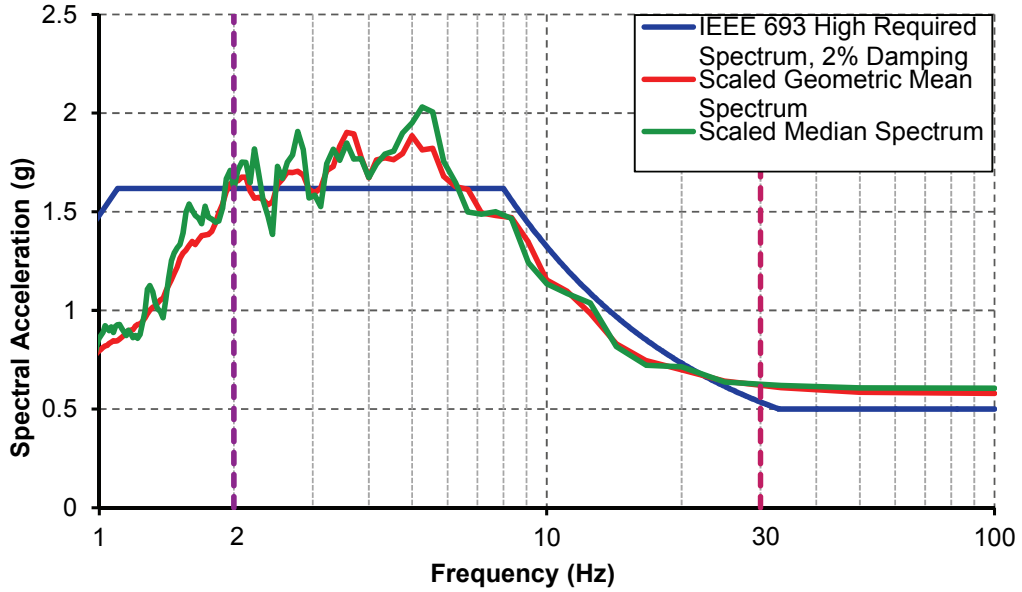

Figure 2-3 Scaling of California Region Ground Motion Ensemble – Ensemble 1 –

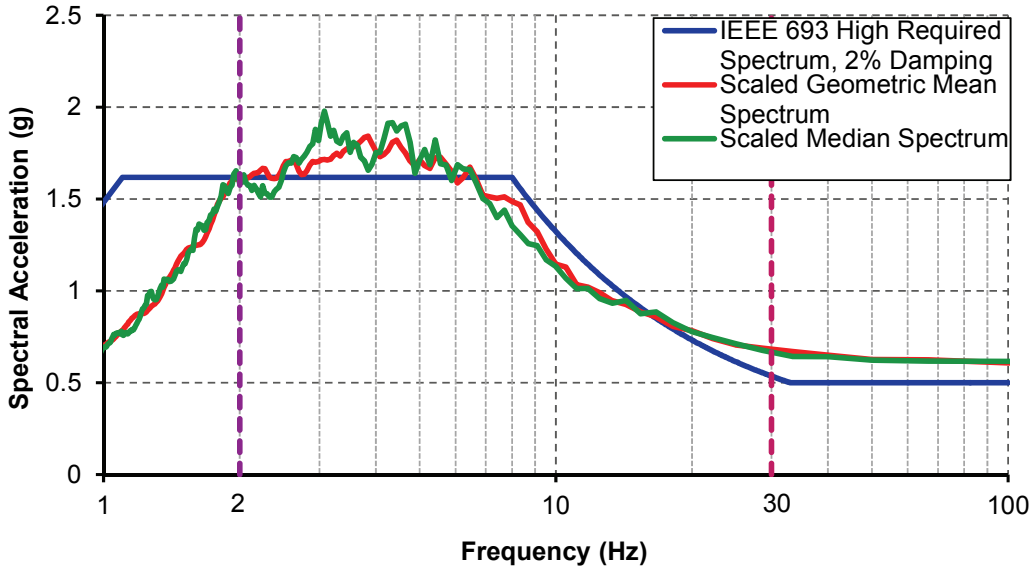

Figure 2-4 Scaling of FEMA P695 Ground Motion Ensemble – Ensemble 2 –

2.4.3. Dynamic Analysis Procedure

For all the transformer-bushings models, linear dynamic time history analyses were performed using both the ground motion ensembles 1 and 2 scaled as described in Section 2.4.2. The models were analyzed in the transverse and the longitudinal direction in all cases. All the analyses performed are summarized in the following table.

Table 2-10 Dynamic Analyses Cases

Direction of motion	Ensemble 1	Ensemble 2 (FEMA P695 -1D)	Ensemble 2 (FEMA P695 - 2D)
Longitudinal	✓	✓	✓
Transverse	✓	✓	

According to Table 2-10, the second ensemble was analyzed as 1D and 2D. The 1D analysis included all the 44 components analyzed in both transverse and longitudinal direction separately, while the 2D analysis included the 22 ground motions combining the two components in the longitudinal and transverse direction, respectively. Two cases were considered for the 2D analysis: "Case 1" applied the component 1 in the longitudinal direction and the component 2 in the transverse, whereas for "Case 2" the directions of the ground motion components were rotated by 90 degrees compared to "Case 1". Note that the effects of vertical ground motions were not considered in this study.

From each analysis, the bending moment at the base of the bushing was obtained in its horizontal axes as a function of time. The maximum bending moment at a given time instant t was calculated as:

$$M^*_{\max}(t) = \max_t \left(\sqrt{M_x^2(t) + M_y^2(t)} \right) \tag{2-4}$$

where $M_x(t)$ and $M_y(t)$ are the moments at the base of the bushing at time t and with respect to the longitudinal and transverse axis of the transformer tank, respectively; while $\max_t$ is the maximum absolute value over the time-history response.

Based on results of all analyses (see Table 2-10), cumulative distribution functions (CDF) associated with the probability of non-exceeding (PoNE) a prescribed maximum moment at the

base of the bushing under the two ensembles of ground motions were calculated. The PoNE was estimated by counting the number of ground motion records causing a prescribed value of the maximum bending moment at the bushing base not to be exceeded and dividing this number by the total number of records considered in the analyses. A lognormal cumulative distribution function was then fitted to the empirical data. The lognormal CDF was defined by the median value (PoNE=50%) of the maximum bending moment and by the dispersion parameter β expressed as the standard deviation of the log of the values of M_{max} .

2.4.4. Dynamic Analysis Results

Linear dynamic time history analyses were conducted for all the analysis cases described in Table 2-10 and the maximum bending moment at the base of the bushing for each of the transformer models was computed according to equation (2-4). Based on the lognormal CDFs shown in the following figures, it can be observed that for all transformer cases, the bushing mounted on the transformer tank is very flexible compared to the bushing mounted on a rigid base. This fact can be easily identified for the maximum moment values of 50% probability of non exceedance that are marked in each lognormal CDF.

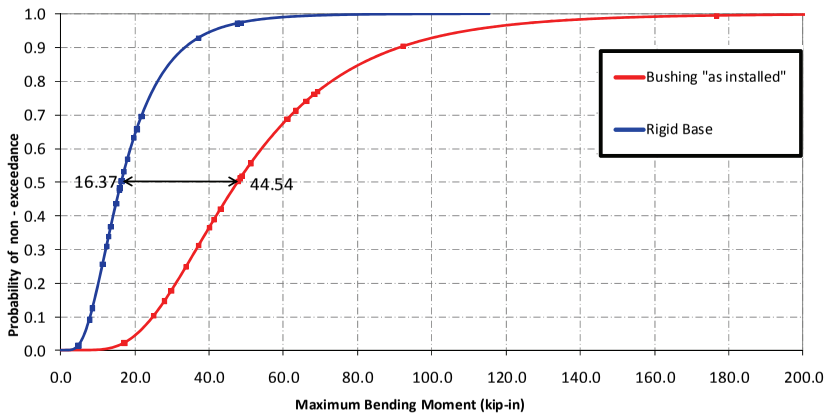

Longitudinal Direction

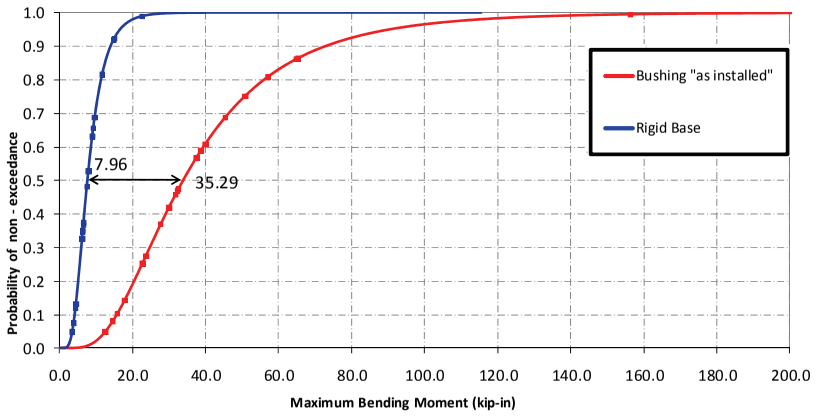

Transverse Direction

Figure 2-5 CDF for Maximum Bending Moments for Westinghouse 525kV Transformer-Bushing Model Ensemble 1

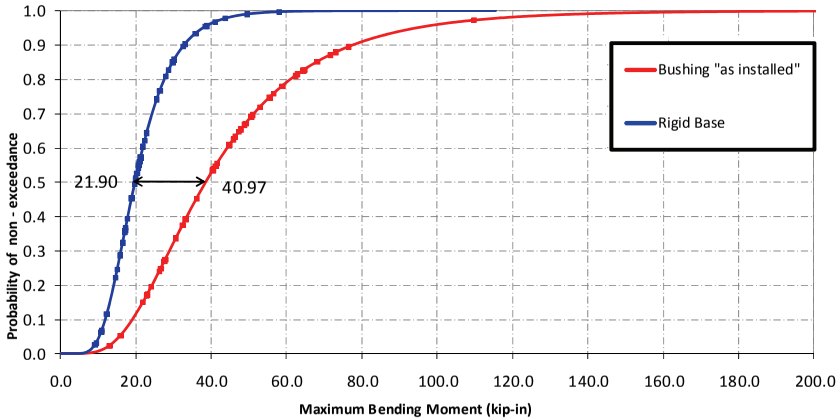

Longitudinal Direction

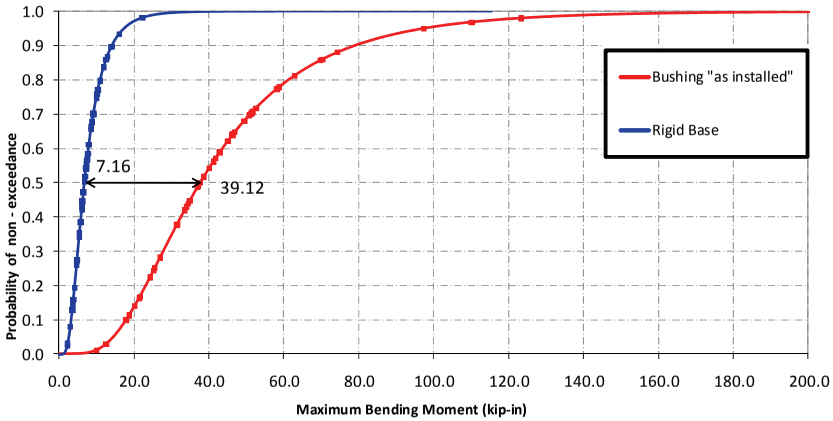

Transverse Direction

Figure 2-6 CDF for Maximum Bending Moments for Westinghouse 525kV Transformer-Bushing Model Ensemble 2 - 1D

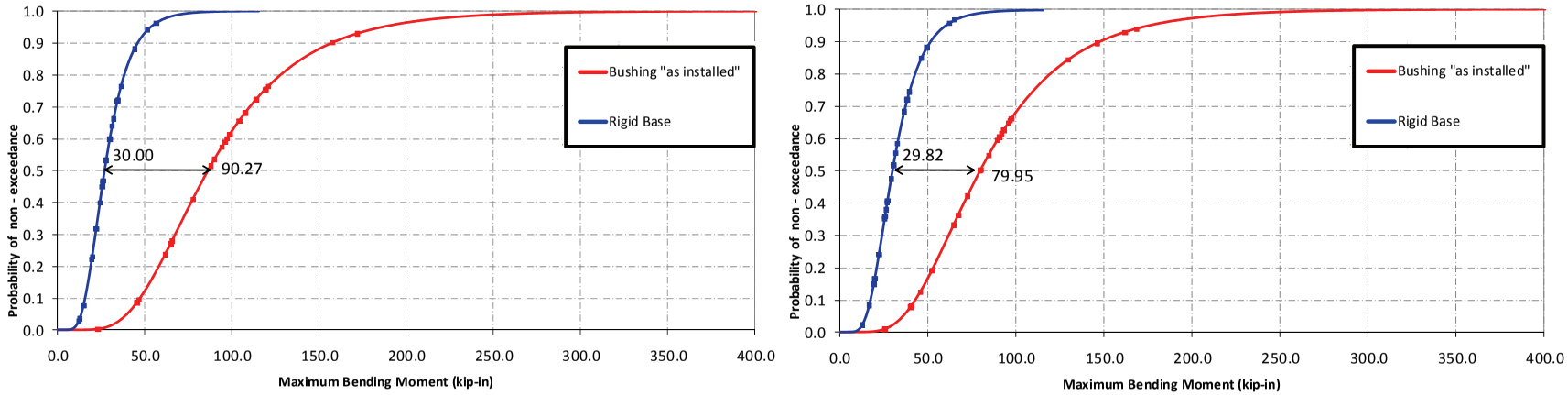

Case 1 Case 2

Figure 2-7 CDF for Maximum Bending Moments for Westinghouse 525kV Transformer-Bushing Model Ensemble 2 – 2D

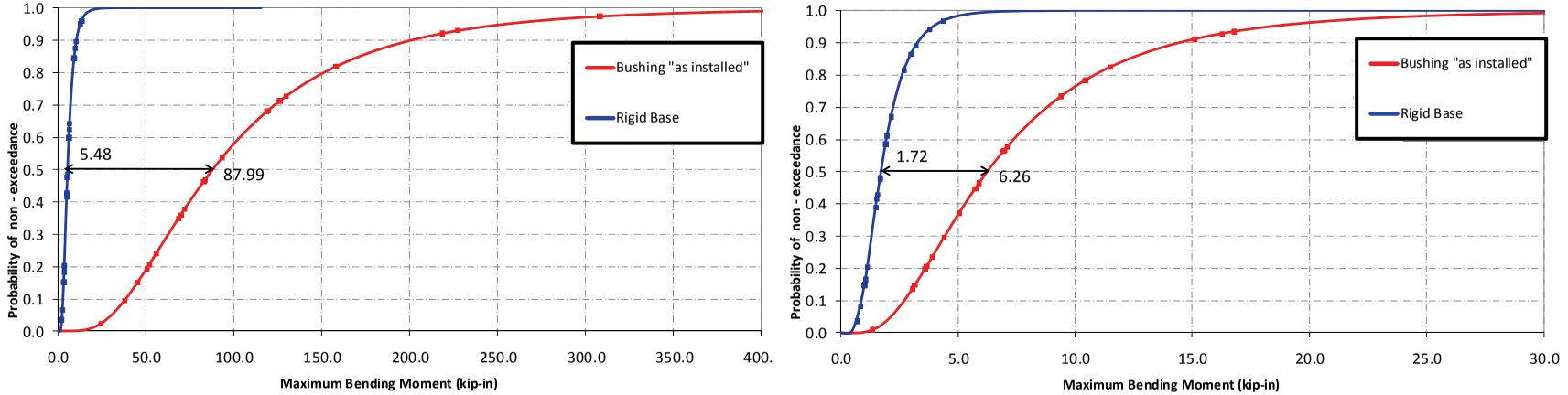

Longitudinal Direction Transverse Direction

Figure 2-8 CDF for Maximum Bending Moments for Siemens 230kV Transformer-Bushing Model Ensemble 1

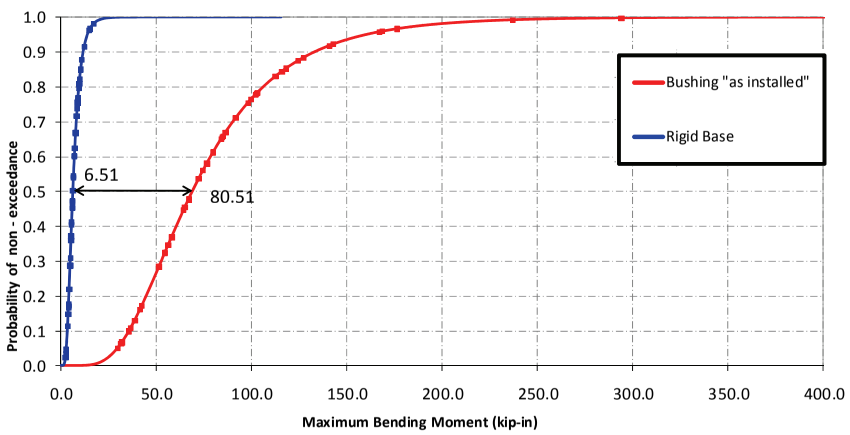

Longitudinal Direction

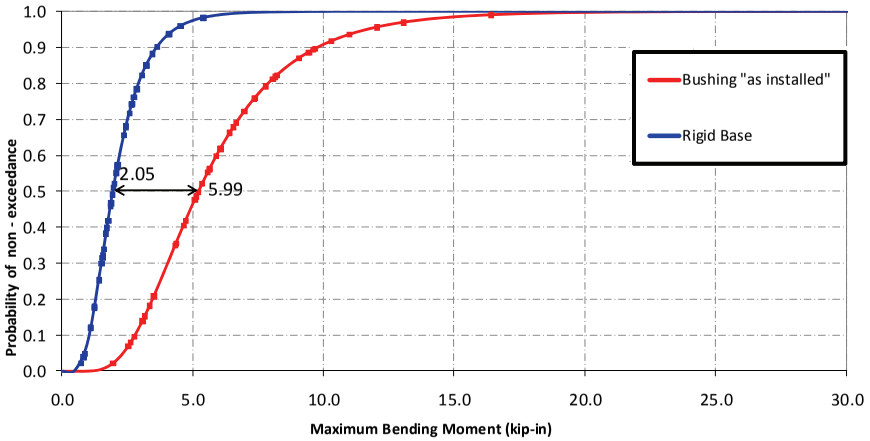

Transverse Direction

Figure 2-9 CDF for Maximum Bending Moments for Siemens 230kV Transformer-Bushing Model Ensemble 2 – 1D

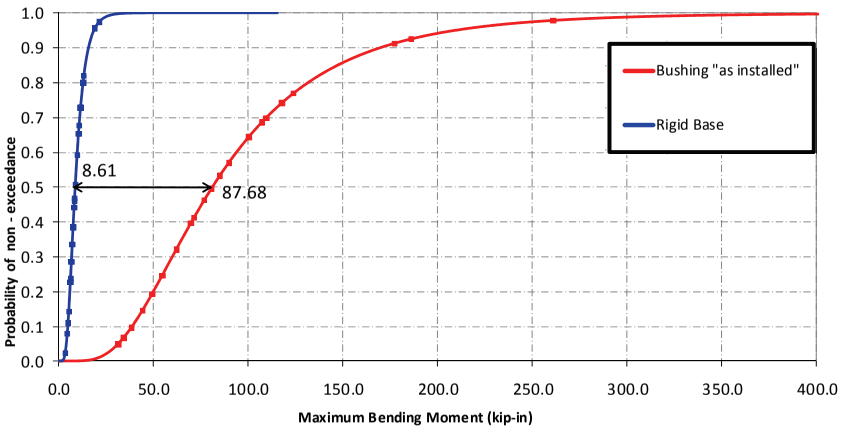

Case 1

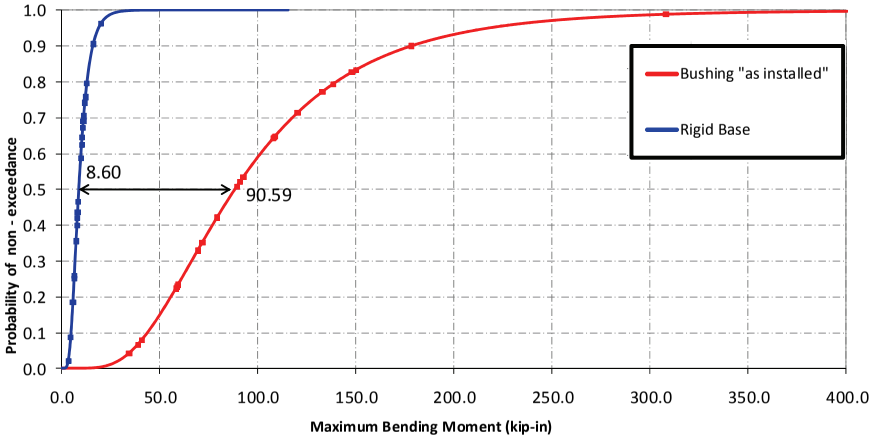

Case 2

Figure 2-10 CDF for Maximum Bending Moments for Siemens 230kV Transformer-Bushing Model Ensemble 2 – 2D

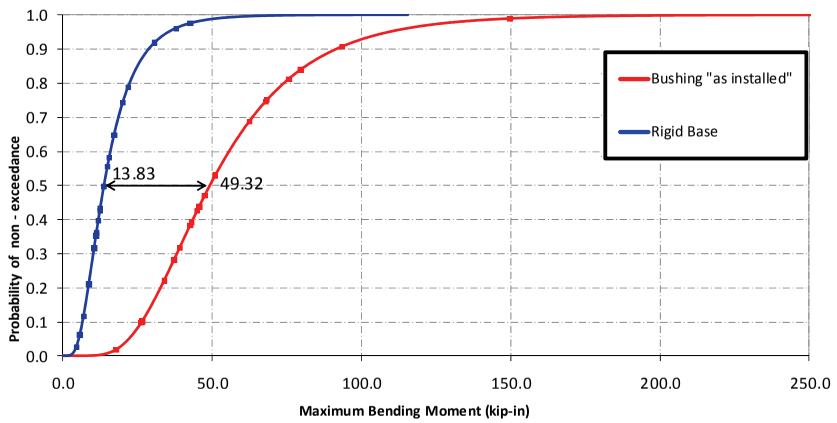

Longitudinal Direction

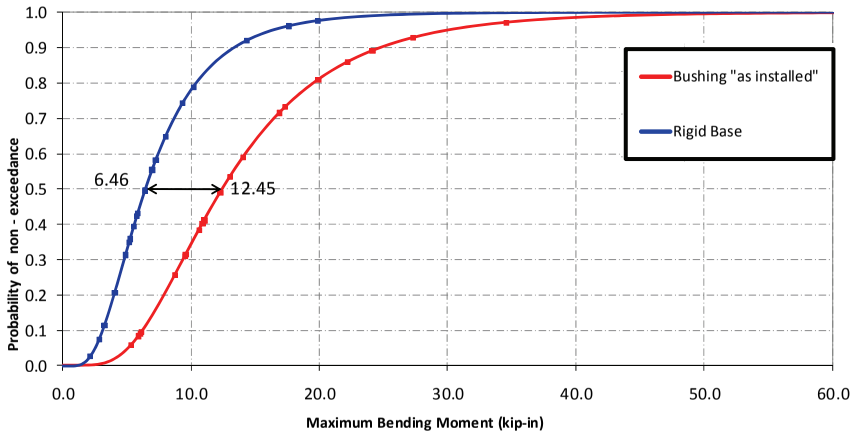

Transverse Direction

Figure 2-11 CDF for Maximum Bending Moments for Siemens 500kV Transformer-Bushing Model Ensemble 1

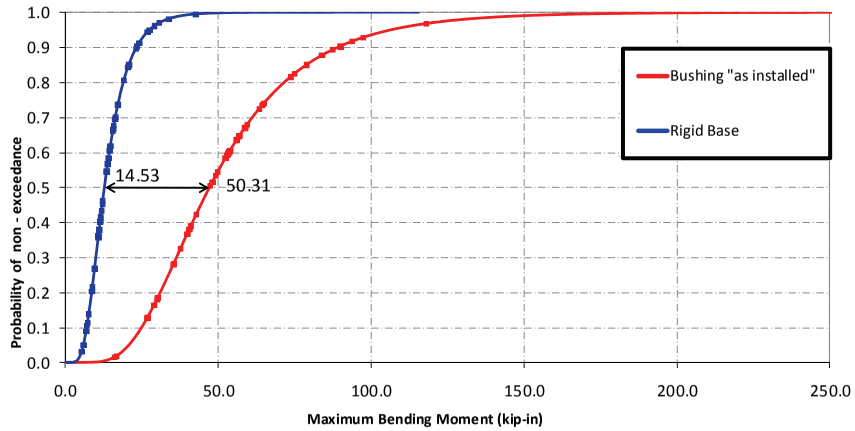

Longitudinal Direction

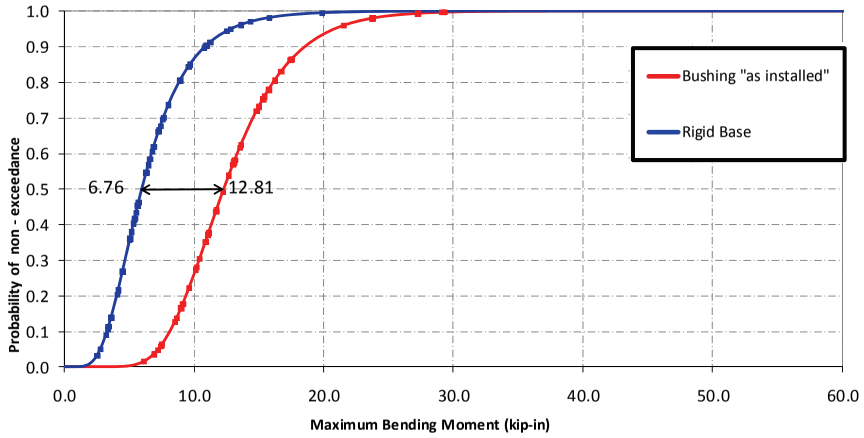

Transverse Direction

Figure 2-12 CDF for Maximum Bending Moments for Siemens 500kV Transformer-Bushing Model Ensemble 2 – 1D

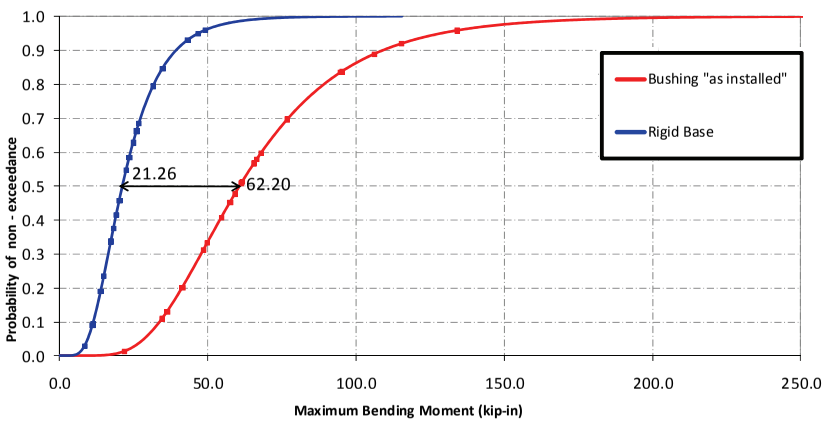

Case 1

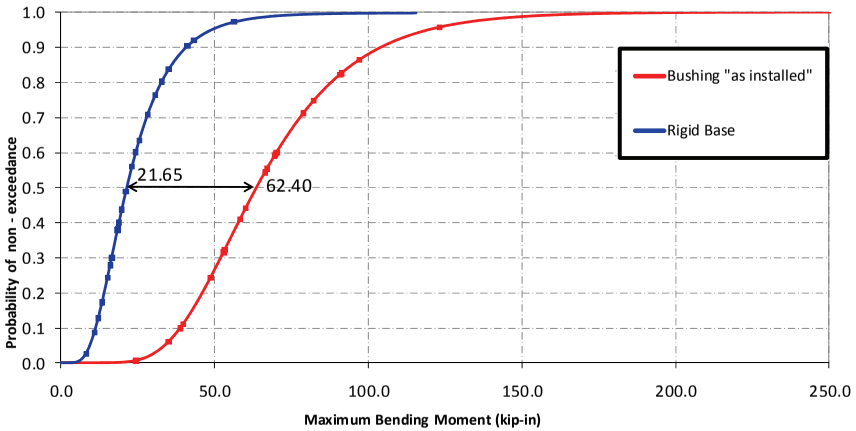

Case 2

Figure 2-13 CDF for Maximum Bending Moments for Siemens 500kV Transformer-Bushing Model Ensemble 2 – 2D

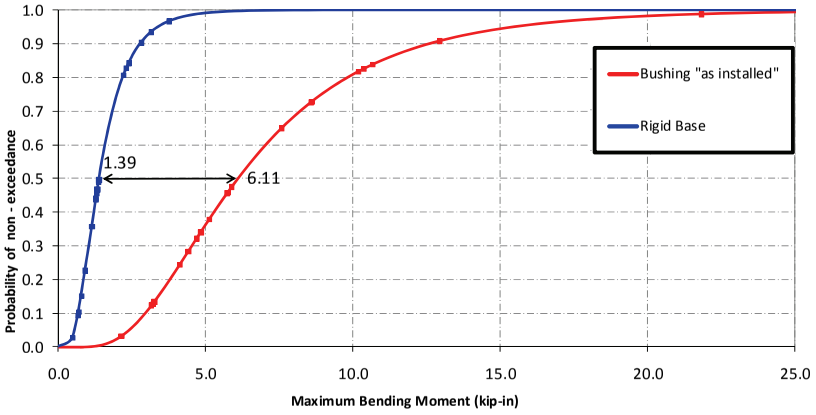

Longitudinal Direction

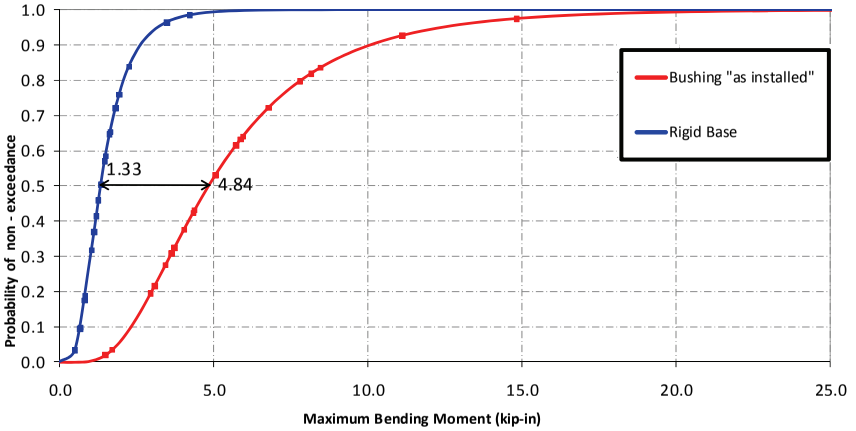

Transverse Direction

Figure 2-14 CDF for Maximum Bending Moments for Ferranti Packard 230kV Transformer-Bushing Model Ensemble 1

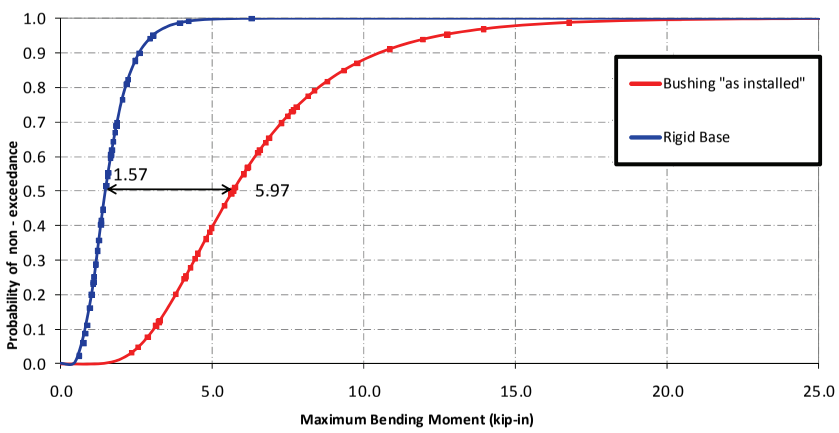

Longitudinal Direction

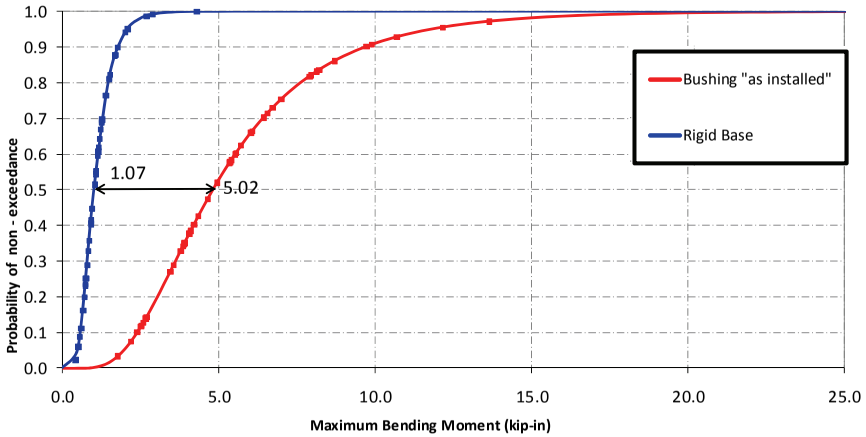

Transverse Direction

Figure 2-15 CDF for Maximum Bending Moments for Ferranti Packard 230kV Transformer-Bushing Model Ensemble 2 – 1D

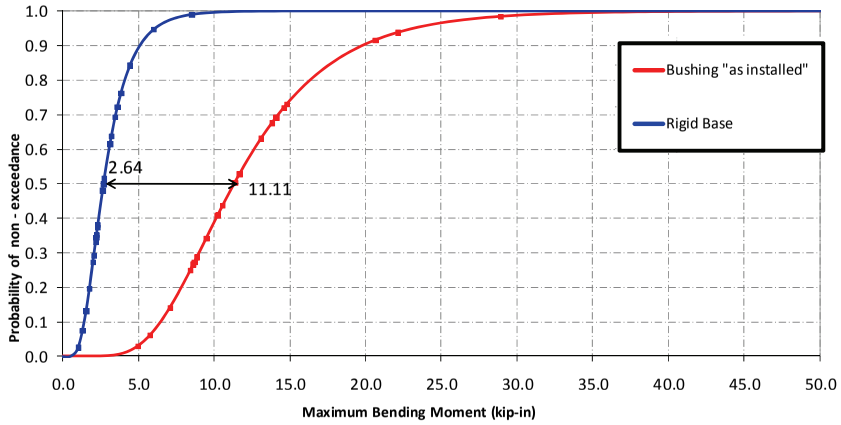

Case 1

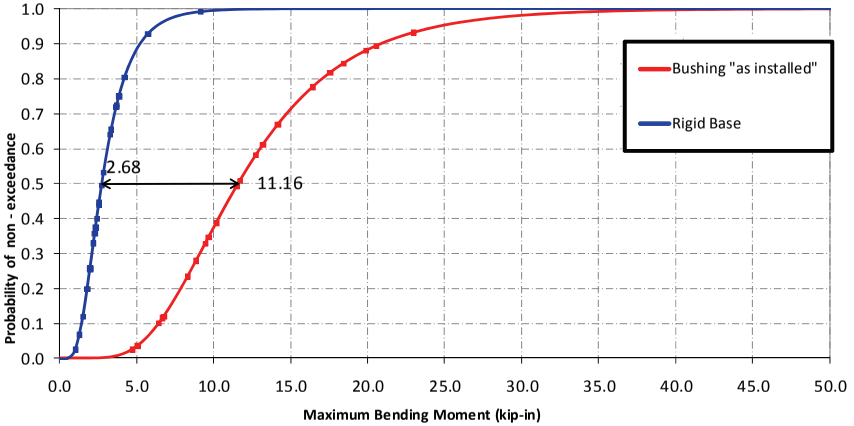

Case 2

Figure 2-16 CDF for Maximum Bending Moments for Ferranti Packard 230kV Transformer-Bushing Model Ensemble 2 – 2D

A *Moment Amplification Factor* (MAF) defined as the ratio of the maximum bending moment at the base of the bushing mounted on the cover plate of the transformer ("as installed" conditions) to the maximum bending moment obtained for the same bushing mounted on a rigid base (see equation (2-5)) was computed for all analysis cases and compared to the amplification factor of two defined by the IEEE-693 Standard.

$$Moment\ Amplification\ Factor = \frac{Moment\ when\ Bushing\ as\ Installed}{Moment\ when\ Bushing\ Mounted\ on\ Rigid\ Base} \tag{2-5}$$

Figure 2-17 to Figure 2-19 present the MAF in the form of empirical and log normal CDFs, while the median values of the MAF-CDFs are compared in Figure 2-20 to Figure 2-22 with the frequency-independent amplification factor of 2 recommended by the IEEE-693 Standard showing that the recommended amplification factor is non-conservative for all the transformer bushing systems. Although not much higher than the proposed amplification factor, the value of that factor computed for all the transformer models appeared to be around three apart from the Siemens 230kV transformer model. The Siemens 230kV model appeared to be the most flexible transformer (especially in the longitudinal direction) since the peak bending moment at the base of the "as installed" bushing was more than 10 times larger than if it was rigidly mounted.

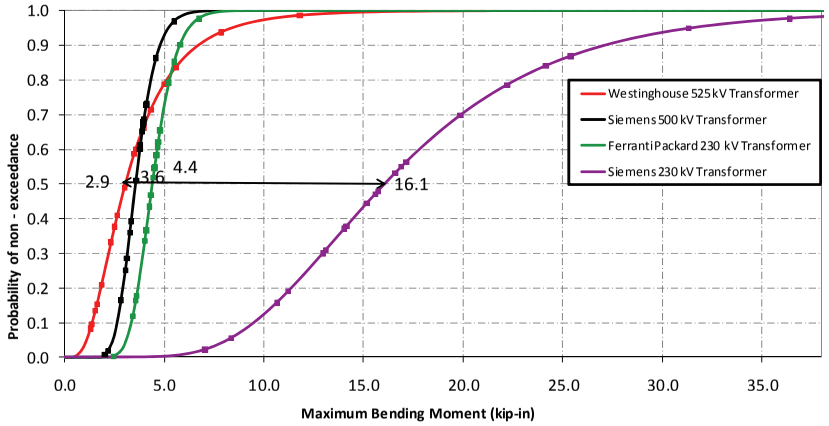

Longitudinal Direction

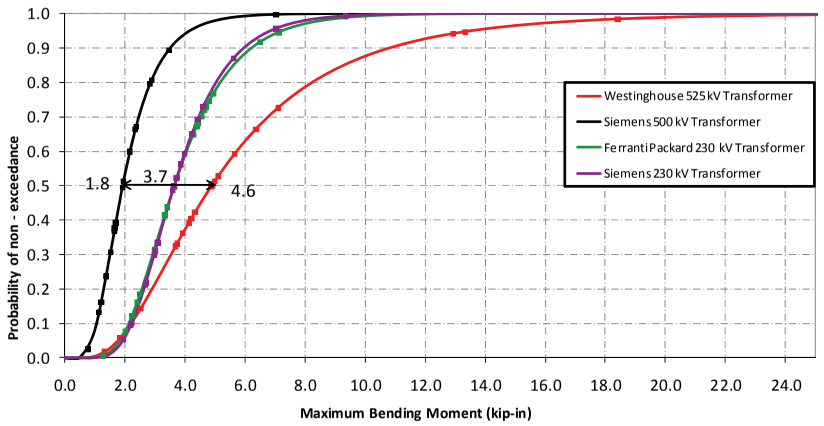

Transverse Direction

Figure 2-17 CDF for Moment Amplification Factors for Ensemble 1

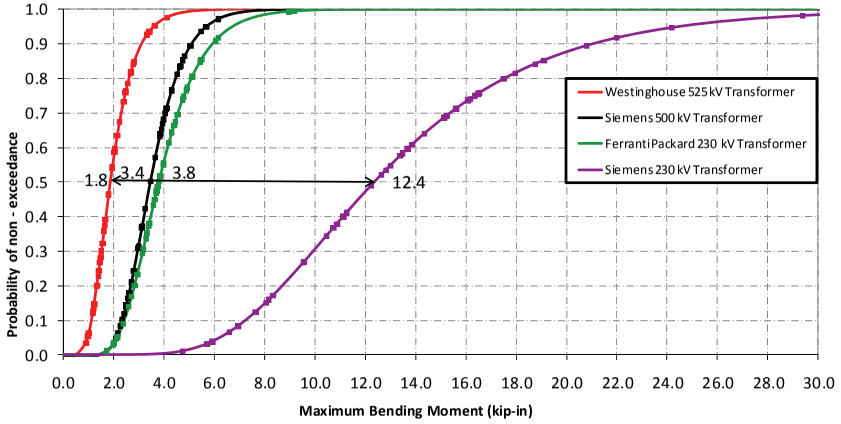

Longitudinal Direction

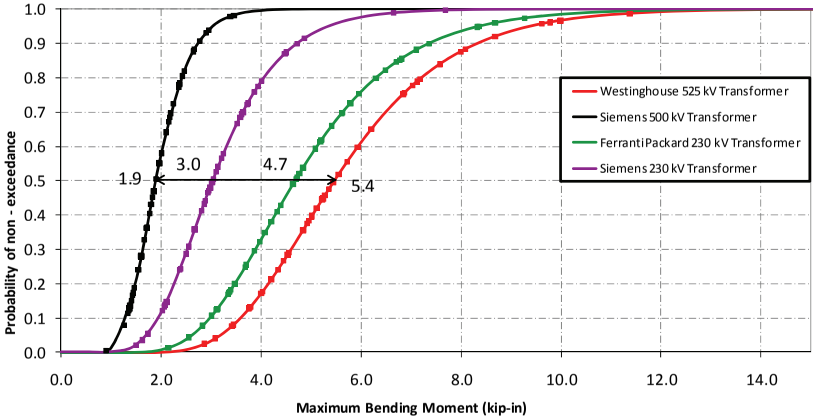

Transverse Direction

Figure 2-18 CDF for Moment Amplification Factors for Ensemble 2 – 1D

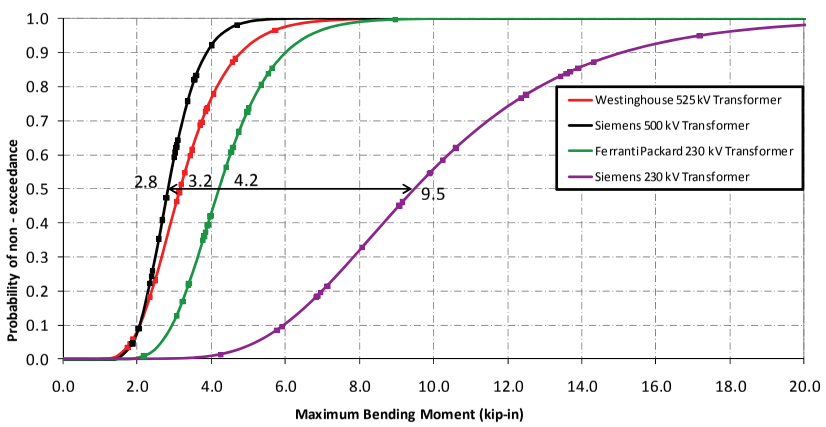

Longitudinal Direction

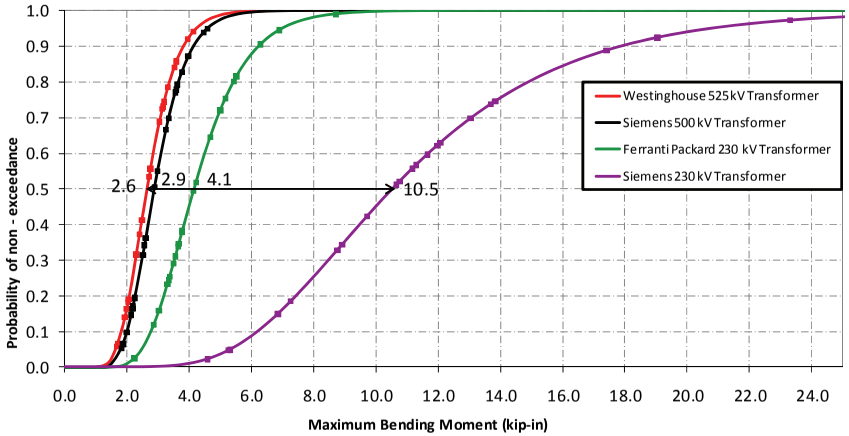

Transverse Direction

Figure 2-19 CDF for Moment Amplification Factors for Ensemble 2 - 2D

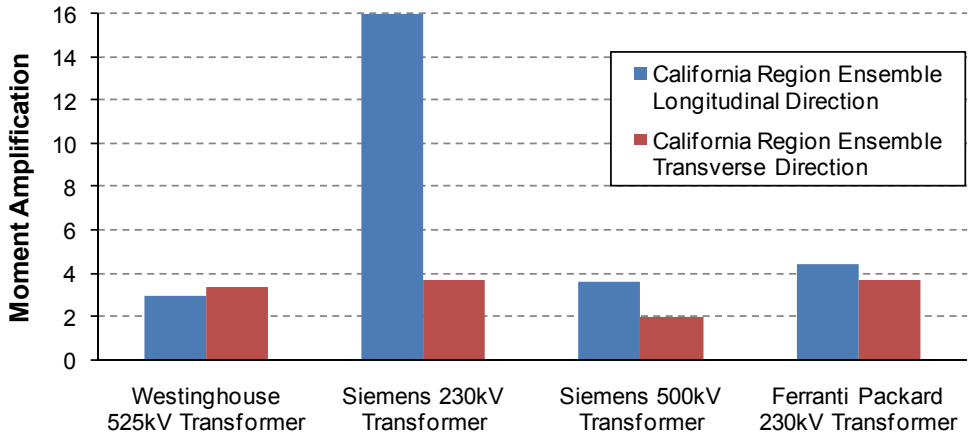

Figure 2-20 Median Values of Moment Amplification Factor for all Four Transformer-Bushing Models for Ensemble 1

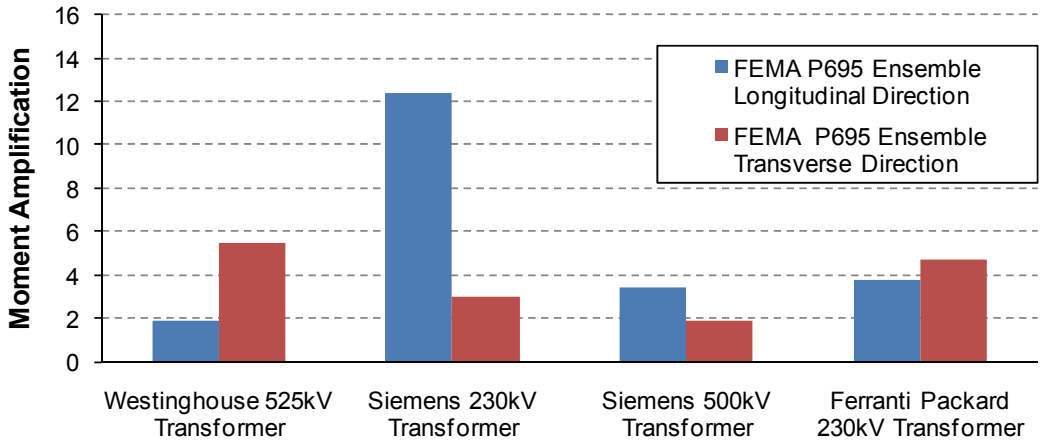

Figure 2-21 Median Values of Moment Amplification Factor for all Four Transformer-Bushing Models for Ensemble 2 – 1D

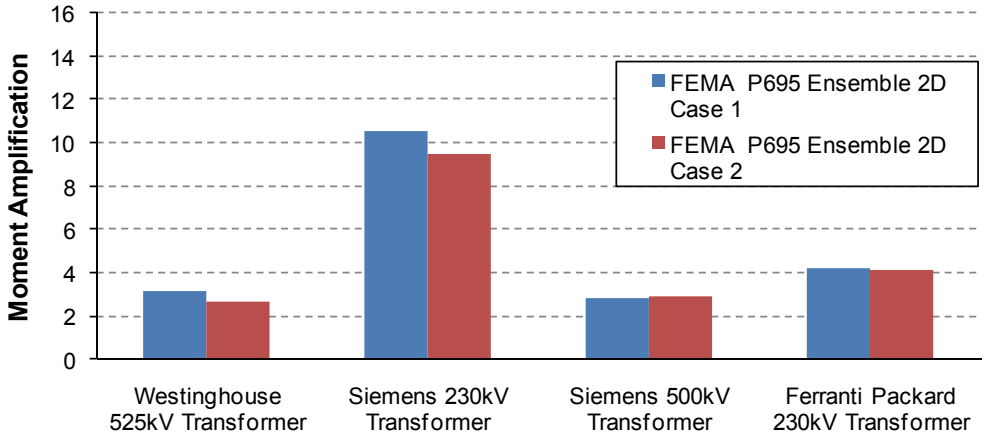

Figure 2-22 Median Values of Moment Amplification Factor for all Four Transformer-Bushing Models for Ensemble 2 – 2D

2.5. Summary and Conclusions

In this section, a preliminary investigation of the seismic response of the bushings mounted on a rigid base and "as installed" on transformer tanks, was conducted by performing modal and linear time history analyses. According to the results, it was observed that the bushing "as installed" is more vulnerable to seismic loading than similar bushings mounted on a rigid base. It is clear that bushings on transformer tanks have to be stiffer in such a way that their response moves closer to the response of the rigid base analysis and therefore the system becomes adequately resistant against intense ground shaking. In order to achieve results close to the ones of the rigid base analysis, various stiffening approaches were investigated and presented in the following section.

SECTION 3

NUMERICAL STUDY OF STIFFENED HIGH VOLTAGE TRANSFORMER-BUSHING SYSTEMS

3.1. Introduction

The objective of this section is to identify feasible approaches to stiffen the base of transformer-bushing systems in order to drive their response as close as possible to the rigid base case associated with much smaller bending moments. For this purpose, several geometrical configurations of stiffeners were implemented on the transformer models and investigated in order to identify those which were the most practical and efficient in reducing the bending moment demand at the base of the bushings.

3.2. Description of Stiffening Techniques Considered

With the aim of reducing the bending moments at the base of transformer bushings, several stiffening approaches were investigated. More specifically, different configurations of axial stiffeners installed in several locations between the bushings and the transformer tank were considered as well as flexural stiffeners incorporated on the tank cover plate.

- **Axial Stiffeners in Transverse and Longitudinal Direction**

As a first stiffening approach, axial stiffeners were added both in the transverse and the longitudinal direction of all models. An example of this approach is shown in Figure 3-1 for the Siemens 230kV transformer-bushing model. These axial stiffeners were installed either between the tank surface and the bushing or between the tank surface and the turret of the bushing depending on the geometry of the models, so that the displacements of the bushing would be decreased. Several configurations of these stiffeners were investigated. More specifically, the effect of stiffening in each direction independently was investigated for several combinations of angles of the axial stiffeners with respect to the horizontal plane and of stiffness values. Three different values for the inclination angle with respect to the horizontal were used (30^o, 45^o and 60^o). It was observed that there was a threshold value in the axial stiffness of the stiffeners which

after it was exceeded; no further increase of the fundamental frequency of the bushing could be achieved. These stiffness threshold values were computed for all models and inclination angles (by conducting modal analysis). The final configuration for each model consisted of the optimum configuration (angle and stiffness yielding the highest natural frequency) determined for each direction independently. It must be mentioned that for the Ferranti Packard 230kV transformer model, due to the geometry of the model, only axial stiffeners with an inclination angle of 45^{o} were considered.

The addition of axial stiffeners in both directions resulted in an increase of the natural frequencies of all systems in comparison to the natural frequencies obtained from the "as installed" conditions. However, the increase was not large enough to reach the frequencies achieved for the rigid base case as shown in the figures presented in Appendix C. The final values of the angle and stiffness used for the analyses are presented in Table 3-1.

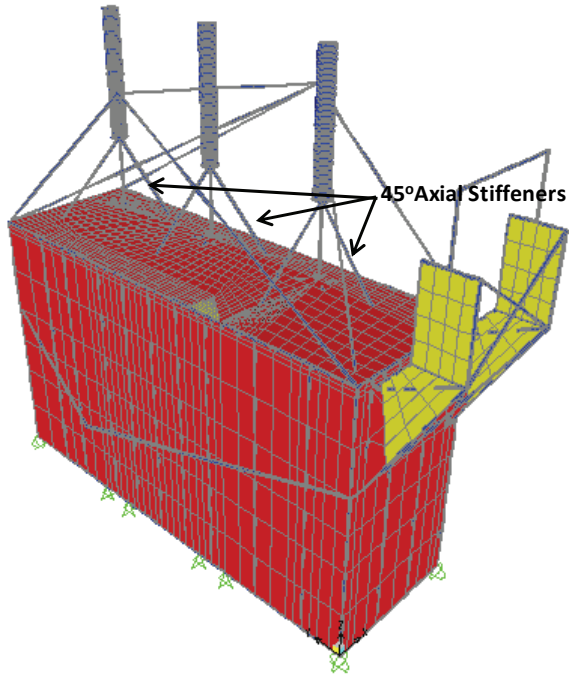

Figure 3-1 Siemens 230kV Transformer-Bushing Model with Axial Stiffeners in Both Directions

Table 3-1 Properties of Axial Stiffeners Installed in Both Directions

Transformer Model	Inclination Angle	Threshold Stiffness (kip/in)
Westinghouse 525kV	45^o	5.0
Siemens 230kV	45^o	10.0
Siemens 500kV	45^o	5.0
Ferranti Packard 230kV	45^o	5.0

- **Axial Stiffeners Connected to the Tank Wall**

The second stiffening approach considered included the installation of two axial stiffeners between the bushing and the wall of each transformer model at an angle of 45^o, in order to decrease the displacements of the bushing compared to the first approach described above. In this case, the change of the natural frequency of each model for different stiffness values was also identified in order to determine the most efficient configuration of this approach and for each finite element model. An example of this stiffening approach is shown in Figure 3-2 for the Siemens 230kV transformer-bushing model. Similarly to the previous stiffening approach (axial stiffeners in both directions), a threshold value of stiffness was determined for the present approach as well. The change of the frequency with respect to the stiffness is presented in Appendix C for all transformer models, while the stiffness values used for dynamic analyses are presented in Table 3-2.

Table 3-2 Properties of Axial Stiffeners connected to the Tank Wall

Transformer Model	Threshold Stiffness (kip/in)
Westinghouse 525kV	1.0
Siemens 230kV	1.0
Siemens 500 V	5.0
Ferranti Packard 230kV	1.0

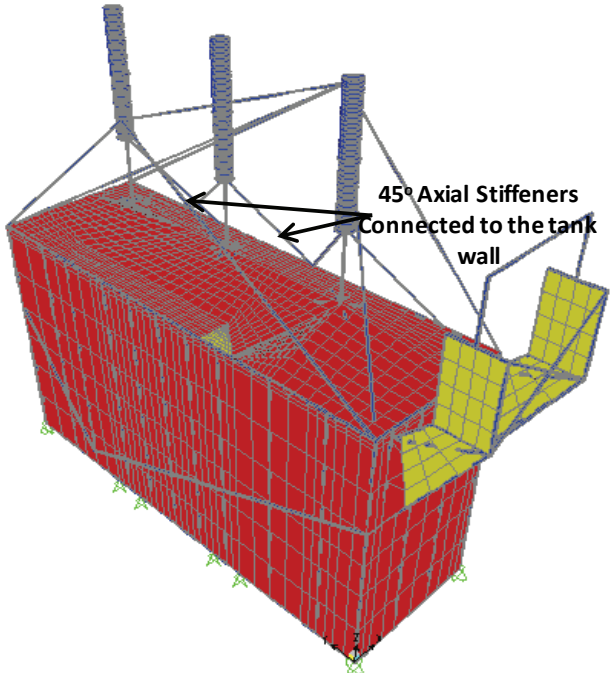

Figure 3-2 Siemens 230kV Transformer-Bushing Model with Axial Stiffeners connected to the Tank Wall

- **Flexural Stiffeners Incorporated on the Top Plate of the Transformer Tank**

This stiffening approach was initially investigated only for the Ferranti Packard 230kV transformer model, which already consisted of three stiffeners in the transverse direction (steel angles L6 x 4 x ½).

The first attempt to stiffen the transformer bushing system, by incorporating flexural stiffeners on the tank top plate, was to increase the stiffness of the existing stiffeners by multiplying it (multiplying the section moment of area I) with a factor varying from 1.5 to 10. According to the results of this investigation, the efficiency of stiffening the base of the bushing by incorporating flexural stiffeners appeared to reach a constant value for factors equal to or greater than 2 (threshold value) as presented in Appendix C.

Furthermore, in order to ensure a better system behavior, this approach was extended in the longitudinal direction as well. Similar flexural stiffeners as those used in the transverse direction, were installed in the longitudinal direction, and analyses were conducted by multiplying their stiffness by a factor varying from 1.5 to 10. Similarly to the transverse direction, the fundamental

frequency of the bushing reached a constant value for factors equal to 2 (threshold value) or greater as presented in Appendix C.

The final proposed configuration consisted of introducing/replacing flexural stiffeners installed in both longitudinal and transverse direction of the cover top plate of the transformer tank. The stiffeners were placed as close as possible to the base of the bushing without interfering with other components of the transformer (see Figure 3-3). For each model, the moment of inertia of the stiffeners was selected to reach or exceed a threshold value required to achieve the maximum possible increase in the bushing fundamental frequencies. This maximum fundamental frequency of a bushing occurred when its base was made locally rigid and was governed by the global flexural flexibility of the tank cover plate and walls.

Note that this stiffening approach is feasible and stiffeners have already been utilized and attached at the top of the transformer tank. Characteristic illustrative examples are the transformer tanks of Figure 3-4 and Figure 3-5.

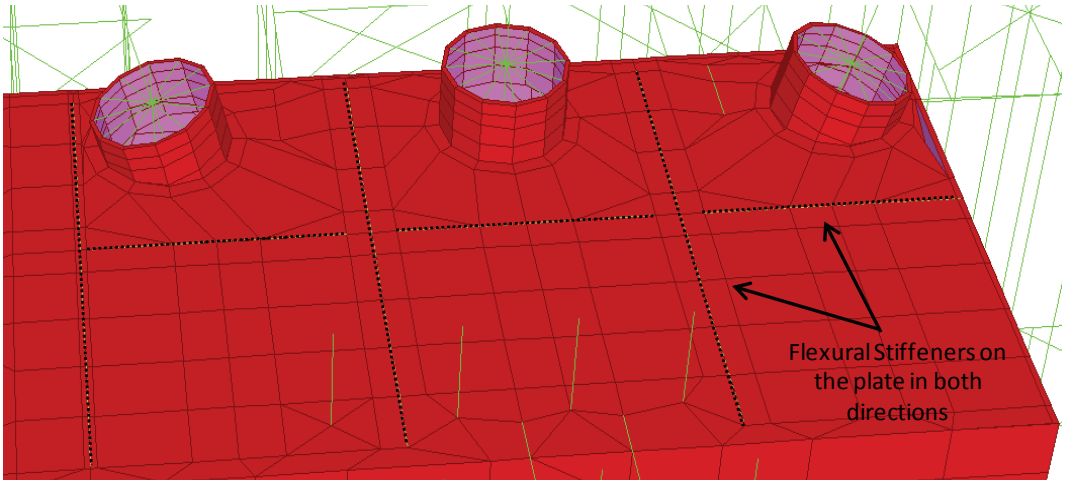

Figure 3-3 Ferranti Packard 230kV Transformer Incorporating Flexural Stiffeners on the Tank Top Plate

Figure 3-4 Underside of 230kV Transformer Cover showing Stiffening Members (courtesy of Schiff, 2011)

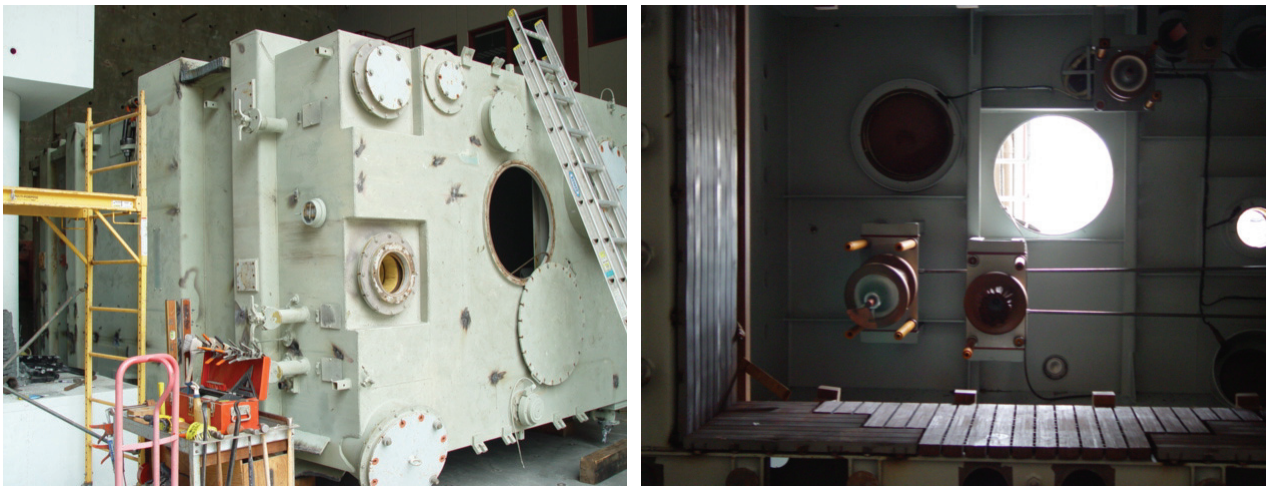

Figure 3-5 525kV Transformer Tank Incorporating Stiffening Elements Composed of Thin Plates and Channels (Matt & Filiatrault, 2004)

3.3. Dynamic Analysis Procedure

Linear dynamic time history analyses were conducted for all the bushings models using both the ground motion ensembles 1 and 2 described in Section 2. From each analysis, the maximum moment at the base of the bushing was calculated in its horizontal axes according to equation (2-4). Taking into consideration the results of all analyses, lognormal cumulative distribution functions were generated for the probability of non-exceeding (PoNE) a prescribed maximum moment at the base of the bushing. Moreover, in order to evaluate and quantify the performance

of the systems incorporating flexural stiffeners on the tank top plate, an *Efficiency Factor*, *E*, was defined for the median values (PoNE = 50%) of maximum bending moments at the base of the bushings as shown in equation (3-1):

$$E = \left(\frac{M_{STIFFENED} - M_{INSTALLED}}{M_{RIGID} - M_{INSTALLED}} \right) * 100\% \qquad (3\text{-}1)$$

where $M_{STIFFENED}$ is the median maximum moment at the base of the bushing for the stiffened case, $M_{INSTALLED}$ is the median maximum moment at the base of the bushing "as installed" and M_{RIGID} is the median maximum moment at the base of the bushing when the bushing is mounted on a rigid base.

According to the definition of equation (3-1), a value of $E = 0\%$ indicates that the evaluated stiffening technique does not improve the response of the bushing system at all. On the contrary, a value of $E = 100\%$ indicates that the stiffened transformer-bushing system achieves the same seismic response as of the bushing mounted on a rigid base. This *Efficiency Factor* was computed for all stiffening techniques implemented in the four transformer-bushing models investigated.

3.4. Analysis Results

According to the CDFs, shown in Figure 3-6 to Figure 3-17, the response (in terms of moment at the base of the bushing) of the stiffening approach with axial stiffeners in both directions is in between the response obtained from the rigid base case and the response of the bushing "as installed". For the case of introducing axial stiffeners connected from the bushing to the wall of the tank, the response of each model is between the response obtained from the rigid base case and the response of the first stiffening approach considered. Furthermore, the response of the stiffening approach incorporating flexural stiffeners on the top plate of the transformer tank appeared to be the closest possible to the rigid base response.

The *Efficiency Factor* was computed for all analysis cases based on the median values of the maximum moments at the base of the bushing obtained from the fragility curves shown in Figure

3-6 to Figure 3-17. The median moment values are presented in Appendix B, while the figures below indicate the *Efficiency Factor* of each analysis and for each transformer model separately.

For the Westinghouse 525kV transformer, higher values of the efficiency factor were obtained using axial stiffeners connected to the wall compared to the efficiency factor obtained by adding axial stiffeners in both directions. In fact, the *Efficient Factor* for axial stiffeners connected to the wall reached an average value of 90% (see Figure 3-18) indicating the high efficiency of this approach for the stiffening of this transformer model.

Similarly to the Westinghouse 525kV transformer, for the Siemens 230kV transformer and Siemens 500kV transformer, higher values of the efficiency factor were obtained using axial stiffeners connected to the wall compared to the efficiency factor obtained by adding stiffeners in both directions. Note that for both transformer models, the efficiency factor obtained in the transverse direction was smaller than that in the longitudinal direction. However, considering the total response, it seems that using stiffeners connected to the wall is an efficient stiffening approach, since the average value of the efficiency factor was over 70% (see Figure 3-19 and Figure 3-20).

As for the Ferranti Packard 230kV transformer, it seems that both stiffening approaches (either adding stiffeners in both directions or installing stiffeners connected to the wall) were not as efficient as for the rest of the transformer models. In fact, the computed average efficiency was between 40% - 50%, which does not seem to be a satisfactory performance. However, adding stiffeners on the cover plate appeared to be the most efficient stiffening technique for this transformer, since in this case the efficiency factor reached an average value of 80% as shown in Figure 3-21.

The amplification factor of the maximum bending moment at the base of the bushing for the stiffened mounting conditions was computed according to equation (2-5) for all analysis cases and compared with the amplification factor obtained from the transformer tank case (bushing as installed).

Lognormal cumulative distribution functions generated for the moment amplification factor are presented below (Figure 3-22 to Figure 3-33). According to these curves, the moment

amplification factor decreased by using the proposed stiffening techniques, while their median values were less than the amplification factor of two recommended in the IEEE-693 Standard.

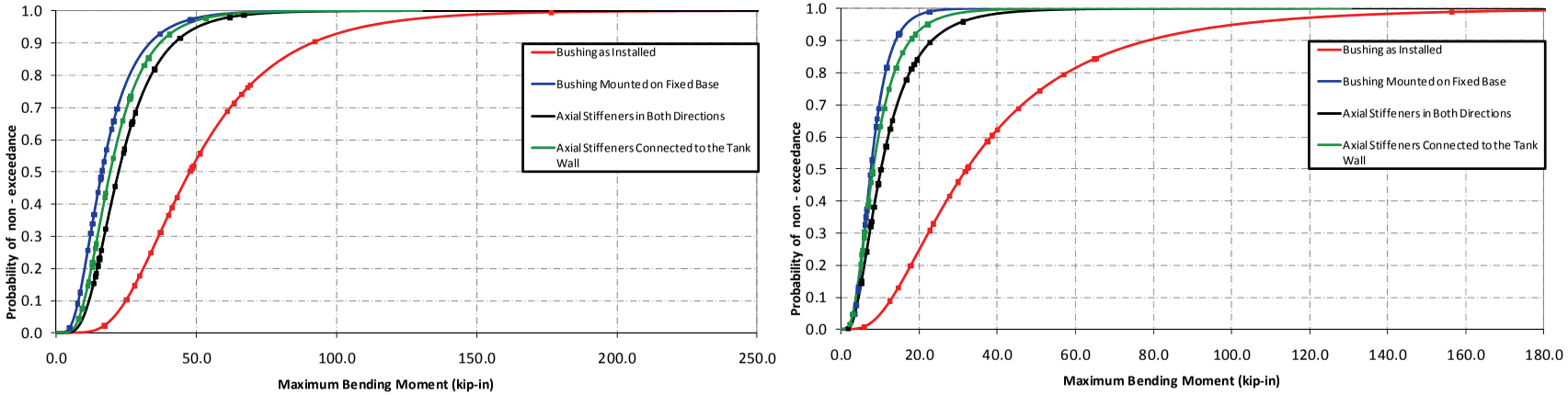

Figure 3-6 CDF for Maximum Bending Moments for Westinghouse 525kV Transformer-Bushing Model Ensemble 1

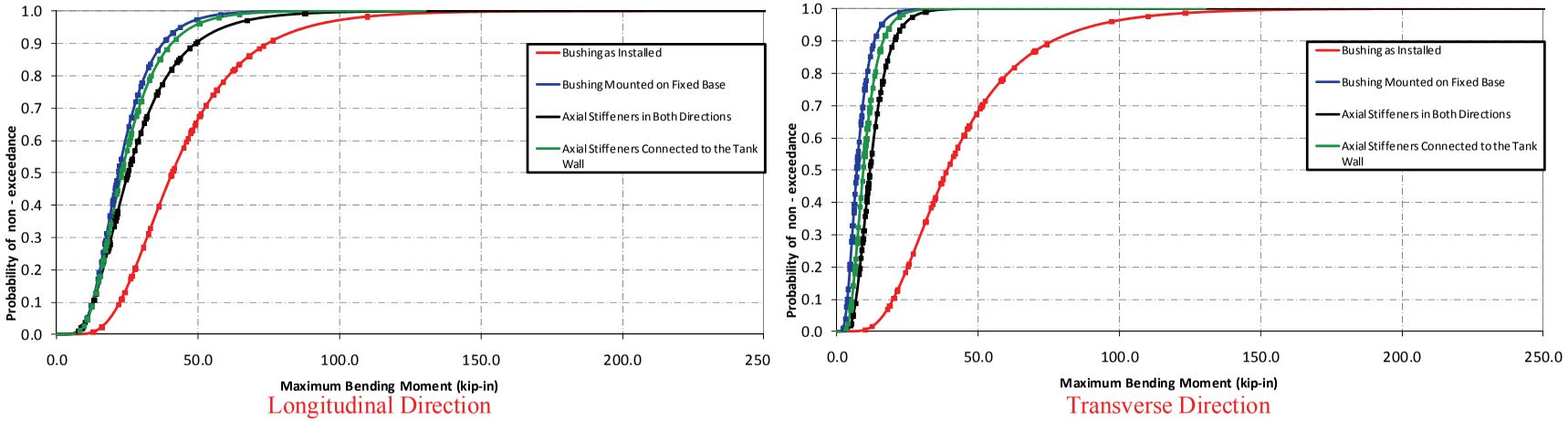

Figure 3-7 CDF for Maximum Bending Moments for Westinghouse 525kV Transformer-Bushing Model Ensemble 2– 1D

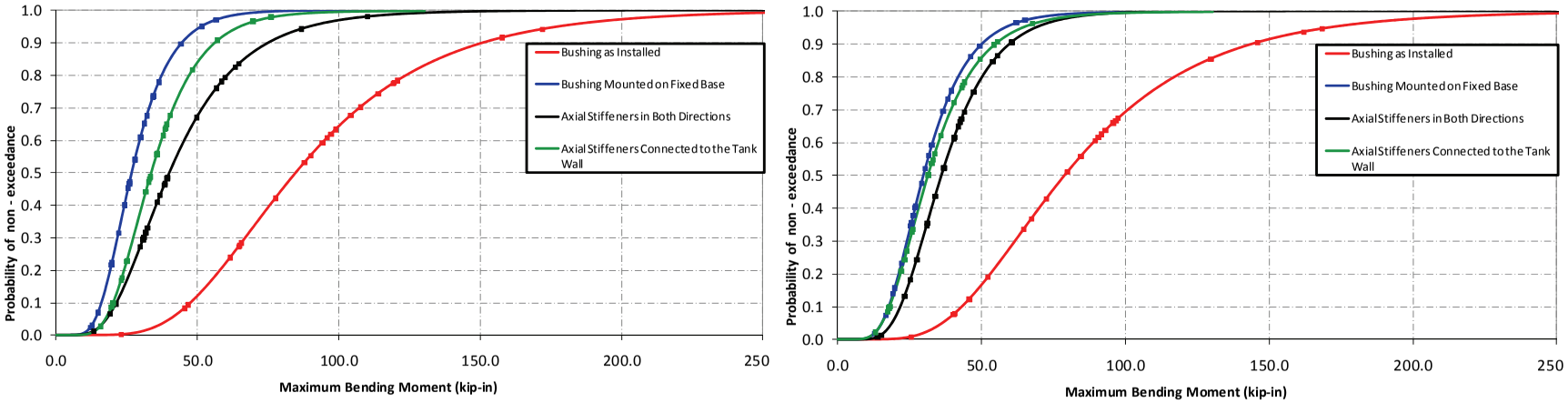

Figure 3-8 CDF for Maximum Bending Moments for Westinghouse 525kV Transformer-Bushing Model Ensemble 2– 2D

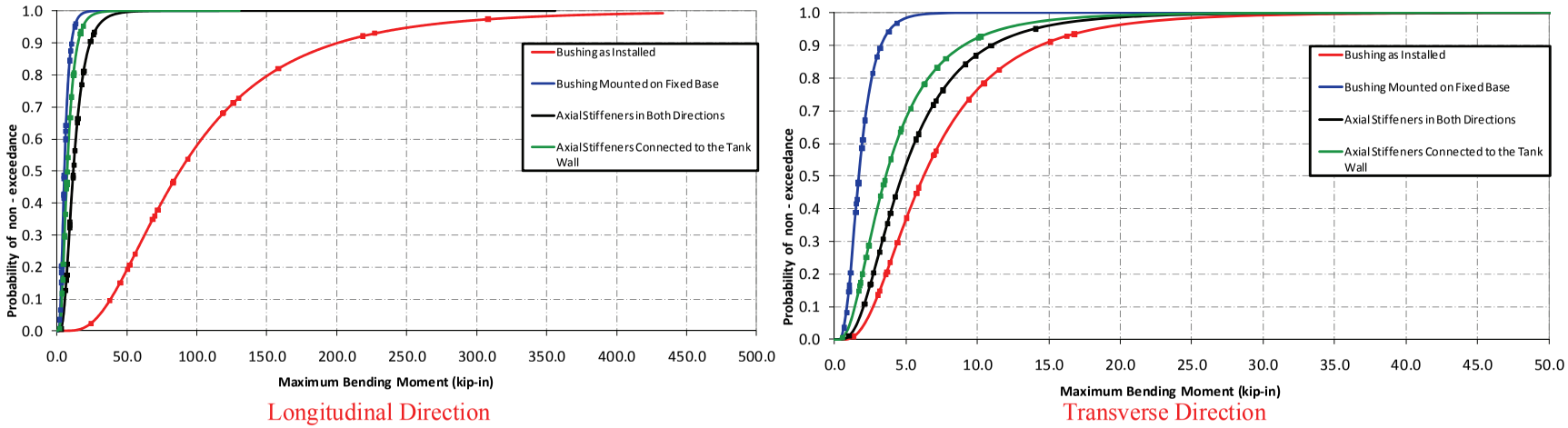

Figure 3-9 CDF for Maximum Bending Moments for Siemens 230kV Transformer-Bushing Model Ensemble 1

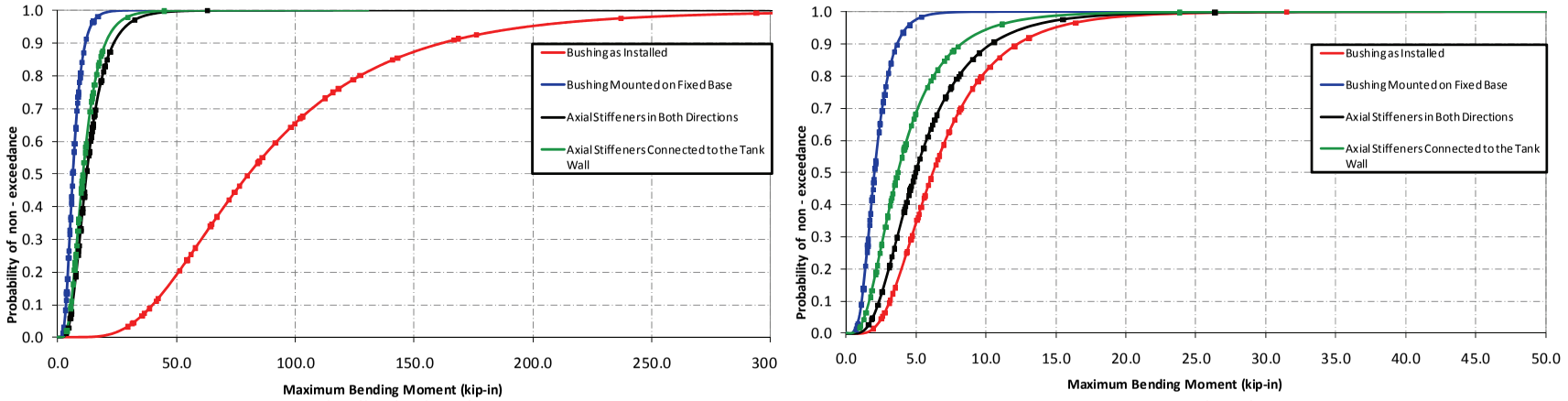

Figure 3-10 CDF for Maximum Bending Moments for Siemens 230kV Transformer-Bushing Model Ensemble 2– 1D

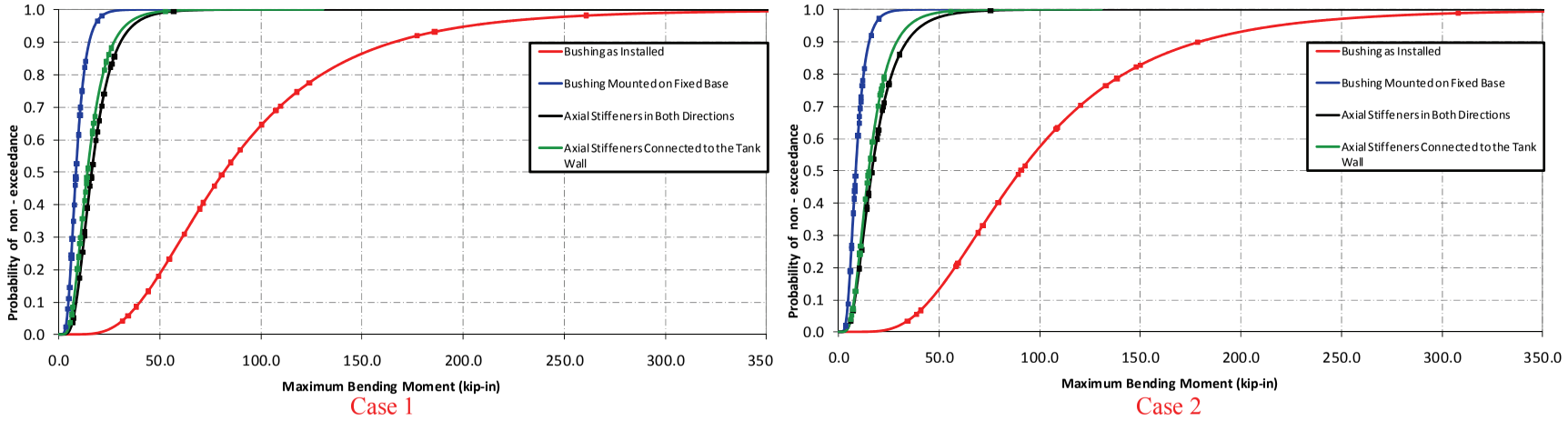

Figure 3-11 CDF for Maximum Bending Moments for Siemens 230kV Transformer-Bushing Model Ensemble 2– 2D

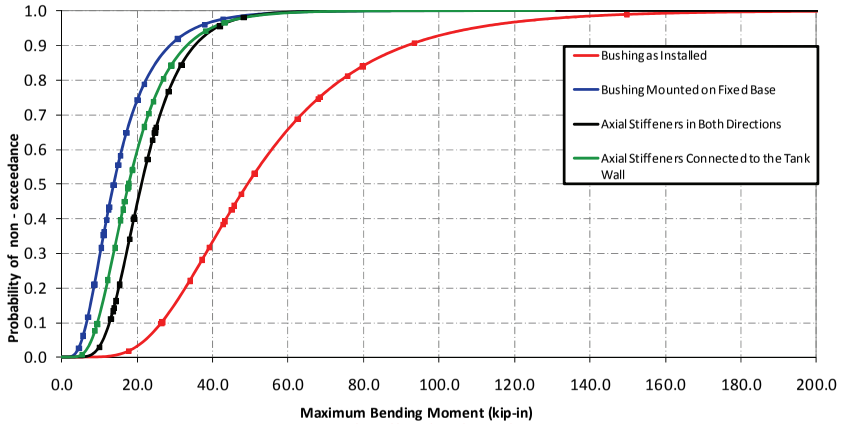

Longitudinal Direction

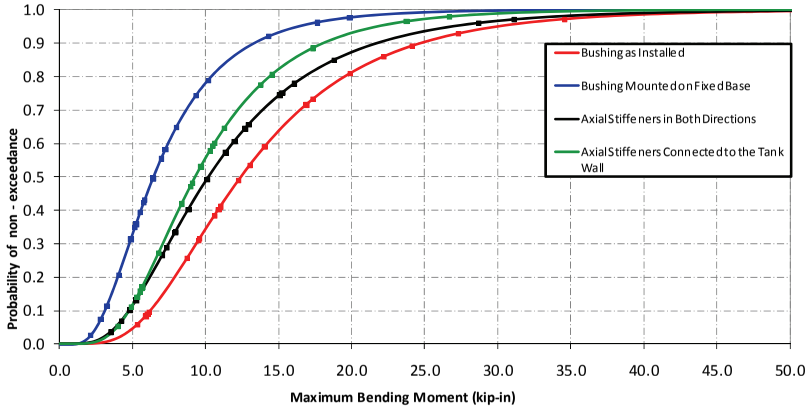

Transverse Direction

Figure 3-12 CDF for Maximum Bending Moments for Siemens 500kV Transformer-Bushing Model Ensemble 1

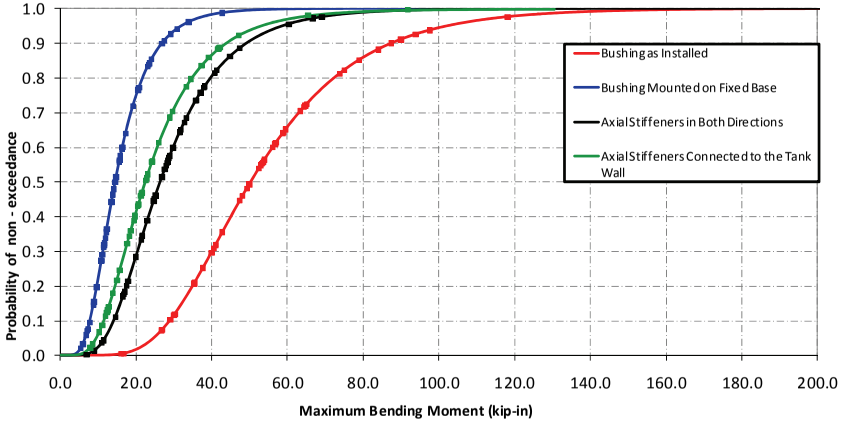

Longitudinal Direction

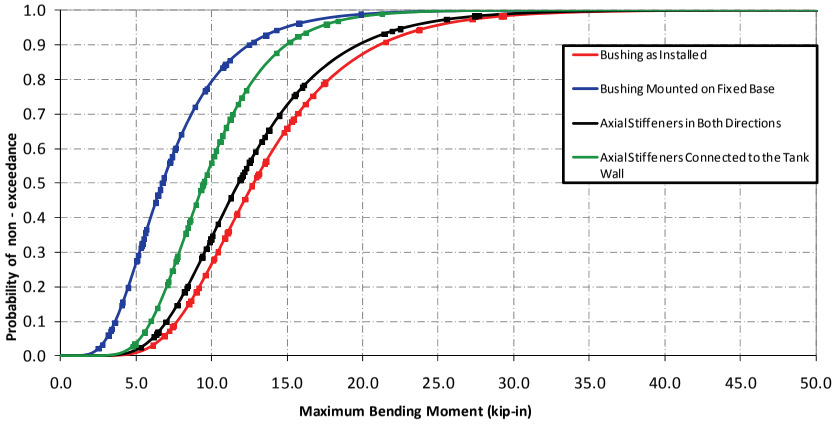

Transverse Direction

Figure 3-13 CDF for Maximum Bending Moments for Siemens 500kV Transformer-Bushing Model Ensemble 2– 1D

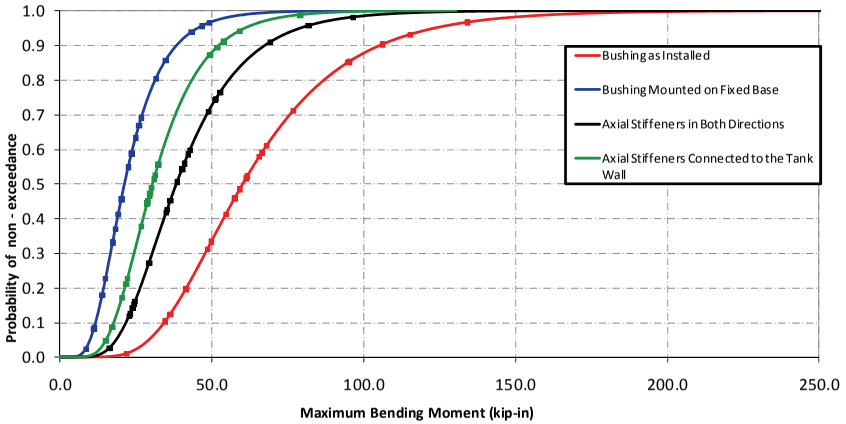

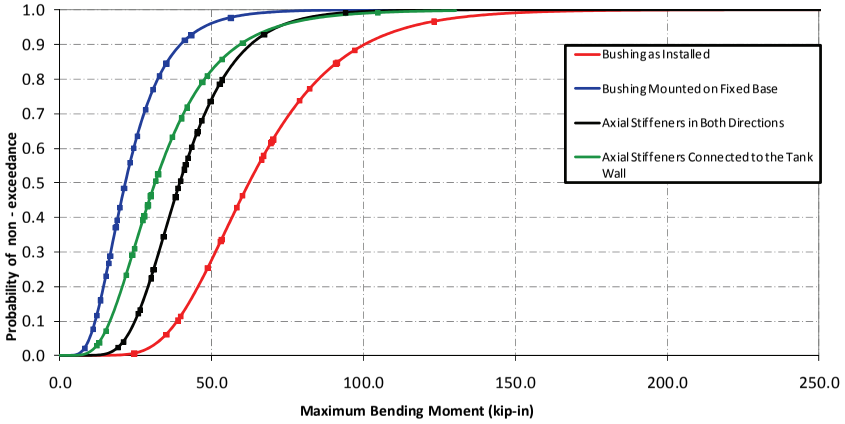

Figure 3-14 CDF for Maximum Bending Moments for Siemens 500kV Transformer-Bushing Model Ensemble 2– 2D

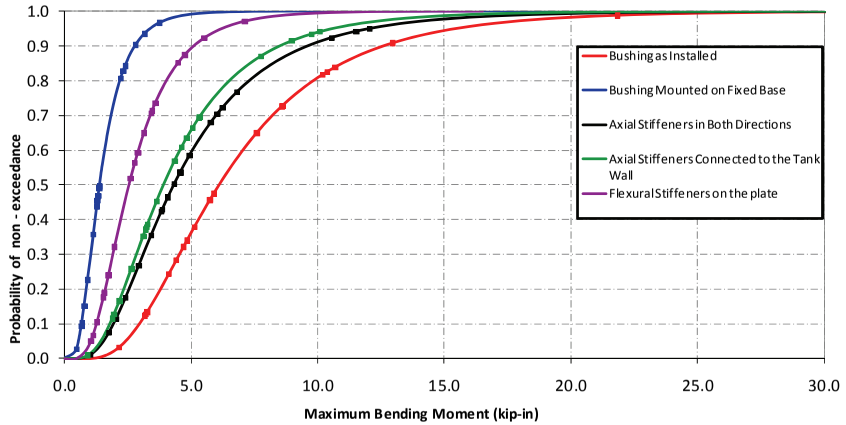

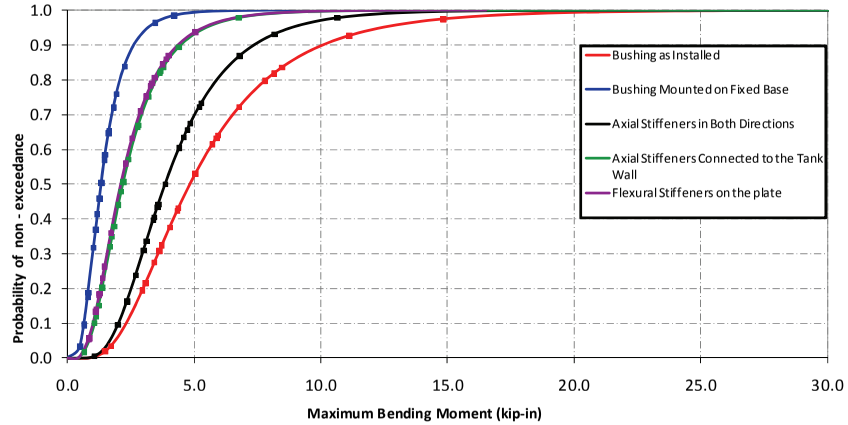

Figure 3-15 CDF for Maximum Bending Moments for Ferranti Packard 230kV Transformer-Bushing Model Ensemble 1

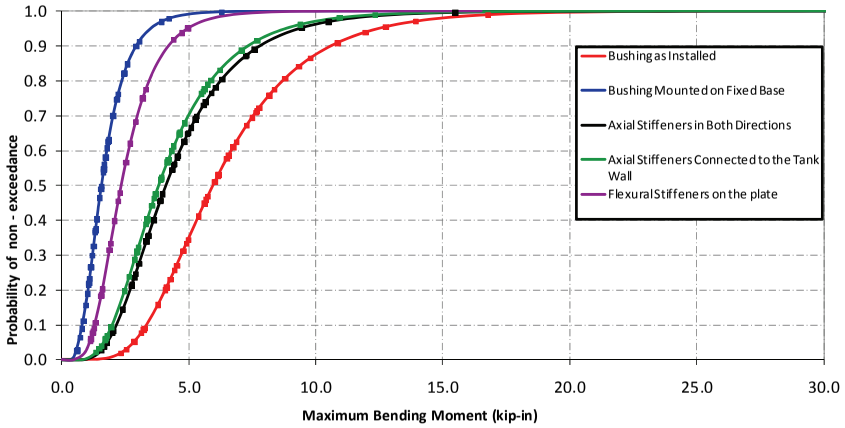

Longitudinal Direction

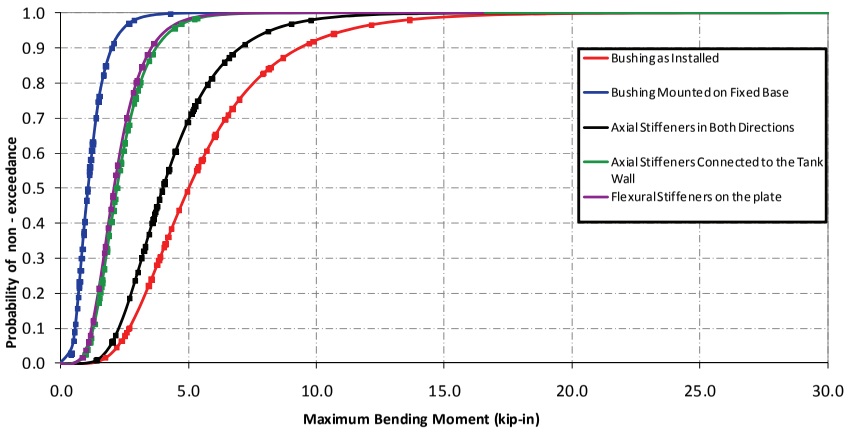

Transverse Direction

Figure 3-16 CDF for Maximum Bending Moments for Ferranti Packard 230kV Transformer-Bushing Model Ensemble 2– 1D

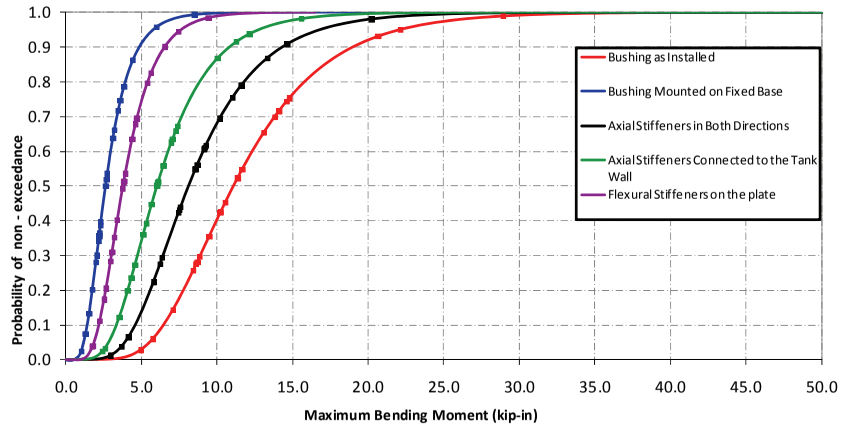

Case 1

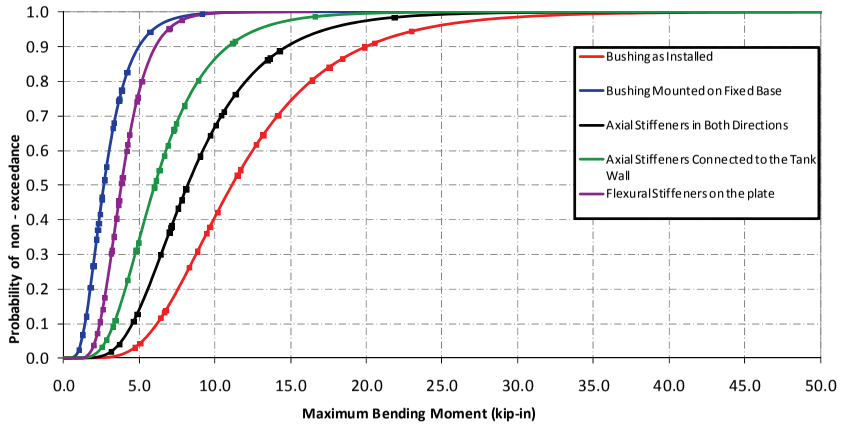

Case 2

Figure 3-17 CDF for Maximum Bending Moments for Ferranti Packard 230kV Transformer-Bushing Model Ensemble 2– 2D

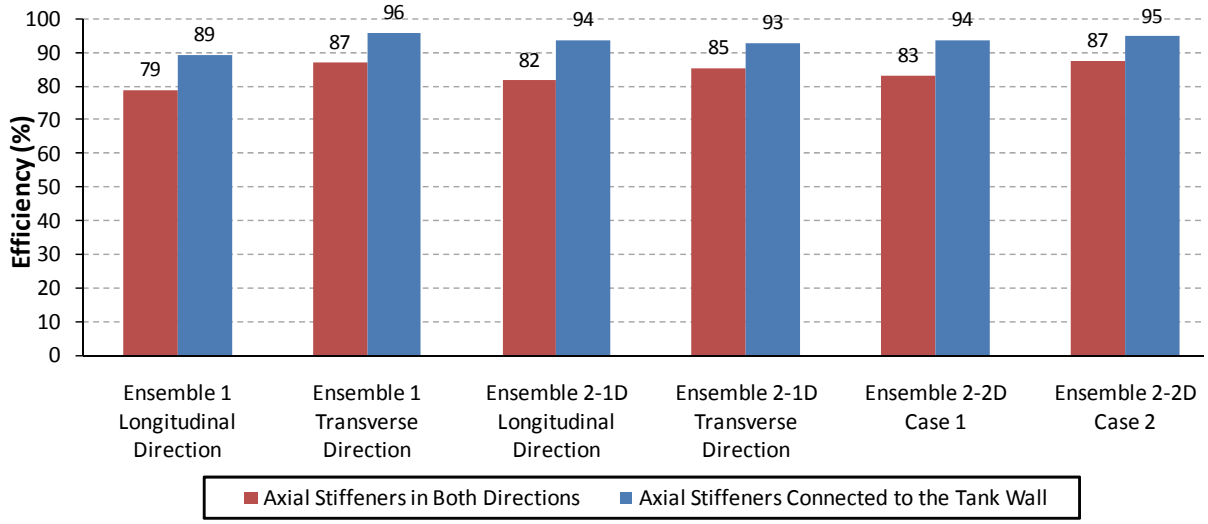

Figure 3-18 Efficiency Factor of Stiffening Techniques for Westinghouse 525kV Transformer Model

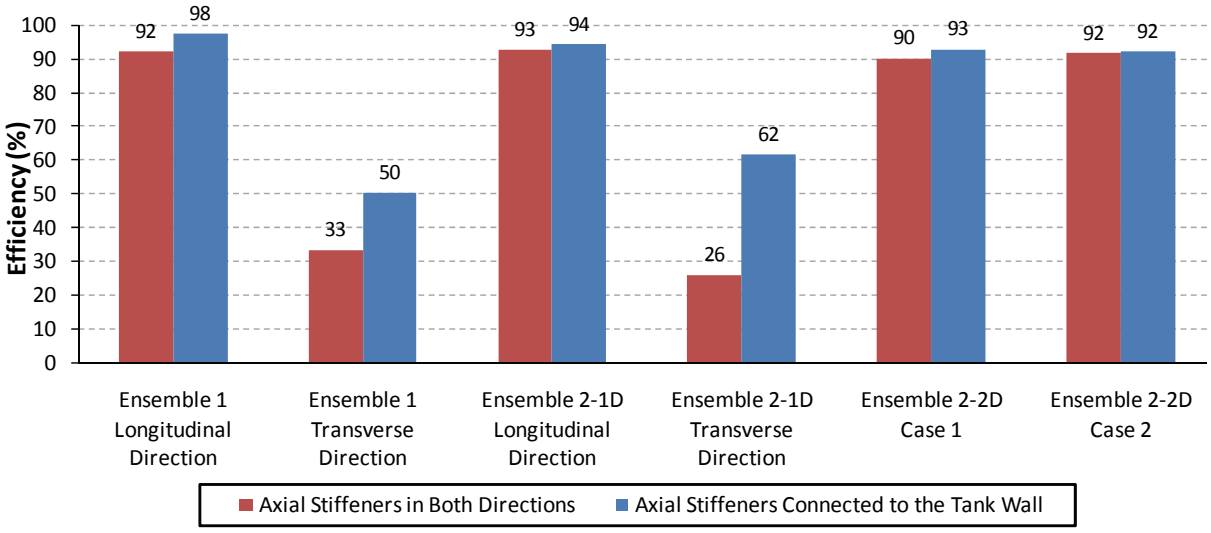

Figure 3-19 Efficiency Factor of Stiffening Techniques for Siemens 230kV Transformer Model

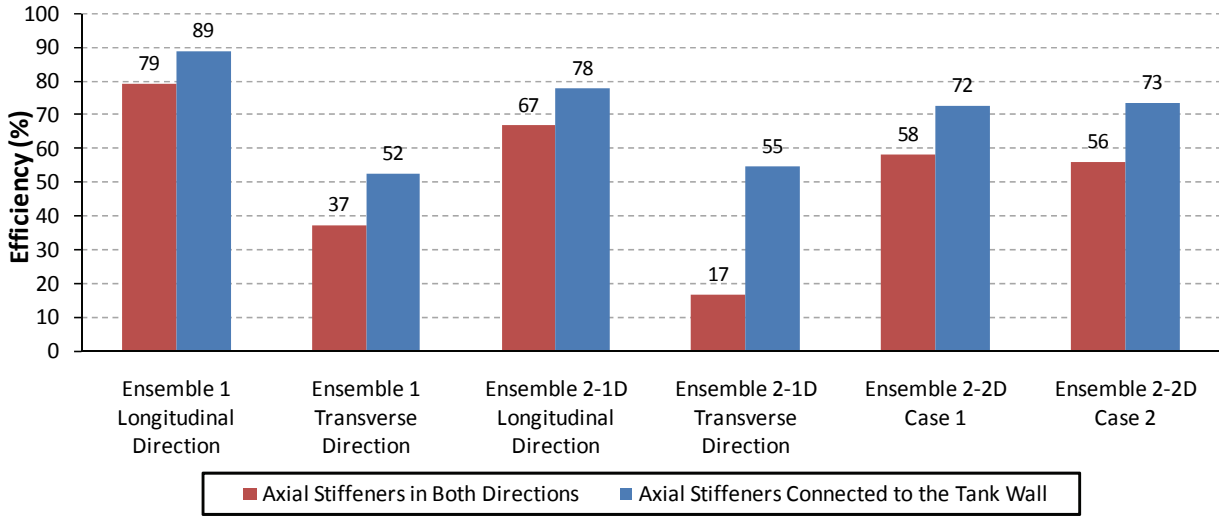

Figure 3-20 Efficiency Factor of Stiffening Techniques for Siemens 500kV Transformer Model

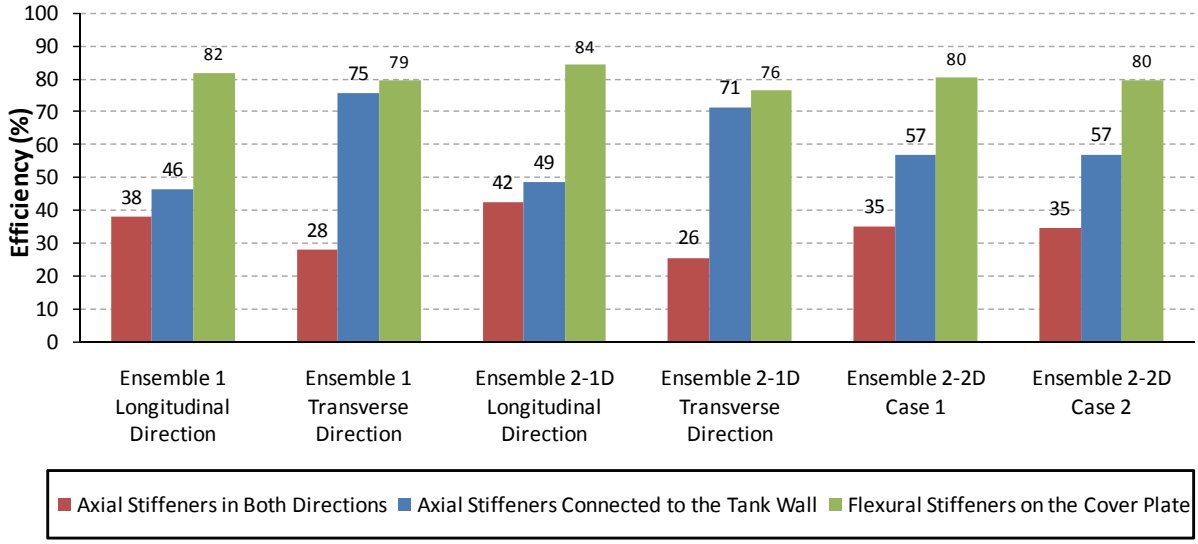

Figure 3-21 Efficiency Factor of Stiffening Techniques for Ferranti Packard 230kV Transformer Model

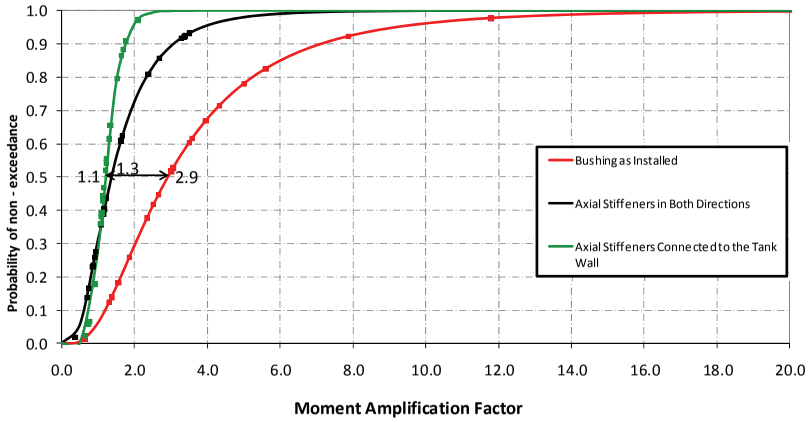

Longitudinal Direction

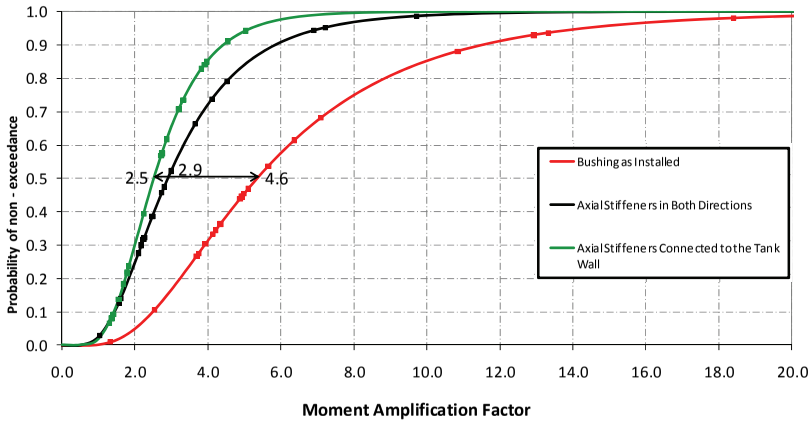

Transverse Direction

Figure 3-22 CDF for Moment Amplification Factors for Westinghouse 525kV Transformer Model Ensemble 1

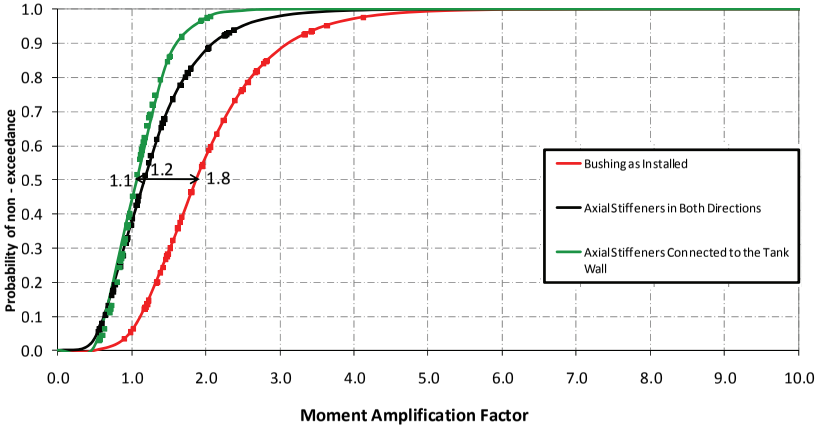

Longitudinal Direction

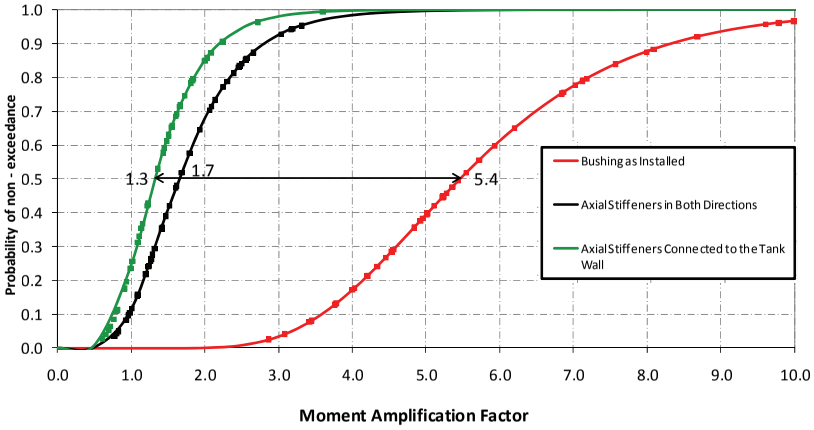

Transverse Direction

Figure 3-23 CDF for Moment Amplification Factors for Westinghouse 525kV Transformer Model Ensemble 2– 1D

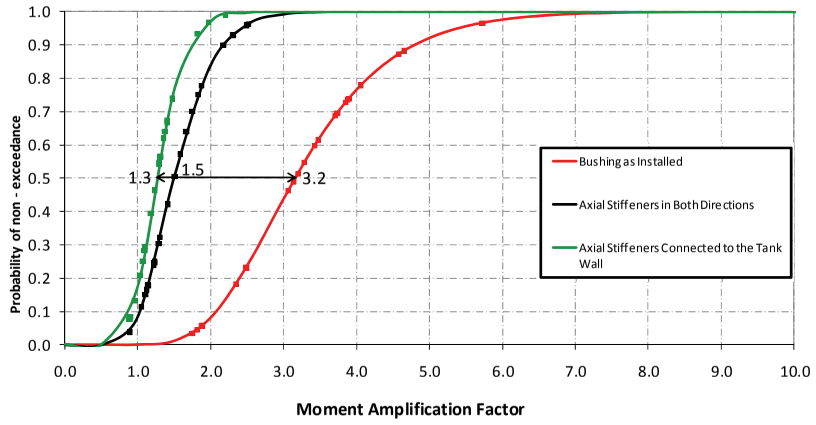

Case 1

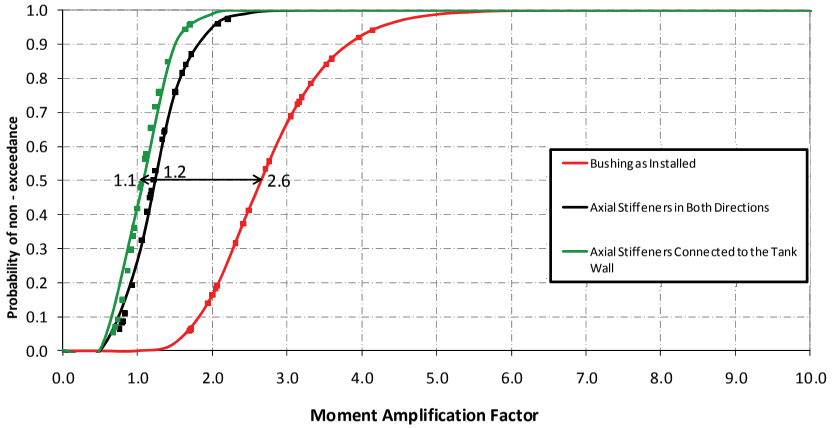

Case 2

Figure 3-24 CDF for Moment Amplification Factors for Westinghouse 525kV Transformer Model Ensemble 2– 2D

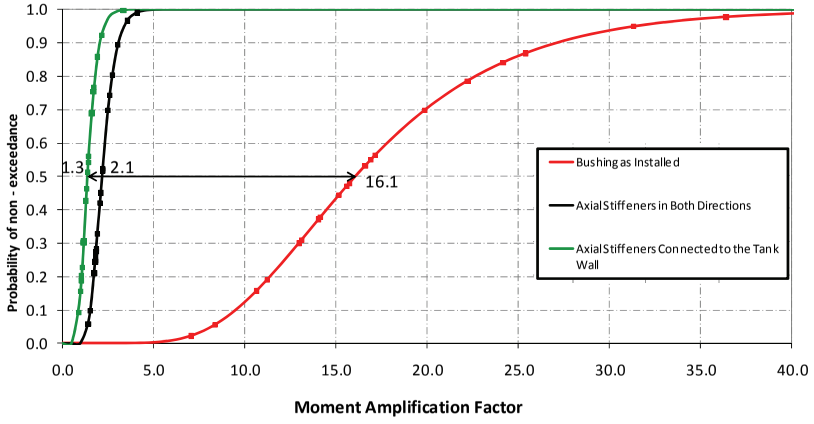

Longitudinal Direction

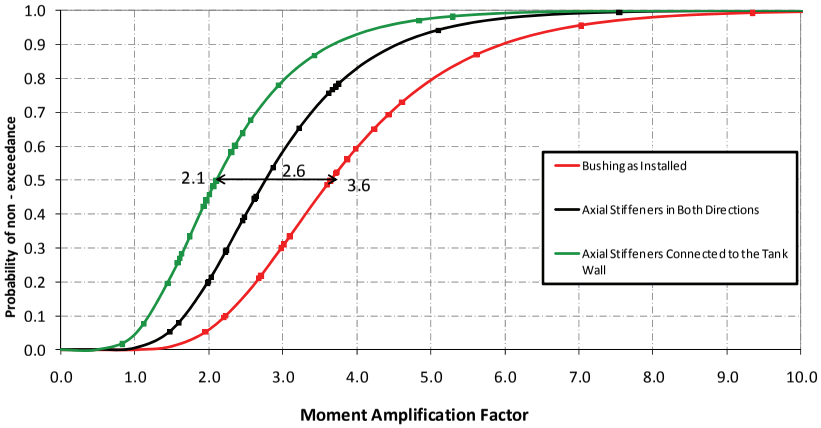

Transverse Direction

Figure 3-25 CDF for Moment Amplification Factors for Siemens 230kV Transformer Model Ensemble 1

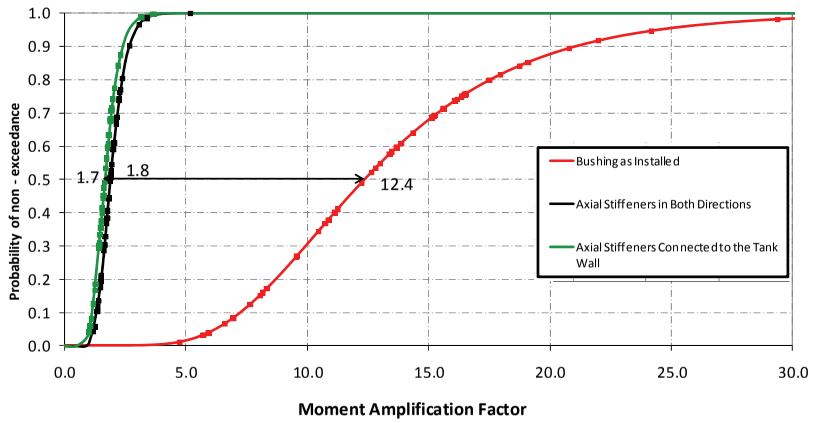

Longitudinal Direction

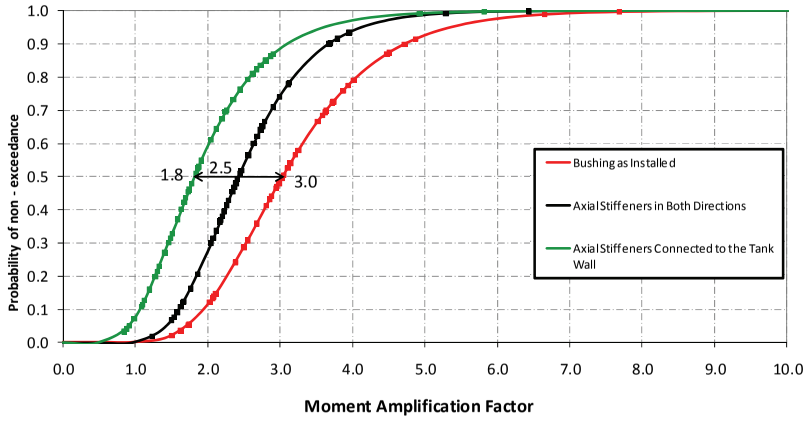

Transverse Direction

Figure 3-26 CDF for Moment Amplification Factors for Siemens 230kV Transformer Model Ensemble 2– 1D

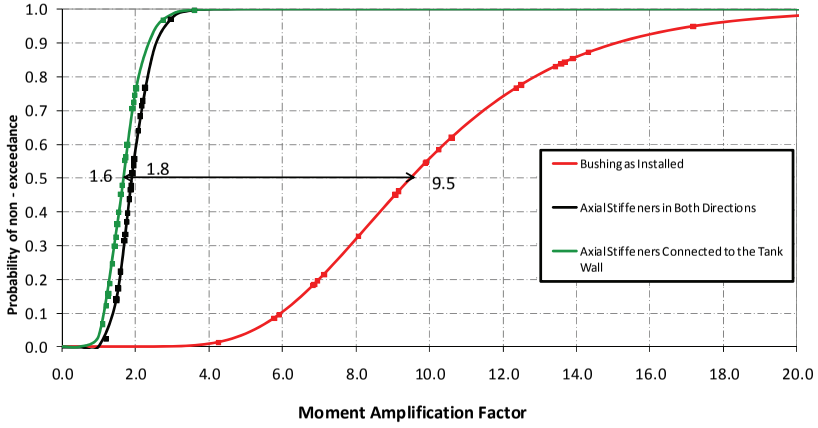

Case 1

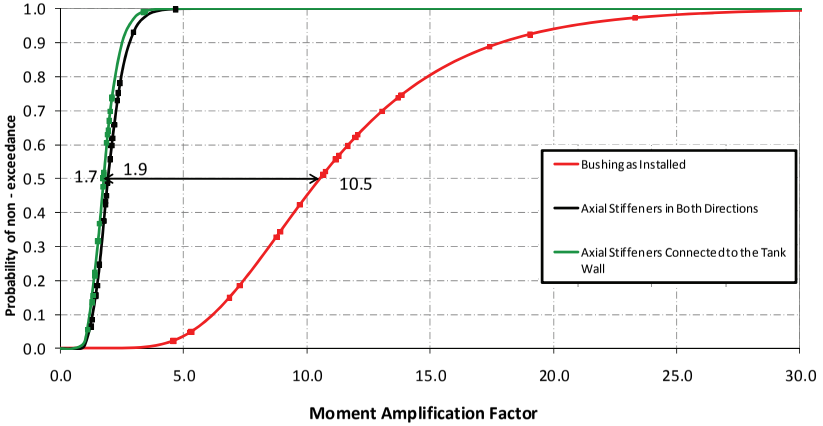

Case 2

Figure 3-27 CDF for Moment Amplification Factors for Siemens 230kV Transformer Model Ensemble 2– 2D

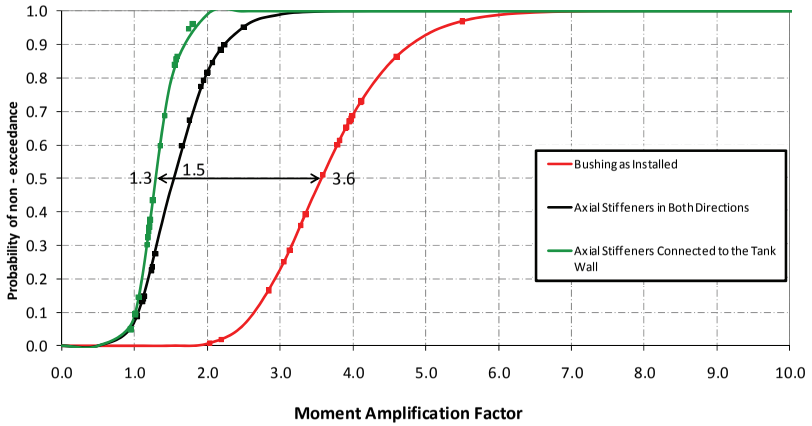

Longitudinal Direction

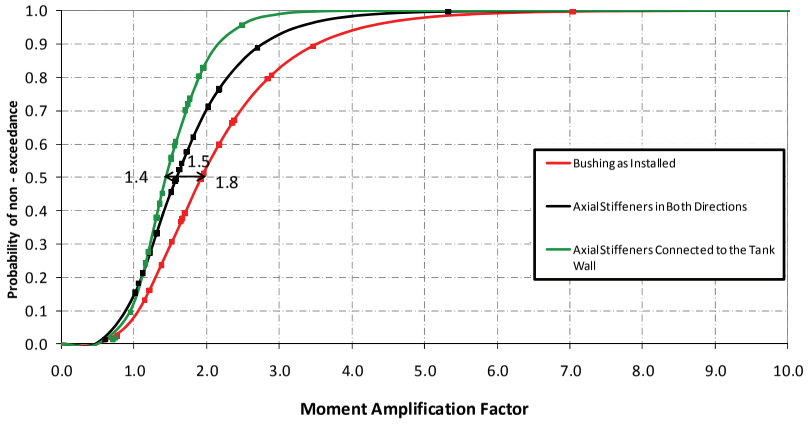

Transverse Direction

Figure 3-28 CDF for Moment Amplification Factors for Siemens 500kV Transformer Model Ensemble 1

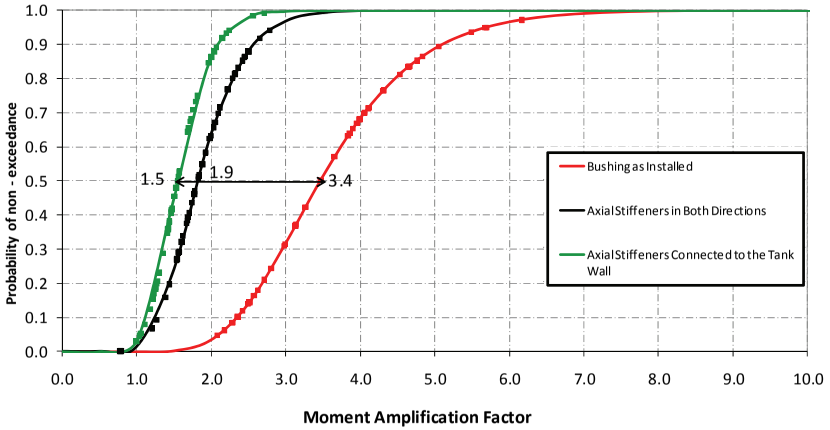

Longitudinal Direction

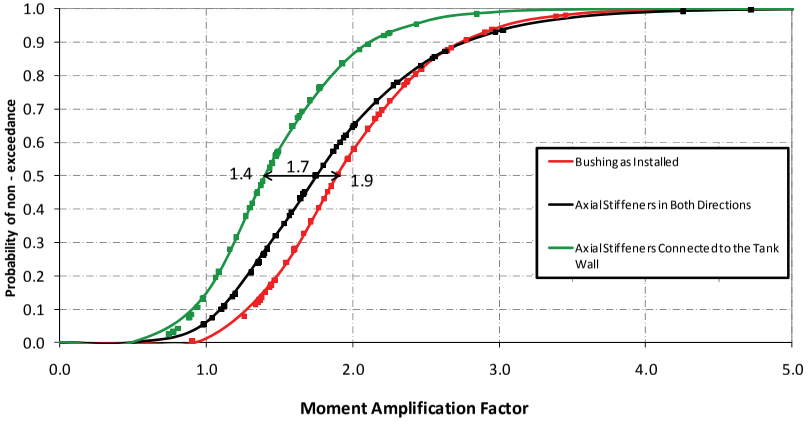

Transverse Direction

Figure 3-29 CDF for Moment Amplification Factors for Siemens 500kV Transformer Model Ensemble 2– 1D

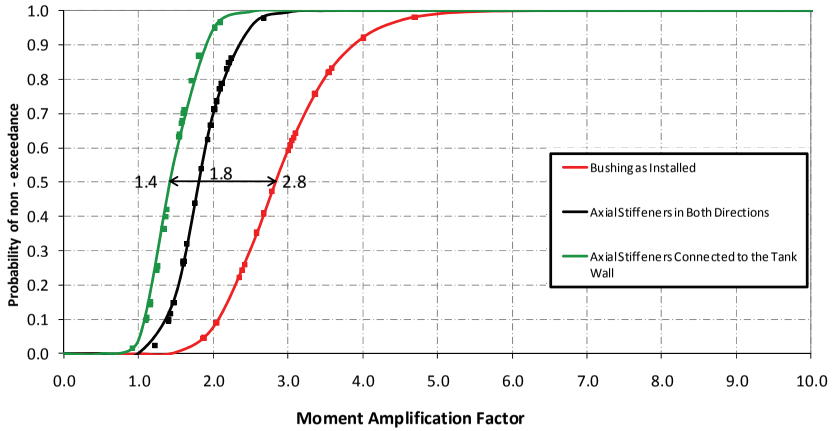

Case 1

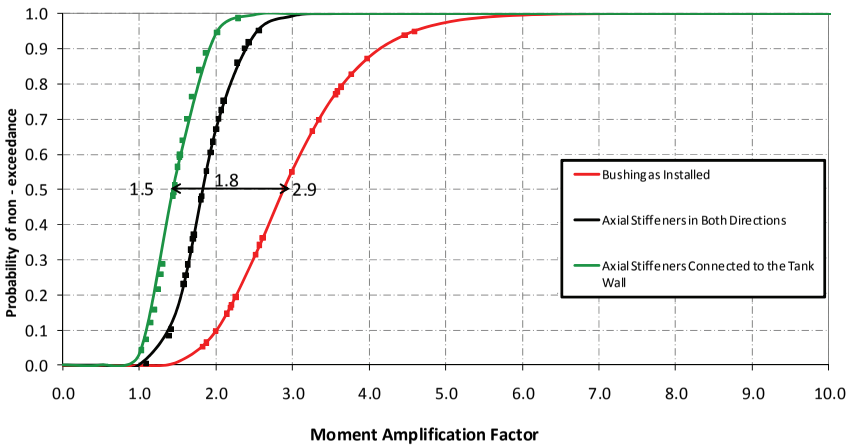

Case 2

Figure 3-30 CDF for Moment Amplification Factors for Siemens 500kV Transformer Model Ensemble 2– 2D

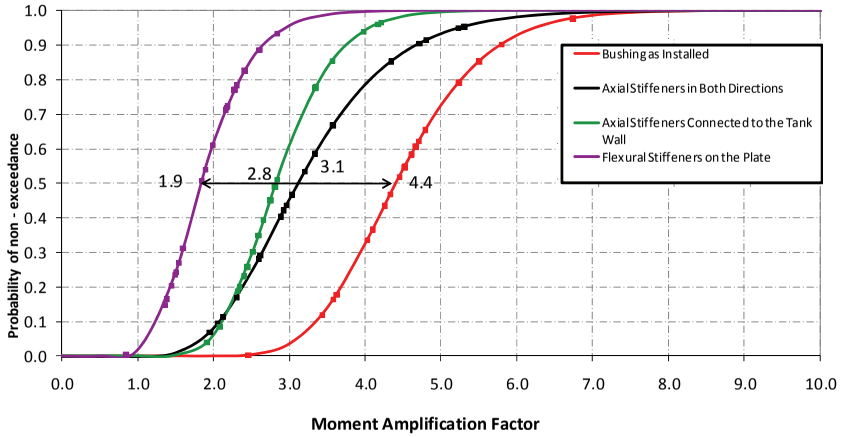

Longitudinal Direction

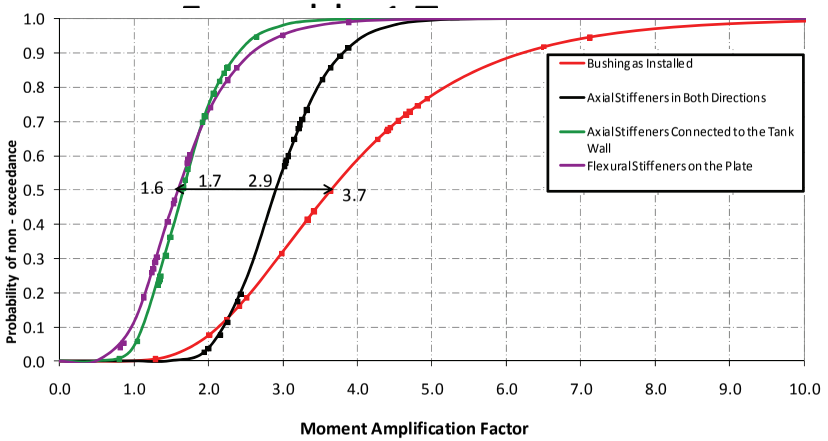

Transverse Direction

Figure 3-31 CDF for Moment Amplification Factors for Ferranti Packard 230kV Transformer Model Ensemble 1

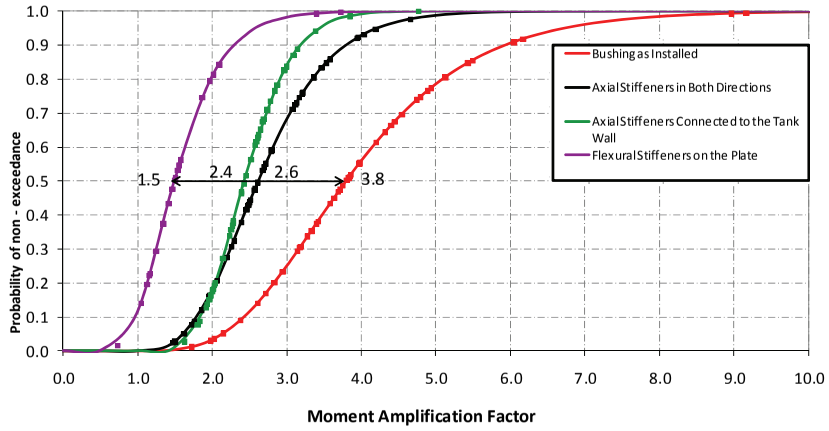

Longitudinal Direction

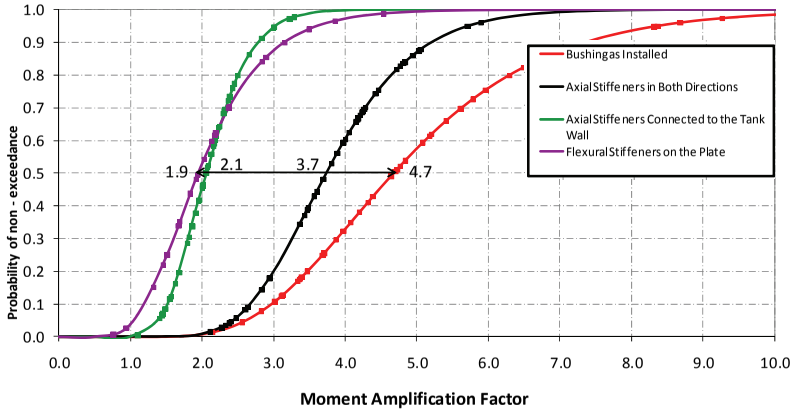

Transverse Direction

Figure 3-32 CDF for Moment Amplification Factors for Ferranti Packard 230kV Transformer Model Ensemble 2– 1D

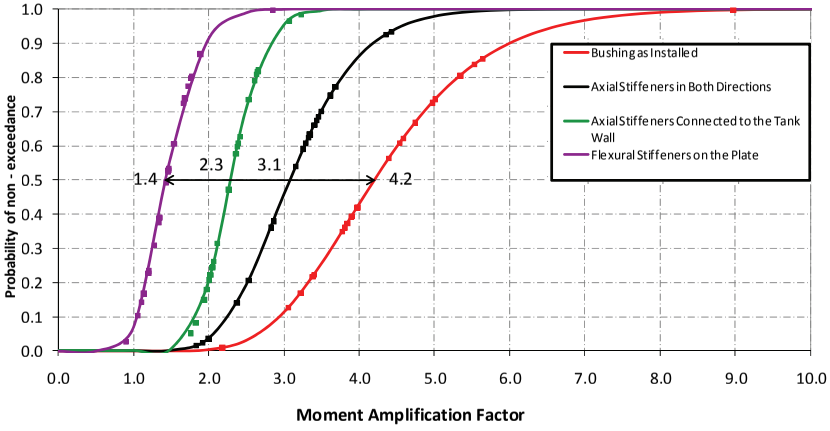

Case 1

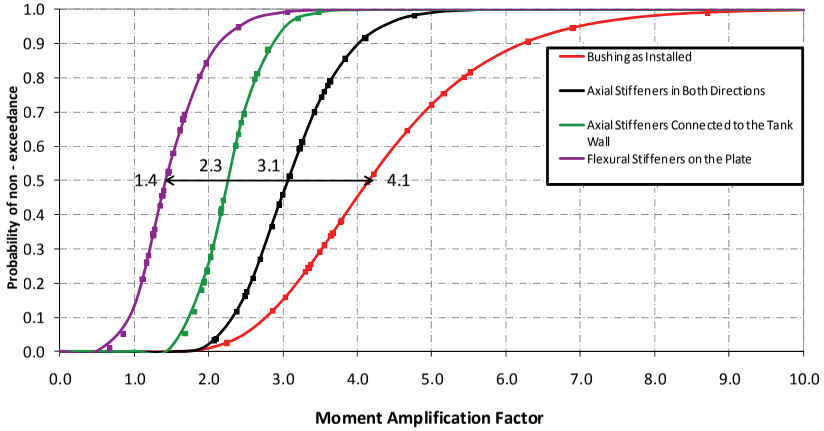

Case 2

Figure 3-33 CDF for Moment Amplification Factors for Ferranti Packard 230kV Transformer Model Ensemble 2– 2D

3.5. Flexural Stiffeners Incorporated at the Transformer Top Plate Implemented as Proposed Stiffening Technique

The stiffening approach of incorporating flexural stiffeners on the cover plate of the transformer tank was found to be the most efficient method investigated even in cases where the response of the transformer bushing system was significantly influenced by the cover plate. In this section the seismic performance of all four transformer models with three mounting conditions ("as installed", "stiffened" with flexural stiffeners and rigid base) is presented. Note that the "as installed" mounting condition is referred herein as "original stiffener configuration", while the "stiffened" case is referred as "final stiffener configuration". Note that the "original stiffener configuration" corresponds to the original specifications of the transformer manufacturers. Information on the properties of the flexural stiffeners in each of the four transformer-bushing system models is provided in Table 3-3, while a plan view of the transformer tank for each model showing the position of the flexural stiffeners is presented in Figure 3-34.

Table 3-3 Flexural Stiffeners on the Top Tank Plate for Existing and Stiffened Models (Koliou et al., 2012)

Transformer Model	Stiffener Configurations for Existing Models	Stiffener Configurations for Stiffened Models
Westinghouse 525kV	5-5x1/2 Plates: 5 in Longitudinal Direction; 3-L7.5x4x1/2:	5-5x1/2 Plates: 5 in Longitudinal Direction; 3 L8x6x1/2: 2 in Transverse Direction; 1in Longitudinal Direction
Siemens 230kV	No stiffener	6-L8x6x1/2: 3 in Transverse Direction; 3 in Longitudinal Direction
Siemens 500kV	No stiffener	5-L8x6x1/2: 2 in Transverse Direction; 3 in Longitudinal Direction
Ferranti Packard 230kV	3-L6x4x1/2: 3 in Transverse Direction	6-L8x6x1/2: 3 in Transverse Direction; 3 in Longitudinal Direction

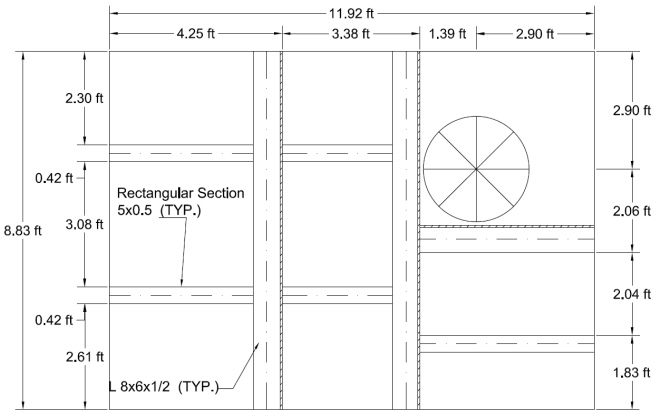

a. Westinghouse 525kV

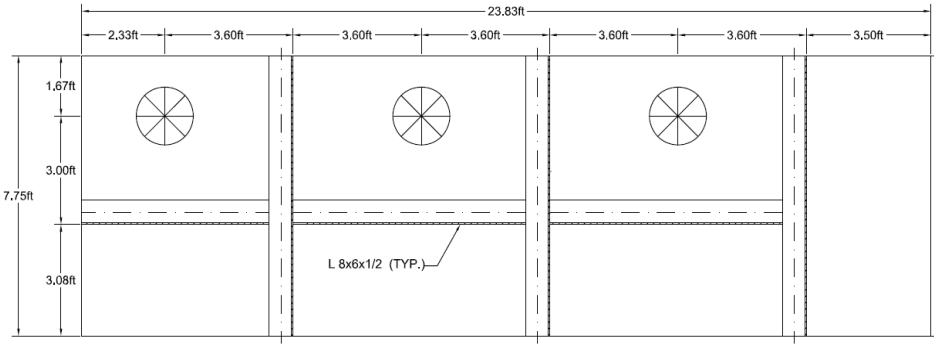

b. Siemens 230kV

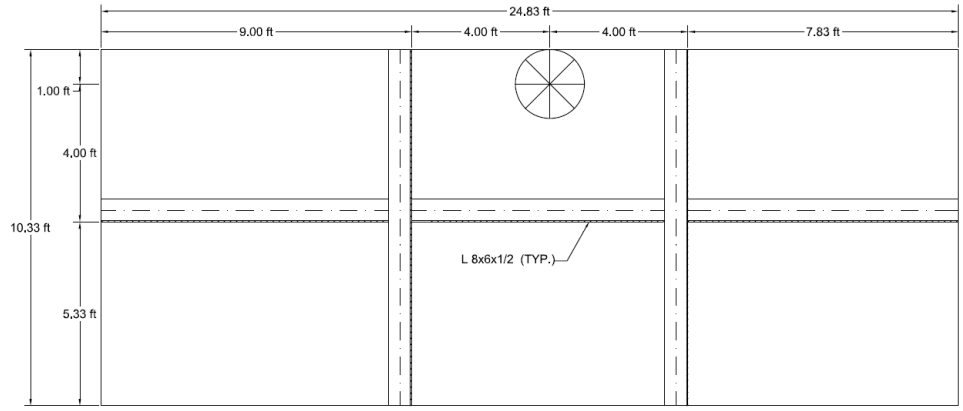

c. Siemens 500kV

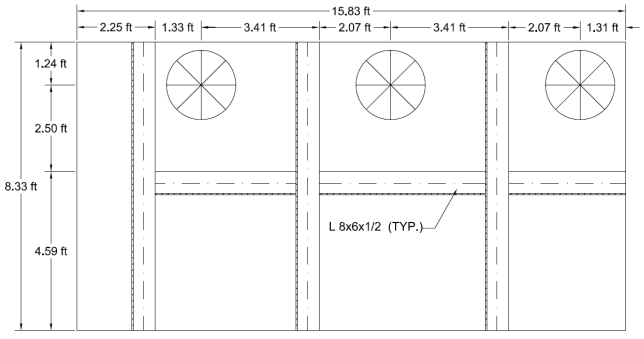

d. Ferranti Packard 230kV

Figure 3-34 Plan View of Transformer-Bushing Model showing the Location of Flexural Stiffeners on the Tank Cover Plate (Circles Indicate Locations of High Voltage Bushings) (Koliou et al., 2012)

The lognormal CDF associated with the probability of non-exceeding (PoNE) a value of maximum bending moment at the base of the bushing under the ensemble of ground motions is shown for each transformer-bushing model and for each mounting condition in Figure 3-35 to Figure 3-38, while the results of the free vibration analyses performed for all four models in order to compute the fundamental frequencies of the bushing systems are presented in Table 3-4.

The *Efficiency Factor*, *E*, as shown in Figure 3-39, varies from 80% to 97% for the four transformer-bushing models verifying that incorporating flexural stiffeners on the cover plate of the transformer tank substantially reduces the induced base bending moments. The MAF, defined earlier, was computed at the base of the bushings incorporating both the "original" and the "final" stiffener configurations. The results of Figure 3-40 to Figure 3-43 are presented in form of empirical and lognormal CDFs, while the median values of the MAF-CDFs are compared in Figure 3-44 with the frequency independent amplification factor of 2 recommended by IEEE-693 Standard.

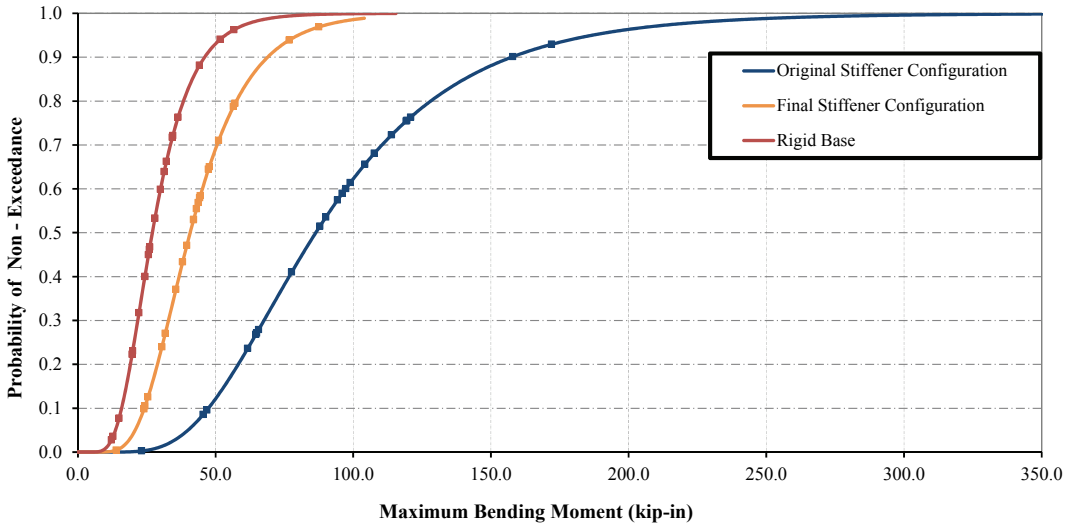

Figure 3-35 CDF for Maximum Bending Moments for Westinghouse 525kV Transformer-Bushing System Model Incorporating Flexural Stiffeners on the Cover Tank Plate (Koliou et al., 2012)

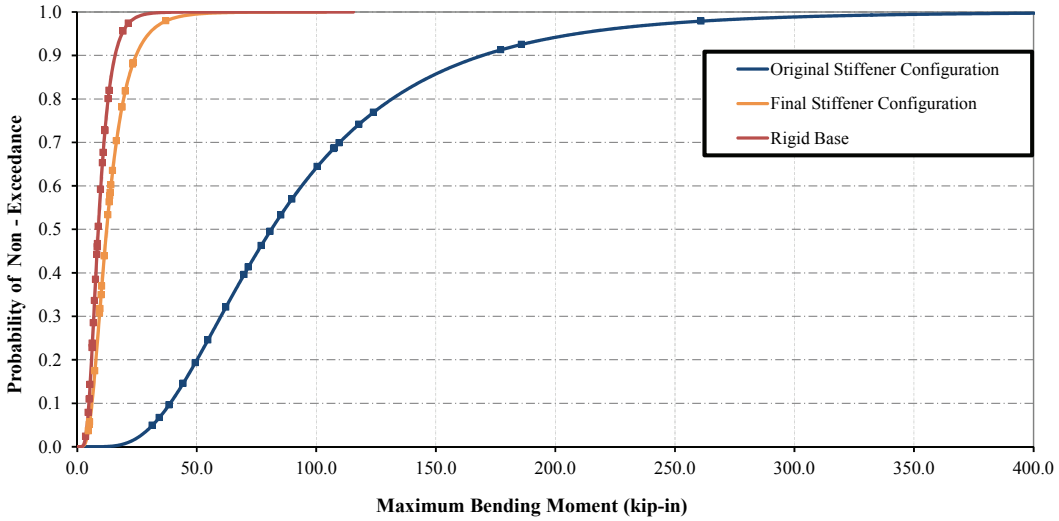

Figure 3-36 CDF for Maximum Bending Moments for Siemens 230kV Transformer-Bushing System Model Incorporating Flexural Stiffeners on the Cover Tank Plate (Koliou et al., 2012)

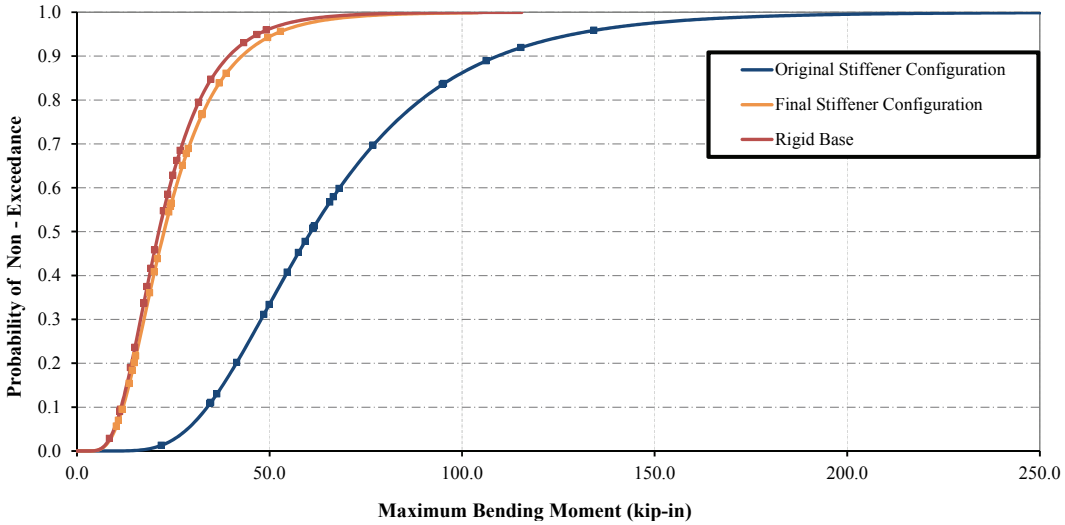

Figure 3-37 CDF for Maximum Bending Moments for Siemens 500kV Transformer-Bushing System Model Incorporating Flexural Stiffeners on the Cover Tank Plate (Koliou et al., 2012)

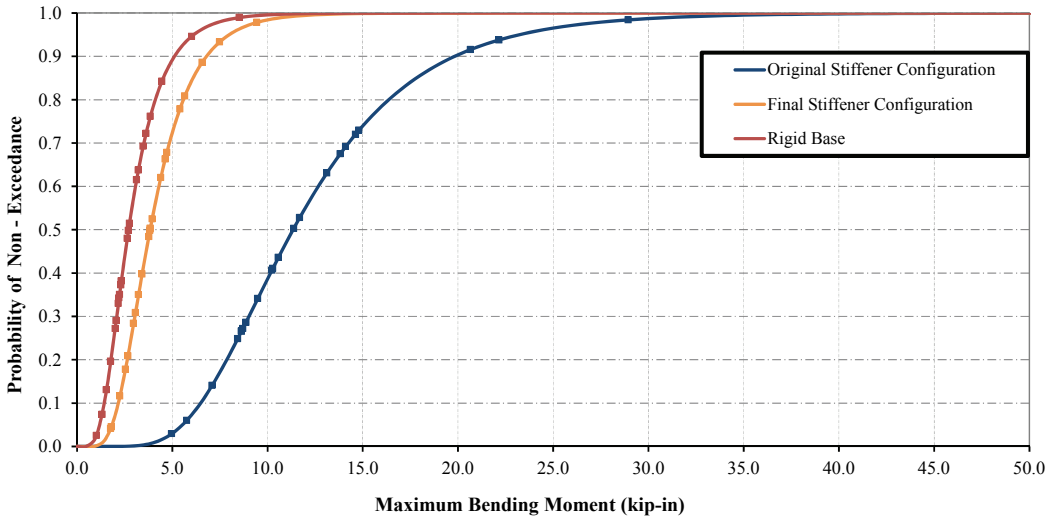

Figure 3-38 CDF for Maximum Bending Moments for Ferranti Packard 230kV Transformer-Bushing System Model Incorporating Flexural Stiffeners on the Cover Tank Plate (Koliou et al., 2012)

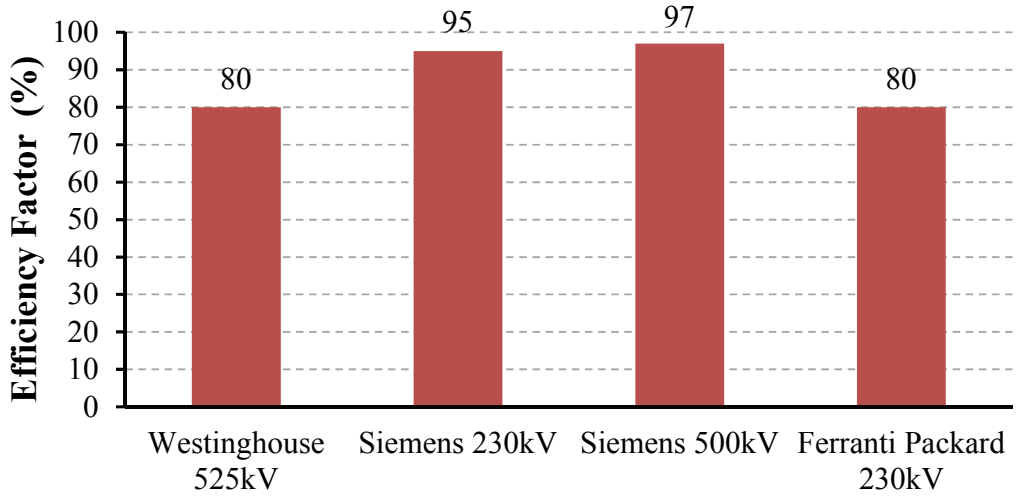

Figure 3-39 Efficiency Factors, E, for Four Transformer-Bushing System Models Incorporating Flexural Stiffeners on the Cover Top Plate (Koliou et al., 2012)

Table 3-4 Computed Fundamental Frequencies of Bushings for Different Mounting Conditions (Koliou et al., 2012)

	Bushings Fundamental Frequency (Hz)			
Mounting Condition	Westinghouse 525kV	Siemens 230kV	Siemens 500kV	Ferranti Packard 230kV
Original Stiffener Configuration	2.92	9.14	3.42	4.76
Final Stiffener Configuration	3.50	11.0	4.05	5.75
Rigid Base	9.27	16.9	8.75	16.8

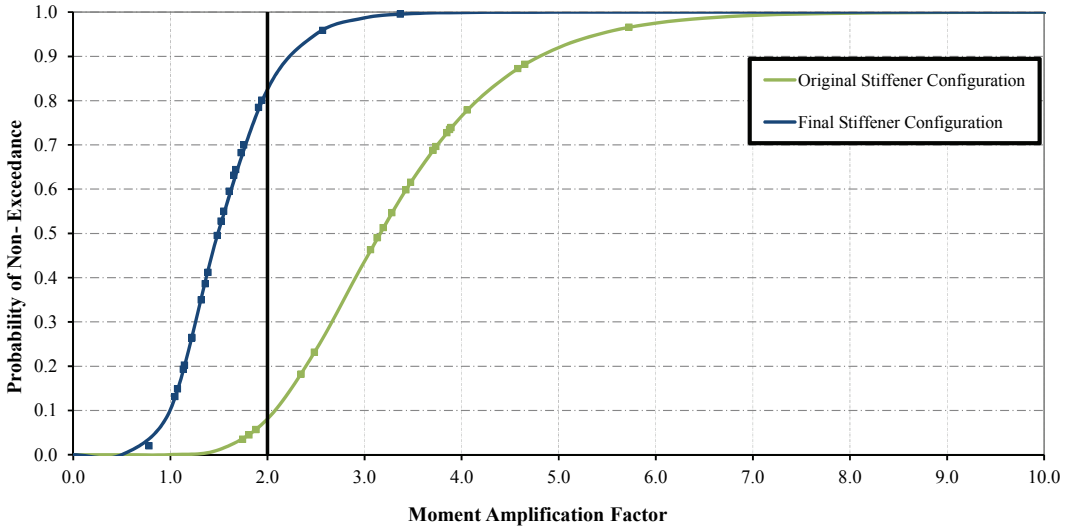

Figure 3-40 CDF for Moment Amplification Factors for Westinghouse 525kV Transformer Model Incorporating Flexural Stiffeners on the Cover Tank Plate (Koliou et al., 2012)

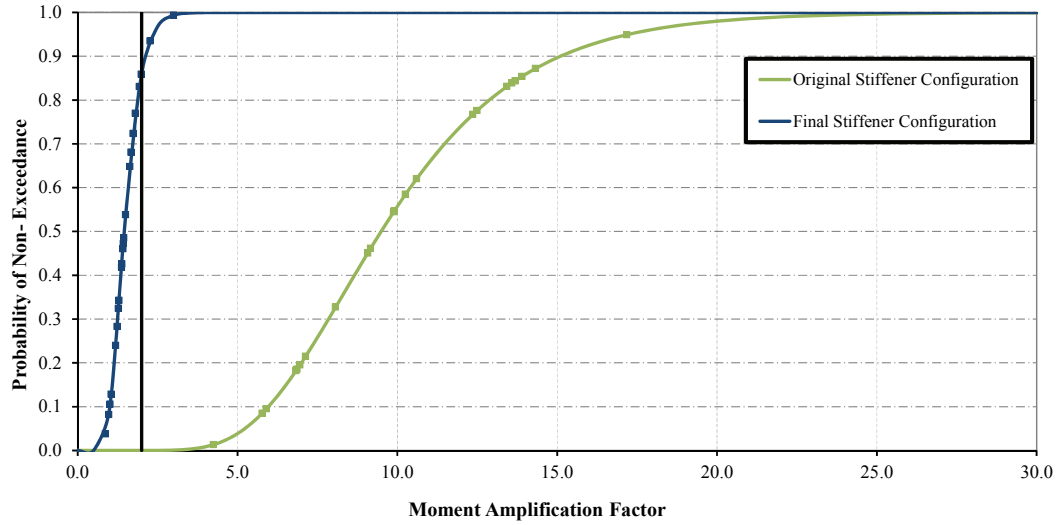

Figure 3-41 CDF for Moment Amplification Factors for Siemens 230kV Transformer Model Incorporating Flexural Stiffeners on the Cover Tank Plate (Koliou et al., 2012)

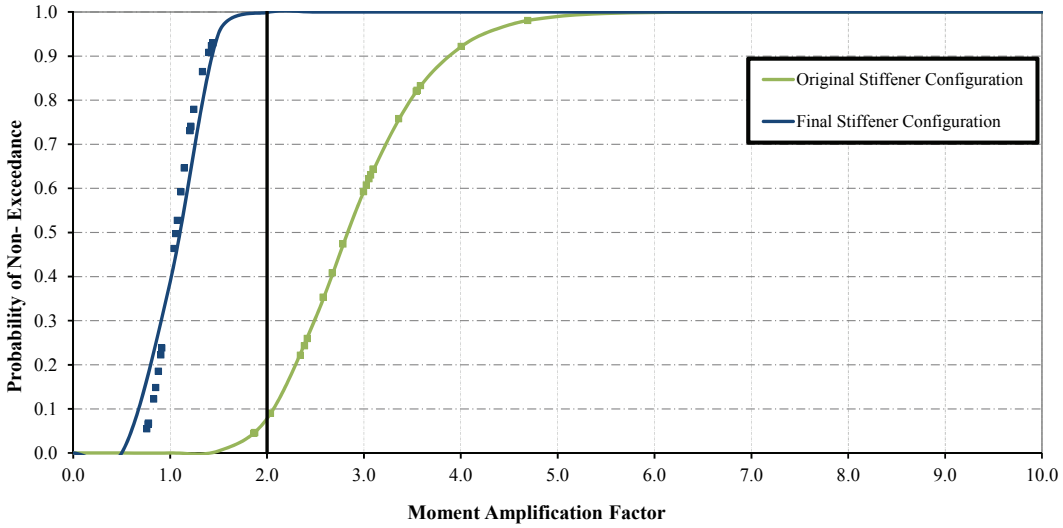

Figure 3-42 CDF for Moment Amplification Factors for Siemens 500kV Transformer Model Incorporating Flexural Stiffeners on the Cover Tank Plate (Koliou et al., 2012)

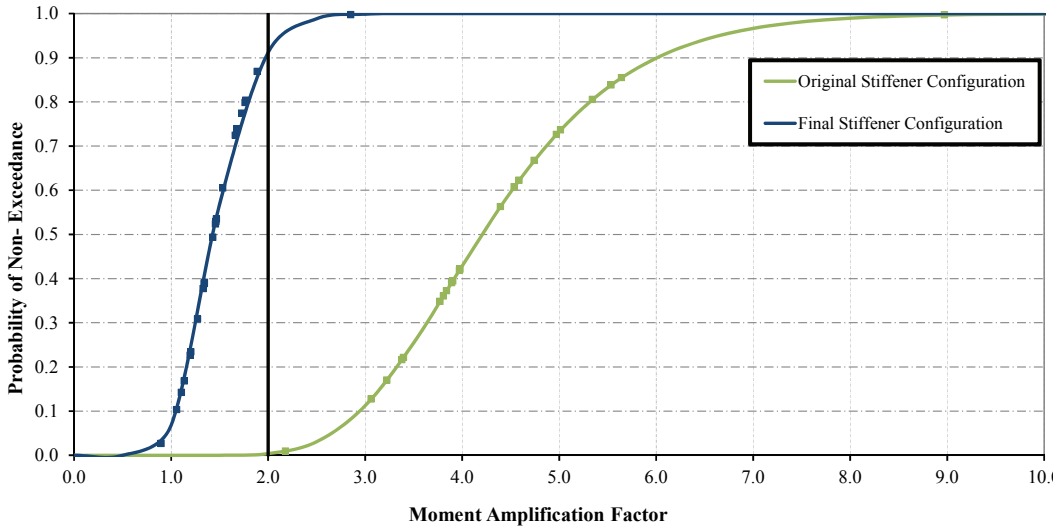

Figure 3-43 CDF for Moment Amplification Factors for Ferranti Packard 230kV Transformer Model Incorporating Flexural Stiffeners on the Cover Tank Plate (Koliou et al., 2012)

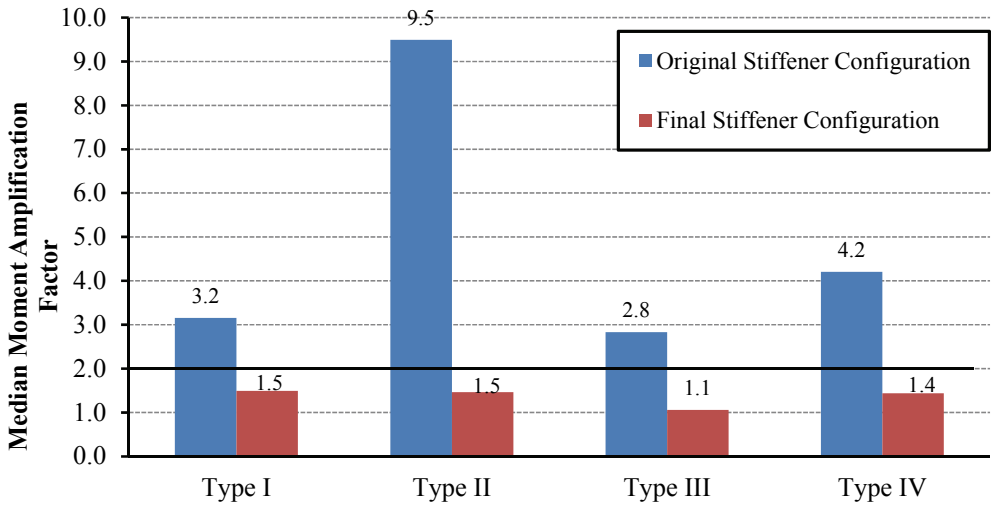

Figure 3-44 Median Values of Moment Amplification Factor Four Transformer-Bushing System Models and Different Mounting Conditions (Koliou et al., 2012)

3.6. Discussions

In summary, the numerical analyses presented, so far, within this section showed that the efficiency of the stiffening approaches considered was satisfactory. By introducing axial stiffeners between the bushing and tank plate or wall or flexural stiffeners on the tank plate, the maximum bending moment at the base of the bushing decreased moving closer to the rigid base results, while the moment amplification factor decreased as well reaching values lower than the amplification factor of 2 recommended in IEEE-693 Standard (IEEE, 2005).

It was observed that adding axial stiffeners, either in both directions or connected to the wall, was an efficient solution, however, incorporating flexural stiffeners on the cover plate appeared to be the most efficient solution even in cases where the response of the transformer bushing system was significantly influenced by the cover plate (Ferranti Packard 230kV model). Thus, it may be inferred that incorporating flexural stiffeners on the cover plate can improve the performance of transformer-bushing systems, so that they behave similarly to the rigid base case.

Since the stiffening approach of incorporating flexural stiffeners was found to be most effective technique of reducing the seismic demand and improving the seismic response of transformer bushing systems, it was implemented in the rest three models (Westinghouse 525kV, Siemens 230kV and Siemens 500kV). Note that the 2D analysis case of ensemble 2 was only considered

since it was already shown, through the current section, that the response trends are pretty similar for all analysis cases.

In order to further investigate the efficiency of this stiffening technique on the dynamic response of transformer-bushing systems, an experimental study was conducted and is presented in the next two sections.

SECTION 4

SYSTEM IDENTIFICATION TESTING

4.1. Introduction – Objectives of Testing

The results of the numerical study presented in the previous section clearly showed that the transformer-bushing system may behave similarly to the rigid base mounting case by using appropriate stiffening techniques. The incorporation of flexural stiffeners on the cover plate of the transformer tank was found to be the most efficient stiffening approach, among all the techniques investigated numerically, since the seismic demand on the bushings (in terms of bending moment at their base) decreased significantly compared to the bushings installed on the unstiffened transformer tanks ("as installed" conditions).

The major objective of the experimental investigation conducted in the context of this research was to validate the results of the numerical study for the stiffening approach of incorporating flexural stiffeners on the cover plate of a transformer tank. For this reason, a two stage experimental study consisting of system identification tests and dynamic (shake table) tests was conducted in the Structural Engineering and Earthquake Simulation Laboratory (SEESL) of the University at Buffalo.

In this section, the system identification testing of the bushing structure, by a series of impact hammer tests and pull tests is presented, while the results of the shake table tests are discussed in Section 5.

4.2. Scope of System Identification Testing

The system identification testing aimed mainly to investigate if the bushing specimen was damaged during previous tests conducted in the Structural Engineering and Earthquake Simulation Laboratory (SEESL) of the University at Buffalo during the summer of 2009 (Muhammad, 2012). More specifically, a series of impact hammer tests and pull-back tests were conducted for the bushing specimen mounted on a rigid base so that the fundamental frequencies of the bushing structure were measured and compared to the frequencies from the previous tests.

4.3. Test Setup Overview

4.3.1. Specimen Description

The specimen used in the system identification tests consisted of a 230kV porcelain bushing bolted on a reinforced concrete slab mounted on the strong floor of the Structural Engineering and Earthquake Simulation Laboratory (SEESL) of the University at Buffalo (UB), as shown in Figure 4-1. More specifically, the bushing was 151.4" tall (see Figure 4-2), while the concrete slab used to simulate the rigid (fixed) base, had plane dimensions 8'x 8' and thickness of 1'. A steel plate was embedded in the top surface of the concrete slab to provide a suitable base for bolting the bushing structure. Note that extra weight of 25lbs was added at the top of the bushing specimen as required per IEEE-693 Standard (IEEE, 2005) for the qualification testing of electrical equipment. In Figure 4-3, Figure 4-4 and Figure 4-5, detailed drawings of the reinforced concrete slab are provided, while the properties/specifications of the bushing structure considered for this experimental study are summarized in Table 4-1.

Table 4-1 Properties of Bushing Used

Manufacturer	N/A	ABB
Material of Insulator	N/A	Porcelain
Voltage Capacity	(kV)	230
Total Height	(in)	151.4
Length over Mounting Flange	(in)	91.4
Length below Mounting Flange	(in)	60.0
Max. Diameter over Mounting Flange	(in)	11.8
Max. Diameter below Mounting Flange	(in)	10.0
Diameter of Mounting Flange	(in)	24.0
Bolt Pattern of Mounting Flange (per flange diameter)	(in)	12-Φ 1 1/4 / Φ21**
Total Weight	(lbs)	840
Location of Center of Gravity (CG) above Flange	(in)	14.0
Upper Unit Weight	(lbs)	447
Location of Upper Unit Center of Gravity (CG)	(in)	34.0
Lower Unit Weight	(lbs)	293
Location of Lower Unit Center of Gravity (CG)	(in)	28.0

** 12-Φ 1 ¼" refers to the minimum edge distance (15"), while 21" represents the largest diameter of the bolt pattern to accommodate several positions of the bushing on the top/relocatable plate

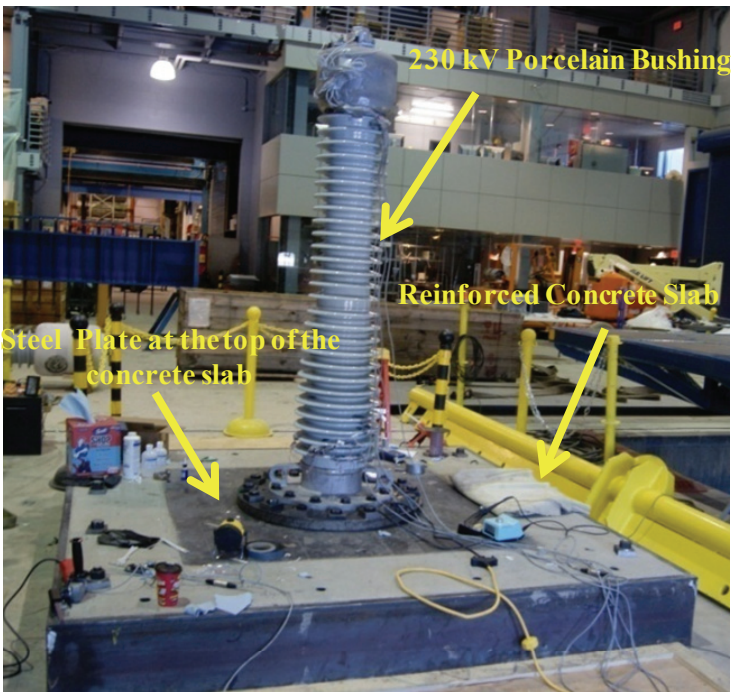

Figure 4-1 Experimental Set-Up of the System Identification Testing

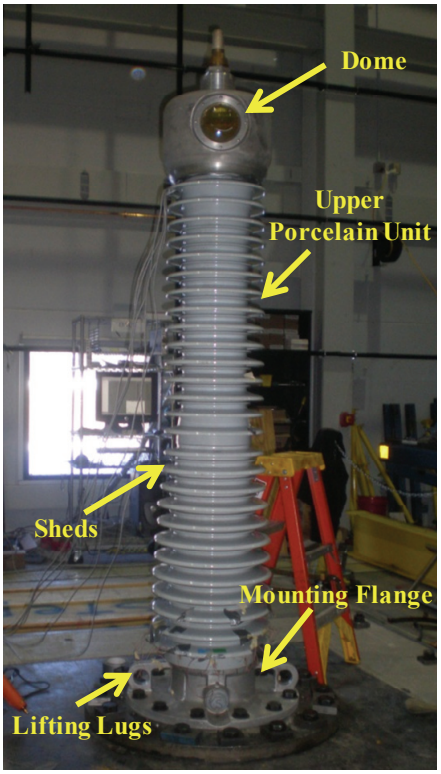

Figure 4-2 230kV Bushing Structure used for the Experimental Studies

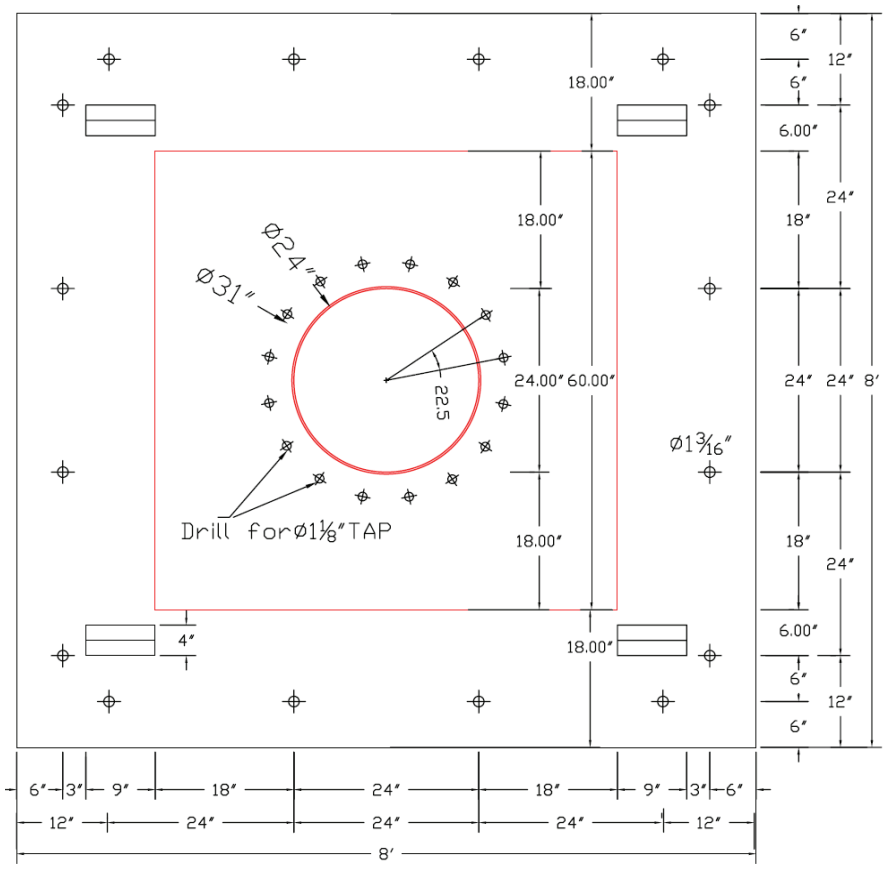

Figure 4-3 Plan View of the Reinforced Concrete Slab (Muhammad, 2012)

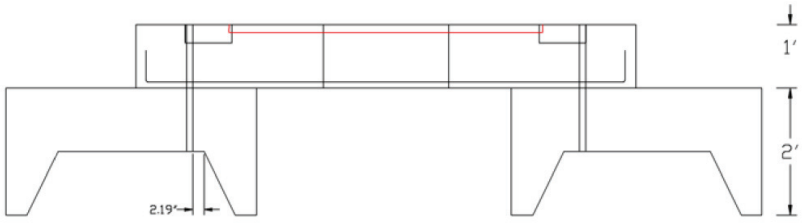

Figure 4-4 Front View of the Reinforced Concrete Slab (Muhammad, 2012)

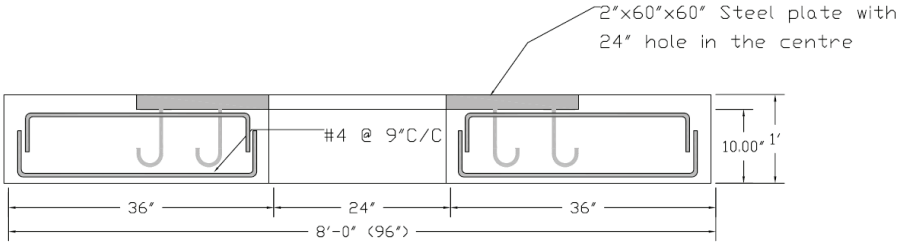

Figure 4-5 Geometric Section of the Reinforced Concrete Slab (Muhammad, 2012)

4.3.2. Loading System

- **Hammer Tests**

Impact hammer tests were conducted by hitting the top of bushing with a hammer in the North-South, North-East and East-West direction to evaluate the natural frequencies and damping characteristics of the bushing specimen. Figure 4-6a shows the hammer test being conducted in the North-South direction.

- **Pull-Back Tests**

The objective of the pull-back tests was to evaluate the static lateral stiffness of the bushing by pulling its top with two different levels of external forces (one of 300lbs and one of 600lbs) in the East-West and North-South direction. In order to conduct the pull-back tests, the external force was applied at the top of the bushing by a forklift or by hand (manually). For this purpose, a band was tied at the top of the bushing and was connected to a load cell and then to another band that was already tied to the forklift. Then the forklift moved slowly away from the specimen and applied a horizontal force. As soon as the force in the band reached the desired maximum value, the band was slowly released. The configuration used for the pull- back tests is presented in Figure 4-6b , while the load cell used for this type of testing is shown in Figure 4-7 .

a) Impact Hammer Test

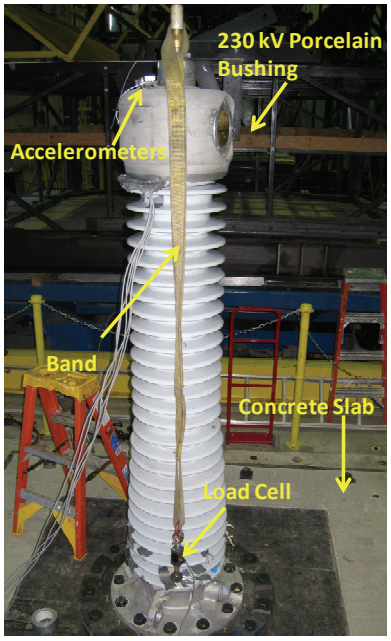

b) Specimen Configuration for the Pull-Back Testing

Figure 4-6 System Identification Testing Configurations

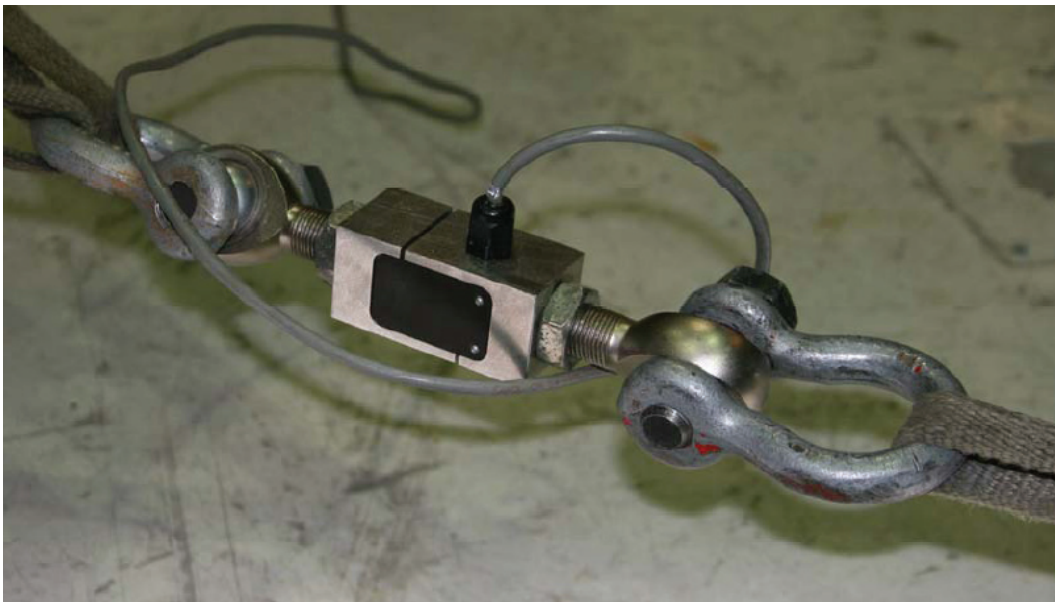

Figure 4-7 Load Cell used for the Pull-Back Tests

4.3.3. Instrumentation Setup

The response of the bushing was recorded by 20 instruments. More specifically, five accelerometers, four strain rosettes (3 strain gauges each one), two linear potentiometers (string pots) and one load cell were used. The accelerometers were attached at the top of the bushing oriented as shown in Figure 4-8. As for the strain rosettes, one rosette was placed at the base of the bushing on each face (north, south, east and west) as shown in Figure 4-9, Figure 4-10 and Figure 4-11. Each one of the rosettes consisted of three strain gauges whose axes were 45^{o} apart. An example of this configuration is presented in Figure 4-12 for the strain rosette in the west direction. Note that the strain rosettes in the east and west direction were attached very close to the lifting lugs of the bushing. Finally, the two linear potentiometers were attached at the top of the bushing as indicated in Figure 4-13. A summary of the instrumentation list for the system identification tests is provided in tabular and graphic form in Table 4-2 and Figure 4-14, respectively.

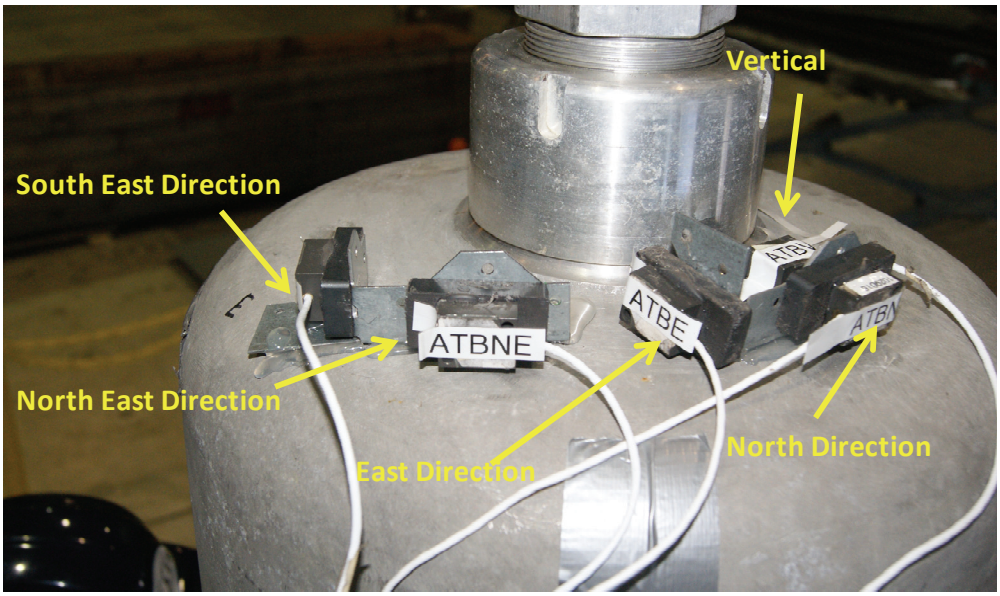

Figure 4-8 Accelerometers Attached at the Top of the Bushing

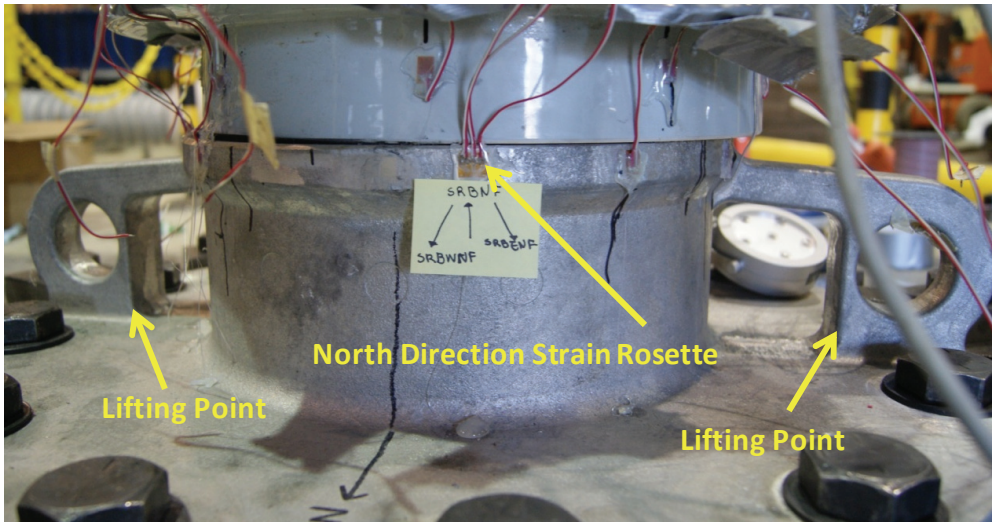

Figure 4-9 Strain Rosette in the North Direction

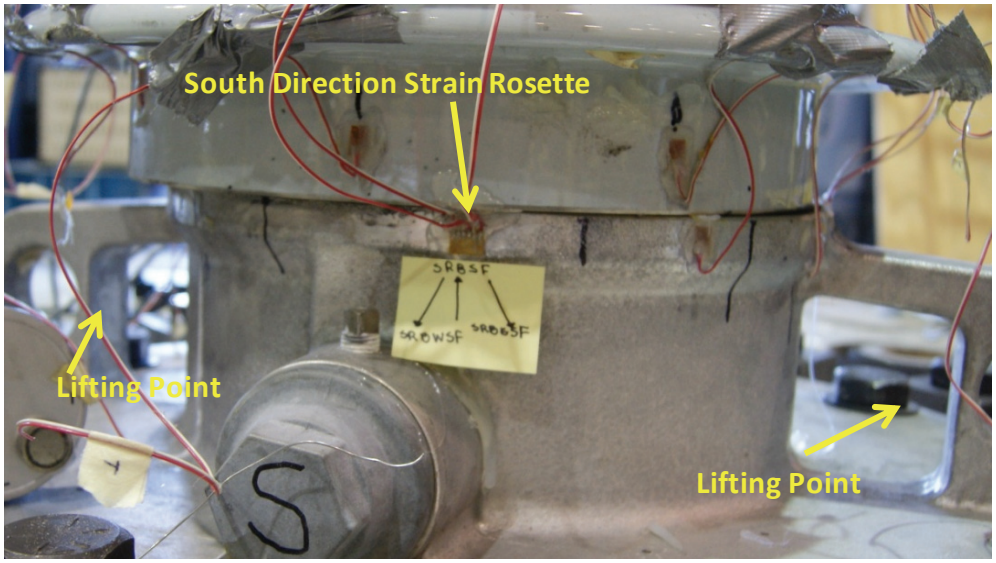

Figure 4-10 Strain Rosette in South Direction

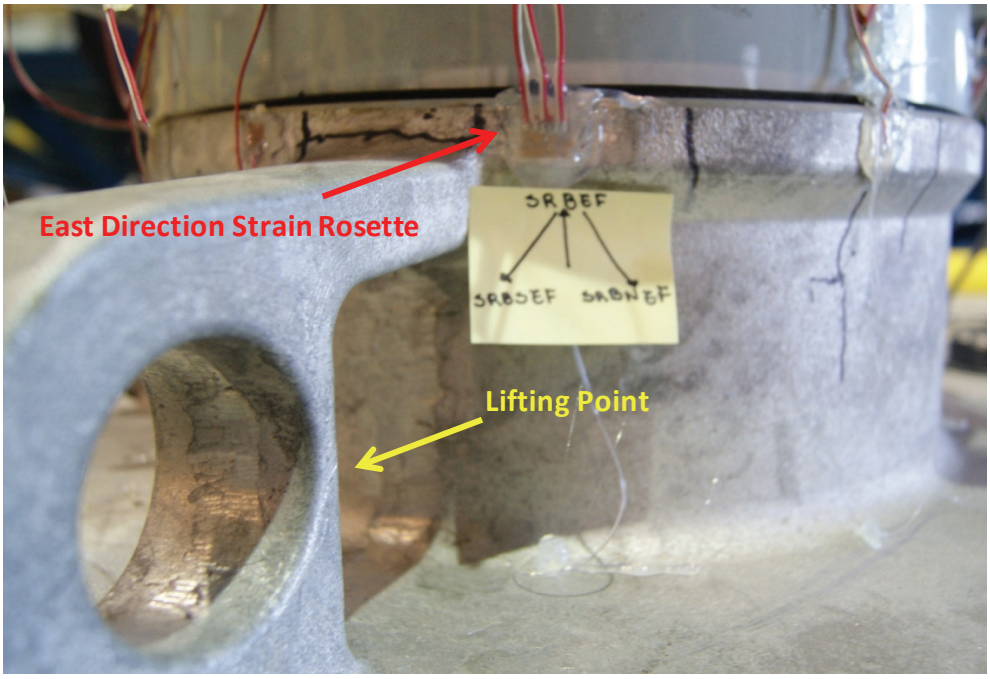

Figure 4-11 Strain Rosette in East Direction

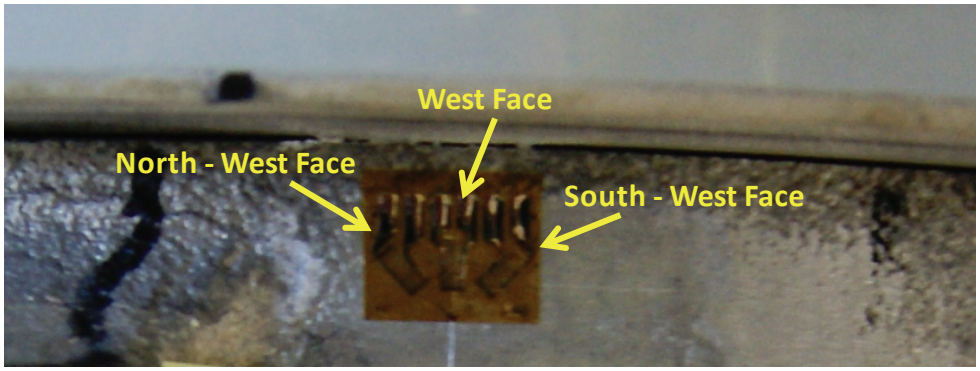

Figure 4-12 Detailed View of the Strain Rosette in West Direction

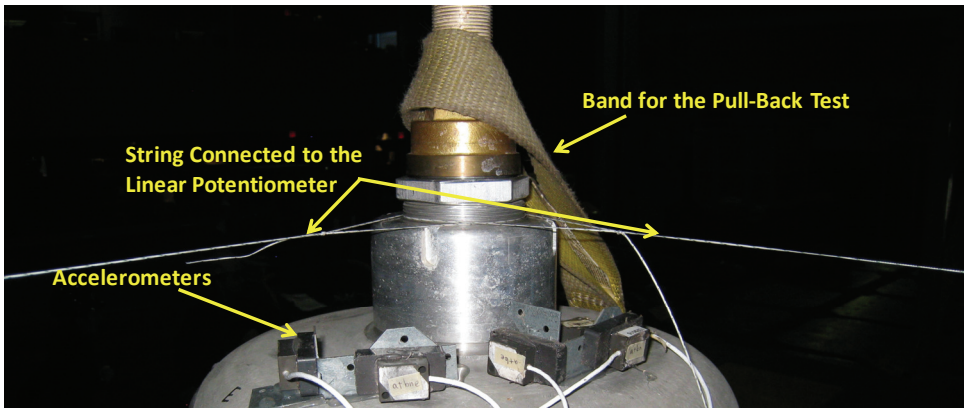

Figure 4-13 Instrumentation Setup during the System Identification Tests

Table 4-2 Instrumentation List for System Identification Testing

Tag Name	Sensor Type	Measurement	Position
ATBV	Accelerometer	Acceleration (g)	Top of the bushing – Vertical
ATBN	Accelerometer	Acceleration (g)	Top of the bushing – North Direction
ATBNE	Accelerometer	Acceleration (g)	Top of the bushing – North East Direction
ATBE	Accelerometer	Acceleration (g)	Top of the bushing – East Direction
ATBSE	Accelerometer	Acceleration (g)	Top of the bushing – South East Direction
DSTE	Linear Potentiometer	Displacement (in)	Top of the bushing – East Direction
DSTN	Linear Potentiometer	Displacement (in)	Top of the bushing – North Direction
SRBWNF	Strain Gauge	Strain (Ustrain)	Base of the bushing – North face and West Direction
SRBNF	Strain Gauge	Strain (Ustrain)	Base of the bushing – North face
SRBENF	Strain Gauge	Strain (Ustrain)	Base of the bushing – North face and East Direction
SRBNEF	Strain Gauge	Strain (Ustrain)	Base of the bushing – East face and North Direction
SRBEF	Strain Gauge	Strain (Ustrain)	Base of the bushing – East face
SRBSEF	Strain Gauge	Strain (Ustrain)	Base of the bushing – East face and South Direction
SRBESF	Strain Gauge	Strain (Ustrain)	Base of the bushing – South face and East Direction
SRBSF	Strain Gauge	Strain (Ustrain)	Base of the bushing – South face
SRBWSF	Strain Gauge	Strain (Ustrain)	Base of the bushing – South face and West Direction
SRBSWF	Strain Gauge	Strain (Ustrain)	Base of the bushing – West face and South Direction
SRBWF	Strain Gauge	Strain (Ustrain)	Base of the bushing – West face
SRBNWF	Strain Gauge	Strain (Ustrain)	Base of the bushing – West face and North Direction
LC	Load Cell	Force (kip)	In series with band for the pull-back test

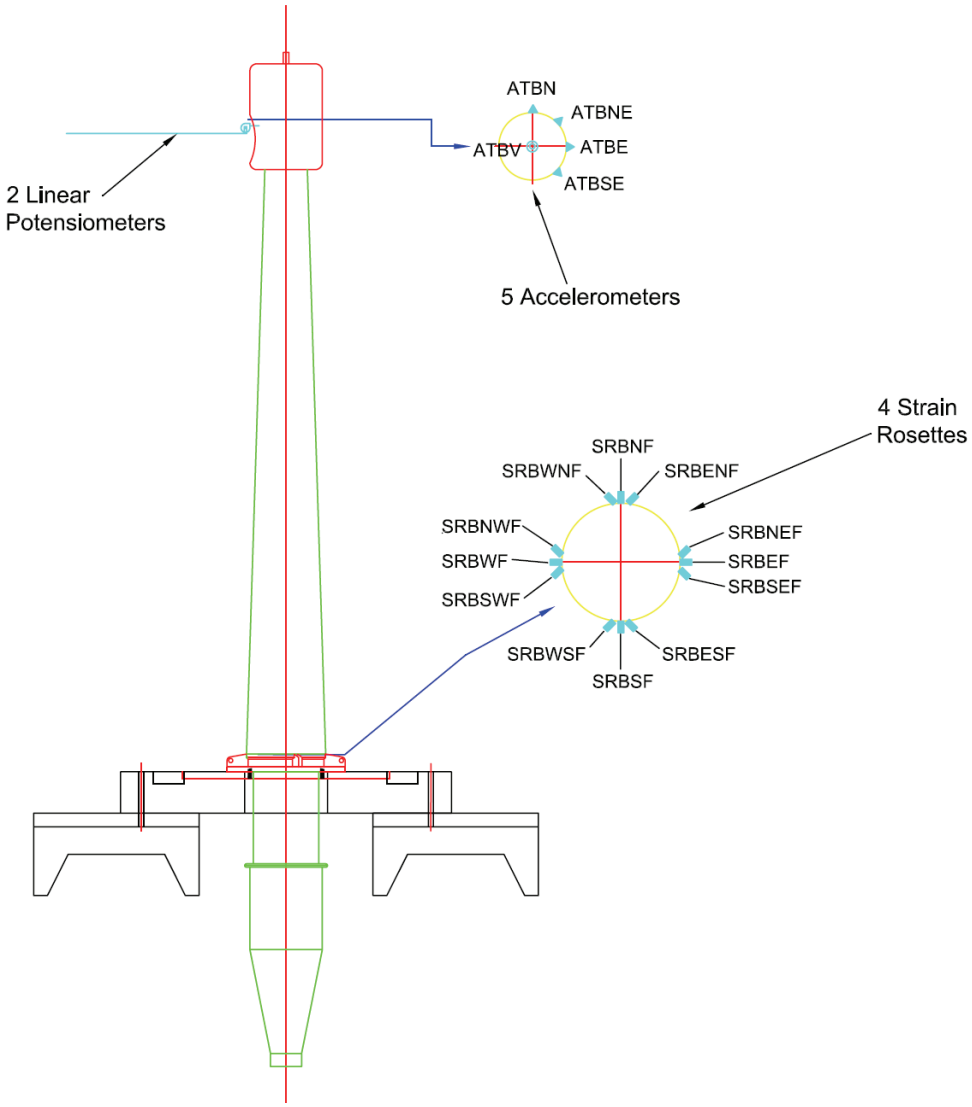

Figure 4-14 View of Total Instrumentation Setup of Bushing Structure

4.4. Test Procedures

The experimental process for the system identification testing was divided into two phases; the impact hammer tests and the pull-back tests. Impact hammer tests were conducted in the North-South, South-East and East-West direction as described in the previous section. As for the pull-back tests, two different forces were applied at the top of the bushing; one of 300lbs and one of 600lbs in both the East-West and North-South directions. The testing sequence which was followed during this experimental investigation is presented in Table 4-3. Note that the force was applied during the pull-back tests by a forklift in the North-South direction, and was applied manually in the East-West direction due to space limitations.

Table 4-3 System Identification Test Sequence

Test ID	Location of Bushing	Test Direction	Test Description
TB - 8 - NS-IH	Concrete Slab	North-South	Impact Hammer Test
TB - 9 -NE-IH	Concrete Slab	North-East	Impact Hammer Test
TB - 10 -EW-IH	Concrete Slab	East-West	Impact Hammer Test
TB - 11 -PL300 EW	Concrete Slab	East-West	300lbs Pull-Back Test at Top
TB - 12 - PL300 NS	Concrete Slab	North-South	300lbs Pull-Back Test at Top
TB - 13 -NS-IH	Concrete Slab	North-South	Impact Hammer Test
TB - 14 -NE-IH	Concrete Slab	North-East	Impact Hammer Test
TB - 15 -EW-IH	Concrete Slab	East-West	Impact Hammer Test
TB - 16 -PL600 NS	Concrete Slab	North-South	600lbs Pull-Back Test at Top
TB - 17 -PL600 EW	Concrete Slab	East-West	600lbs Pull-Back Test at Top

4.5. Test Results

4.5.1. Raw Data

Digitized signals obtained at the end of each test from all the instruments are presented in this section. Note that the experimental results of one series of impact hammer tests and pull-back tests are presented. More specifically, raw data from the following tests are presented: (i) TB-13-NS-IH, (ii) TB-14- NE-IH, (iii) TB-15- EW-IH, (iv) TB-16- PL600 NS and (v) TB-17- PL600 EW. The results are provided in Figure 4-15 to Figure 4-19 in the form of time histories with a sampling rate of 256Hz.

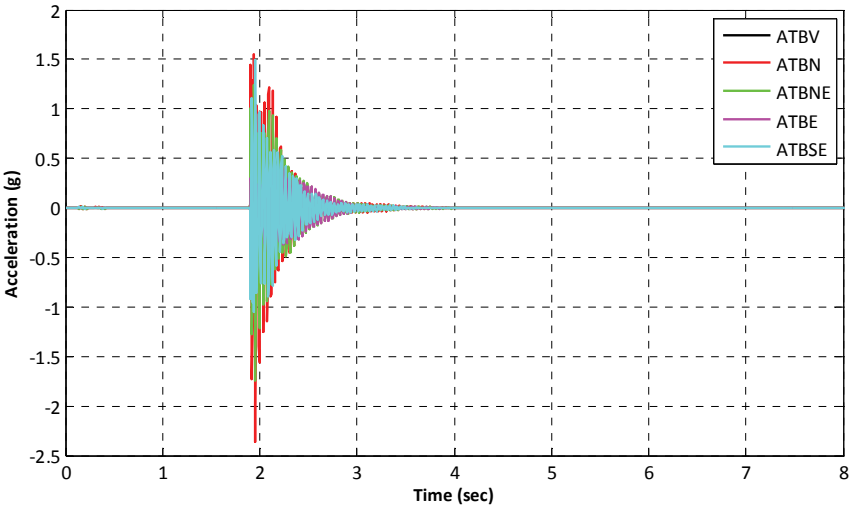

(a)

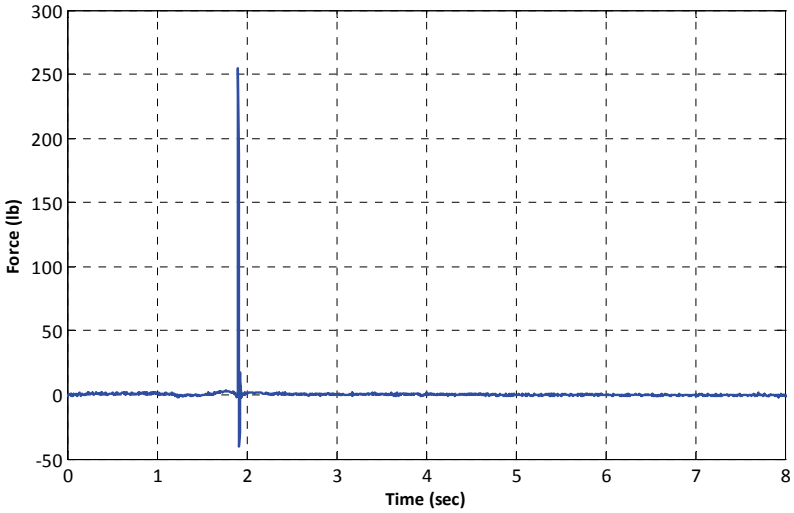

(b)

Figure 4-15 Raw Data from Test TB-13- NS-IH: (a) Acceleration Time Histories and (b) Applied Force Time History

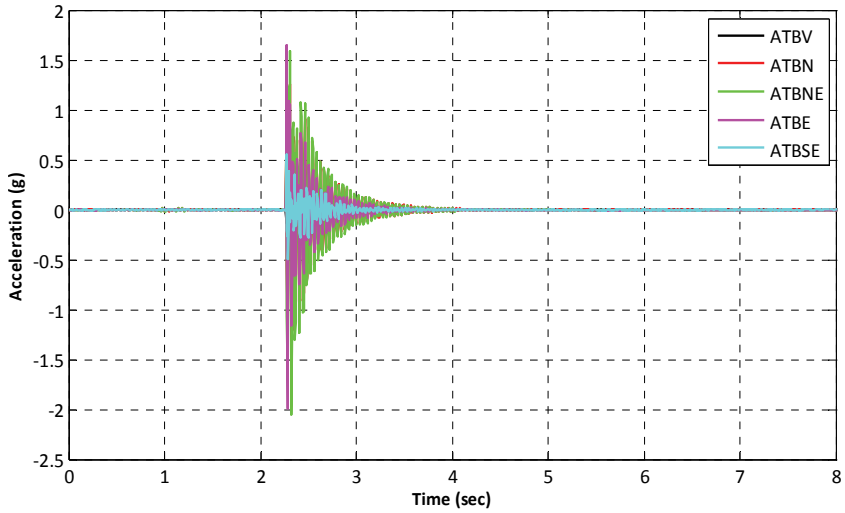

(a)

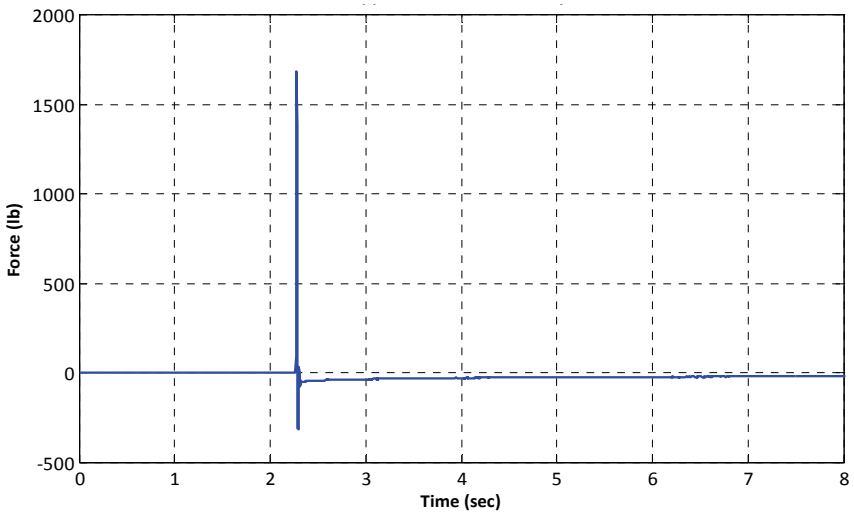

(b)

Figure 4-16 Raw Data from Test TB-14- NE-IH: (a) Acceleration Time Histories and (b) Applied Force Time History

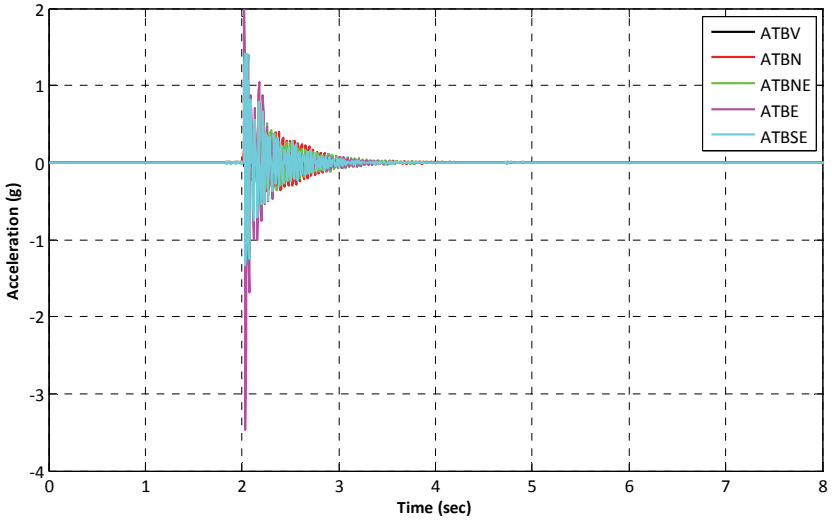

(a)

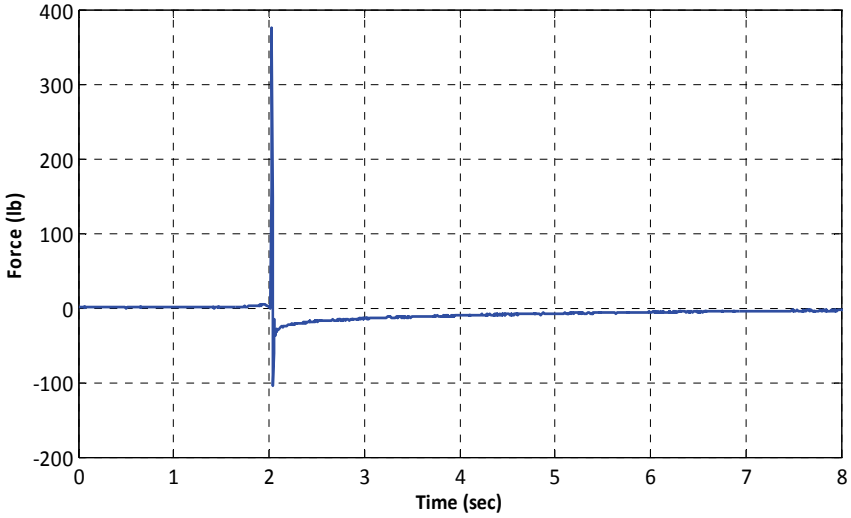

(b)

Figure 4-17 Raw Data from Test TB-15- EW-IH: (a) Acceleration Time Histories and (b) Applied Force Time History

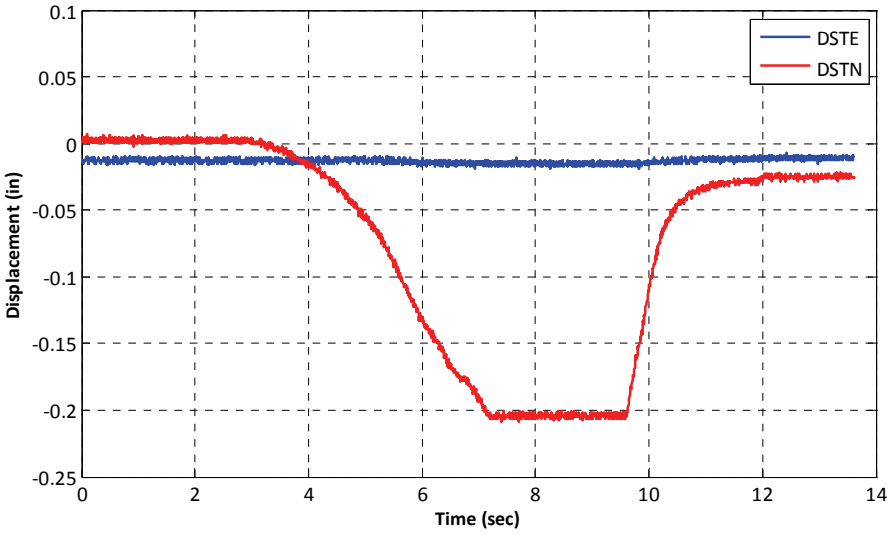

(a)

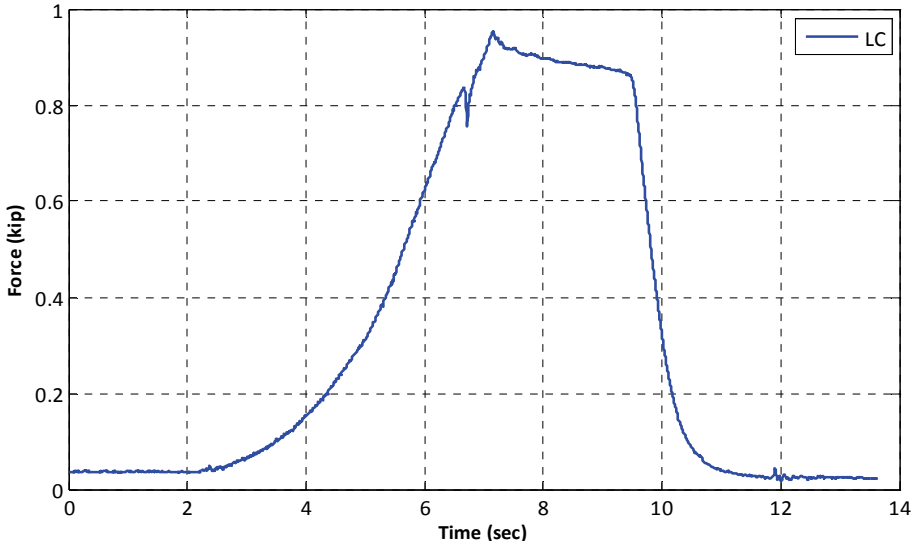

(b)

Figure 4-18 Raw Data from Test TB-16- PL600 NS: (a) Displacement Time Histories and (b) Applied Force Time History

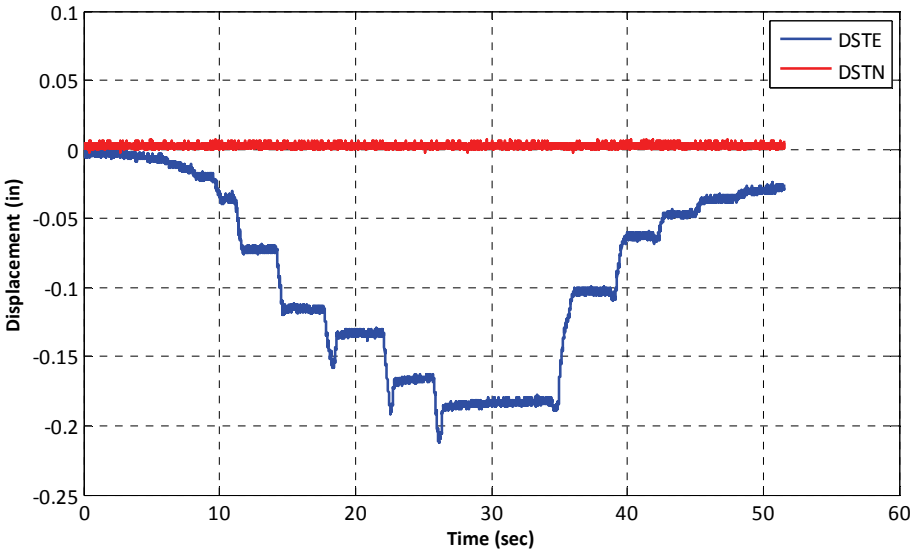

(a)

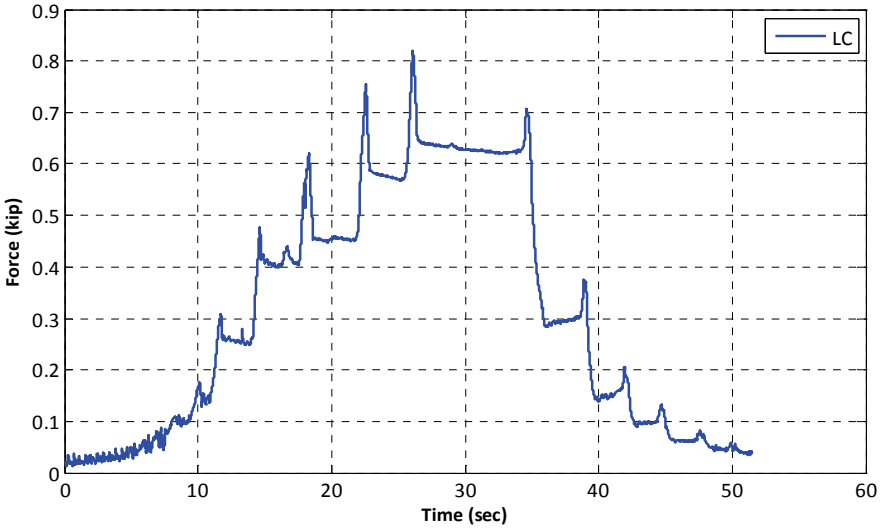

(b)

Figure 4-19 Raw Data from Test TB-17- PL600 EW: (a) Displacement Time Histories and (b) Applied Force Time History

4.5.2. Data Processing

4.5.2.1. Results of Frequency Evaluation Tests

The Fourier Amplitude Spectrum from the acceleration time histories was plotted for each impact hammer test using data collected from the accelerometers. From these plots, the fundamental frequency of the bushing specimen was identified as shown in Figure 4-20. Note that prior to conducting the system identification tests, the fundamental frequency of the 230kV porcelain bushing was expected to vary between 20Hz to 22Hz based on previous experimental and numerical investigations. According to the experimental results of this testing sequence, the fundamental frequency of the bushing was identified to be approximately 25Hz. Based on these results, it may be assumed that the bushing structure was not damaged from the previous experiments.

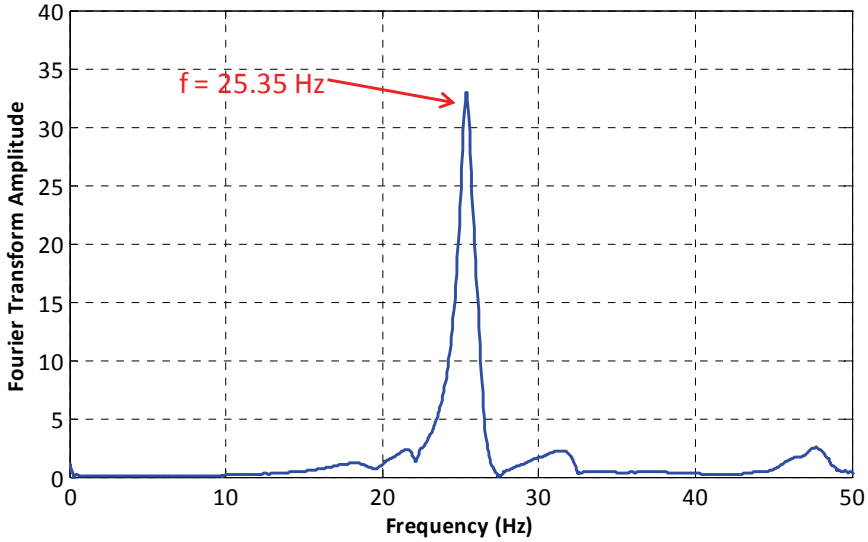

(a)

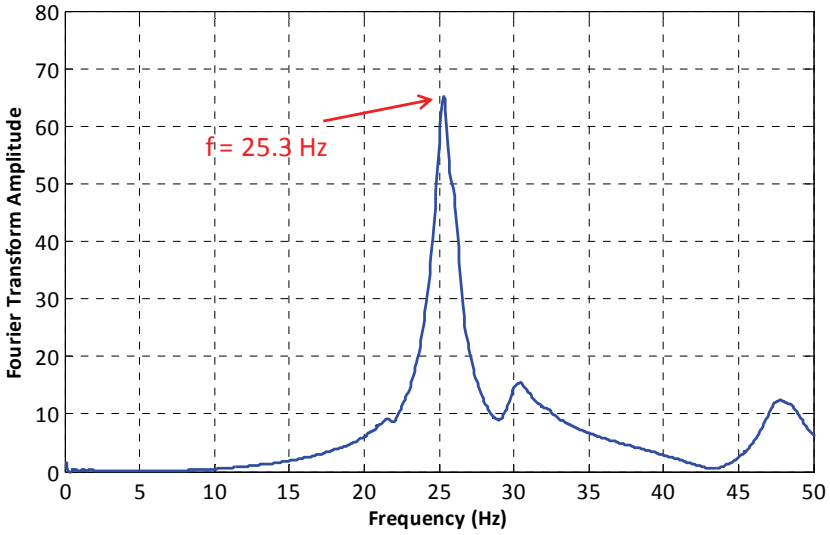

(b)

Figure 4-20 Frequency Results obtained from Impact Hammer Tests: (a) East-West Direction and (b) North-South Direction

4.5.2.2. Results of Damping Ratio Evaluation

The first mode viscous damping ratio of the 230kV porcelain bushing was estimated using the *Half-Power Bandwidth Method*. According to this procedure, the kth mode damping factor, ξ_k, is determined from the frequencies at which the amplitude of the response at the kth natural frequency, ρ_{f_k}, is reduced by $(1/\sqrt{2})$ or frequencies at which the power input is half the input.

The determination of the damping ratio at that mode is presented graphically in Figure 4-21, while mathematically is given by the following equation (Bracci et al., 1992):

$$\xi_k = \frac{f_2 - f_1}{f_2 + f_1} = \frac{f_2 - f_1}{2 f_k} \tag{4-1}$$

where f_2, f_1 are the frequencies when $\rho_{f_1}, \rho_{f_2} = \left(1/\sqrt{2}\right)\rho_{f_k}$ and f_k is the kth natural frequency.

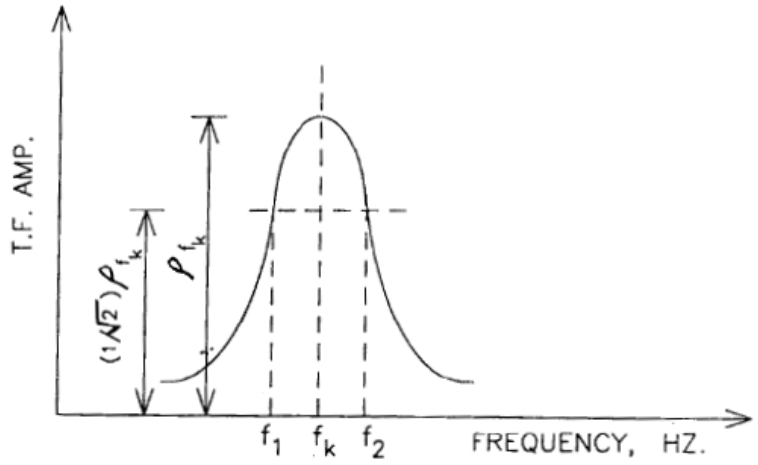

Figure 4-21 Half-Power Bandwidth Method (Bracci et al., 1992)

The results obtained from the impact hammer tests for the modal participation factors are presented in Table 4-4.

Table 4-4 Modal Damping Ratios computed from the Impact Hammer Tests

Test Direction	Frequency (Hz)	Damping Ratio ξ (%)
North-South	25.30	2.3
East-West	25.35	2.1

4.5.2.3. Results of Stiffness Evaluation

The static lateral stiffness of the bushing structure was estimated using the results obtained from the pull-back tests (see Table 4-5). More specifically, the force vs. displacement curves were plotted for the East-West direction of testing, since the instruments in the North-South direction were malfunctioning resulting in noisy measurements. Note that the force displacement curves were developed using the results of the plateau of the displacement time histories and force time histories.

Table 4-5 Stiffness Values Computed from the Pull-Back Tests

Test Direction	Stiffness k (lbs/in)
North-South	4517
East-West	N/A

4.6. Summary

In this section, the system identification testing on a typical porcelain 230kV bushing was presented. More specifically, a detailed presentation including the test specimen, experimental instrumentation, test procedure and recorded data was provided. The section ends with the post-processing of the recorded data from all the identification tests. The following section presents the dynamic (shake table) tests conducted as the second stage of the experimental investigation.

SECTION 5

SEISMIC TESTING

5.1. Introduction

In this section, the second stage of the experimental study is presented. The major objective of the shake table tests, as described in the previous section, was to experimentally investigate the efficiency of the stiffening approach of incorporating flexural stiffeners on the cover plate of the transformer tank and validate the results achieved from the numerical studies. The experimental procedure and the results obtained from the dynamic tests are presented in this section.

5.2. Description of UB SEESL Facility

The seismic tests were performed on one of the two high-performance, six degree of freedom shake tables in the Structural Engineering and Earthquake Simulation Laboratory (SEESL) of the University at Buffalo. The twin shake tables, shown in Figure 5-1 and Figure 5-2, are relocatable and may be rapidly repositioned from being adjacent to being apart up to a distance of 100 feet (center to center). Together, the tables can host specimens of up to 100 metric tons and up to 120 feet long, and subject them to fully in-phase or totally uncorrelated dynamic excitations (see http://seesl.buffalo.edu/).

The parent platform of each shake table is 3.6 meters x 3.6 meters, while their deployable surface may be increased to 7 meters x 7 meters with the installation of extension platforms allowing testing of larger test specimens without significant change in the shake table performance. Note that these extensions can be removed to access the original platforms if required. The theoretical dynamic performance of the twin shake tables is summarized in Table 5-1.

Table 5-1 Theoretical Dynamic Performance of Twin Shake Tables at SEESL (from http://seesl.buffalo.edu/)

Table platform size w/o table extension	3. 6 meter x 3.6 meter
Table size w/ extension platform in place	7 meter x 7 meter
Maximum specimen mass	50 ton maximum / 20 ton nominal
Maximum specimen mass with table extension platform in place	40 ton maximum
Maximum Overturning Moment	46 ton meter
Maximum Off Center Loading Moment	15 ton meter
Frequency of operation	0.1~50 hertz nominal/100 hertz maximum
Nominal Performance	X axis Y axis Z axis
Stroke	±.150 m ±.150 m ±.075 m
Velocity	1250 mm/sec 1250 mm/sec 500 mm/sec
Acceleration	±1.15 g ±1.15 g ±1.15 g (w/20ton specimen)

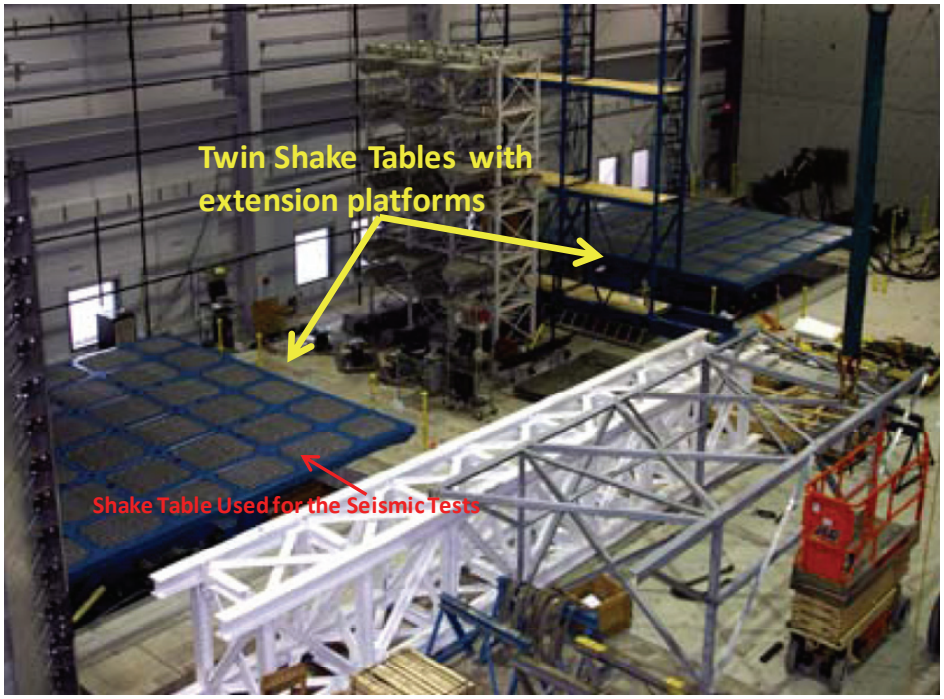

Figure 5-1 Twin Shake Tables of Structural Engineering and Earthquake Simulation Laboratory (SEESL) of the University at Buffalo

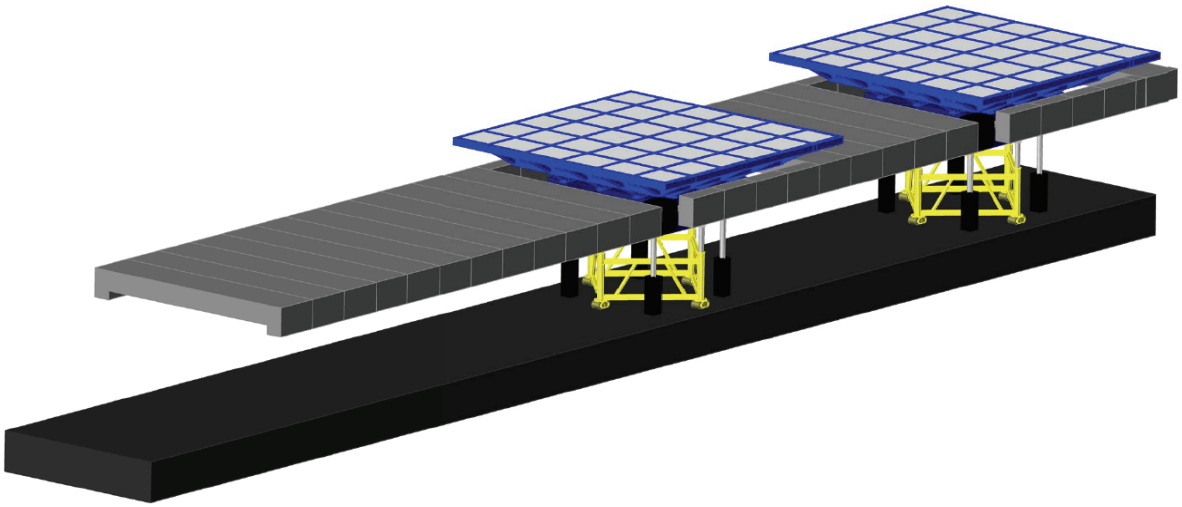

Figure 5-2 3D View of the Structural Engineering and Earthquake Simulation Laboratory (SEESL) of the University at Buffalo Shake Table Facility

5.3. Test Setup Overview

5.3.1. Specimen Description

The specimen used for seismic testing consisted of the 230kV porcelain bushing, described in Section 4, as well as a support structure representing a generic transformer tank (see Figure 5-3). Due to the various structural systems of transformer tanks, developing a supporting frame representative of the lateral stiffness of all transformer tanks of interest appeared to be practically infeasible. Thus, it was considered to be more appropriate to design the support structure stiff enough to prevent amplification of the imposed ground motions in all directions for frequencies below 33Hz (Kong, 2010; Muhammad, 2012).

The support structure consisted of a rigid frame, a relocatable top plate and an adaptor plate (attached at the top plate) as shown in Figure 5-3. The rigid frame was of dimensions 8’ x 8’ x 8’ (height x length x width), while the four faces of the rigid frame were reinforced by cross bracing of angle sections L 5” x 5” x ¾”. Figure 5-5 illustrates a front view of the rigid frame. A steel square tube of TS 5” x 5” x ½” was used for the four columns at the corners, while the top of the columns was connected with angle sections L 5” x 5” x ¾” (Kong, 2010; Muhammad, 2012). The top plate was of dimensions 127” x 127” x ¾”, as shown in Figure 5-7. Note that more bolt holes than those originally needed for this study were drilled on the plate to account for possible relocation of the bushing that might have been required later on in the course of this study.

Finally, the adaptor plate was designed to be placed between the top plate and the bushing mounting flange. Due to the four different bolt hole patterns on the adaptor plate (see Figure 5-6), different types of bushings could be mounted on the support structure (Kong, 2010). Note that for the stiffening of the cover plate, steel angle sections were used (L8"x6"x½" and L6"x4"x½") in different positions in order to simulate the flexural stiffeners' properties.

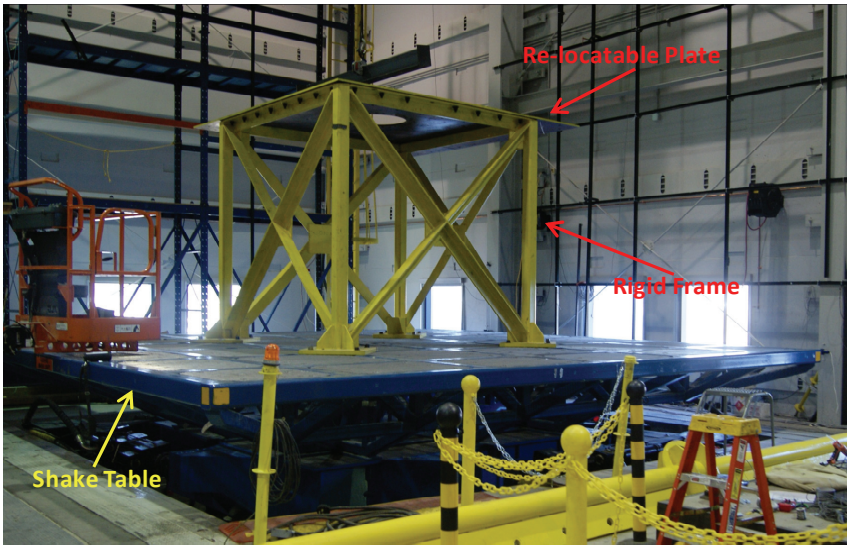

Figure 5-3 Support Structure on the Shake Table

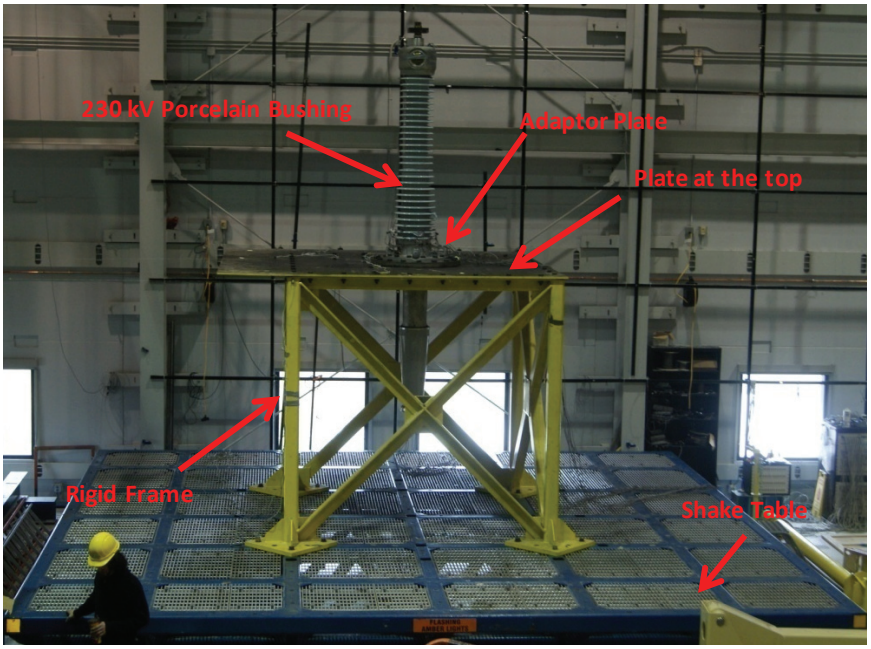

Figure 5-4 Specimen used for Seismic Testing

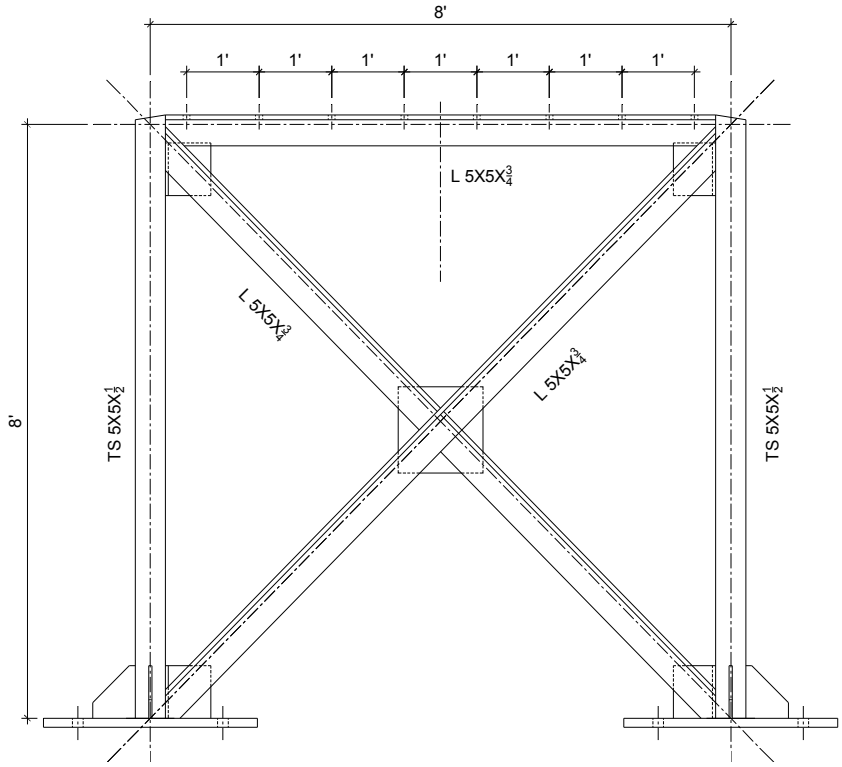

Figure 5-5 Front View of Rigid Frame (Kong, 2010)

Figure 5-6 Adaptor Plate

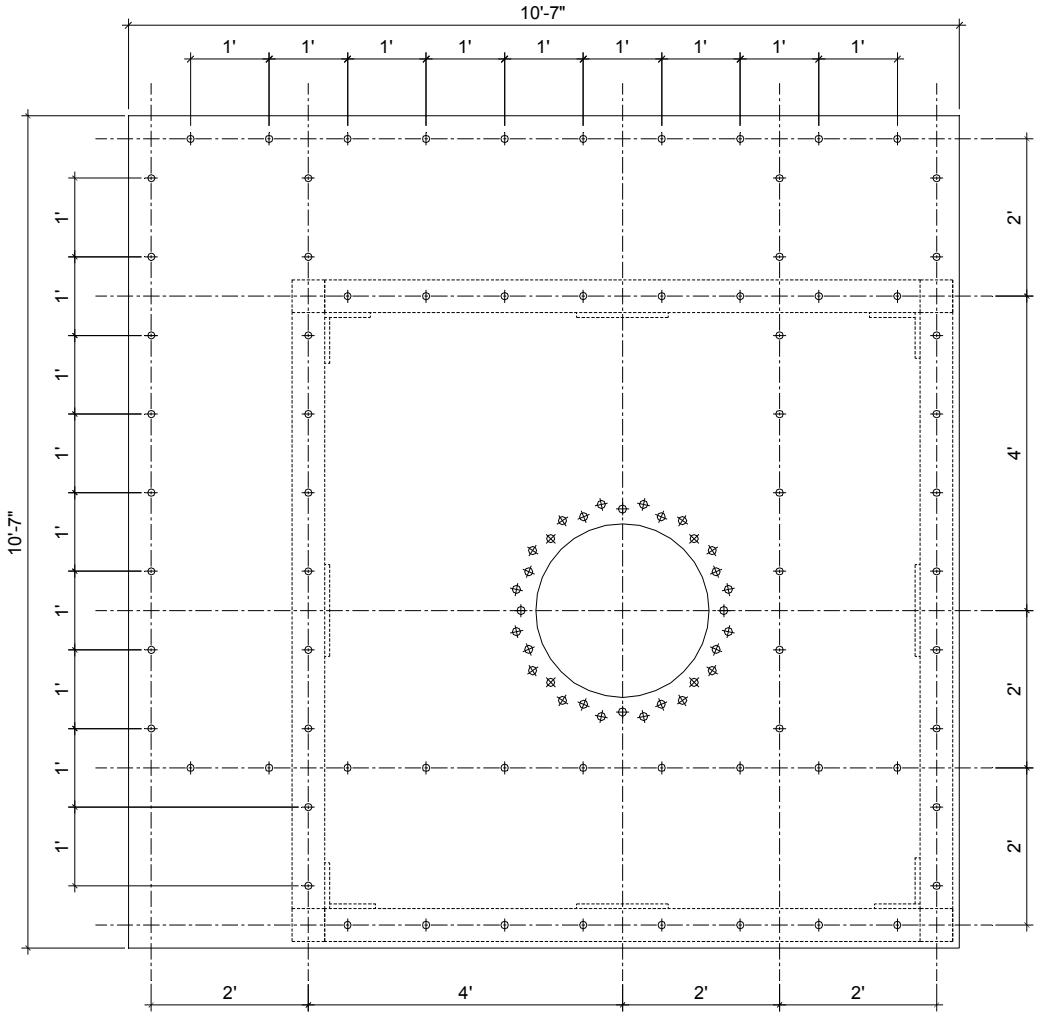

Figure 5-7 Plan View of the Relocatable Plate (Kong, 2010)

5.4. Instrumentation Setup

The dynamic response of the transformer-bushing structure was recorded by more than 40 sensors. More specifically, 20 instruments were installed on the bushing structure (five accelerometers, four strain rosettes -3 strain gauges each one-, two linear potentiometers -string pots- and one load cell). Note that these instruments (accelerometers and strain rosettes) were used to direct measure the moments and shear forces at the base of the bushing structure. In addition, 7 instrumentation channels, consisting of 3 accelerometers (west, south and vertical direction) and 4 linear potentiometers (north-west, north-east, west-north and west-south face) were used in order to measure the dynamic response of the steel/rigid frame. Furthermore, 13 accelerometers were placed on the cover plate: three of them were installed in the north, east and vertical direction in order to record the response of the plate, while the rest (ten), were place on

the cover plate providing measurements in the vertical direction and were distributed along two perpendicular lines close to the bushing base as shown in Figure 5-8. Finally, three accelerometers (north, east and vertical direction) and four linear potentiometers (north-west, north-east, west-north and west-south) were placed on the shake table in order to record the achieved input motions. Details about the type of sensors and their positions on the specimen structure are presented in Table 5-2, while detailed drawings and photos showing the positions of all sensors are provided in Figure 5-8 to Figure 5-11.

Table 5-2 Instrumentation List for System Testing

Tag Name	Sensor Type	Measurement	Position
ATBV	Accelerometer	Acceleration (g)	Top of bushing – Vertical
ATBN	Accelerometer	Acceleration (g)	Top of bushing – North Direction
ATBNE	Accelerometer	Acceleration (g)	Top of bushing – North East Direction
ATBE	Accelerometer	Acceleration (g)	Top of bushing – East Direction
ATBSE	Accelerometer	Acceleration (g)	Top of bushing – South East Direction
AFW	Accelerometer	Acceleration (g)	Rigid Frame – West Direction
AFS	Accelerometer	Acceleration (g)	Rigid Frame – South Direction
AFV	Accelerometer	Acceleration (g)	Rigid Frame – Vertical
ATN	Accelerometer	Acceleration (g)	Shake Table – North Direction
ATV	Accelerometer	Acceleration (g)	Shake Table – Vertical
ATE	Accelerometer	Acceleration (g)	Shake Table – East Direction
APE	Accelerometer	Acceleration (g)	Top of Plate – East Direction
APN	Accelerometer	Acceleration (g)	Top of Plate – North Direction
APV	Accelerometer	Acceleration (g)	Top of Plate – Vertical
APBR1	Accelerometer	Acceleration (g)	Top of Plate – Close to Bushing
APBR2	Accelerometer	Acceleration (g)	Top of Plate – Close to Bushing
APBR3	Accelerometer	Acceleration (g)	Top of Plate – Close to Bushing
APBR4	Accelerometer	Acceleration (g)	Top of Plate – Close to Bushing
APBR5	Accelerometer	Acceleration (g)	Top of Plate – Close to Bushing
APBR6	Accelerometer	Acceleration (g)	Top of Plate – Close to Bushing
APBR7	Accelerometer	Acceleration (g)	Top of Plate – Close to Bushing
APBR8	Accelerometer	Acceleration (g)	Top of Plate – Close to Bushing
APBR9	Accelerometer	Acceleration (g)	Top of Plate – Close to Bushing
APBR10	Accelerometer	Acceleration (g)	Top of Plate – Close to Bushing
DSTE	Linear Potentiometer	Displacement (in)	Top of bushing – East Direction
DSTN	Linear Potentiometer	Displacement (in)	Top of bushing – North Direction

Table 5-2 contd.

SPFNW	Linear Potentiometer	Displacement (in)	Top of Rigid Frame – North West Direction
SPFNE	Linear Potentiometer	Displacement (in)	Top of Rigid Frame – North East Direction
SPFWN	Linear Potentiometer	Displacement (in)	Top of Rigid Frame –West North Direction
SPFWS	Linear Potentiometer	Displacement (in)	Top of Rigid Frame –West South Direction
SPTNW	Linear Potentiometer	Displacement (in)	Shake Table – North West Direction
SPTNE	Linear Potentiometer	Displacement (in)	Shake Table – North East Direction
SPTWN	Linear Potentiometer	Displacement (in)	Shake Table –West North Direction
SPTWS	Linear Potentiometer	Displacement (in)	Shake Table –West South Direction
SRBWNF	Strain Gauge	Strain (Ustrain)	Base of the bushing – North face and West Direction
SRBNF	Strain Gauge	Strain (Ustrain)	Base of the bushing – North face
SRBENF	Strain Gauge	Strain (Ustrain)	Base of the bushing – North face and East Direction
SRBNEF	Strain Gauge	Strain (Ustrain)	Base of the bushing – East face and North Direction
SRBEF	Strain Gauge	Strain (Ustrain)	Base of the bushing – East face
SRBSEF	Strain Gauge	Strain (Ustrain)	Base of the bushing – East face and South Direction
SRBESF	Strain Gauge	Strain (Ustrain)	Base of the bushing – South face and East Direction
SRBSF	Strain Gauge	Strain (Ustrain)	Base of the bushing – South face
SRBWSF	Strain Gauge	Strain (Ustrain)	Base of the bushing – South face and West Direction
SRBSWF	Strain Gauge	Strain (Ustrain)	Base of the bushing – West face and South Direction
SRBWF	Strain Gauge	Strain (Ustrain)	Base of the bushing – West face
SRBNWF	Strain Gauge	Strain (Ustrain)	Base of the bushing – West face and North Direction

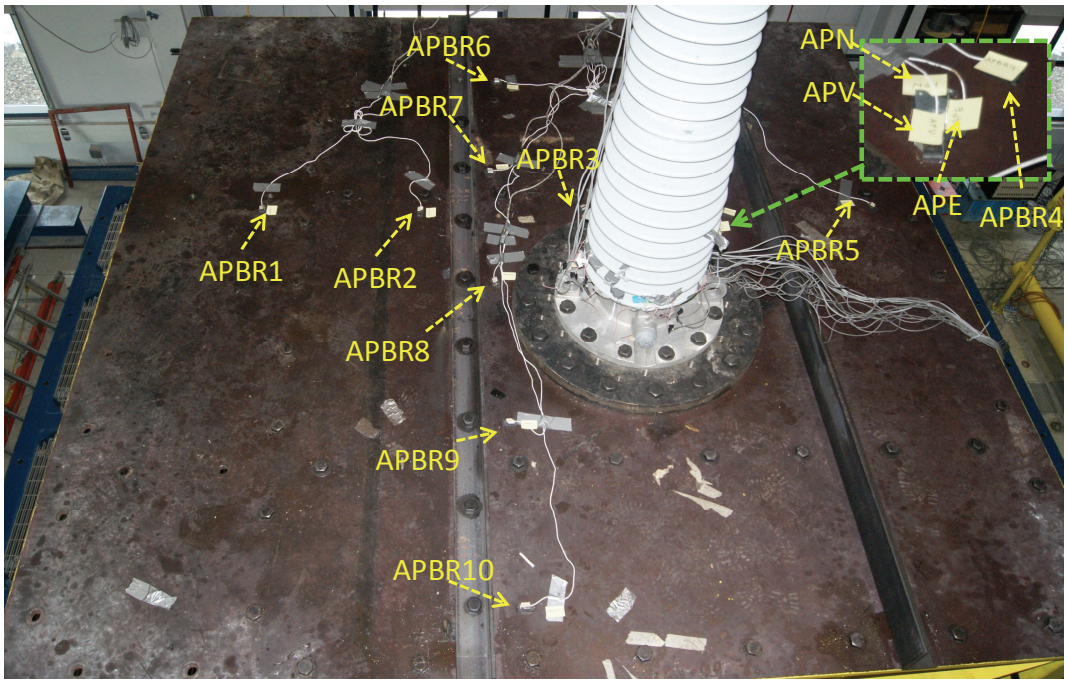

Figure 5-8 Plan View of the Instrumentation Setup on the Top Plate

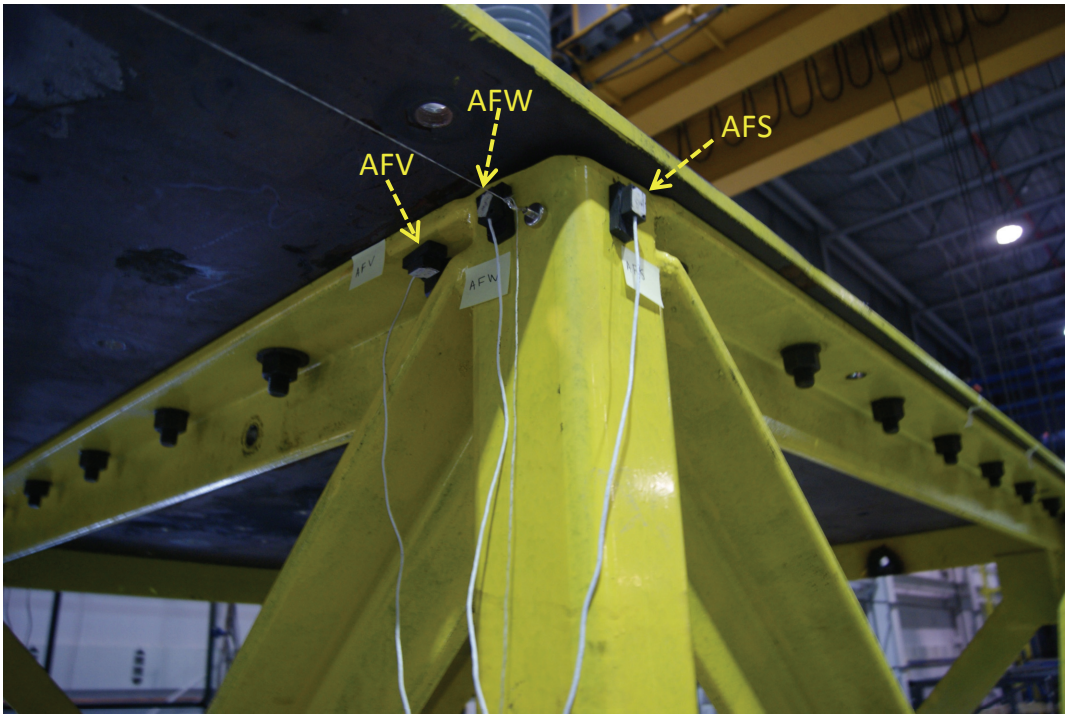

Figure 5-9 Accelerometers on the Rigid Frame

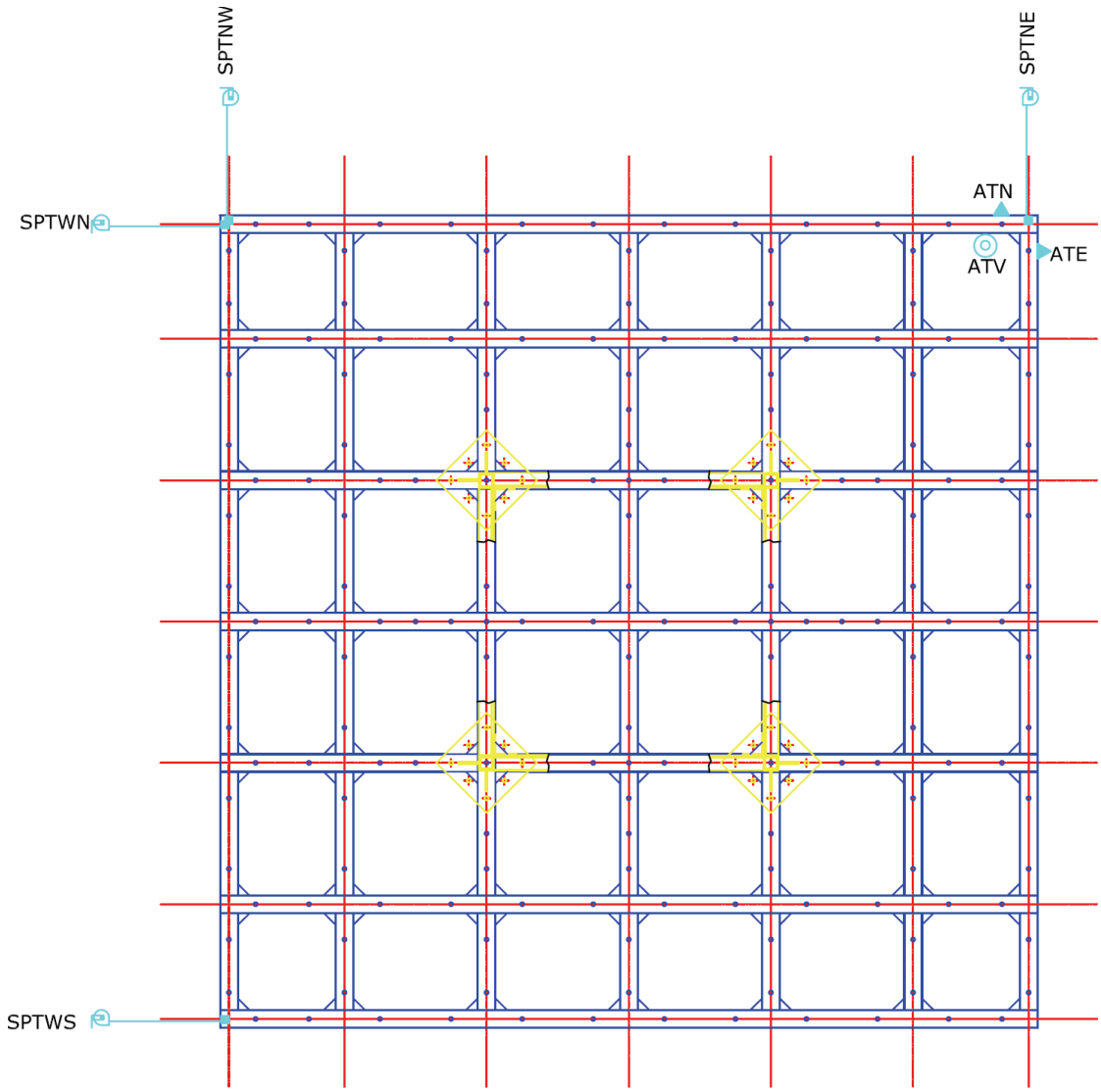

Figure 5-10 Plan View of the Instrumentation Setup of the Shake Table

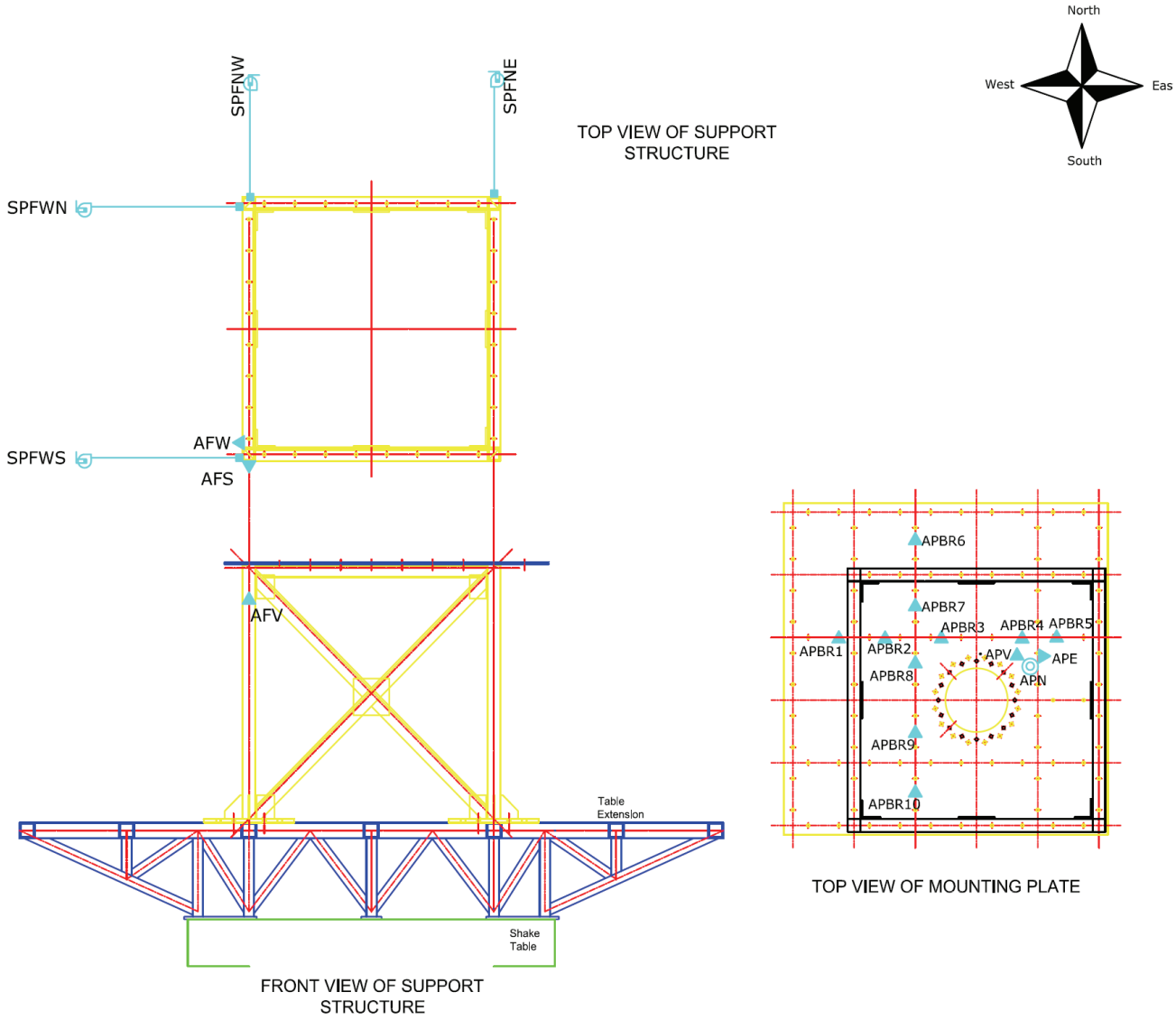

Figure 5-11 Instrumentation Setup of the Support Structure Test Procedures

5.4.1. Test Schedule

The experimental procedure for the seismic testing was divided into three phases: (i) the first phase referred to the specimen stiffened by using flexural stiffeners on the cover (relocatable) plate with the installation of angle sections L8”x6”x½”, (ii) in the second phase, the stiffening case of installing smaller sections of stiffeners (L6”x4”x½”) was investigated, and (iii) in the last phase the test specimen used referred to the unstiffened case (“as installed” conditions). Figure 5-12 illustrates the flexural stiffeners (angle sections) installed in both directions (two at the top of the plate and two at the bottom). Note that during the first phase of testing, the angle sections

installed at the bottom of the plate were fixed (bolted) on the rigid frame, while the angle sections of the second phase of testing were not fixed (shorter sections), as shown in Figure 5-13. Moreover, it has to be mentioned that the testing sequence (see Table 5-3, Table 5-4 and Table 5-5), started with the most efficient approach of adding stiffeners L8"x6"x½", which was expected to result in the least seismic demand (as concluded by the numerical studies in Section 3) and finished with testing the "as installed" bushing, which was the case expected to impose the most seismic demand to the system.

Figure 5-12 Steel Angles Installed on the Plate

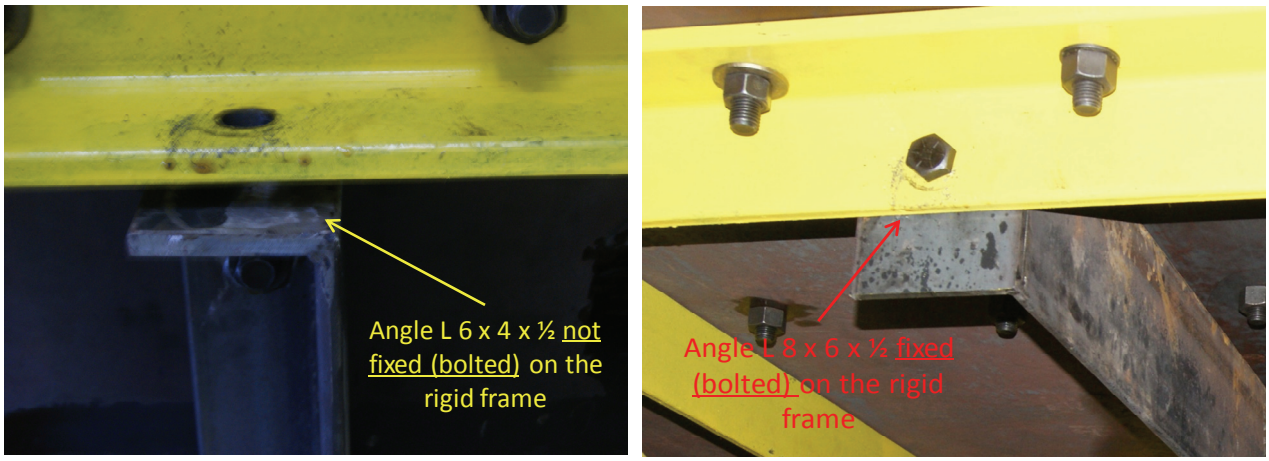

Figure 5-13 Details on the Connections of Steel Angles

Table 5-3 Seismic Test Sequence Phase 1 (Stiffeners L8x6x½ on the plate)

Test ID	Location of Bushing	Test Description
TB - 18 - WN	Center of Frame	White Noise Test (0-50Hz, 0.1 g)
TB - 19 -TBI	Center of Frame	Table Impulse Test
TB - 20 - AHSEST2	Center of Frame	Acceleration Time History Test (EQ 12041)
TB - 21 - WN	Center of Frame	White Noise Test (0-50Hz, 0.1 g)
TB - 22 - TBI	Center of Frame	Table Impulse Test
TB - 23 - AHSEST1	Center of Frame	Acceleration Time History Test (EQ 12011)
TB - 24 - WN	Center of Frame	White Noise Test (0-50Hz, 0.1 g)
TB - 25 - TBI	Center of Frame	Table Impulse Test
TB - 26 - AHSEST3	Center of Frame	Acceleration Time History Test (EQ 12072)
TB - 27 - WN	Center of Frame	White Noise Test (0-50Hz, 0.1 g)
TB - 28 - TBI	Center of Frame	Table Impulse Test
TB - 29 - AHSEST4	Center of Frame	Acceleration Time History Test (EQ 12092)
TB - 30 - WN	Center of Frame	White Noise Test (0-50Hz, 0.1 g)
TB - 31 - TBI	Center of Frame	Table Impulse Test
TB - 32 - AHSEST5	Center of Frame	Acceleration Time History Test (EQ 12132)
TB - 33 - WN	Center of Frame	White Noise Test (0-50Hz, 0.1 g)
TB - 34 - TBI	Center of Frame	Table Impulse Test

Table 5-4 Seismic Test Sequence Phase 2 (Stiffeners L6x4x½ on the plate)

Test ID	Location of Bushing	Test Description
TB - 35 - WN	Center of Frame	White Noise Test (0-50Hz, 0.1 g)
TB - 36 -TBI	Center of Frame	Table Impulse Test
TB - 37 - AHSEST2	Center of Frame	Acceleration Time History Test (EQ 12041))
TB - 38 - WN	Center of Frame	White Noise Test (0-50Hz, 0.1 g)
TB - 39 - TBI	Center of Frame	Table Impulse Test
TB - 40 - AHSEST1	Center of Frame	Acceleration Time History Test (EQ 12011)
TB - 41 - WN	Center of Frame	White Noise Test (0-50Hz, 0.1 g)
TB - 42 - TBI	Center of Frame	Table Impulse Test
TB - 43 - AHSEST3	Center of Frame	Acceleration Time History Test (EQ 12072)
TB - 44 - WN	Center of Frame	White Noise Test (0-50Hz, 0.1 g)
TB - 45 - TBI	Center of Frame	Table Impulse Test
TB - 46 - AHSEST4	Center of Frame	Acceleration Time History Test (EQ 12092)
TB - 47 - WN	Center of Frame	White Noise Test (0-50Hz, 0.1 g)
TB - 48 - TBI	Center of Frame	Table Impulse Test
TB - 49 - AHSEST5	Center of Frame	Acceleration Time History Test (EQ 12132)
TB - 50 - WN	Center of Frame	White Noise Test (0-50Hz, 0.1 g)
TB - 51 - TBI	Center of Frame	Table Impulse Test

Table 5-5 Seismic Test Sequence Phase 3 ("as installed" Bushing)

Test ID	Location of Bushing	Test Description
TB - 52 - WN	Center of Frame	White Noise Test (0-50Hz, 0.1 g)
TB - 53 -TBI	Center of Frame	Table Impulse Test
TB - 54 - AHSEST2	Center of Frame	Acceleration Time History Test (EQ 12041)
TB - 55 - WN	Center of Frame	White Noise Test (0-50Hz, 0.1 g)
TB - 56 - TBI	Center of Frame	Table Impulse Test
TB - 57 - AHSEST1	Center of Frame	Acceleration Time History Test (EQ 12011)
TB - 58 - WN	Center of Frame	White Noise Test (0-50Hz, 0.1 g)
TB - 59 - TBI	Center of Frame	Table Impulse Test
TB - 60 - AHSEST3	Center of Frame	Acceleration Time History Test (EQ 12072)
TB - 61 - WN	Center of Frame	White Noise Test (0-50Hz, 0.1 g)
TB - 62 - TBI	Center of Frame	Table Impulse Test
TB - 63 - AHSEST4	Center of Frame	Acceleration Time History Test (EQ 12092)
TB - 64 - WN	Center of Frame	White Noise Test (0-50Hz, 0.1 g)
TB - 65 - TBI	Center of Frame	Table Impulse Test
TB - 66 - AHSEST5	Center of Frame	Acceleration Time History Test (EQ 12132)
TB - 67 - WN	Center of Frame	White Noise Test (0-50Hz, 0.1 g)
TB - 68 - TBI	Center of Frame	Table Impulse Test

5.4.2. Selection of Input Ground Motions

In order to maintain consistency with the numerical studies, the FEMA P695 Far Field Ground Motion Set (original un-normalized ground motions) was used as input for the seismic tests (FEMA P695, 2009). To limit the number of tests, a reduced ground motion ensemble, consisting of five motions of two components each, was considered, which was selected to be consistent with the initial ensemble of 22 ground motions.

The selection criteria for the reduced ground motion ensemble were: (i) both ensembles have very close values for several statistical measures (e.g. median, arithmetic mean, geometric mean, standard deviation, maximum and minimum) of parameters of interest (e.g. spectral values, PGA, etc.) at a range of frequencies between 10Hz and 25Hz and (ii) the reduced ground motion ensemble included no more than one motion from the same event. The fundamental steps of the selection process are summarized below:

1. For each motion, the geometric mean of $S_{a,xy}$ of the two components ($S_{a,x}$ and $S_{a,y}$) was calculated, such that there was a characteristic parameter for each motion at all frequencies between 10Hz and 25Hz.
2. The geometric mean of the $S_{a,xy}$ in the frequency range of 10Hz to 25Hz was calculated, such that there is one value of the characteristic parameter of each motion at the selected frequency range.
3. The statistical values (median, average, geometric mean, standard deviation, maximum and minimum) of the characteristic parameter were computed for the 22 motions.
4. Based on the value of the characteristic parameter, the motions were listed in ascending order, and different combinations of 5 motions were investigated. The combination that provided statistical values that matched better the statistical values of the 22 motions (or 22 pairs of accelerograms) was the one which was selected for the dynamic tests.

Note that the geometric mean was selected as a characteristic value because it is assumed to provide an orientation-independent measure of earthquake intensity (Boore et al., 2006). The basic concept of this selection process was introduced by Sideris (2008) and also presented in Sideris et al. (2010) for the experimental seismic testing of palletized merchandise in steel storage racks, where ten ground motions were selected out of the forty four of the initial ensemble to be used in seismic tests.

According to the approach described above, five pairs of ground motions were selected to match as close as possible the total twenty two pairs of ground motions of the FEMA P695 Far-Field ground motion ensemble. The selected reduced ensemble is presented in Table 5-6, while a comparison of the statistical parameters of interest for the full and the reduced FEMA P695 Far Field Ground Motion Set is presented numerically in Table 5-7 and in Figure 5-14 and Figure 5-15, graphically. Note that a comparison between the original ensemble of 22 pairs of motions and the reduced ensemble of 5 pairs of motions as well as between the original ensemble of 44 ground motions and the reduced ensemble of 10 ground motions are presented in these figures.

Table 5-6 Motions of Reduced Earthquake Ensemble

EQ. Index	Earthquake Event				Recording Station	PGA(g)
	Name		Year	M_w		
	EQ_ID.	Earthquake				
1	12011	Northridge	1994	6.7	Beverly Hills – Mulhol	0.52
2	12041	Duzce, Turkey	1999	7.1	Bolu	0.82
3	12072	Kobe, Japan	1995	6.9	Shin – Osaka	0.24
4	12092	Landers	1992	7.3	Coolwater	0.42
5	12132	Cape Mendocino	1992	7.0	Rio Dell Overpass	0.55

Table 5-7 Comparison of Statistical Parameters for 2% Damped Spectral Acceleration in the Frequency Range of Interest (10Hz to 25Hz) between the Full and Reduced Ground Motion Sets

Statistical Values	Ensemble of 22 Pairs of EQS	Reduced Ensemble of 5 Pairs of EQS	Ensemble of 44 EQS	Reduced Ensemble of 10 EQS
	Spectral Acceleration (g) for ζ=2%			
Median	0.909	0.924	0.920	0.928
Arithmetic Mean	1.026	1.011	1.031	1.018
Geometric Mean	0.927	0.903	0.927	0.903
Standard Deviation	0.495	0.529	0.501	0.518
Maximum	2.531	1.825	2.751	2.002
Minimum	0.412	0.426	0.353	0.404

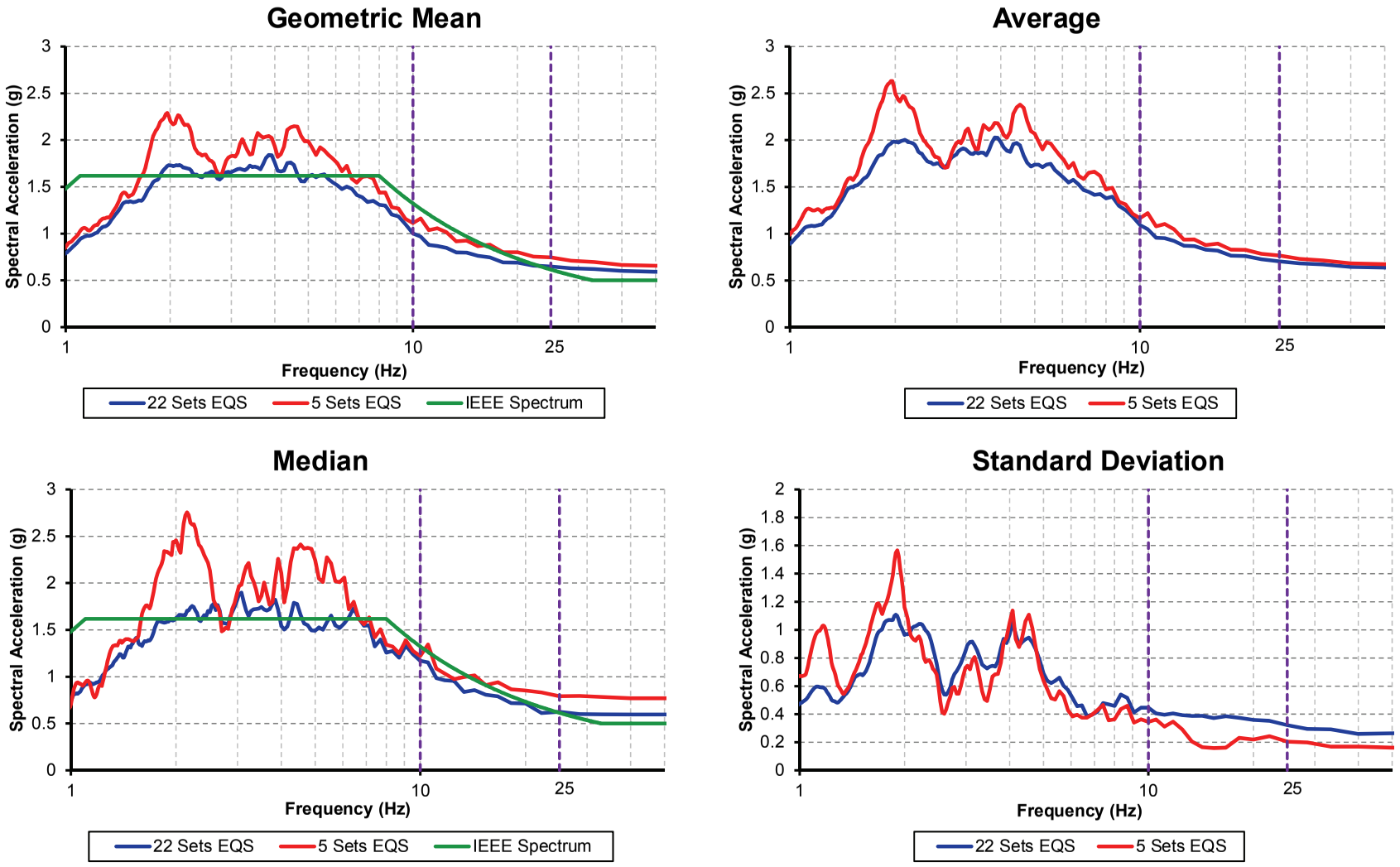

Figure 5-14 Comparison of Statistical Parameters in Full and Reduced Ground Motion Sets (22 Sets and 5 Sets)

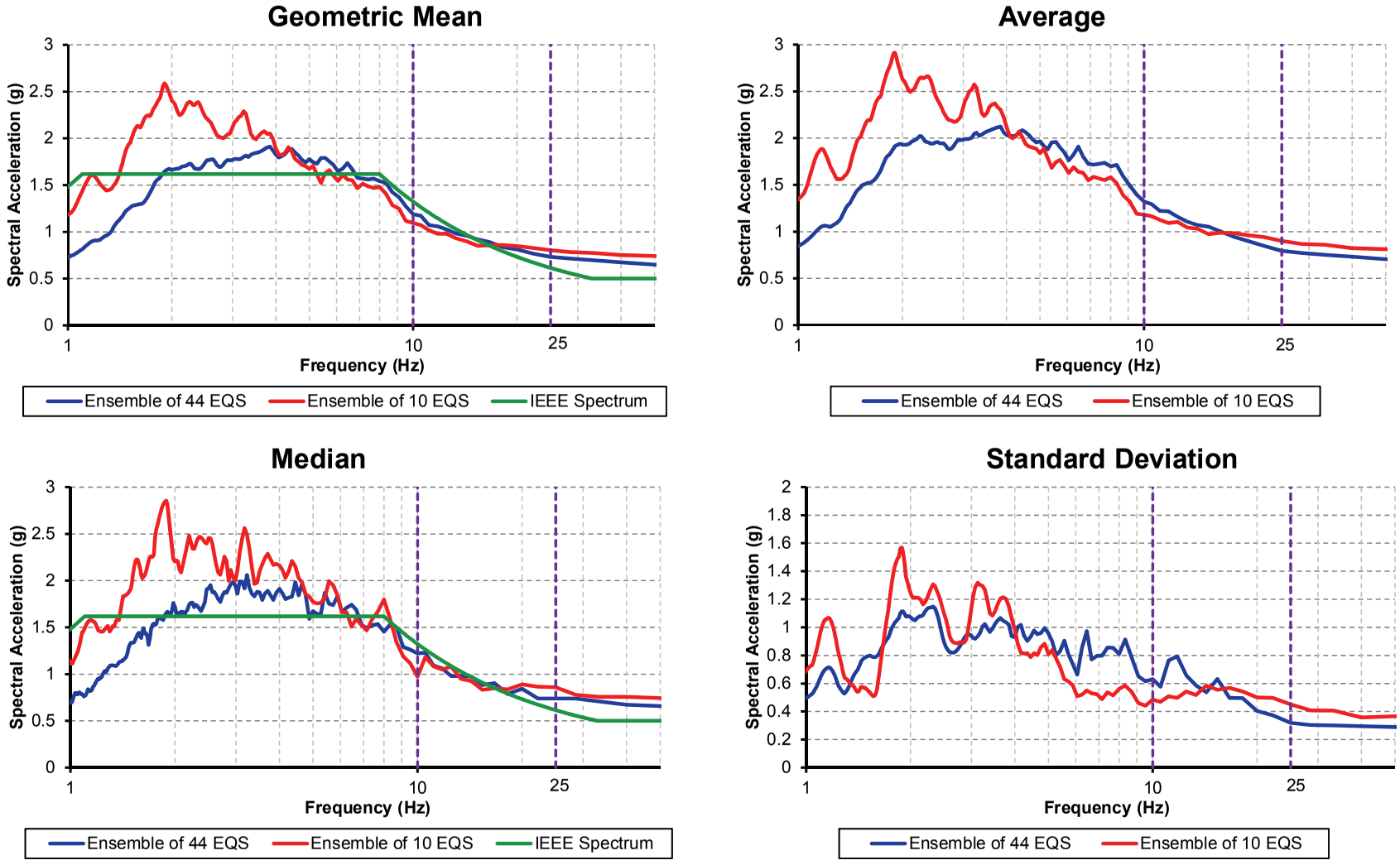

Figure 5-15 Comparison of Statistical Parameters in Full and Reduced Ground Motion Sets (44 EQS and 10 EQS)

5.5. Test Results

5.5.1. Raw Data

In this section, digitized signals obtained from all instruments are presented. For brevity, only one test from each phase was selected and presented. Note that the selected test was the one with the strongest ground motion in terms of peak ground acceleration (ID #: 12041 – Duzce, Turkey). More specifically, raw data from the following tests are presented: (i) TB-20-AHSEST2, (ii) TB-37- AHSEST2, (iii) TB-54- AHSEST2. The results are illustrated in Figure 5-16 to Figure 5-18 in the form of time histories with a sampling rate of 256Hz.

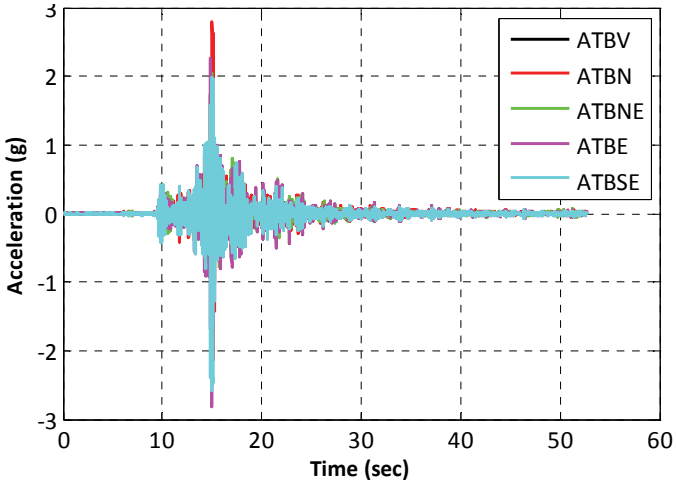

(a)

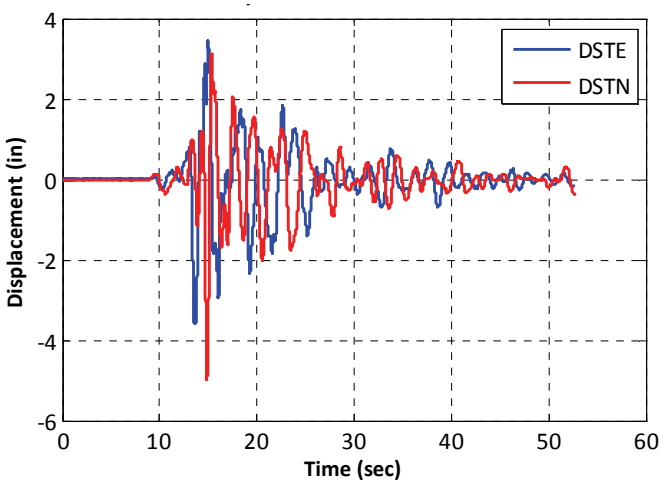

(b)

Figure 5-16 Raw Data from test TB-20- AHSEST2: (a) Acceleration Time Histories and (b) Displacement Time Histories

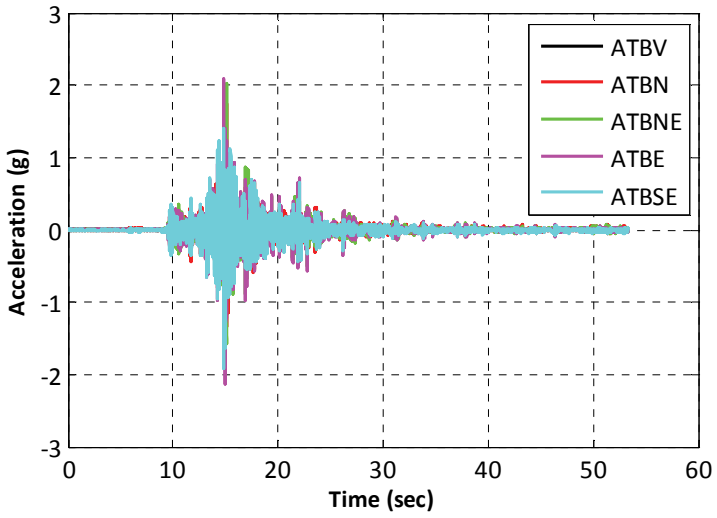

(a)

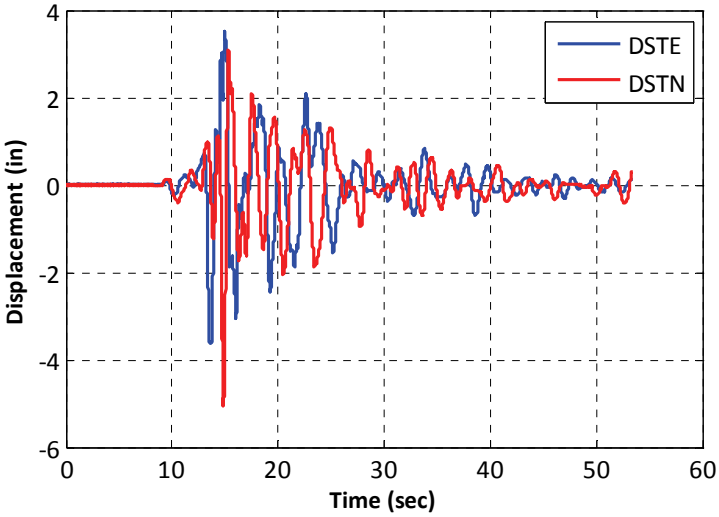

(b)

Figure 5-17 Raw Data from test TB-37- AHSEST2: (a) Acceleration Time Histories and (b) Displacement Time Histories

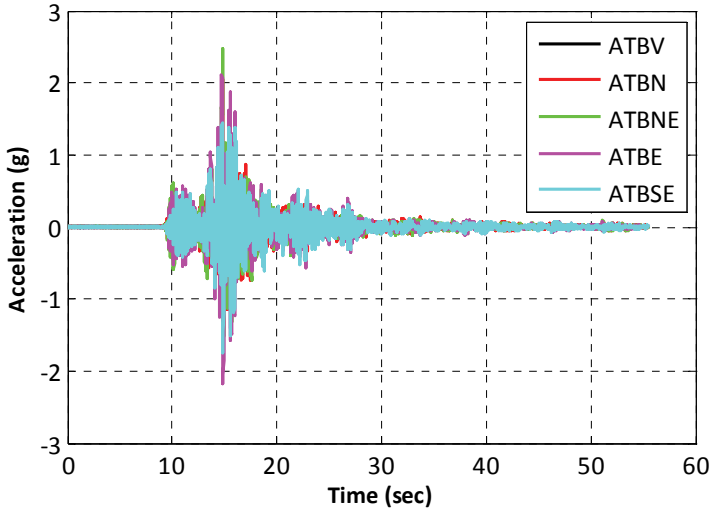

(a)

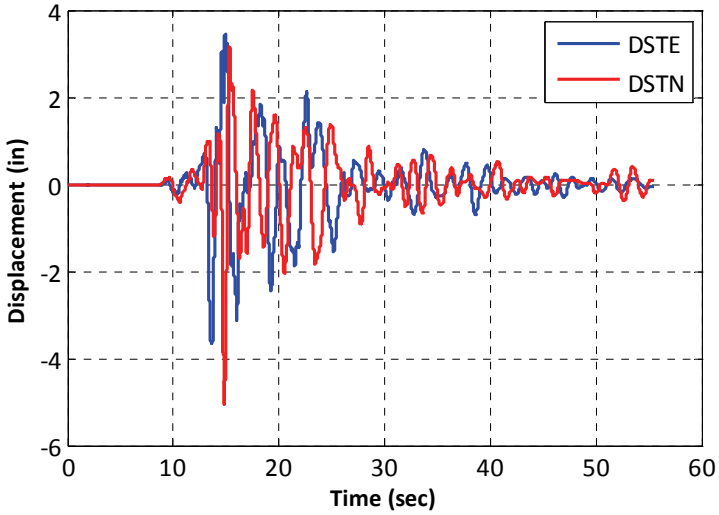

(b)

Figure 5-18 Raw Data from test TB-54- AHSEST2: (a) Acceleration Time Histories and (b) Displacement Time Histories

5.5.2. Data Processing

5.5.2.1. Results of Frequency and Damping Tests

The Fourier Amplitude Spectra of the Acceleration Time Histories were plotted for white noise tests performed during the three phases of the seismic testing. From these plots, the fundamental frequency of the bushing structure was identified as shown in Figure 5-19 for the three different

configurations, which increases with the size of the flexural stiffeners as expected from previous numerical analysis presented in Section 3.

The viscous damping ratio for the first mode of vibration of the 230kV porcelain bushing was estimated using the *Half-Power Bandwidth Method* as described in the previous section. The results obtained for the three different configurations of the specimen are presented in the following table.

Table 5-8 Modal Damping Ratios Computed for Each Test Phase

Test Phase	Frequency (Hz)	Damping Ratio ξ (%)
Phase 1: Stiffeners L8x6x½	16.14	4.1
Phase 2: Stiffeners L6x4x½	15.13	3.2
Phase 3: Bushing "as installed"	10.11	1.9

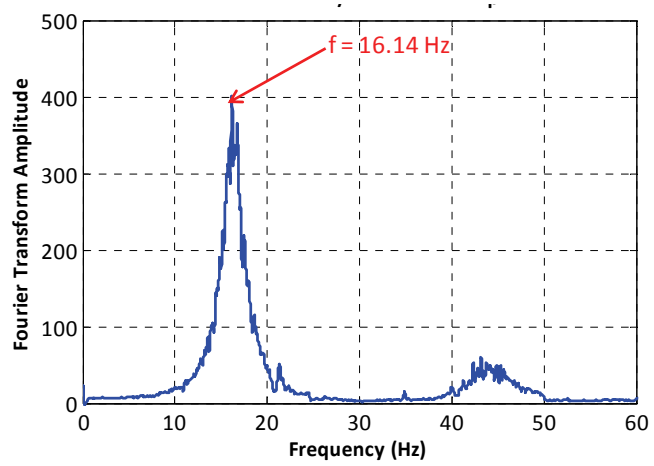

(a)

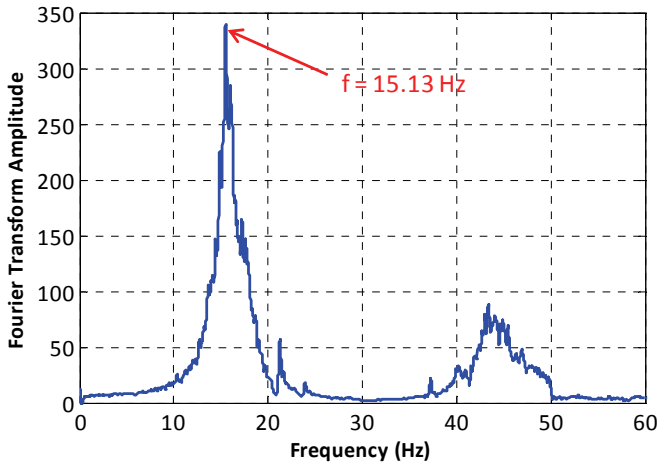

(b)

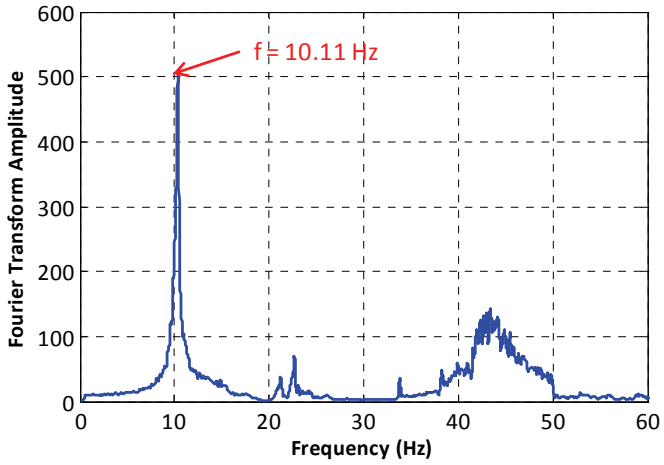

(c)

Figure 5-19 Fundamental Frequency of Bushing Structure in the Three Test Phases: (a) Stiffeners L8x6x½, (b) Stiffeners L6x4x½ and (c) Bushing "as installed"

5.5.2.2. Seismic Response of Bushing

During the data processing, the measurements obtained from all the instruments were used to evaluate the dynamic characteristics of the bushing structure. More specifically, the maximum bending moment and the shear force at the base of the bushing were computed for the first time in two ways: (i) using strain gauge measurements, and (ii) using accelerometer measurements, while the peak displacement and acceleration at the top of the bushing were obtained by linear potentiometer and accelerometer measurements, respectively.

Note that differences in the moment and force results computed with the two approaches were observed as shown in Table 5-9. The moments measured by the strain gauges were larger by 17% than the ones computed from the acceleration measurements, whereas the forces obtained from the strain gauge measurements were smaller by 20% than the ones calculated from the acceleration measurements. Furthermore, the position of the center of inertia of the bushing structure was found to be higher by 39%-130% than the estimated position mentioned in the previous section (see Table 4-1).

Table 5-9 Acceleration and Strain Gauges Measurements

From Accelerometers Measurements						From Strain Gauges Measurements						Ratios –"Strain Gauges" to "Accelerations"							
MOMENTS AT THE BASE (kip-in)												**MOMENTS AT THE BASE (kip-in)**							
Bushing "as installed" (f=10.11Hz)												***Bushing "as installed" (f=10.11Hz)***							
	EQ1	**EQ2**	**EQ3**	**EQ4**	**EQ5**		**EQ1**	**EQ2**	**EQ3**	**EQ4**	**EQ5**		**EQ1**	**EQ2**	**EQ3**	**EQ4**	**EQ5**	**AVG**	**1/AVG**
(1)	(2)	(3)	(4)	(5)	(6)	(7)	(8)	(9)	(10)	(11)	(12)	(1)	(2)	(3)	(4)	(5)	(6)	(7)	(8)
NS	20.57	21.53	4.62	9.78	16.72	**NS**	28.15	27.97	4.87	10.00	19.21	**NS**	1.37	1.30	1.05	1.02	1.15	1.18	0.85
EW	11.29	20.02	7.71	13.01	11.59	**EW**	13.79	25.55	8.43	15.07	12.58	**EW**	1.22	1.28	1.09	1.16	1.09	1.17	0.86
SRSS	23.47	29.40	8.98	16.28	20.34	**SRSS**	31.35	37.88	9.74	18.09	22.96	**SRSS**	1.34	1.29	1.08	1.11	1.13	1.19	0.84
Stiffeners L6x4x1/2 (f=15.13Hz)												***Stiffeners L6x4x1/2 (f=15.13Hz)***							
NS	13.06	14.98	3.37	8.01	8.53	**NS**	23.33	21.98	6.85	13.83	18.82	**NS**	1.79	1.47	2.03	1.73	2.21	1.84	0.54
EW	8.01	16.24	3.34	5.84	7.40	**EW**	14.31	14.09	5.43	6.56	8.78	**EW**	1.79	0.87	1.62	1.12	1.19	1.32	0.76
SRSS	15.32	22.10	4.75	9.92	11.29	**SRSS**	27.37	26.10	8.74	15.31	20.77	**SRSS**	1.79	1.18	1.84	1.54	1.84	1.64	0.61
Stiffeners L8x6x1/2 (f=16.14Hz)												***Stiffeners L8x6x1/2 (f=16.14Hz)***							
NS	11.95	10.08	3.81	9.14	8.64	**NS**	22.44	11.99	4.56	10.01	10.89	**NS**	1.88	1.19	1.20	1.10	1.26	1.32	0.76
EW	9.18	13.70	4.14	6.27	7.34	**EW**	13.57	16.88	6.50	7.15	10.60	**EW**	1.48	1.23	1.57	1.14	1.44	1.37	0.73
SRSS	15.07	17.01	5.62	11.08	11.33	**SRSS**	26.23	20.70	7.94	12.30	15.20	**SRSS**	1.74	1.22	1.41	1.11	1.34	1.36	0.73
SHEAR FORCE AT THE BASE (kip)												**SHEAR FORCE AT THE BASE (kip)**							
Bushing "as installed" (f=10.11Hz)												***Bushing "as installed" (f=10.11Hz)***							
NS	1.47	1.54	0.33	0.70	1.19	**NS**	1.30	1.32	0.37	0.64	0.75	**NS**	0.88	0.86	1.13	0.92	0.63	0.88	1.13
EW	0.81	1.43	0.55	0.93	0.83	**EW**	0.70	0.85	0.50	0.54	0.69	**EW**	0.86	0.59	0.91	0.58	0.84	0.76	1.32
SRSS	1.68	2.10	0.64	1.16	1.45	**SRSS**	1.48	1.57	0.63	0.84	1.02	**SRSS**	0.88	0.75	0.97	0.72	0.70	0.81	1.24
Stiffeners L6x4x1/2 (f=15.13Hz)												***Stiffeners L6x4x1/2 (f=15.13Hz)***							
NS	0.93	1.07	0.24	0.57	0.61	**NS**	0.76	0.99	0.28	0.54	0.52	**NS**	0.82	0.93	1.16	0.95	0.85	0.94	1.06
EW	0.57	1.16	0.24	0.42	0.53	**EW**	0.18	0.37	0.10	0.16	0.19	**EW**	0.32	0.32	0.44	0.39	0.36	0.36	2.76
SRSS	1.09	1.58	0.34	0.71	0.81	**SRSS**	0.79	1.06	0.30	0.57	0.55	**SRSS**	0.72	0.67	0.88	0.80	0.69	0.75	1.33
Stiffeners L8x6x1/2 (f=16.14Hz)												***Stiffeners L8x6x1/2 (f=16.14Hz)***							
NS	0.85	0.72	0.27	0.65	0.61	**NS**	0.79	1.05	0.21	0.47	0.50	**NS**	0.93	1.45	0.76	0.72	0.81	0.94	1.07
EW	0.66	0.88	0.30	0.45	0.52	**EW**	0.34	0.44	0.18	0.28	0.41	**EW**	0.52	0.50	0.62	0.63	0.78	0.61	1.64
SRSS	1.08	1.14	0.40	0.79	0.80	**SRSS**	0.86	1.14	0.28	0.55	0.64	**SRSS**	0.80	1.00	0.69	0.69	0.80	0.80	1.26
MOMENT TO SHEAR FORCE RATIOS (in)												**MOMENT TO SHEAR FORCE RATIOS (in)**							
Bushing "as installed" (f=10.11Hz)												***Bushing "as installed" (f=10.11Hz)***							
NS	14.00	14.00	13.97	14.00	14.01	**NS**	21.65	21.16	13.01	15.54	25.70	**NS**	1.55	1.51	0.93	1.11	1.83	1.39	0.72
EW	14.00	14.00	14.00	14.00	14.00	**EW**	19.77	30.11	16.83	27.74	18.15	**EW**	1.41	2.15	1.20	1.98	1.30	1.61	0.62
Stiffeners L6x4x1/2 (f=15.13Hz)												***Stiffeners L6x4x1/2 (f=15.13Hz)***							
NS	14.00	14.00	14.15	14.00	14.00	**NS**	30.54	22.12	24.78	25.54	36.13	**NS**	2.18	1.58	1.75	1.82	2.58	1.98	0.50
EW	14.00	14.00	14.15	14.00	14.00	**EW**	30.54	22.12	24.78	25.54	36.13	**EW**	2.18	1.58	1.75	1.82	2.58	1.98	0.50
Stiffeners L8x6x1/2 (f=16.14Hz)												***Stiffeners L8x6x1/2 (f=16.14Hz)***							
NS	14.00	14.00	14.00	13.98	14.16	**NS**	28.34	11.44	21.91	21.32	21.96	**NS**	2.02	0.82	1.57	1.53	1.55	1.50	0.67
EW	14.00	15.58	14.00	14.00	14.00	**EW**	39.95	38.08	35.64	25.41	25.77	**EW**	2.85	2.44	2.55	1.82	1.84	2.30	0.43

These observed differences in the results may be easily proven by the theoretical investigation that follows.

The demand at the base of the bushing structure is a function of the inertia forces and damping as shown according to the following equations assuming an approximation of mass and acceleration distribution as illustrated in Figure 5-20.

$$V_B = \int_0^H m(z)\cdot a(z)\,dz + c(z)v(z)\,dz$$
$$M_B = \int_0^H m(z)\cdot a(z)\cdot z\,dz + c(z)\cdot v(z)\cdot z\,dz \qquad (5\text{-}1)$$

where $m(z)$, $a(z)$, $c(z)$ and $v(z)$ are the mass, acceleration, damping, velocity profiles along the height z of the bushing structure

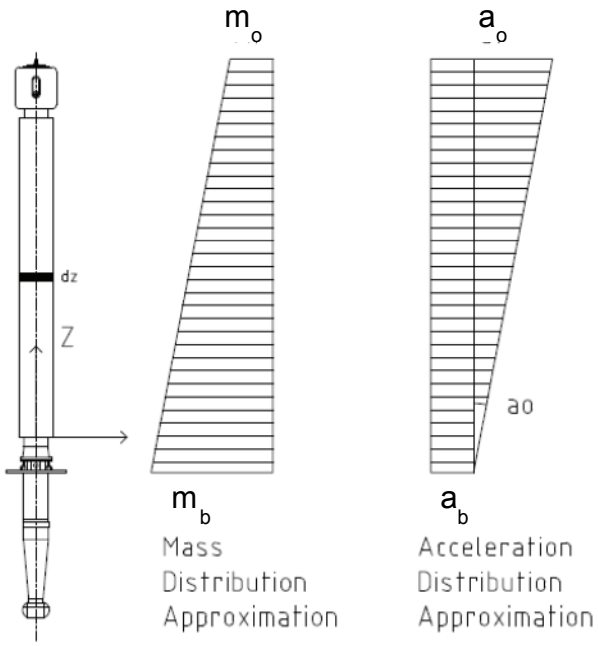

Figure 5-20 Mass and Acceleration Approximated Distribution

The damping force, which contributes with an out-of phase behavior, may be excluded. However, by neglecting the damping, the first term of equation (5-1) is dominant, and therefore the forces become dependent on mass and acceleration response distributions ($m(z)$ and $a(z)$)

as presented in equation (5-2). Note that the general expression of equation (5-2) can be further simplified depending on the mass and acceleration response distributions along the height of the bushing. Two different assumptions of the acceleration profile were considered: (i) *uniform acceleration distribution* and (ii) *linearly variable acceleration distribution*.

$$V_B = \int_0^H m(z) \cdot a(z)\, dz$$
$$M_B = \int_0^H m(z) \cdot a(z) \cdot z dz \tag{5-2}$$

1. *Uniform Acceleration ($a(z) = a_o$)*

For a uniform acceleration profile, the shear force and the moment at the base of the bushing can be computed according to equation (5-3). Note that this approach is based on the assumption that a_o is measured at an arbitrary or crudely approximated point in space, z_{CG},defined as "center of gravity CG". The parameter z_{CG} must not be arbitrary, but the precise result of the mass distribution of all components of the bushing above the flange. Therefore, with the distribution assumed constant and the approximated location of the center of the mass, the acceleration values determined using the above formulas are only rough approximations.

$$V_B = a_b \int_0^H m(z)\, dz = \frac{W}{g} a_b = \frac{W}{g} a_{CG}$$
$$M_B = a_b \int_0^H m(z)\, z\, dz = a_b \int_0^H m(z)\, dz \times \frac{\int_0^H m(z)\, z\, dz}{\int_0^H m(z)\, dz} = \frac{W}{g} a_b Z_{CG} = \frac{W}{g} a_{CG} Z_{CG} \tag{5-3}$$

where W is the weight of the bushing structure above the flange section

2. *Linearly variable acceleration distribution*

By assuming a different acceleration distribution from the one described above, where acceleration is not uniform, but varies linearly, and the mass is also linearly varying along the

height as per equations (5-4) and (5-5), while the base shear and moment can be computed from equations (5-6) and (5-7), respectively.

$$a(z) = a_b + (a_o - a_b)\left(\frac{z}{H}\right) \tag{5-4}$$

$$m(z) = m_b - (m_b - m_o)\left(\frac{z}{H}\right) \tag{5-5}$$

where a_o is the acceleration at the top of the bushing structure, a_b is the acceleration at the base of the bushing structure, m_o is the mass at the top of the bushing structure and m_b is the mass at the base of the bushing structure

The shear force can be calculated as:

$$\begin{aligned} V_B &= \int_0^H \left[m_b - (m_b - m_o)\left(\frac{z}{H}\right)\right]\left[a_b + (a_o - a_b)\left(\frac{z}{H}\right)\right] dz \Rightarrow \\ V_B &= \frac{m_b H a_o}{6}\left[(2a_b / a_o + 1) + \frac{m_o}{m_b}(a_b / a_o + 2)\right] \end{aligned} \tag{5-6}$$

Similarly, the moment at the base of the bushing structure shall be computed as:

$$\begin{aligned} M_B &= \int_0^H \left[m_b - (m_b - m_o)\left(\frac{z}{H}\right)\right]\left[a_b + (a_o - a_b)\left(\frac{z}{H}\right)\right] z dz \Rightarrow \\ M_B &= \frac{m_b H^2 a_o}{12}\left[(a_b / a_o + 1) + \frac{m_o}{m_b}(a_b / a_o + 3)\right] \end{aligned} \tag{5-7}$$

Summarizing the cases presented above, the moment and shear force values can vary based on the assumptions made for the mass and acceleration profile. More specifically:

- ✓ If $a_o = a_b \; and \; m_o = m_b$ (constant acceleration and mass distribution), the moment and the shear force at the base of the bushing are:

  $$V_1 = m_b H a_o \; and \; M_1 = \frac{m_b H^2 a_o}{2}$$

- ✓ If $a_b = 0 \, and \, m_o = m_b$ (inverted triangular acceleration and constant mass), the moment and the shear force at the base of the bushing are:

$$V_2 = \frac{m_b H a_o}{2} = \frac{V_1}{2} = 0.50 \, V_1 \, and \, M_2 = \frac{m_b H^2 a_o}{3} = \frac{M_1}{1.5} = 0.667 M_1$$

- ✓ If $a_b = 0 \, and \, m_o = \frac{m_b}{2}$ (inverted triangular acceleration and variable mass), the moment and the shear force at the base of the bushing are:

$$V_3 = \frac{m_b H a_o}{3} = \frac{V_1}{3} = 0.33 \, V_1 \, and \, M_3 = \frac{m_b H^2 a_o}{4.8} = \frac{M_1}{2.4} = 0.417 M_1$$

Note that the current practice recommends multiplying the weight of the structure by the acceleration at the center of gravity (CG) - to calculate the shear force - and then multiply by the elevation of the center of gravity z_{CG} - to calculate the base moment, which appears to be valid only for a constant acceleration response along the height of the structure, as presented in equation (5-3).

According to the results in Table 5-9, the moments and the shear forces at the base of the bushing structure for the stiffened specimen were smaller compared to the ones of the unstiffened specimen ("as installed" bushing) by an average ratio of 38% (from acceleration measurements) or 29-39% (from strain gauges measurements) for the testing motion ensemble. Moreover, the moments at the base of the bushing reduce significantly by incorporating flexural stiffeners of the transformer top plate compared to the moments obtained for the unstiffened case (phase 3). When steel angles L6x4x½ (smaller sections/smaller stiffness) were used as stiffeners, the maximum bending moment at the base of the bushing was in between the other two cases. These response trends are also demonstrated in Figure 5-21, where the lognormal cumulative distribution functions (CDF) for the probability of non-exceeding (PoNE) a prescribed maximum moment at the base of the bushing are plotted for the three experimental phases. The same trend was also observed for the relative displacement and the absolute acceleration at the top of the bushing structure. However, as illustrated in Figure 5-22 and Figure 5-23, unlike the acceleration values, the displacement values did not decrease significantly.

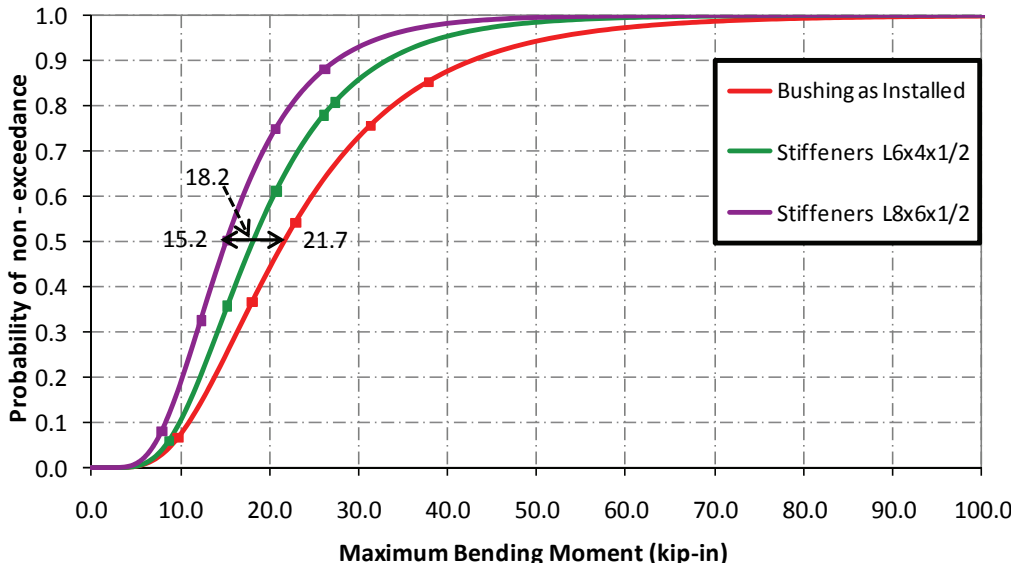

(a)

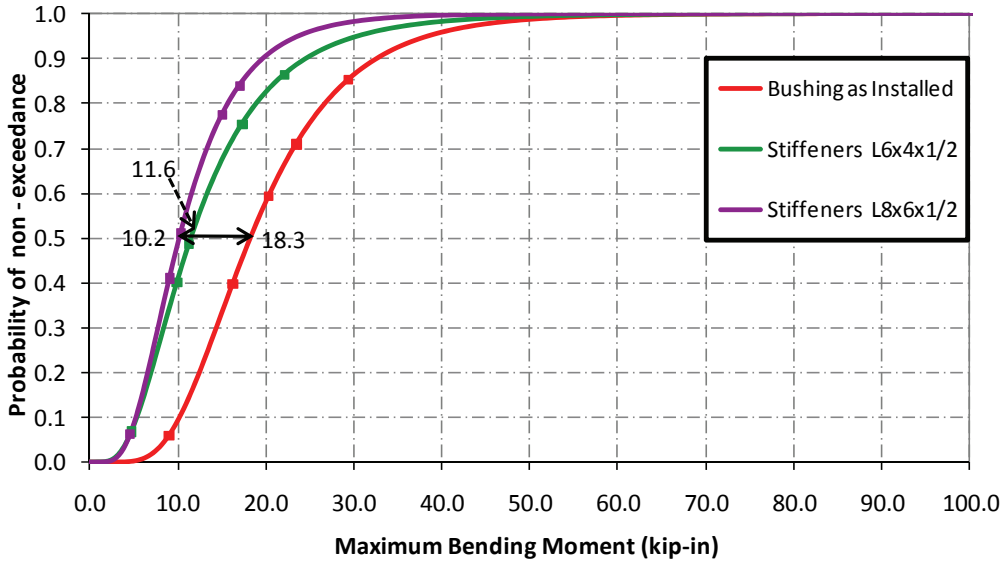

(b)

Figure 5-21 CDF for Maximum Bending Moments obtained by: (a) Strain Gauges Measurements and (b) Acceleration Measurements

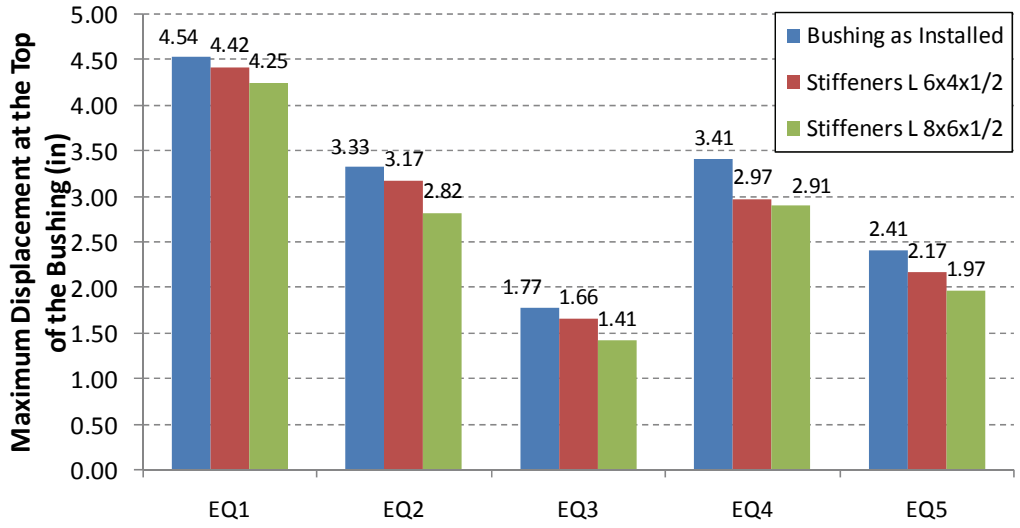

Figure 5-22 Maximum Relative Displacements Measured at the Top of the Bushing

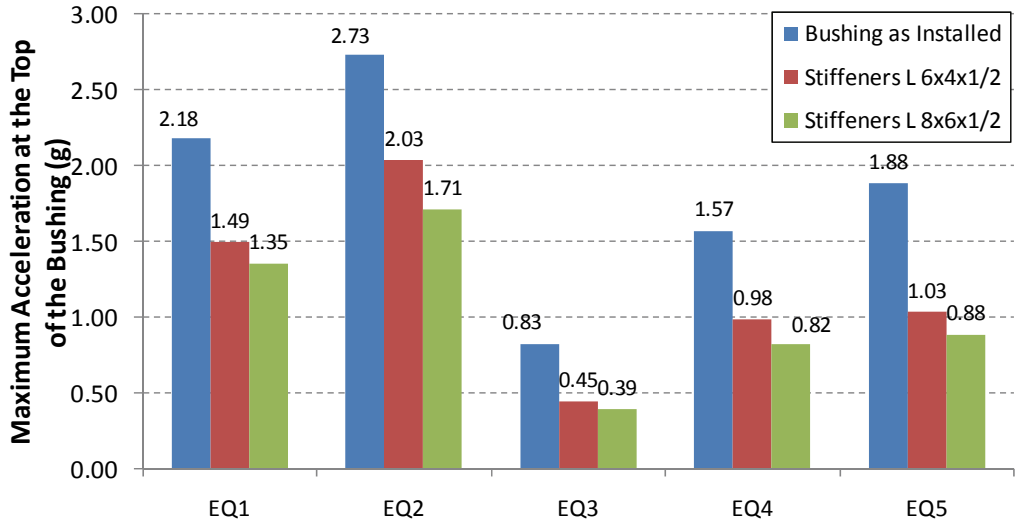

Figure 5-23 Maximum Absolute Accelerations Measured at the Top of the Bushing

5.6. Discussions

In summary, the experimental investigation presented within this section verified the efficiency of the stiffening approach incorporating flexural stiffeners on the top plate of the transformer structure. More specifically, by introducing stiffeners in the configuration of steel angles L8x6x½ the response of the bushing improved significantly compared to the response obtained not only when the bushing was mounted on the transformer structure ("as installed" conditions), but when smaller sections (smaller stiffness) of stiffeners were used. Note that the *Efficiency Factor* defined in Section 3 was not computed for this experimental investigation, since the case

of the bushing mounted on a rigid base was not tested under seismic conditions. However, reduction in the maximum base bending moment was clearly identified from the CDFs provided earlier in this section. Furthermore, finite element models of the specimen configurations were developed in order to match the results obtained during the dynamic tests. The numerical models and the results obtained from the analyses are presented in the following section, while a comparison between the numerical and the experimental results of the specimen configuration is also provided.

SECTION 6

COMPARISON OF NUMERICAL AND EXPERIMENTAL RESULTS

6.1. Introduction

This section presents the finite element models of the specimen configurations used for the system identification and seismic testing (see Sections 4 and 5, respectively), which were developed in order to predict the experimental response of the system. The section is divided into two parts: the first part presents the numerical models considered for the analyses, while the second part provides a comparison between numerical and experimental findings.

6.2. Description of Numerical Models

Two different finite element models were developed in the commercial structural analysis program *SAP2000 Advanced V.14.1.0* (Computers and Structures, 2009). The first model represented the configuration of the specimen used for the system identification testing, which consisted of the fixed concrete slab and the 230kV bushing structure as shown in Figure 6-1. The second model was developed based on the dimensions and the geometry of the specimen used for the shake table tests, which consisted of the rigid frame, top plate, adaptor plate and the bushing structure, as illustrated in Figure 6-2. Note that the numerical model of Figure 6-2 was modified by adding steel angles of the same dimensions and geometry as in the experimental procedure in order to simulate the stiffening cases.

The high voltage bushing, in both models, was modeled by multiple beam elements with the appropriate geometry, stiffness and mass assembled in series in order to represent the 230kV bushing structure used for the experimental investigation. All the components of the rigid frame were modeled as beam elements of the steel sections used in the actual frame. More specifically, the frame was of dimensions 8’ x 8’ x 8’, its four columns were modeled as beam elements of sections TS 5” x 5” x ½”, while the top of the columns was connected with angle sections L 5” x 5” x ¾”. A more detailed view of the finite element model of the rigid frame is presented in Figure 6-3. Shell elements of appropriate mass and thickness were used to model the adaptor plate as well as the top plate of the generic transformer tank (see Figure 6-4), while beam

elements were used to model the flexural stiffeners (L8x6x1/2 or L6x4x1/2) attached to the top plate.

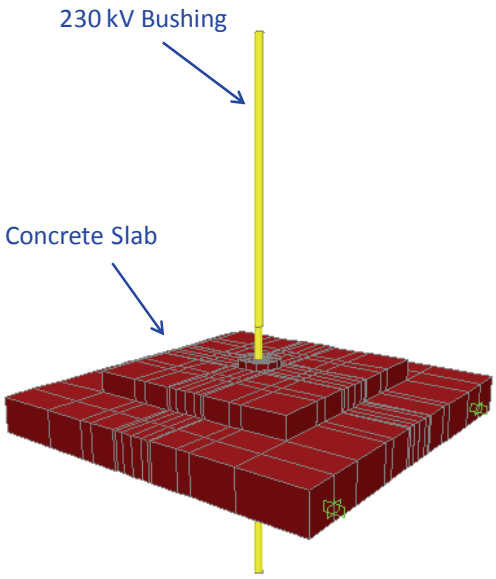

Figure 6-1 Finite Element Model of the Testing Configuration for the System Identification Testing

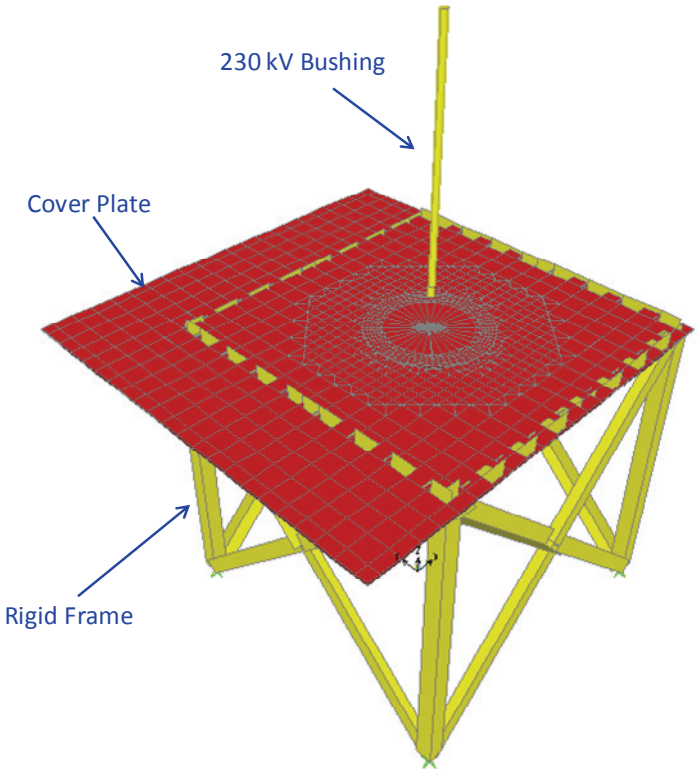

Figure 6-2 Finite Element Model of the Shake Table Testing

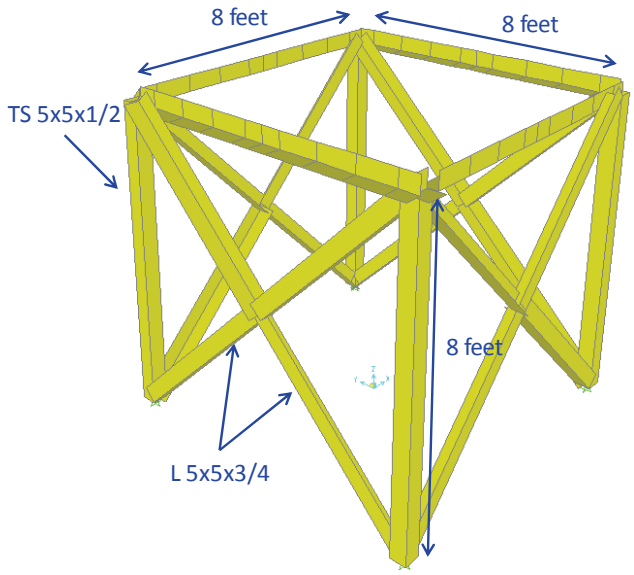

Figure 6-3 Isometric View of the Finite Element Model Representing the Rigid Frame

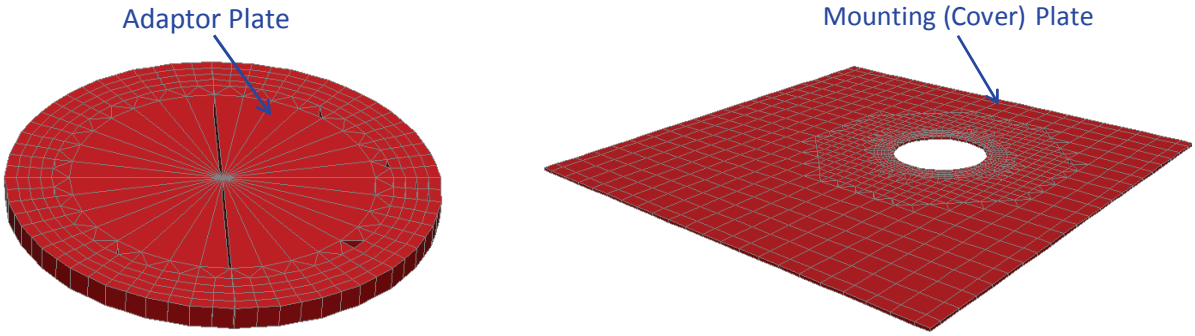

Figure 6-4 Finite Element Mesh used for the Modeling of the Adaptor Plate and Cover Plate

6.3. Analysis Procedure and Results

Modal and linear dynamic time history analyses were performed for both models using the reduced ensemble of five motions which was defined during the experimental investigation (see Section 5). Note that the ground motions recorded from the shake table tests (achieved motions) as well as with the damping ratios measured during testing were considered for performing the analyses in order to compare the experimental and numerical findings. A comparison between the response spectra of the theoretical motions and the recorded motions from the shake table tests is provided in Appendix D.

6.3.1. Modal Analyses Results

Based on the modal analyses performed for both models, the frequencies computed by the finite element models were very close to the experimental ones as shown in Table 6-1. According to these results, the finite elements models appeared to predict very well the frequency range of the bushing in the different configurations, since the difference between the computed fundamental frequencies and the measured fundamental frequencies on either stiffened or unstiffened transformer tank deviated between 3% and 9% (see Table 6-1). However, for the bushing structure mounted on a rigid base, the computed frequency of 21Hz differed 20% from the measured value of frequency (25Hz).

Table 6-1 Bushing Fundamental Frequency from Numerical Models and Experimental Investigation

Bushing Configuration	Numerical Models	Hammer Tests	White Noise Tests	Difference (%)
	Fundamental Frequency (Hz)			
Bushing "as installed"	11.20	N/A	10.11	9.70
Stiffeners L6x4x½	14.60	N/A	15.13	3.60
Stiffeners L8x6x½	15.15	N/A	16.14	6.50
Rigid base	21.00	25.30	N/A	20.50

6.3.2. Dynamic Analyses Results

After comparing the modal properties of the bushing structure for the different configurations both numerically and experimentally, dynamic time history analyses were performed. Note that the dynamic time history analyses were conducted by using the recorded motions from the shake table tests as well as the modal damping ratios measured during the testing. Figure 6-5 illustrates the results obtained from the numerical analyses in the form of lognormal cumulative distribution function (CDF) for the probability of non-exceeding (PoNE) a prescribed maximum moment at the base of the bushing. It was clearly identified from the numerical analyses that the stiffening approach of incorporating flexural stiffeners L8x6x½ on the top (cover) plate is an effective measure since the moments at the base of the bushing decreased significantly compared to the bushing "as installed" and moved towards the rigid base response.

In order to compare the numerical and experimental findings, the moments at the base of the bushing for all motions considered as well as the median values for each case are presented

numerically in Table 6-2 and graphically in Figure 6-6. According to these results, the finite element models appeared to slightly overestimate the moments at the base of the bushing structure for all the analysis cases as shown in Table 6-3. More specifically, the numerical results for the configurations with stiffeners differed by 3% to 5% from the experimental results, while for the bushing without stiffeners ("as installed" conditions), the difference between the experimental and numerical results reached an average value of 10%.

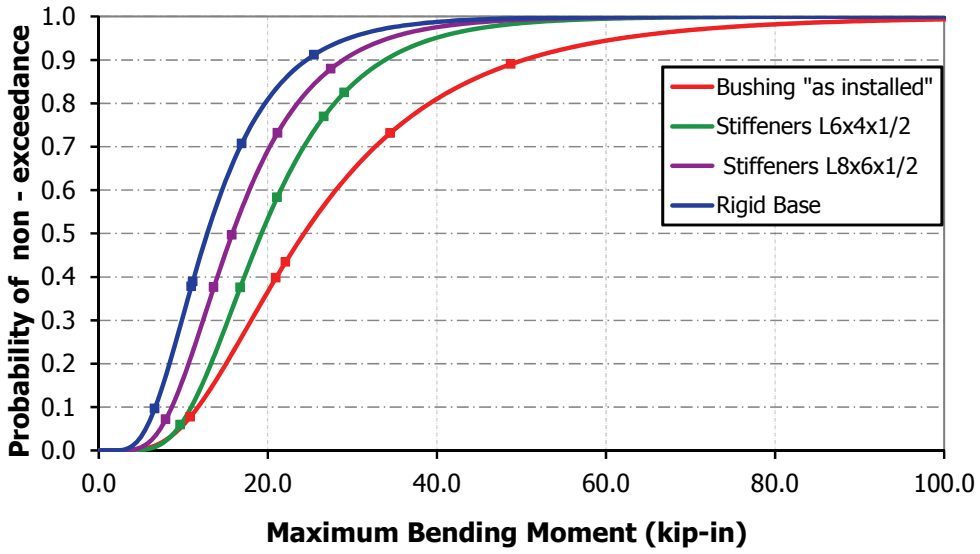

Figure 6-5 CDF for Maximum Bending Moments for Finite Element Models of Experimental Configurations

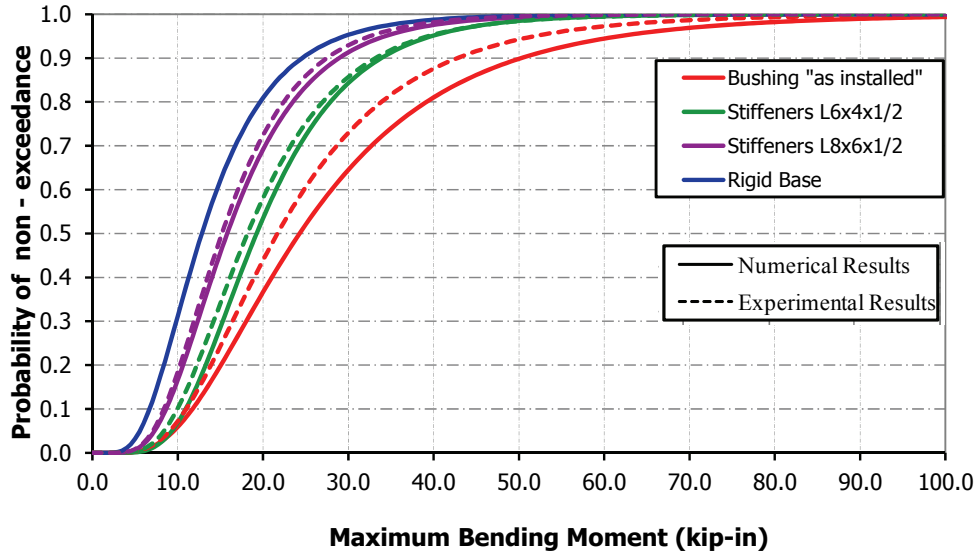

Figure 6-6 CDF for Maximum Bending Moments obtained by Numerical and Experimental Investigation

Table 6-2 Maximum Moment at the Base of the Bushing for Numerical and Experimental Investigation

EQ ID.	*Analytical Results*				*Experimental Results*			
	Rigid Base	**Bushing "as installed"**	**Stiffeners L8x6x½**	**Stiffeners L6x4x½**	**Rigid Base**	**Bushing "as installed"**	**Stiffeners L8x6x½**	**Stiffeners L6x4x½**
	Maximum Moment at the base of the bushing (kip-in)							
EQ 1 (12011)	16.92	34.47	27.45	29.05	N/A	31.35	26.23	27.37
EQ 2 (12041)	25.47	48.76	21.15	26.63	N/A	37.88	20.70	26.10
EQ 3 (12072)	6.62	10.84	7.92	9.66	N/A	9.74	7.94	8.74
EQ 4 (12092)	10.95	20.96	13.61	16.73	N/A	18.09	12.30	15.31
EQ 5 (12132)	11.12	22.11	15.73	21.11	N/A	22.96	15.20	20.77
Median Moment Value	12.83	24.28	15.80	17.27	N/A	21.69	15.18	18.18

Table 6-3 Differences between Numerical and Experimental Results of the Maximum Moment at the Base of the Bushing

	Difference (%) between Numerical and Experimental Results		
EQ ID.	**Bushing "as installed"**	**Stiffeners L8x6x½**	**Stiffeners L6x4x½**
EQ 1 (12011)	9.05	4.44	6.78
EQ 2 (12041)	22.31	2.13	1.99
EQ 3 (12072)	10.15	0.25	9.52
EQ 4 (12092)	13.69	9.63	8.49
EQ 5 (12132)	3.84	3.37	1.61
Median Moment Value	10.15	2.39	4.46

The *Efficiency Factor* for the experimental results was computed by using equation (3-1) and considering the values of maximum bending moments at the base of the bushing predicted by the numerical model (see Figure 6-7) since no seismic test was conducted for the rigid base condition.

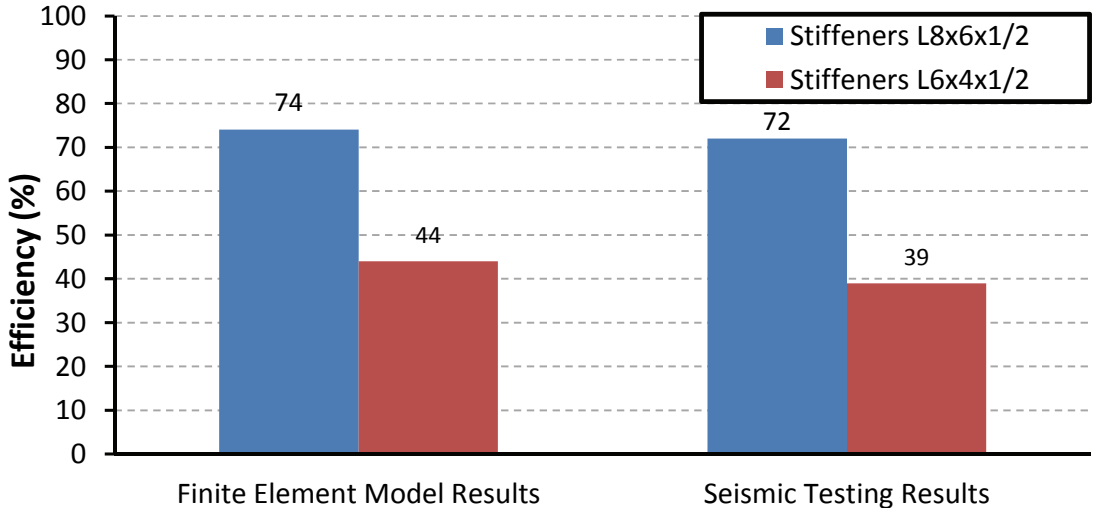

Figure 6-7 Measured and Computed Efficiency Factors for Stiffened Bushing on Support Structure

The moment amplification factors were calculated for each case according to equation (2-5) taking into consideration the results of the moments at the base of the bushing presented earlier. In Table 6-4, the moment amplification factors computed both experimentally and numerically are presented, and the median values of the amplification factors for all cases are shown in Figure 6-8. It is clearly shown that the amplification factor reduced by stiffening the base of the bushing was as expected based on the numerical investigation discussed in Section 3. Furthermore, the trend of the differences between the numerical and the experimental results did not change for this component of the comparison since the moment amplification factor computed for the numerical models was slightly larger than the factor computed from the experimental results (see Table 6-4). However, the differences of the amplification factors did not exceed an average value of 6%, which verified that the finite element models captured well the response of the bushing during the experimental investigation.

Table 6-4 Moment Amplification Factors computed from Experimental and Numerical Results

EQ ID	*Analytical Results*			*Experimental Results*		
	Bushing "as installed"	**Stiffeners L8x6x½**	**Stiffeners L6x4x½**	**Bushing "as installed"**	**Stiffeners L8x6x½**	**Stiffeners L6x4x½**
	Moment Amplification Factor					
EQ 1 (12011)	2.04	1.62	1.72	1.95	1.63	1.70
EQ 2 (12041)	1.91	0.83	1.05	1.57	0.86	1.08
EQ 3 (12072)	1.64	1.20	1.46	1.55	1.26	1.39
EQ 4 (12092)	1.91	1.24	1.53	1.74	1.18	1.47
EQ 5 (12132)	1.99	1.41	1.90	2.17	1.44	1.97

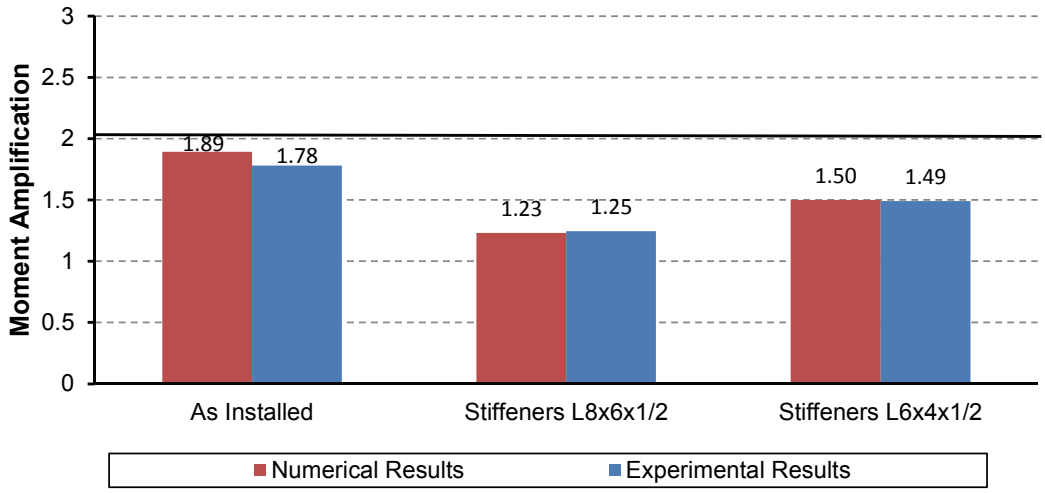

Figure 6-8 Median Values of Moment Amplification Factor computed from Experimental and Numerical Results

6.4. Discussions

In summary, the numerical analyses presented within this section showed that the finite element models for the different configurations of the bushing structure predicted the experimental results with relatively good accuracy. More specifically, the fundamental frequencies of the bushing as they were predicted by these models matched very well the corresponding recorded values with an average deviation of 10%, while the predicted values of moment at the base of the bushing were slightly larger than those recorded during the seismic tests (see Table 6-2). The deviation between the experimental and analytical results of the moments was between 5% and 10%. Finally, it was clearly shown that the stiffening approach of incorporating flexural stiffeners on

the top (cover) plate is a very efficient stiffening technique since the *Efficiency Factor* computed from both analytical and experimental results reached an average value of 70%.

SECTION 7

ANALYTICAL FREQUENCY EVALUATION OF BUSHING MOUNTED ON TRANSFORMER COVER

7.1. Introduction

Analytical background and simplified methods for evaluation of fundamental frequencies of bushing structures were developed and presented in this section. The simplified equations derived verify the validity of the concept of stiffening the base of the bushing in order to move the fundamental frequencies closer to the rigid base ones and consequently reduce the seismic demand. It is clearly shown by the analytical derivations of this section that the variation of frequencies is dependent on the relative stiffness of the bushing and the transformer cover, which is not included in the current practice (Reinhorn et al., 2011).

Analytical derivations of approximate frequencies of three different bushing "cases" are presented within this section: (a) cantilever (bushing structure) with distributed mass and elasticity mounted on rotational spring, (b) cantilever of distributed mass and elasticity with an extra lumped mass at the top mounted on rotational spring and (c) cantilever with lumped mass at the top mounted on rotational spring (without distributed mass and elasticity). Note that the mounting on the rotational spring was utilized to represent the flexibility of the tank top plate.

7.2. Analytical Derivations of Approximate Frequencies

7.2.1. Cantilever with Distributed Mass and Elasticity Mounted on a Rotational Spring

An approximation to the frequency ratio curves was obtained using the Southwell-Dunkerley method (Newmark & Rosenblueth, 1971) as presented below. The cantilever bushing on a flexible base was treated as the sum of a flexible system on a fixed base and a rigid system on a flexible base, with both systems having the same uniform mass distribution as shown in Figure 7-1.

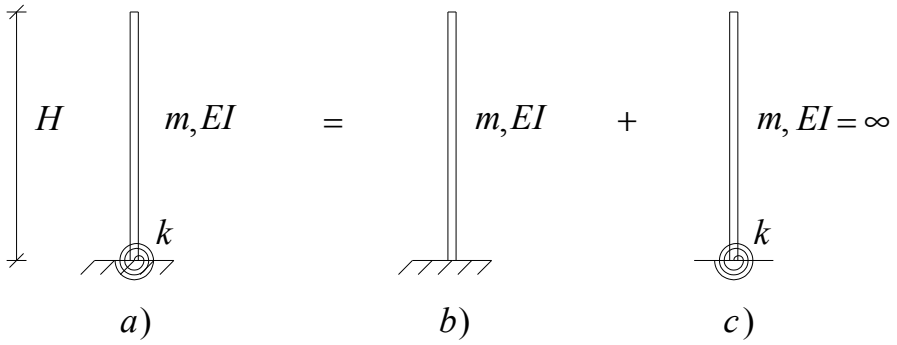

Figure 7-1 System Decomposition: (a) Flexible Base Cantilever, (b) Fixed Base Cantilever and (c) Rigid System on Flexible Base

The frequency of the system on a flexible base was evaluated as follows:

$$\frac{1}{f_k^2} = \frac{1}{f_{\text{fixed}}^2} + \frac{1}{f_{\text{rigid}}^2} \tag{7-1}$$

where f_k, f_{fixed} and f_{rigid} are the frequencies of the systems shown in Figure 7-1 (a), (b) and (c) respectively. equation (7-1) was manipulated to yield:

$$f_k = f_{\text{fixed}} \sqrt{\frac{1}{1 + (f_{\text{fixed}} / f_{\text{rigid}})^2}} \tag{7-2}$$

The square of the first mode frequency of the cantilever beam on a fixed base and that of the rigid beam with a spring at the base were evaluated as:

$$f_{\text{fixed}}^2 = \frac{(3.516)^2}{(2\pi)^2} \frac{EI}{mH^4} \quad \textit{and} \quad f_{\text{rigid}}^2 = \frac{3}{(2\pi)^2} \frac{k}{mH^3} \tag{7-3}$$

Substituting equation (7-3) into equation (7-2) led to the following expression for the frequency ratio:

$$f_k = f_{\text{fixed}} \sqrt{\frac{1}{1 + \lambda\sigma}} \quad \text{where} \qquad \lambda = \frac{(3.516)^2}{3} = 4.12 \tag{7-4}$$

Figure 7-2 shows the variation of the frequency ratio based on the exact solution versus an approximation using equation (7-4) based on the Southwell-Dunkerley method. Since the differences appear to be negligible, this solution can be used as an extremely good approximation for design purposes.

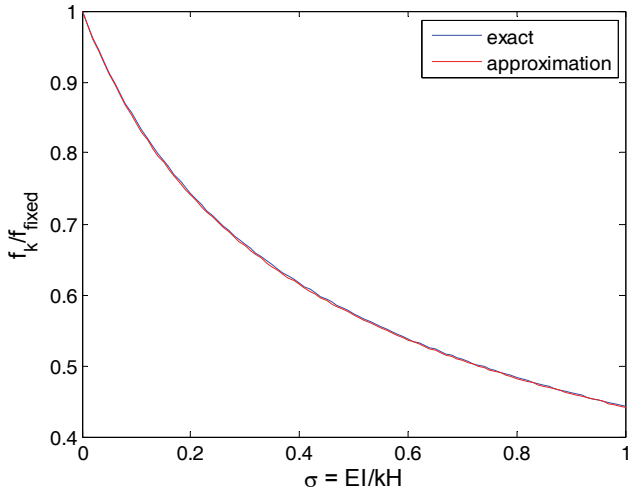

Figure 7-2 Interpolation of Exact Solution

7.2.2. Cantilever with Additional Concentrated Mass at the Top Mounted on Rotational Spring

Similarly to the previous section, an approximation to the frequency ratio curves was obtained using the Southwell-Dunkerley method (Newmark & Rosenblueth, 1971). The cantilever bushing on a flexible base was treated as the sum of a flexible system on a fixed base and a rigid system on a flexible base, with both systems having the same uniform mass distribution m and the same lumped mass ρmH at the top (see Figure 7-3).

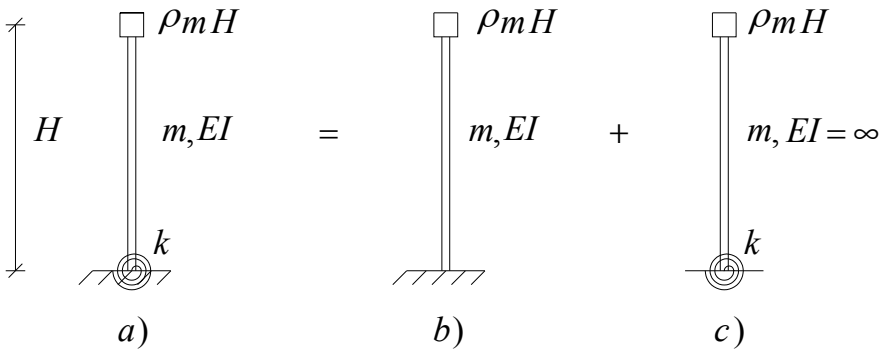

Figure 7-3 System Decomposition: (a) Flexible Base Cantilever with Additional Concentrated Mass at the Top, (b) Fixed Base Cantilever and (c) Rigid System on Flexible Base

The frequency of the system on a flexible base was evaluated per equations (7-1) and (7-2). The square of the frequency of the rigid system shown in Figure 7-3 (c) was computed as:

$$f_{\text{rigid}}^2 = \frac{1}{(2\pi)^2}\frac{3}{(3\rho+1)}\frac{k}{mH^3} \tag{7-5}$$

The square of the first mode frequency of the cantilever beam with a lumped mass at the top and on a fixed base may be evaluated itself using the Southwell-Dunkerley method. For this purpose, the system of Figure 7-3(b) was decomposed in the sum of a cantilever with uniformly distributed mass *m* and one with a lumped mass ρmH at the top, both systems having the same stiffness (see Figure 7-4).

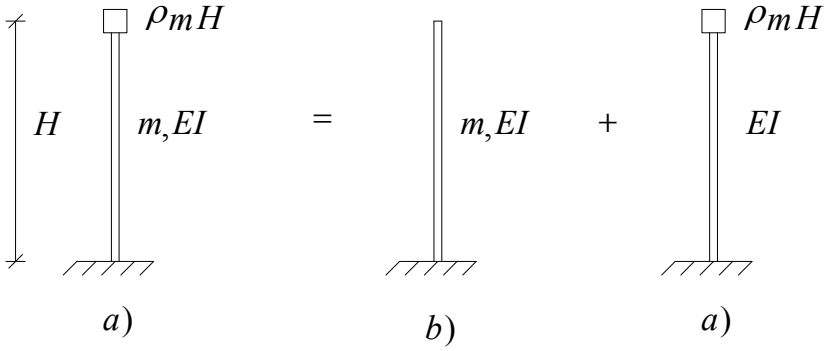

Figure 7-4 System Decomposition: (a) Fixed Base Cantilever with Uniformly Distributed Mass and Lumped Mass at the Top, (b) Fixed Base Cantilever with Uniformly Distributed Mass Only and (c) Fixed Base Cantilever with Lumped Mass at the Top Only

The frequency of the combined system was calculated as follows:

$$\frac{1}{f_{\text{fixed}}^2} = \frac{1}{f_{\text{distributed}}^2} + \frac{1}{f_{\text{lumped}}^2} \tag{7-6}$$

where f_{fixed}, $f_{\text{distributed}}$ and f_{lumped} are the frequencies of the systems shown in Figure 7-4 (a), (b) and (c), respectively, equation (7-6) may be solved for f_{fixed}^2 giving:

$$f_{\text{fixed}}^2 = \frac{f_{\text{distributed}}^2 f_{\text{lumped}}^2}{f_{\text{distributed}}^2 + f_{\text{lumped}}^2} \tag{7-7}$$

The square of the frequencies of the systems shown in Figure 7-4 (b) and (c) was evaluated as:

$$f^2_{\text{distributed}} = (3.516)^2 \frac{EI}{mH^4} \quad and \quad f^2_{\text{lumped}} = \frac{3}{\rho}\frac{EI}{mH^4} \tag{7-8}$$

Substituting equation (7-8) into equation (7-7) resulted in:

$$f^2_{\text{fixed}} = \frac{3}{\rho + \frac{1}{\lambda}}\frac{EI}{mH^4} \quad where \quad \lambda = \frac{(3.516)^2}{3} = 4.12 \tag{7-9}$$

By substituting in equation (7-2) the following expression for the frequency ratio was formulated:

$$f_k = f_{\text{fixed}}\sqrt{\frac{1}{1+\chi\sigma}} \quad where \quad \chi(\rho) = \frac{3\rho+1}{\rho+(1/\lambda)} \quad and \tag{7-10}$$
$$\rho = M/mH \quad \text{and} \quad \lambda = 4.12$$

Figure 7-5 shows the exact variation of frequency versus that obtained by using equation (7-10) in the case of a mass parameter $\rho = M/mH = 1$ In this case, the coefficient χ in equation (7-10) is approximately equal to 3.2. It is shown from equation (7-10) that when $\rho = 0$, meaning that there is no lumped mass at the top of the cantilever, $\chi = \lambda = 4.12$ and as expected equation (7-10) coincides with equation (7-4). When ρ becomes very large, the effect of the distributed mass is negligible compared to that of the lumped mass at the top and $\chi \to 3$.

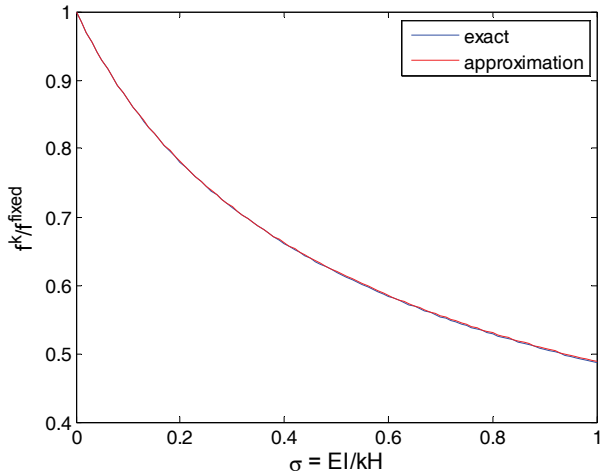

Figure 7-5 - Interpolation of Exact Solution with $\chi = 3.2$ for Systems with $\rho = 1$.

7.2.3. Cantilever with Lumped Mass at the Top Mounted on Spring (No Distributed Mass)

By defining the lateral bending stiffness of the fixed base cantilever as $k_f = 3EI / H^3$, and the lateral stiffness due to the rotational spring at the base as $k_\theta = k / H^2$, the following expression was formulated:

$$k_t = \frac{k_\theta k_f}{k_\theta + k_f} = k_f \frac{1}{1 + k_f / k_\theta} \tag{7-11}$$

The frequency of the fixed base cantilever was expressed by equation (7-12), while the frequency of the system on a flexible base was expressed by equation (7-13) and (7-14).

$$f_{\text{fixed}} = \frac{1}{2\pi}\sqrt{\frac{k_f}{M}} \tag{7-12}$$

$$f_k = \frac{1}{2\pi}\sqrt{\frac{k_t}{M}} = f_{\text{fixed}}\sqrt{\frac{1}{1 + k_f / k_\theta}} = f_{\text{fixed}}\sqrt{\frac{1}{1 + 3EI / kH}} = f_{\text{fixed}}\sqrt{\frac{1}{1 + 3\sigma}} \tag{7-13}$$

$$f_k = f_{\text{fixed}}\sqrt{\frac{1}{1 + 3\sigma}} \qquad \text{where} \qquad \sigma = EI / kH \tag{7-14}$$

From equations (7-11) and (7-13), it was noticed that for a flexible support structure $k_\theta \to 0$, the actual frequency f changes to a value that is very small tending to zero. If the base stiffness is very high, $k_\theta \to \infty$, then the "as-installed" frequency f, is same as for the fixed base f_{fixed}. If the base is more flexible, then the frequency f decreases as the square root quantity increases. For taller bushing structures, although the frequency reduces, the reduction is smaller than for a short bushing structure.

SECTION 8

SUMMARY, CONCLUSIONS AND RECOMMENDATIONS

8.1. Summary

In this report, the dynamic response of high voltage transformer bushing systems under seismic excitation was studied. Possible approaches to stiffen the base of the "as installed" bushings as a measure to mitigate their seismic vulnerability were identified.

Initially, numerical studies were conducted for four different transformer models of various sizes and voltages: (i) the Westinghouse 525kV transformer-bushing model, (ii) Siemens 230kV transformer-bushing model, (iii) Siemens 500kV transformer-bushing model and (iv) Ferranti Packard 230kV transformer-bushing model. For each model, the bushing structure was considered mounted on a rigid base or installed on the top plate of the transformer tank. Two ground motion ensembles were considered for performing linear dynamic time history analyses of the models: (i) Ensemble 1: 20 historical ground motions recorded within the California region, and (ii) Ensemble 2: FEMA P695 Far-field ground motion set. A second numerical study was also conducted investigating the efficiency of the stiffening approaches implemented on these four finite element models to ensure the bushing structural integrity under strong seismic excitation, i.e. (i) axial stiffeners in transverse and longitudinal direction, (ii) axial stiffeners connected to the tank wall, and (iii) flexural stiffeners on the tank top (cover) plate. For both numerical studies, the response parameters of interest were the moments at the base of the high voltage bushings since they could specify the demand due to seismic excitation.

A two stage experimental study, incorporating two types of testing: (i) system identification tests and (ii) shake table tests conducted in the Structural Engineering and Earthquake Simulation Laboratory (SEESL) of the University at Buffalo, was carried out in order to experimentally validate the numerically observed trends. Finally, a finite element model of the specimen configuration was developed in order to predict/match the experimental findings.

Analytical derivations of approximate bushing frequency were presented to verify the validity of the stiffening approach concept.

8.2. Conclusions

Considering the results of all the numerical analyses and the experimental tests presented in this report, the main conclusions are summarized herein:

- The bushing structures "as installed" on transformer top plates appeared to be vulnerable compared to the rigid base mounting because of the reduction in their natural frequencies due to the flexibility of the transformer top (cover) plate.
- Stiffening the base of the bushing was identified as a feasible approach to improve the dynamic response of the high voltage transformer – bushing systems.
- By introducing axial stiffeners between the bushing structure and tank plate or wall or flexural stiffeners on the top (cover) plate, the maximum bending moment at the base of the bushing decreased, moving towards the rigid base results; and the fundamental frequency of the bushing increased also reaching values closer to the rigid base case.
- Adding axial stiffeners, either in both directions or connected to the tank wall, appeared to be an efficient approach for the transformer models considered. However, incorporating flexural stiffeners on the tank top plate appeared to be the most efficient solution even in cases where the response of the transformer bushing system was significantly influenced by the cover plate. Moreover, the approach of incorporating flexural stiffeners was identified as the most practical and economical stiffening solution to be implemented either in existing transformer bushing systems or new ones.
- The moment amplification factor of 2 recommended in the IEEE-693 Standard for the bushing "as installed" was found to be non-conservative for all transformer bushing systems considered in this study. However, stiffening the base of the bushing structure resulted in a reduction of the moment amplification factor, which reached values lower than 2.
- The efficiency of the stiffening technique of incorporating flexural stiffeners on the top (cover) plate of the transformer tank was verified experimentally as well.

- Moments and shear forces at the base of the bushing were directly measured for first time during experimental investigation by using strain gauge measurements. Moments and shear force measurements obtained by using acceleration data (accelerometers at the top of the bushing structure) were compared to the strain gauge measurements and the differences identified were significant.
- The finite element models developed to represent the specimen configurations predicted the experimental results with relatively good accuracy.

8.3. Recommendations for Future Research

Based on the results obtained in this study, the following topics can be considered as potential subjects for future research on the seismic performance of high voltage bushing structures.

- The two ground motion ensembles considered for the numerical and experimental studies consisted of far-field motions. However, the response of the high voltage bushings using near-fault motions is expected to be of great interest for electrical substations close to active faults.
- The analytical and experimental studies were conducted by performing either 1D or 2D analyses using the two ground motion ensembles. Taking into consideration the vertical components of the motions may have an effect on the dynamic response of the high voltage bushing structure.
- The proposed stiffening technique of incorporating flexural stiffeners on the top cover plate of the transformer tank could also be an effective option for improving the response of existing transformers and for the rehabilitation of the existing ones. Transformer manufacturers should consider optimizing the selections and locations of horizontal stiffeners on the cover (top plates) of transformer tanks to improve the seismic response of bushings and reduce damage to transformer-bushing systems in strong earthquakes.

SECTION 9

REFERENCES

Bellorini, S., Bettinali, F., Salvetti, M., & Zafferani, G. (1998). *Seismic Qualification of Transformer High Voltage Bushings*. IEEE Transactions on Power Delivery, 13 (4), pp. 1208–1213

Boore, D., M., Watson-Lamprey, J., & Abrahamson, N., A. (2006). *Orientation-Independent Measures of Ground Motion*. Bulletin of the Seismological Society of America 96, pp. 1502–1511.

Bracci, J., Reinhorn, A., & Mander, J. (1992). *Seismic Resistance of Reinforced Concrete Framed Structures Designed Only for Gravity Loads: Part I - Design and Properties of a One - Third Scale Model Structure*. Technical Report NCEER-92-0027, Buffalo, NY.

Computers and Structures, Inc. (2009). *SAP2000 Advanced V.14.1.0.* Berkeley, CA.

Ersoy, S., & Saadeghvaziri, M. A. (2004). *Seismic Response of Transformer-Bushing Systems*. IEEE Transactions on Power Delivery, 19 (1), pp. 131-137.

Ersoy, S., Saadeghvaziri, M., A., Liu, G., & Mau, S., T. (2001). *Analytical and Experimental Seismic Studies of Transformers Isolated with Friction Pendulum System and Design Aspects*. Earthquake Spectra, 17(4), pp. 569–595

Ersoy, S., Feizi, B., Ashrafi, A., & Saadeghvaziri, A. M. (2008). *Seismic Evaluation and Rehabilitation of Critical Components of Electrical Power Systems*. Technical Report MCEER-08-0011, Buffalo, NY.

Fahad, M., Roh, H., Oikonomou, K. & Reinhorn, A.M. (2010). *Seismic Evaluation of Transformer Bushings*. Abstract and Presentation at 2010 ASCE/SEI Structures Congress, May 12-15, 2010, Orlando, FL.

FEMA P695. (2009). *Quantification of Building Seismic Performance Factors.* Federal Emergency Management, Washington, DC.

Filiatrault, A. & Matt, H. (2006). *Seismic Response of High Voltage Transformer-Bushing Systems*. ASCE Journal of Structural Engineering, 132(2), pp. 287-295.

Gilani, A. S. J., Chavez, J. W., Fenves, G. L., & Whittaker, A. S. (1998). *Seismic Evaluation of 196-kV Porcelain Transformer Bushings*. Report No. PEER 98/02, Pacific Earthquake Engineering Research Center, University of California at Berkeley.

Gilani, A. S. J., Whittaker, A. S., Fenves, G. L., & Fujisaki, E. (1999). *Seismic Evaluation of 550-kV Porcelain Transformer Bushings*. Report No. PEER 99/05, Pacific Earthquake Engineering Research Center, University of California at Berkeley.

Gilani, A. S., Whittaker, A. S., & Fenves, G. L. (2001). *Seismic Evaluation and Retrofit of 230 kV Porcelain Transformer Bushings*. Earthquake Spectra, 17(4), pp.597–616 .

IEEE. (2005). *IEEE Recommended Practice for Seismic Design of Substations.* IEEE-SA Standards Board, NY

Koliou, M., Filiatrault, A. & Reinhorn, A.M. (2012). *Seismic Response of High Voltage Transformer-Bushing Systems Incorporating Flexural Stiffeners I: Numerical Study*. Companion Paper Accepted for Publication in Earthquake Spectra.

Kong, D. (2010). *Protection of High Voltage Electrical Equipment Against Severe Shock and Vibration*. Doctor of Philosophy in Civil Engineering Dissertation, University at Buffalo, The State University of New York, Buffalo, U.S.A.

Matt, H., & Filiatrault, A. (2004). *Seismic Qualification Requirements For Transformer Bushings*. Research Project Report No SSRP-2003-12 Department of Structural Engineering, Univeristy of California, San Diego,La Jolla, CA.

Muhammad, F. (Expected 2012). *Seismic Evaluation of Tranformer Bushings*. Doctor of Philoshophy is Civil Engineering Dissertation, University at Buffalo, The State University of New York, Buffalo, NY, U.S.A.

Murota N. (2003). *Base Isolation for Seismic Protection of Power Transformers*. Doctor of Philoshophy is Civil Engineering Dissertation, University of California Irvine, CA, U.S.A.

Newmark, N.M. & Rosenblueth E. (1971). *Fundamentals of Earthquake Engineering*. Prentice Hall International, London.

Oikonomou, K. (2010). *Modeling of Electrical Transformers and Seismic Performance.* Master of Science of Philoshophy is Civil Engineering Dissertation, University at Buffalo, The State University of New York, Buffalo, NY, U.S.A.

Pansini, A. (1999). *Electrical Transformer and Power Equipment.* Fairmont, GA.

Reinhorn, A. M., Filiatrault, A., Fahad, M., Oliveto, N., Oikonomou, K. & Koliou, M. (2011). *Evaluation of Transformer Bushings: Current and Recommended Practise*. MCEER Task Report TR-11-01, University at Buffalo, The State University of New York, Buffalo, NY.

Schiff, A. J. (1997). *Northridge Earthquake: Lifeline Performance and Post Earthquake Response*. Technical Council on Lifeline Earthquake Engineering (TCLEE), Monograph No. 8, ASCE.

Schiff, A. J. (1998). *Hyogoken Nabu (Kobe) Earthquake of January 17, 1995 Lifeline Performance*. Technical Council on Lifeline Earthquake Engineering (TCLEE), Monograph No. 14, ASCE.

Schiff, A. J. (1999). *Guide to Improved Earthquake Performance of Electric Power Systems*. Manual and Reports on Engineering Practice No.96, ASCE.

Schiff, A. J. (2011). *As-Installed Frequencies of Substation Equipment*. Private Communication.

Schiff, A. J. & Tang, A. K. (2000). *Chi Chi, Taiwan Earthquake of September 21,1999 Lifeline Performance*. Technical Council on Lifeline Earthquake Engineering (TCLEE), Monograph No. 18, ASCE.

Sezen, H., & Whittaker, A. S. (2006). *Seismic Performance of Industrial Facilities Affected by the 1999 Turkey Earthquake.* Journal of Performance of Constructed Facilities, 20(1), pp. 28-36.

Sideris, P., (2008). *Seismic Behavior of Palletized Merchandise in Steel Storage Racks*. Master of Science in Civil Engineering Thesis, University at Buffalo, The State University of New York, Buffalo, U.S.A.

Sideris, P., Filiatrault, A., & Leclerc, M., Tremblay, R., (2010). *Experimental Investigation on the Seismic Behavior of Palletized Merchandise in Steel Storage Racks*. Earthquake Spectra, 26, pp. 209-233.

Structural Engineering and Earthquake Simulation Laboratory (SEESL) of the State University of New York at Buffalo website : *http://seesl.buffalo.edu/*.

Tang, A. K. (2000). *Izmit (Kocaeli), Turkey, Earthquake August 17, 1999 - Including Duzce Earthquake of November 12,1999 - Lifeline Performance*. Technical Council on Lifeline Earthquake Engineering (TCLEE), Monograph No.17, ASCE.

Wang, Y. (2008). *Geologic Hazards in Earthquake Country.* Presentation, Department of Geology and Mineral Industries.

Whittaker, A., S., Fenves, G., L. & Gilani, A., S., J. (2004). *Earthquake Performance of Porcelain Transformer Bushings*. Earthquake Spectra, 20(1), pp. 205-203.

Wilcoski, J., & Smith, S. J. (1997). *Fragility Testing of a Power Transformer Bushing*. USACERL Technical Report 97/57, U.S. Army Corps of Engineers Construction Engineering Research Laboratories, Champaign, IL.

Villaverde, R., Pardoen, G. C. & Carnalla, S. (2001). *Ground Motion Amplification at Flange Level of Bushings Mounted on Electric Substation Transformers*. Earthquake Engineering and Structural Dynamics 30, pp. 621-632.

APPENDIX A

GROUND MOTION TIME HISTORIES AND RESPONSE SPECTRA

In this appendix time histories of the ground motions considered for the numerical analyses in Section 2 and Section 3 are presented. More specifically, the time histories of the 20 historical ground motions of California region (Ensemble 1) are presented as well as the time histories of the ground motions of ensemble 2 (FEMA P695 Far Field Ground Motion Set). Note that for the second ensemble of ground motions, the time histories of both components of each motion are plotted and illustrated in this appendix. Additionally, the response spectra of all the ground motions included in both ensembles and the geometric mean spectrum of each ensemble (unscaled motions) are presented in this appendix.

Cape Mendocino (Fortuna Blvd.)

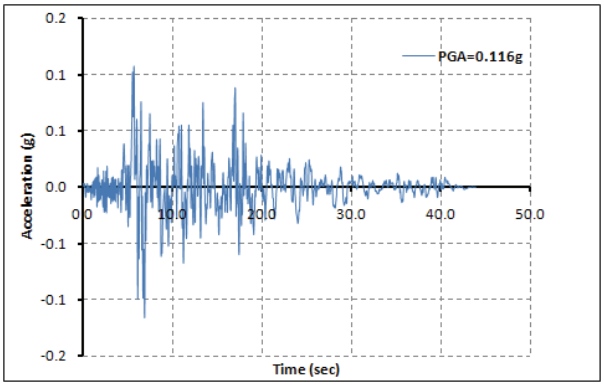

Cape Mendocino (Rio Dell Overpass)

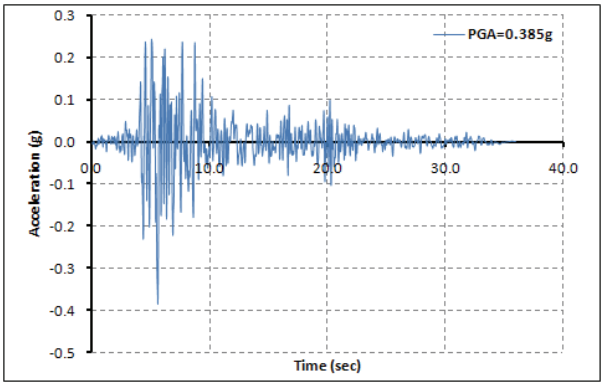

Landers (Hot Springs)

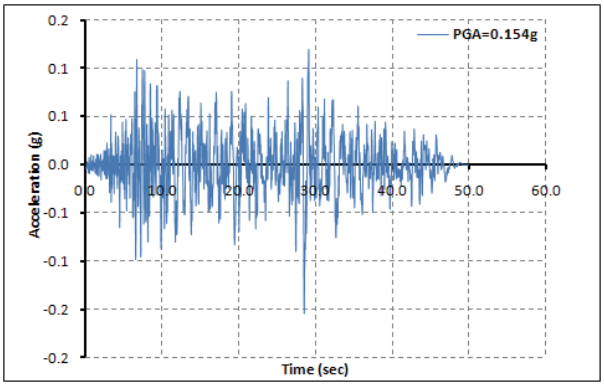

Landers (Yermo Fire Station)

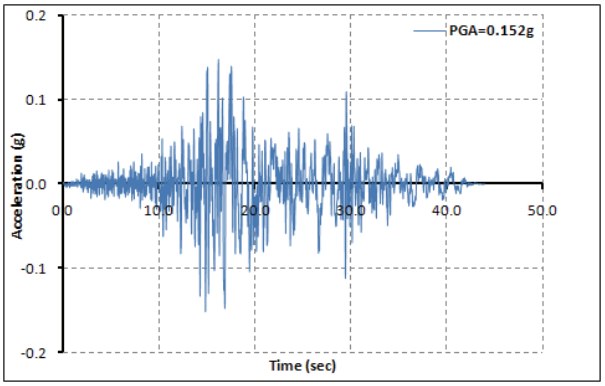

Loma Prieta (Capitola)

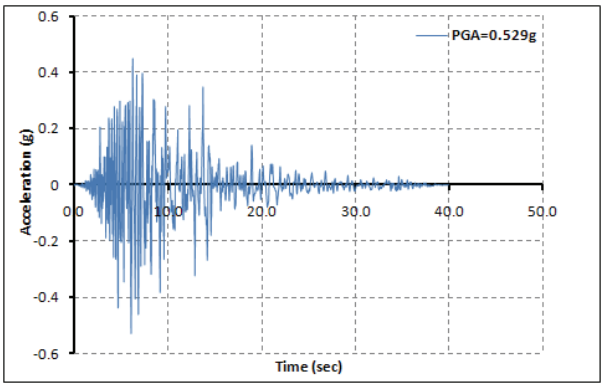

Loma Prieta (Gilroy Array #3)

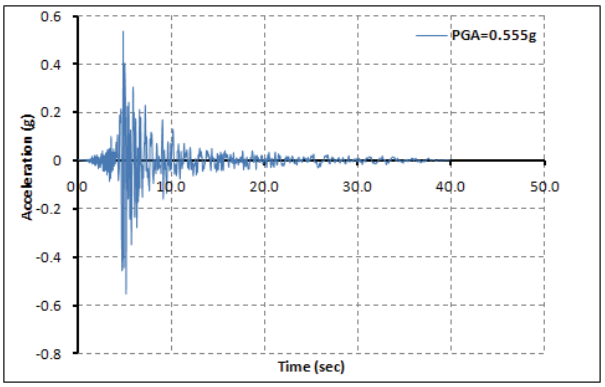

Loma Prieta (Gilroy Array #4)

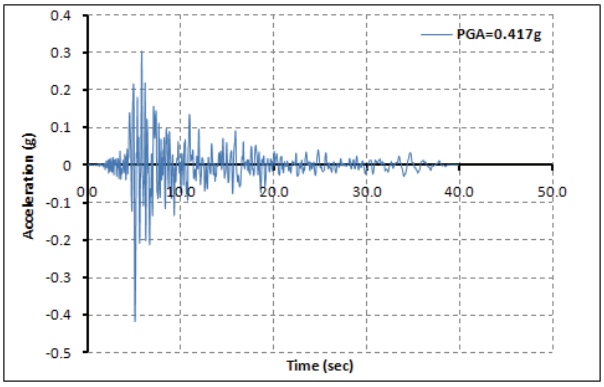

Loma Prieta (Gilroy Array #7)

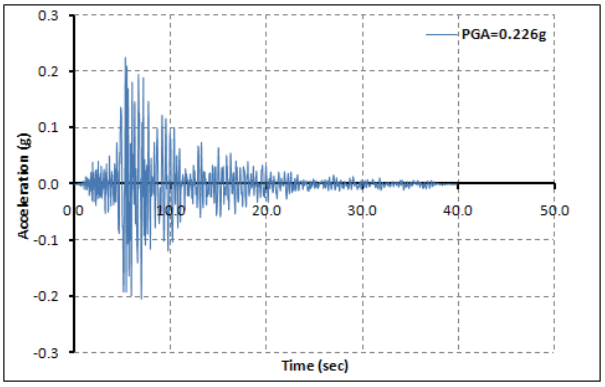

Loma Prieta (Hollister Diff. Array)

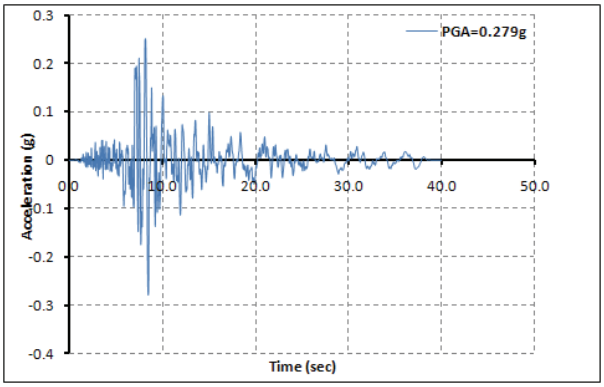

Loma Prieta (Saratoga)

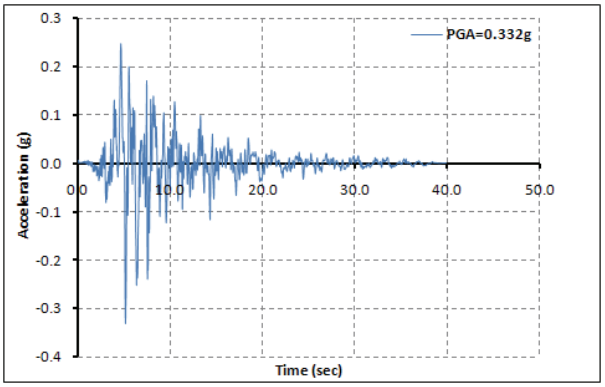

Northridge (Beverly Hills)

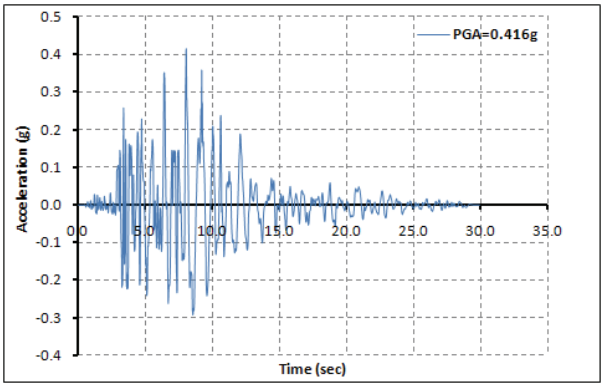

Northridge (Canoga Park)

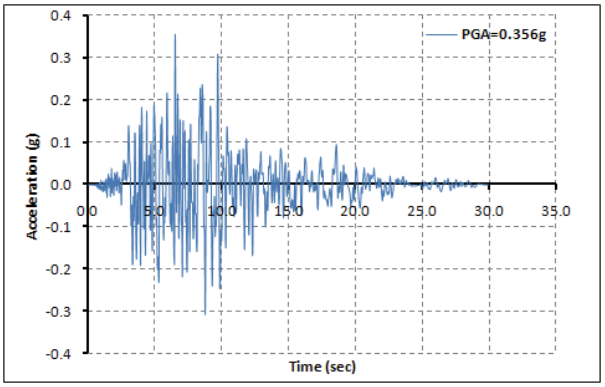

Northridge (Glendale)

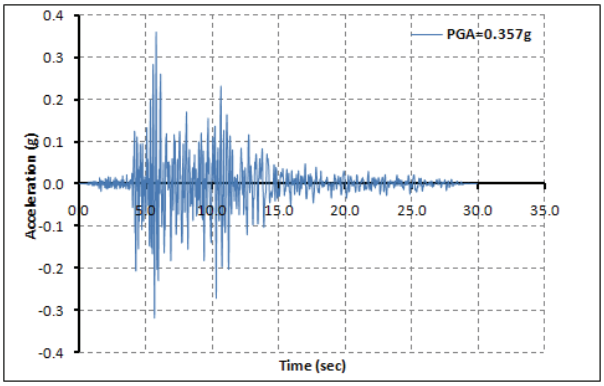

Northridge (LA – Hollywood Stor)

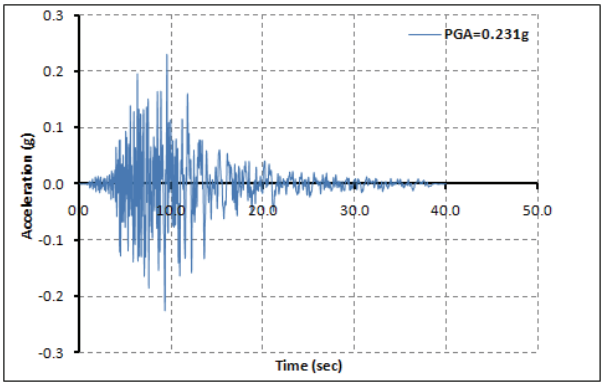

Northridge (LA – Faring Rd.)

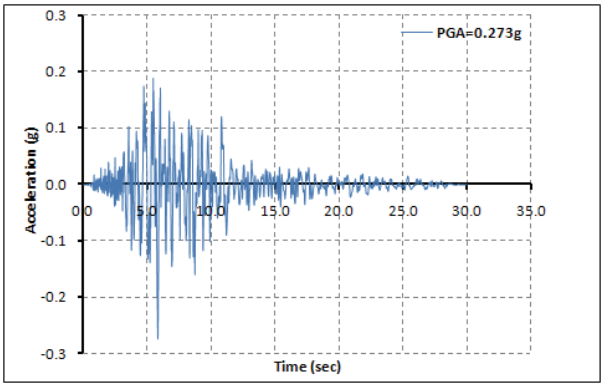

Northridge (N. Hollywood)

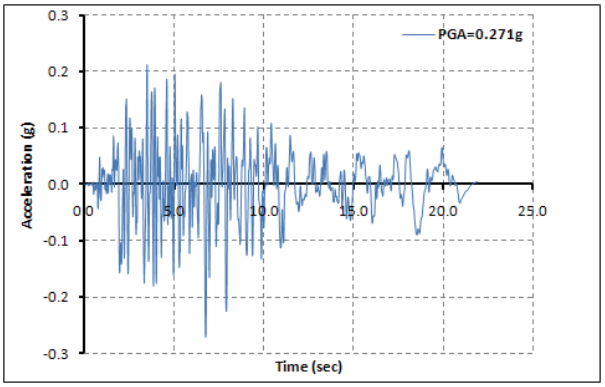

Northridge (Sunland)

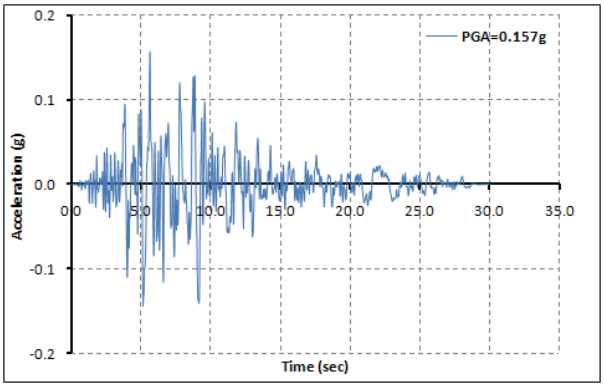

Superstition Hills (Brawley)

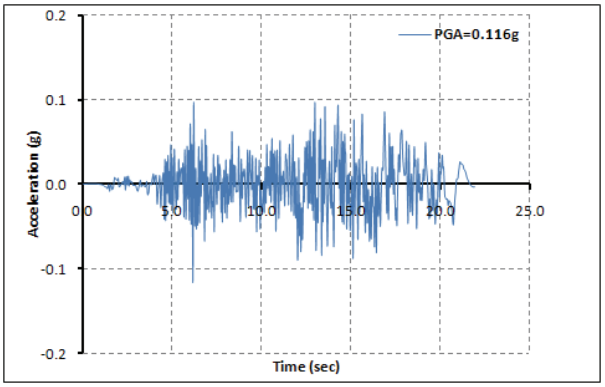

Superstition Hills (El Centro)

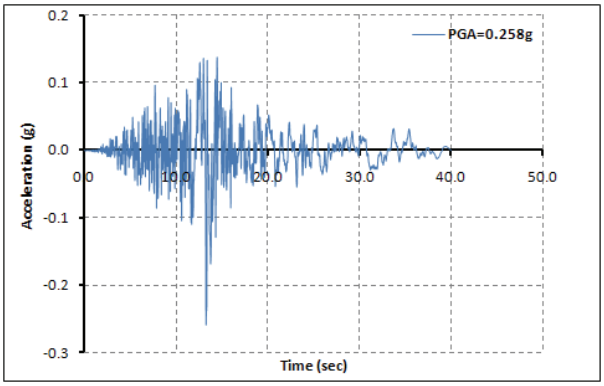

Superstition Hills (Plaster City)

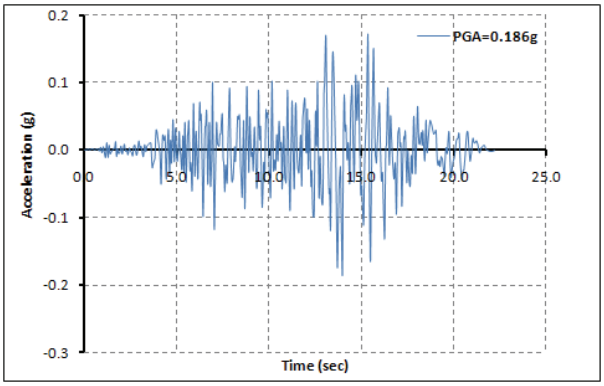

EQ ID: 12011 Component 1

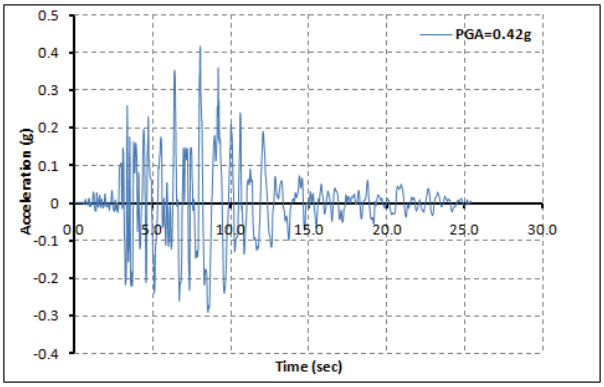

EQ ID: 12011 Component 2

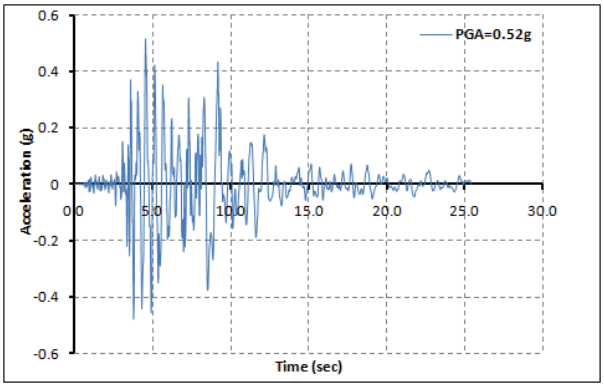

EQ ID: 12012 Component 1

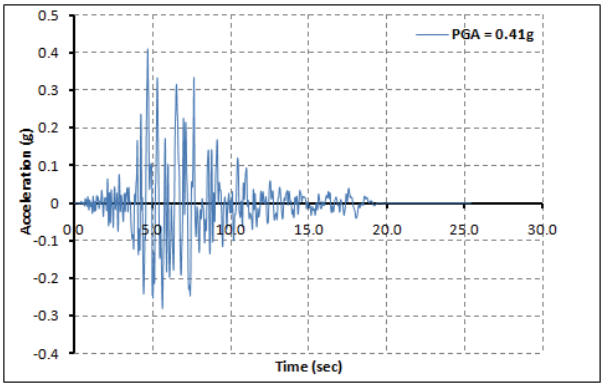

EQ ID: 12012 Component 2

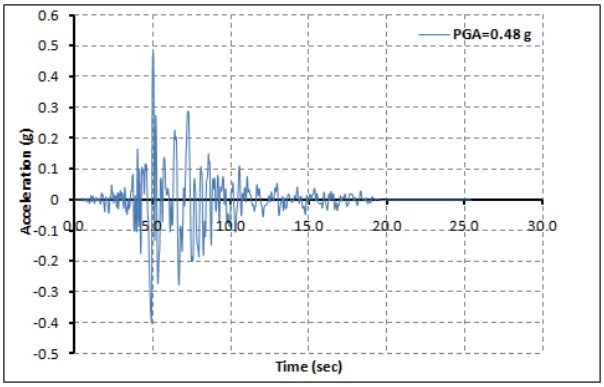

EQ ID: 12041 Component 1

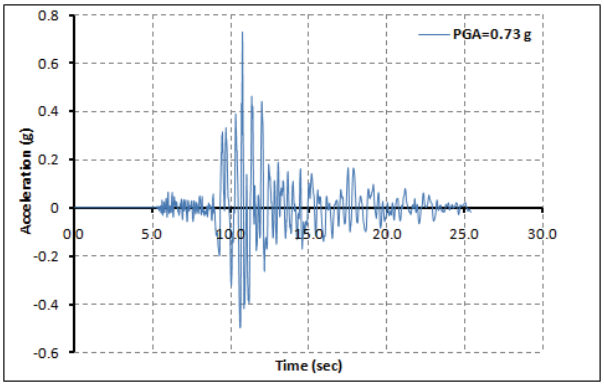

EQ ID: 12041 Component 2

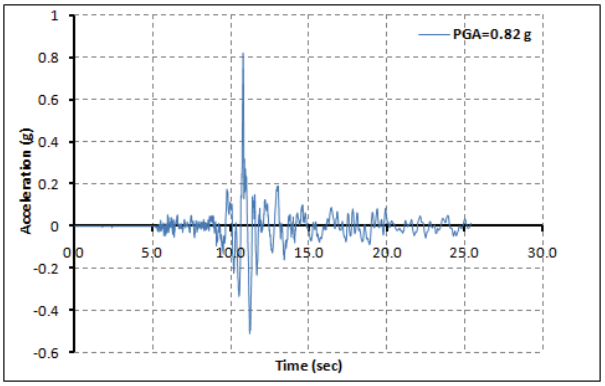

EQ ID: 12052 Component 1

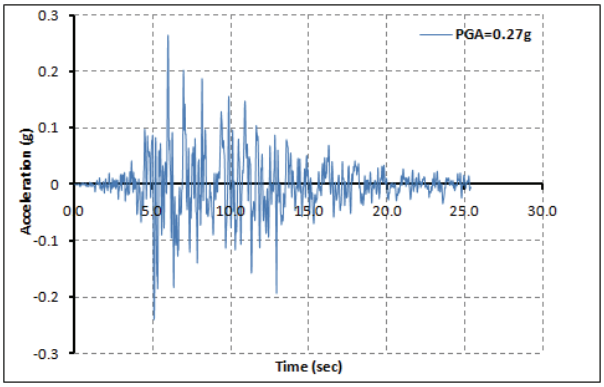

EQ ID: 12052 Component 2

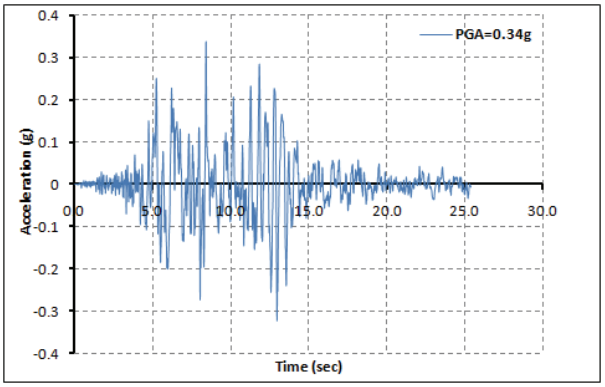

EQ ID: 12061 Component 1

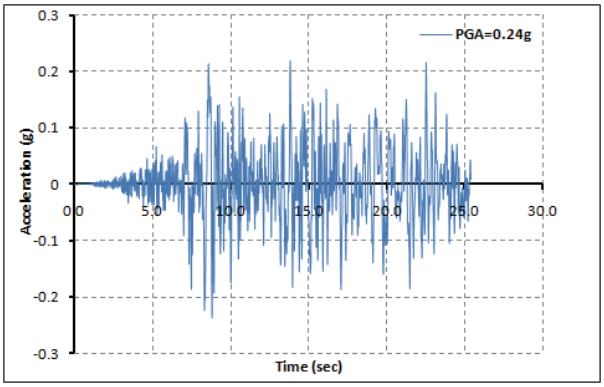

EQ ID: 12061 Component 2

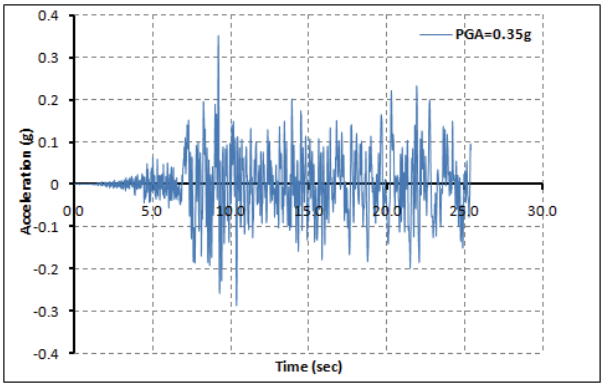

EQ ID: 12062 Component 1

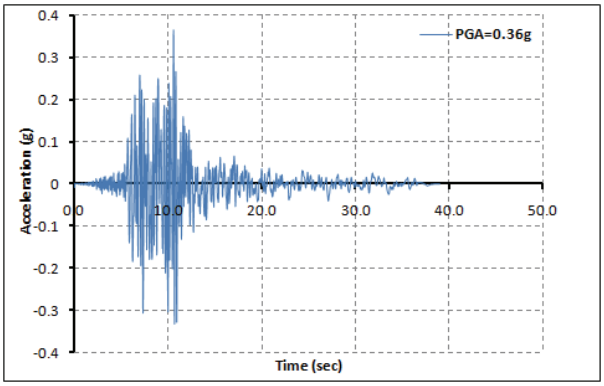

EQ ID: 12062 Component 2

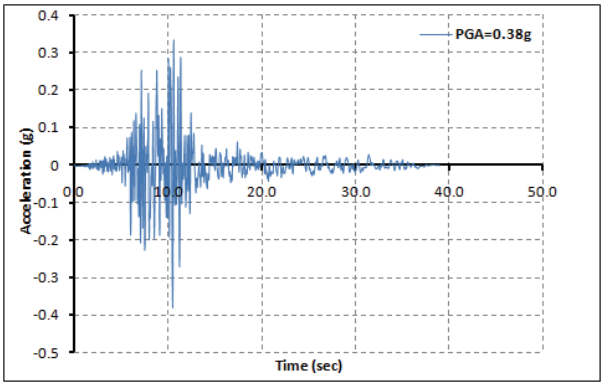

EQ ID: 12071 Component 1

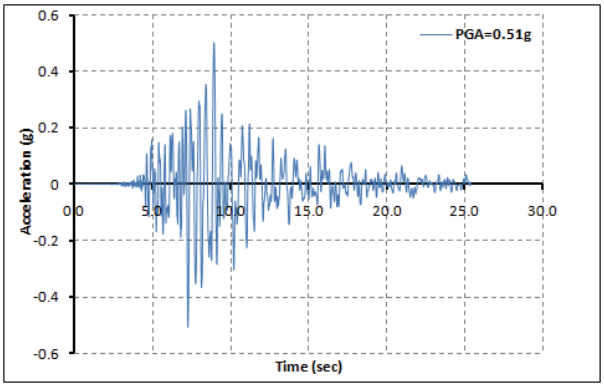

EQ ID: 12071 Component 2

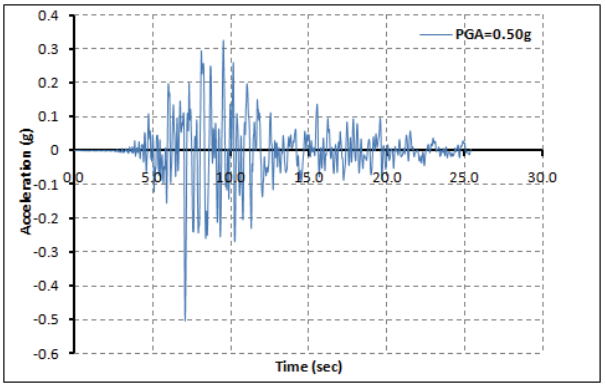

EQ ID: 12072 Component 1

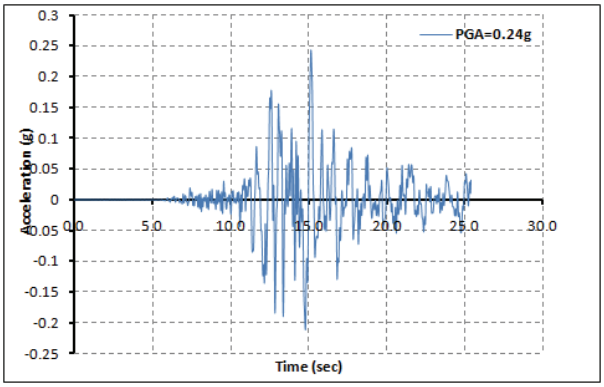

EQ ID: 12072 Component 2

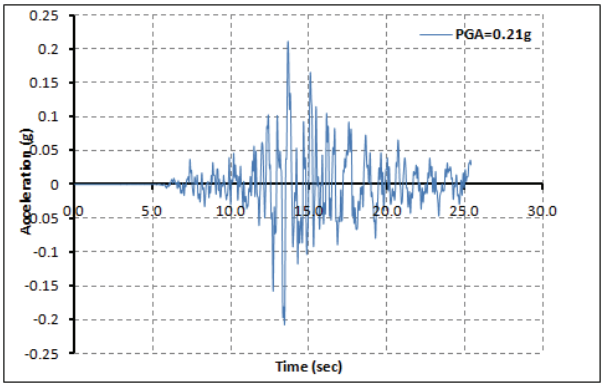

EQ ID: 12081 Component 1

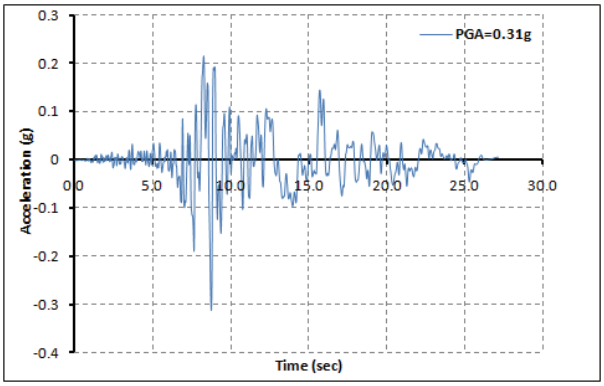

EQ ID: 12081 Component 2

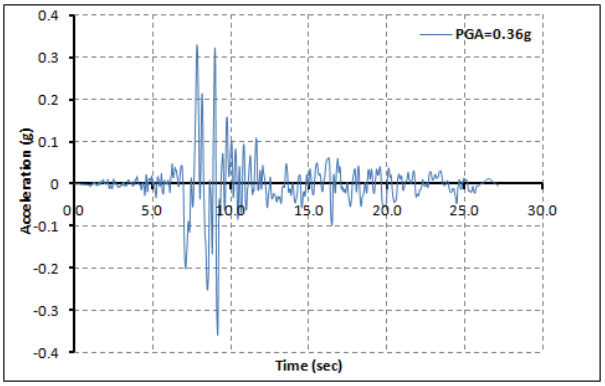

EQ ID: 12082 Component 1

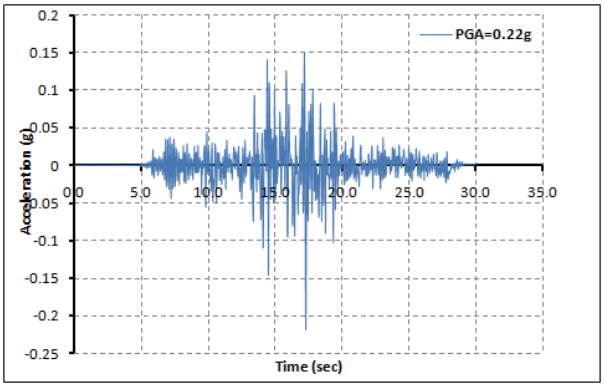

EQ ID: 12082 Component 2

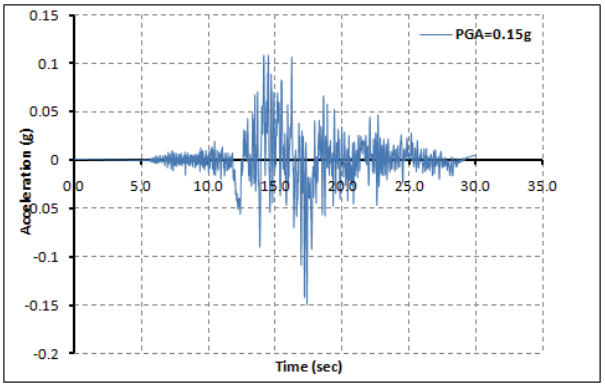

EQ ID: 12091 Component 1

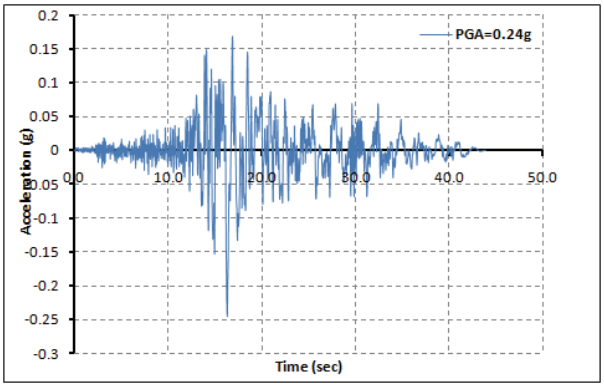

EQ ID: 12091 Component 2

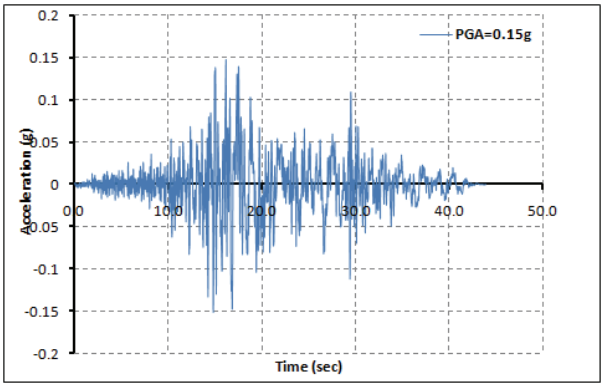

EQ ID: 12092 Component 1

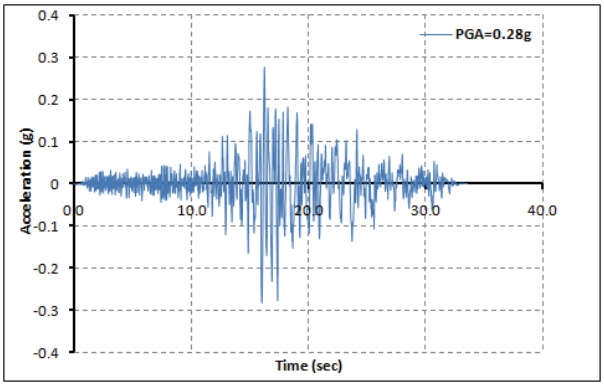

EQ ID: 12092 Component 2

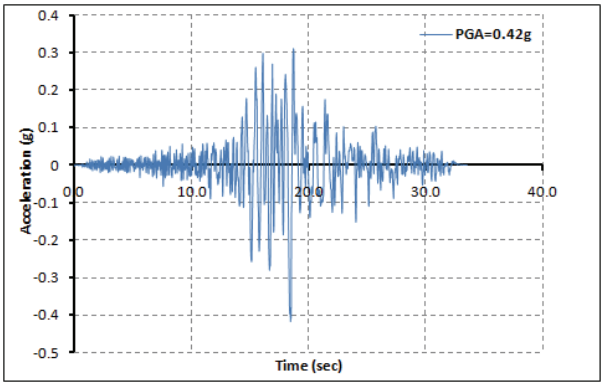

EQ ID: 12101 Component 1

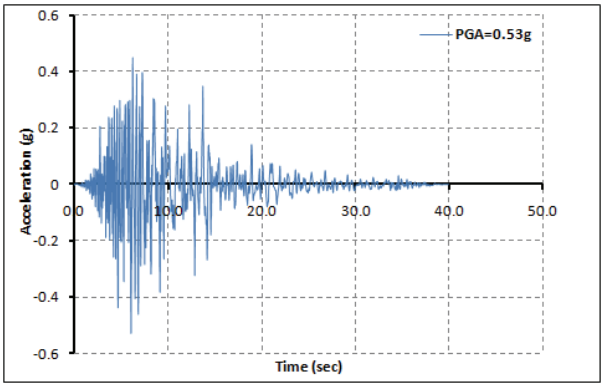

EQ ID: 12101 Component 2

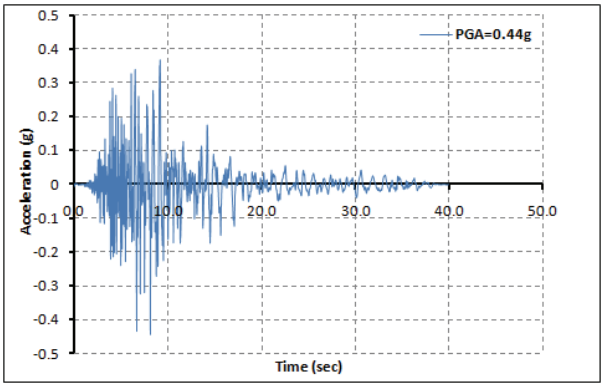

EQ ID: 12102 Component 1

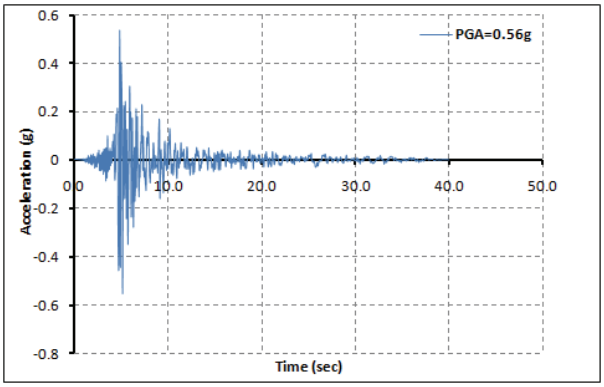

EQ ID: 12102 Component 2

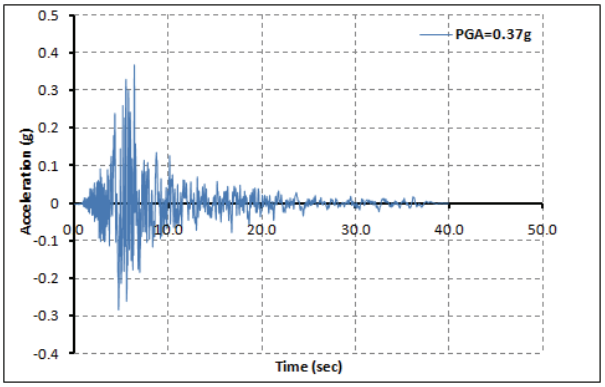

EQ ID: 12111 Component 1

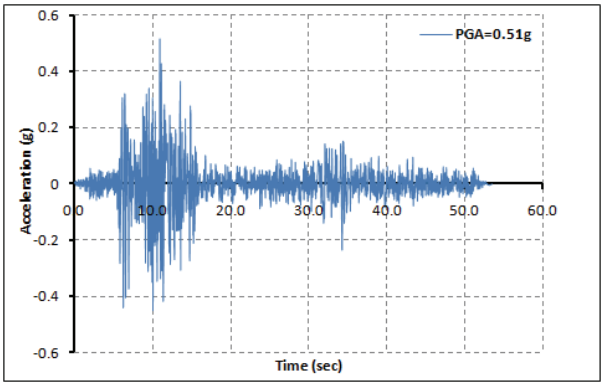

EQ ID: 12111 Component 2

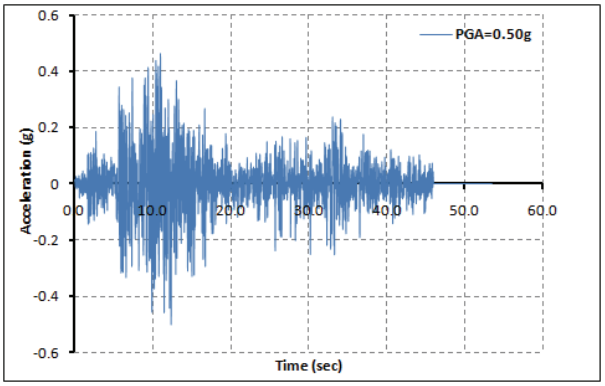

EQ ID: 12121 Component 1

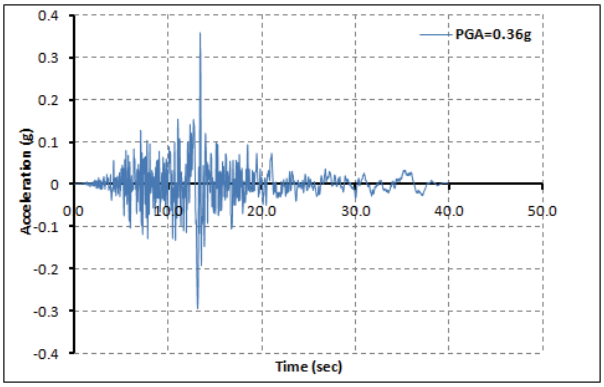

EQ ID: 12121 Component 2

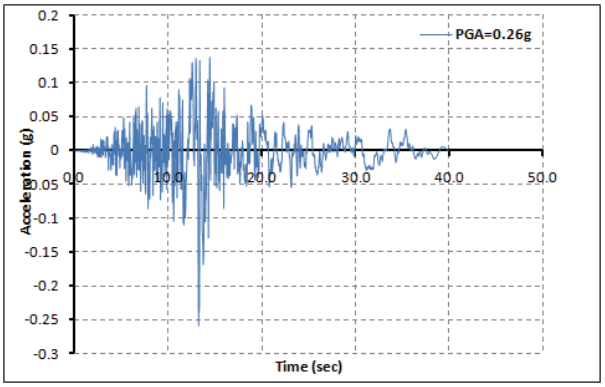

EQ ID: 12122 Component 1

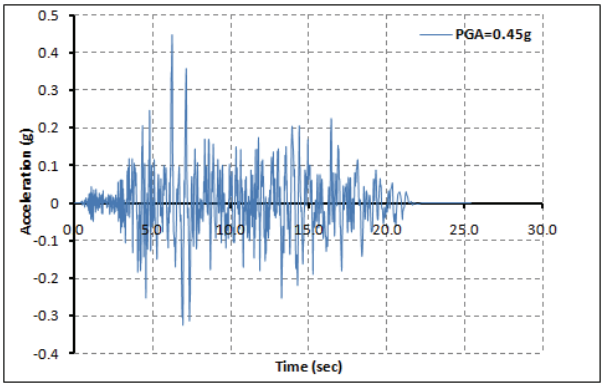

EQ ID: 12122 Component 2

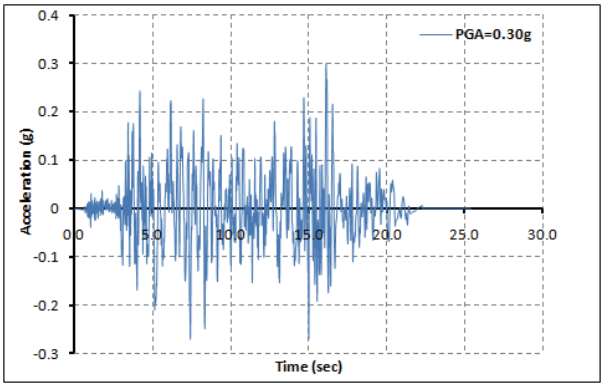

EQ ID: 12132 Component 1

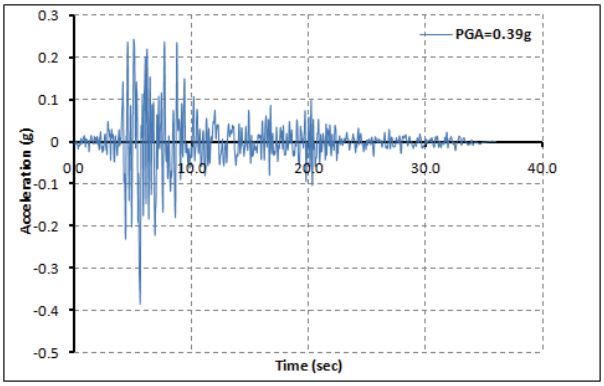

EQ ID: 12132 Component 2

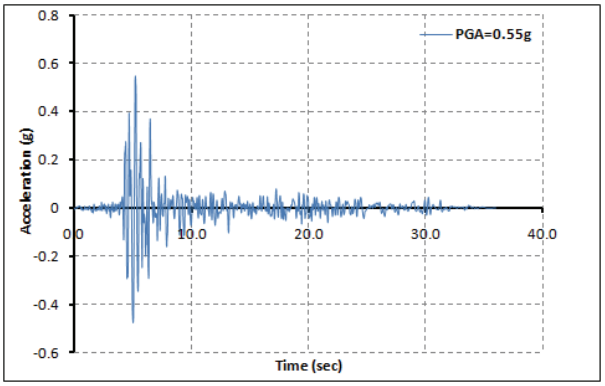

EQ ID: 12141 Component 1

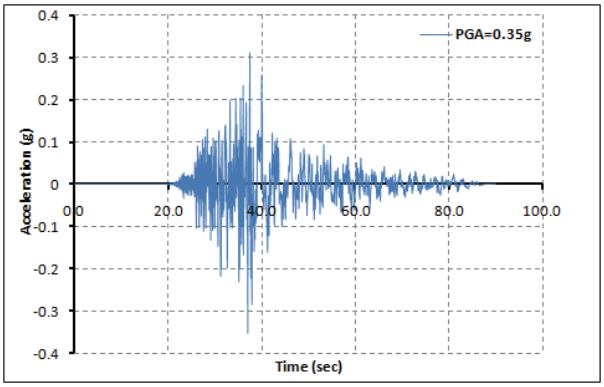

EQ ID: 12141 Component 2

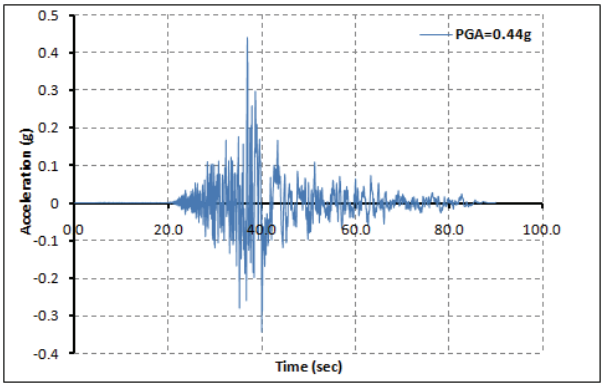

EQ ID: 12142 Component 1

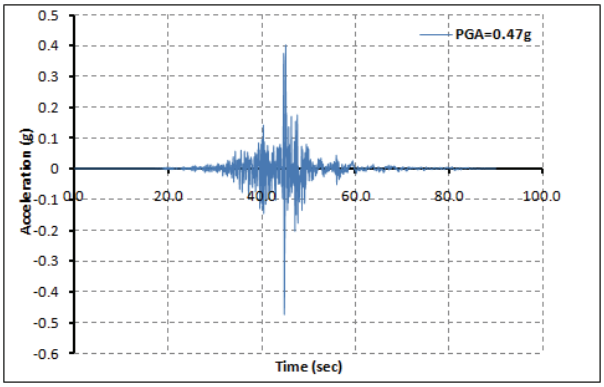

EQ ID: 12142 Component 2

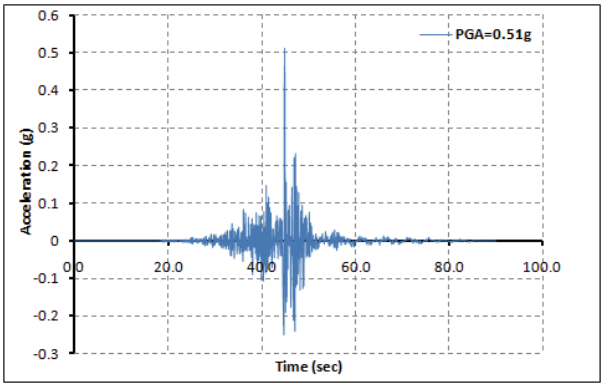

EQ ID: 12151 Component 1

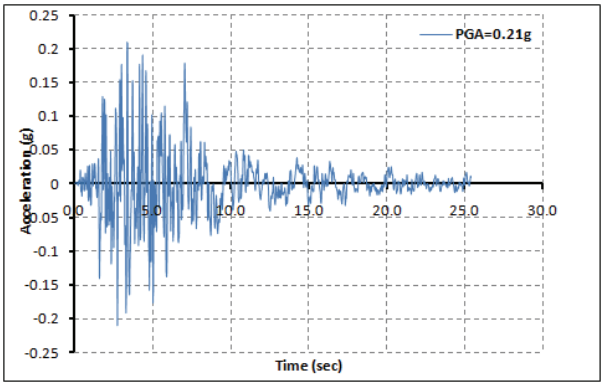

EQ ID: 12151 Component 2

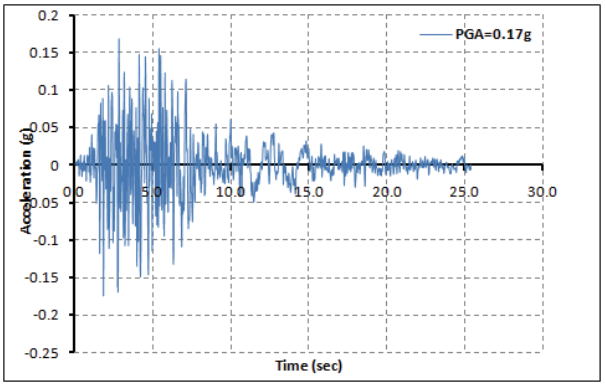

EQ ID: 12171 Component 1

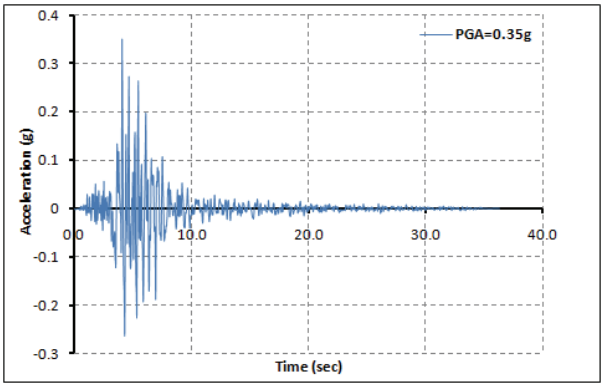

EQ ID: 12171 Component 2

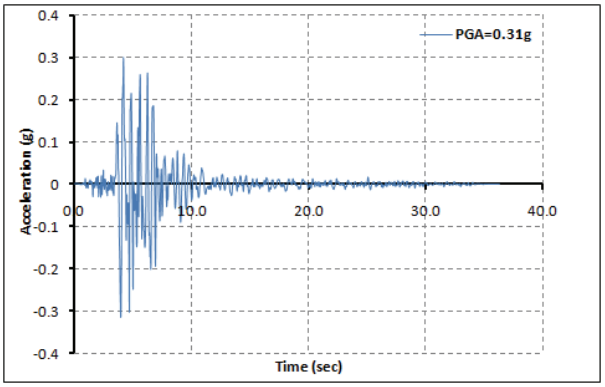

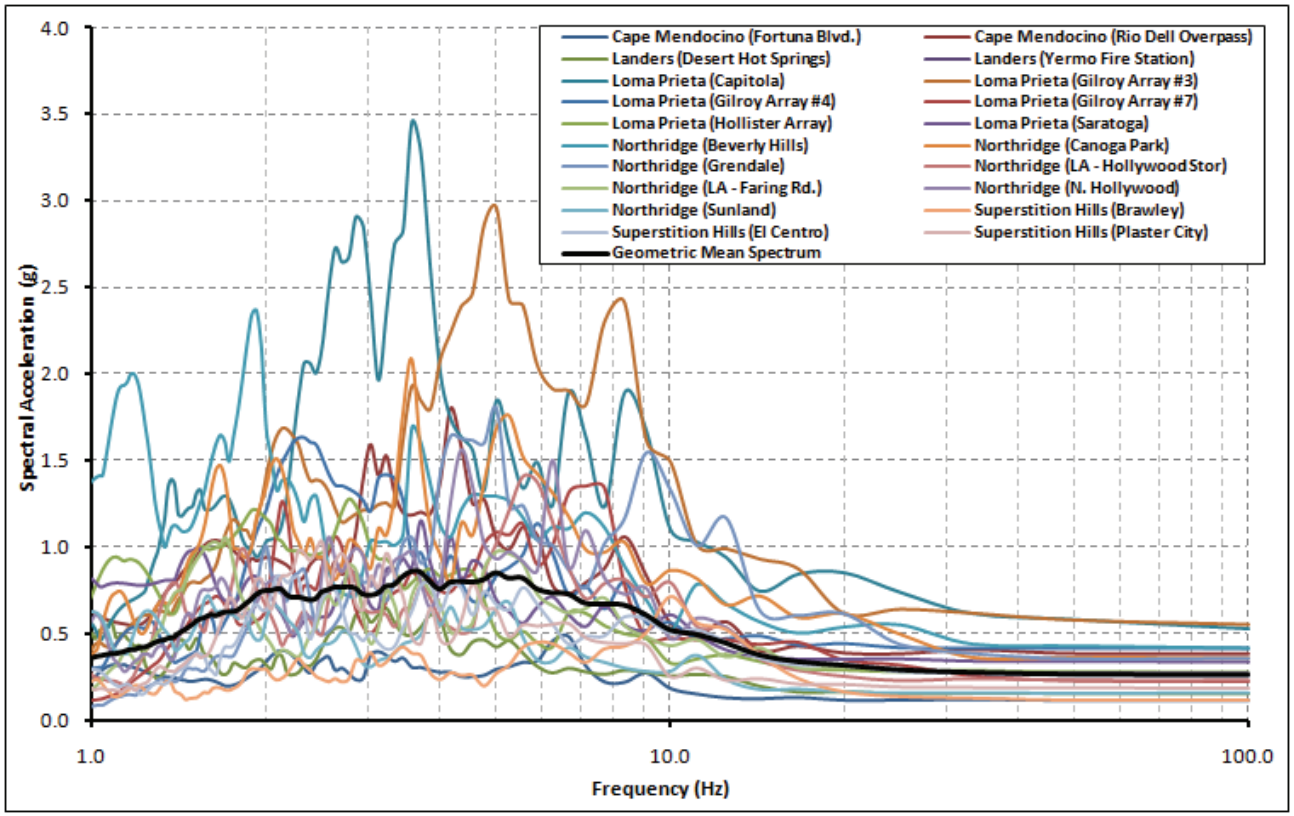

California Region Ground Motion Ensemble (Ensemble 1) Response Spectra (unscaled motions)

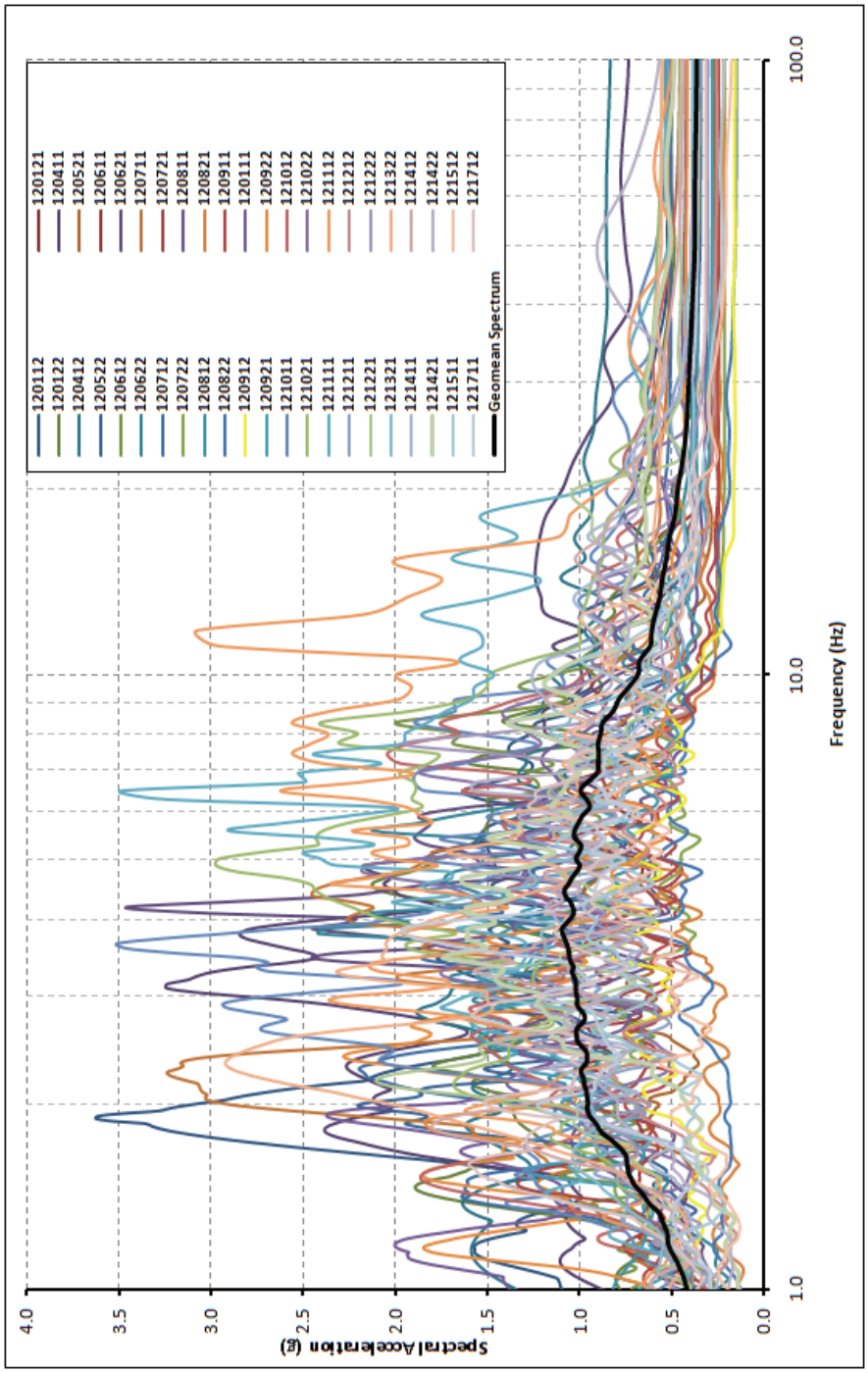

FEMA P695 Far Field Ground Motion Ensemble (Ensemble 2) Response Spectra (unscaled motions)

APPENDIX B

MEDIAN VALUES USED FOR EFFICIENCY FACTOR ESTIMATION

In this appendix the median values of the moments at the base of the bushing for each analysis case and for all the four transformer-bushing models used for the numerical investigation in Section 2 and Section 3 are presented. More specifically, for each ground motion, the median bending moments of the bushing "as installed", mounted on a rigid base, stiffened with axial stiffeners in both longitudinal and transverse direction, stiffened with axial stiffeners connected to the tank wall and stiffened with flexural stiffeners incorporated on the cover plate of the transformer tank (only for Ferranti Packard 230 kV Transformer) are presented. These median moment values presented within this appendix were used for the calculating the *Efficiency Factor* for each stiffening approach considered.

Median Bending Moment Values for Westinghouse 525kV Transformer Model

Analysis Case	Bushing "as installed:	Rigid Base	Axial Stiffeners in both Directions	Axial Stiffeners Connected to the Tank Walls
	Median Bending Moment at the Base of the Bushing Structure (kip-in)			
Ensemble 1 Longitudinal Direction	44.54	16.37	22.32	19.36
Ensemble 1 Transverse Direction	35.29	7.69	11.29	8.84
Ensemble 2 Longitudinal Direction	40.97	21.90	25.39	23.10
Ensemble 2 Transverse Direction	39.12	7.16	11.83	9.46
Ensemble 2 Case 1 (2D Analysis)	90.27	30.00	40.19	33.76
Ensemble 2 Case 2 (2D Analysis)	79.95	29.82	36.12	32.44

Median Bending Moment Values for Siemens 230kV Transformer Model

Analysis Case	Bushing "as installed:	Rigid Base	Axial Stiffeners in both Directions	Axial Stiffeners Connected to the Tank Walls
	Median Bending Moment at the Base of the Bushing Structure (kip-in)			
Ensemble 1 Longitudinal Direction	87.99	5.48	11.87	7.50
Ensemble 1 Transverse Direction	6.26	1.72	4.74	3.97
Ensemble 2 Longitudinal Direction	80.51	6.51	11.82	10.76
Ensemble 2 Transverse Direction	5.99	2.05	4.97	3.56
Ensemble 2 Case 1 (2D Analysis)	87.68	8.61	16.37	14.24
Ensemble 2 Case 2 (2D Analysis)	90.59	8.60	15.47	15.03

Median Bending Moment Values for Siemens 500kV Transformer Model

Analysis Case	Bushing "as installed:	Rigid Base	Axial Stiffeners in both Directions	Axial Stiffeners Connected to the Tank Walls
	Median Bending Moment at the Base of the Bushing Structure (kip-in)			
Ensemble 1 Longitudinal Direction	49.31	13.83	21.21	17.80
Ensemble 1 Transverse Direction	12.45	6.46	10.22	9.31
Ensemble 2 Longitudinal Direction	50.31	14.53	26.40	22.46
Ensemble 2 Transverse Direction	12.81	6.76	11.81	9.50
Ensemble 2 Case 1 (2D Analysis)	62.20	21.26	38.55	32.52
Ensemble 2 Case 2 (2D Analysis)	62.40	21.65	39.57	32.46

Median Bending Moment Values for Ferranti Packard 230 kV Transformer Model

Analysis Case	Bushing "as installed:	Rigid Base	Axial Stiffeners in both Directions	Axial Stiffeners Connected to the Tank Walls	Flexural Stiffeners on the Cover Plate
	Median Bending Moment at the Base of the Bushing Structure (kip-in)				
Ensemble 1 Longitudinal Direction	6.11	1.39	4.32	3.92	2.24
Ensemble 1 Transverse Direction	4.84	1.33	3.86	2.19	2.05
Ensemble 2 Longitudinal Direction	5.97	1.57	4.11	3.83	2.27
Ensemble 2 Transverse Direction	5.02	1.07	4.01	2.20	2.14
Ensemble 2 Case 1 (2D Analysis)	11.11	2.64	8.14	6.30	4.31
Ensemble 2 Case 2 (2D Analysis)	11.16	2.68	8.23	6.32	4.40

**__Ensemble 1:__ California Region Ensemble of Ground Motions & __Ensemble 2:__ FEMA P695 Far Field Ground Motion Set

APPENDIX C

VARIATION OF FREQUENCY AND EFFICIENCY FACTOR FOR DIFFERENT STIFFENING APPROACHES

In this appendix the variation of frequency and *Efficiency Factor* for the stiffening approaches considered in this research are presented. More specifically, for the approach of adding axial stiffeners in both longitudinal and transverse direction, the variation of frequency is illustrated for the cases of adding stiffeners in each direction separately and in three different angles of inclination. Note that these results are presented for all four finite element models considered for numerical analysis (see Section 2). Moreover, for the stiffening approach of incorporating flexural stiffeners on the cover plate of the transformer tank (only Ferranti Packard 230 kV Transformer), the variation of the *Efficiency Factor* by increasing the stiffness, is presented.

According to the results adding axial stiffeners in both directions did not increase the frequency significantly for the Westinghouse 525kV transformer model, while by adding stiffeners connected to the tank wall appeared to be more efficient (in terms of frequency increase) since the frequency increases almost 50% compared to the bushing "as installed".

As for the Siemens 230kV transformer model and Siemens 500kV transformer model, the approach of adding axial stiffeners in both directions appeared to work better for the transverse direction (direction of first mode of bushing structure), while the frequency did not change considerably by adding axial stiffeners connected to the tank walls.

Finally, for the Ferranti Packard 230kV transformer model, as mentioned in earlier in this report, the approach of adding axial stiffeners was not efficient, since not only the decrease of moments at the base of the bushing was not significant (see Section 3) but the fundamental natural frequency did not change as shown in Figure s below.

Note that from all the graphs presented below the threshold value of stiffness considered for the numerical analysis was identified (for the stiffening approaches).

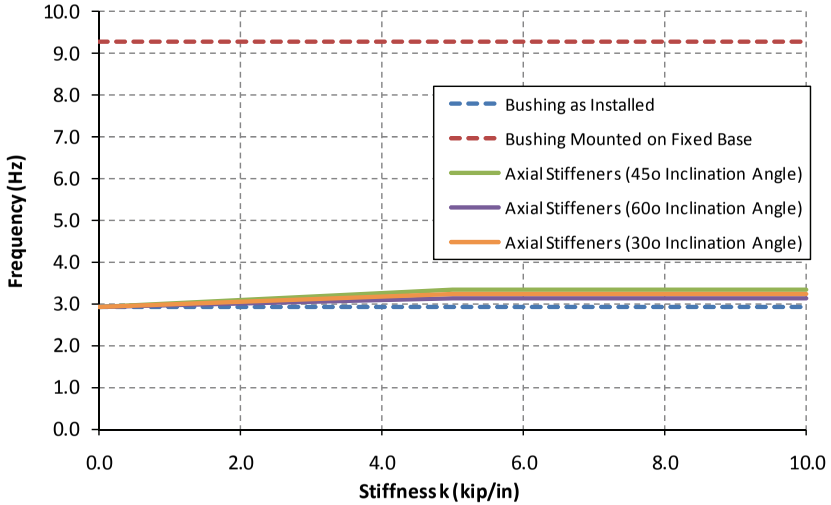

Axial Stiffeners in Longitudinal Direction only

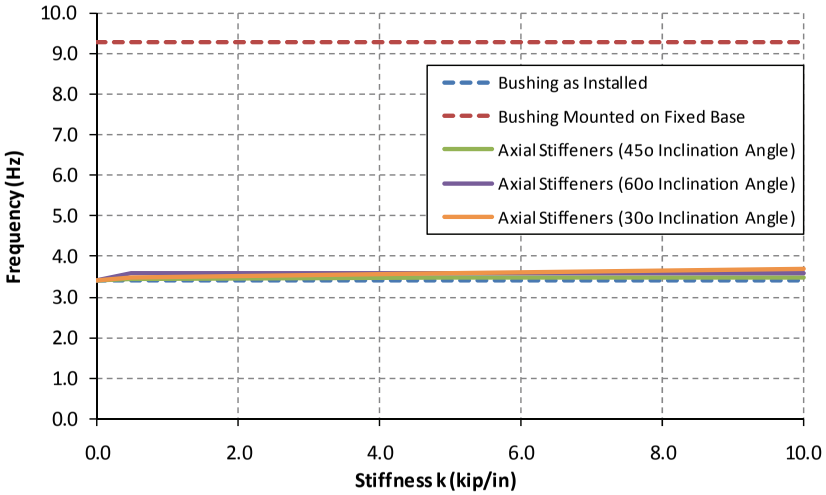

Axial Stiffeners in Transverse Direction only

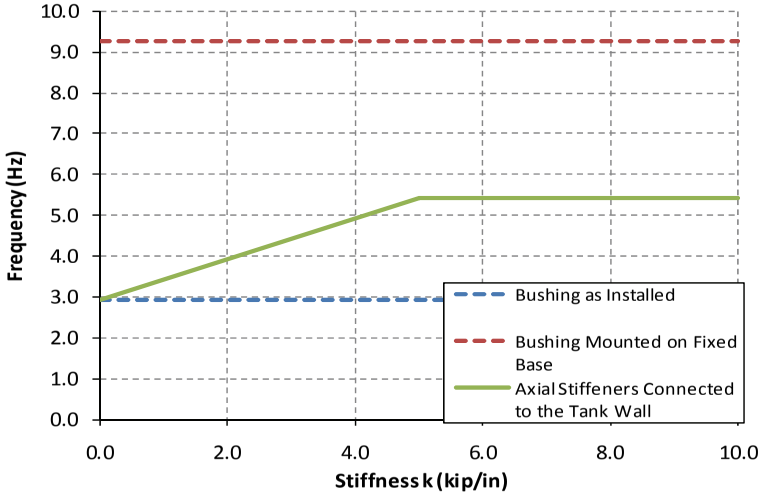

Axial Stiffeners Connected to the Tank Walls

Variation of Frequency for Westinghouse 525kV Transformer Model for the Different Stiffening Techniques considered

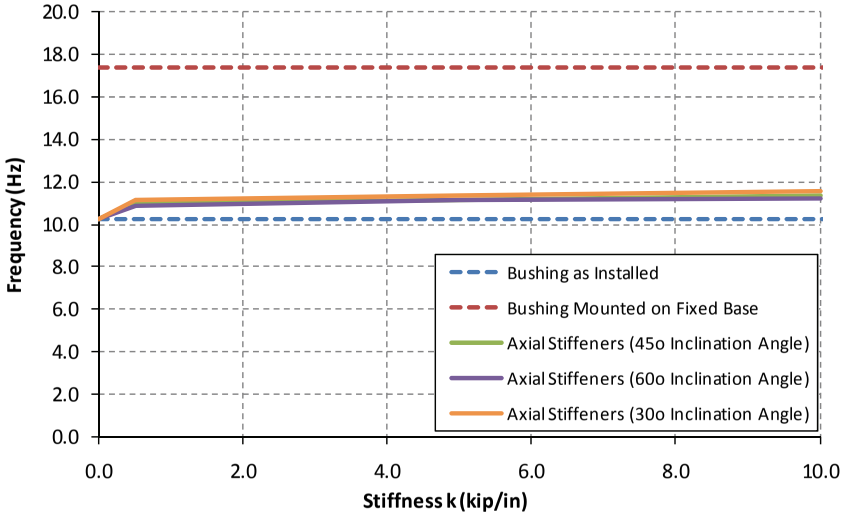

Axial Stiffeners in Longitudinal Direction only

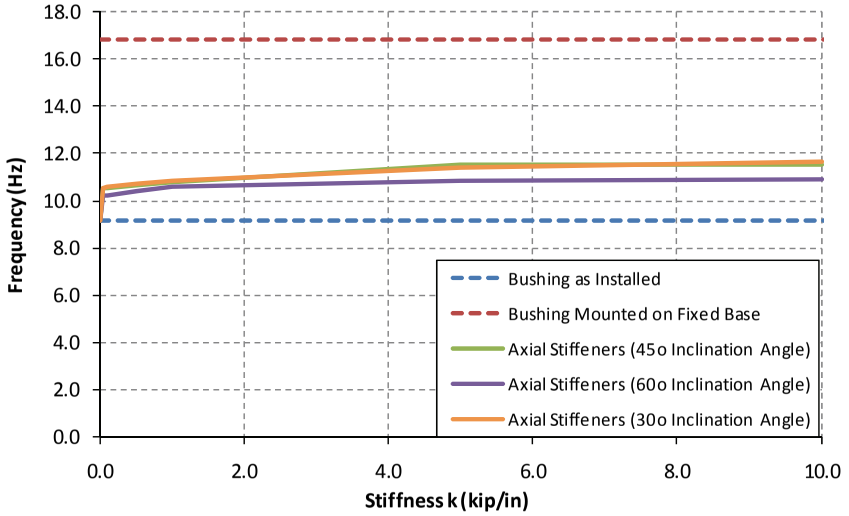

Axial Stiffeners in Transverse Direction only

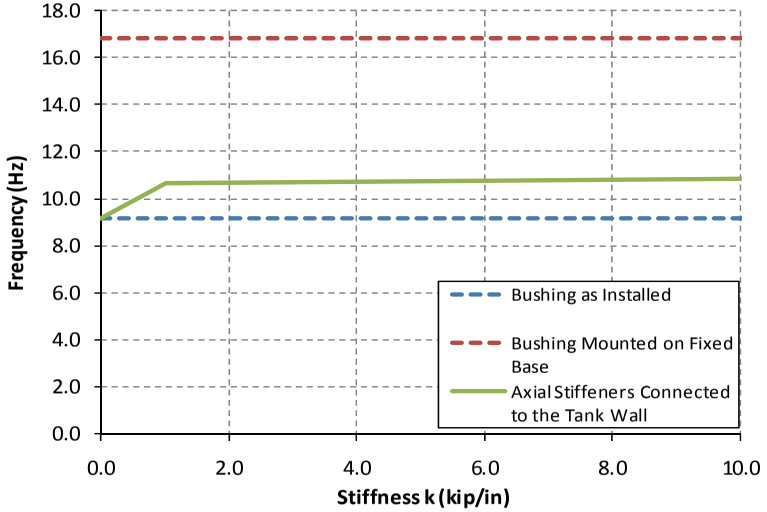

Axial Stiffeners Connected to the Tank Walls

Variation of Frequency for Siemens 230kV Transformer Model for the Different Stiffening Techniques considered

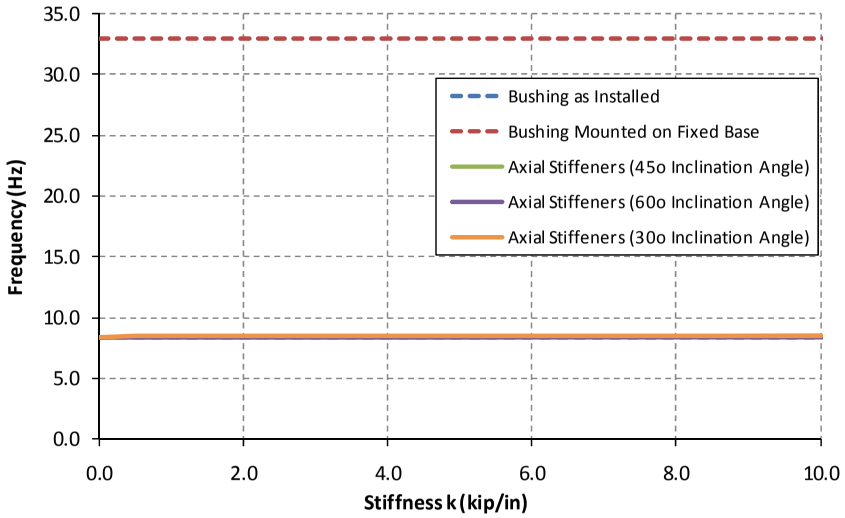

Axial Stiffeners in Longitudinal Direction only

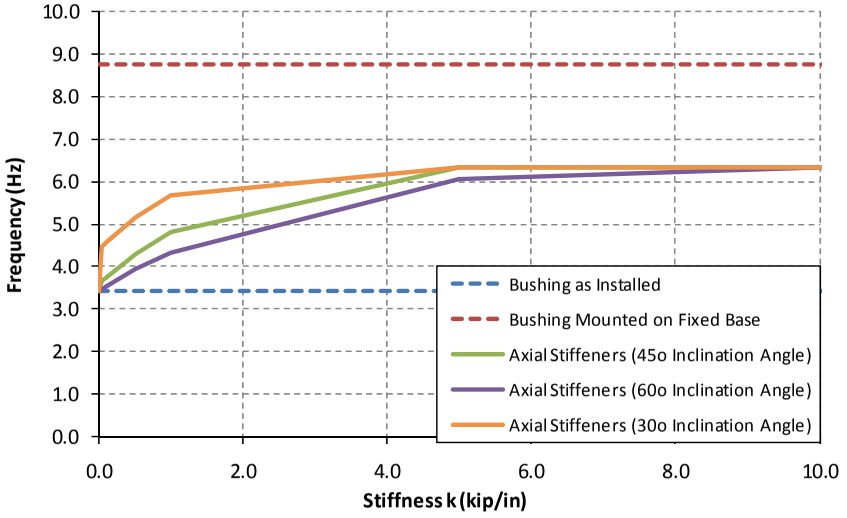

Axial Stiffeners in Transverse Direction only

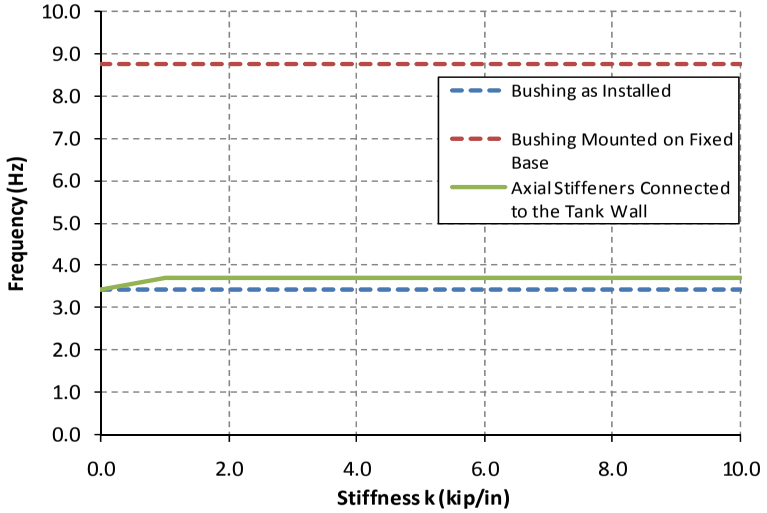

Axial Stiffeners Connected to the Tank Walls

Variation of Frequency for Siemens 500kV Transformer Model for the Different Stiffening Techniques considered

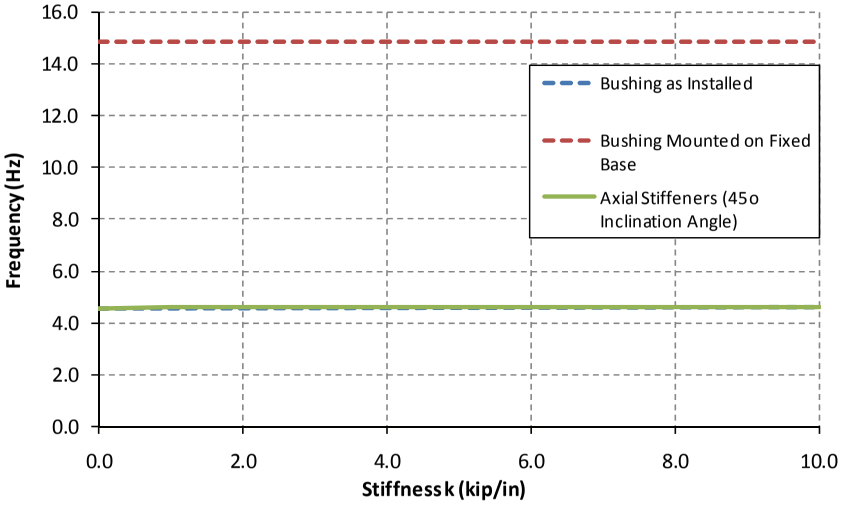

Axial Stiffeners in Longitudinal and Transverse Direction

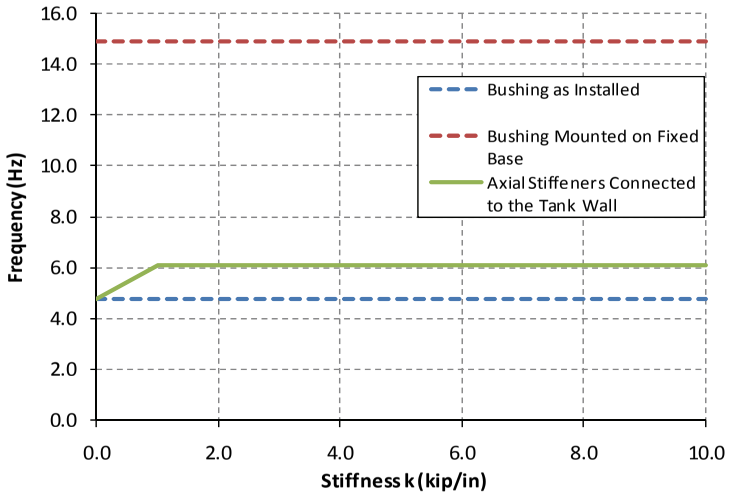

Axial Stiffeners Connected to the Tank Walls

Variation of Frequency for Ferranti Packard 230 kV Transformer Model for the Different Stiffening Techniques considered (axial stiffeners only)

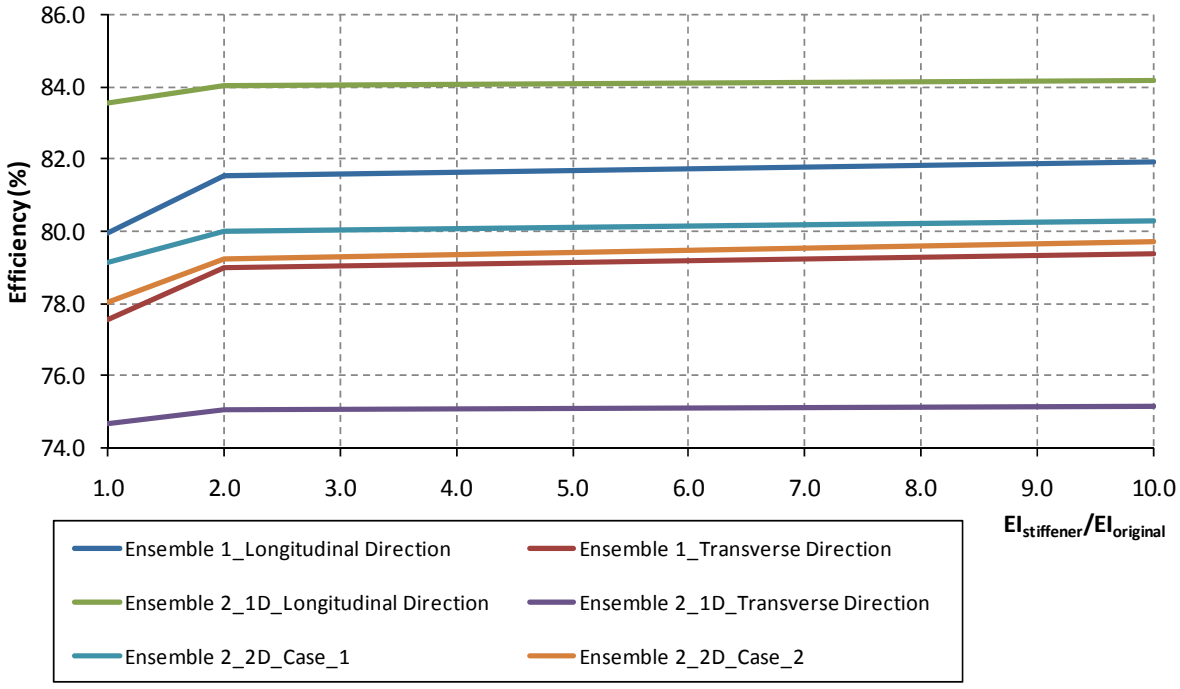

a) Flexural Stiffeners on the Cover Plate of Transformer Tank in Longitudinal and Transverse Direction

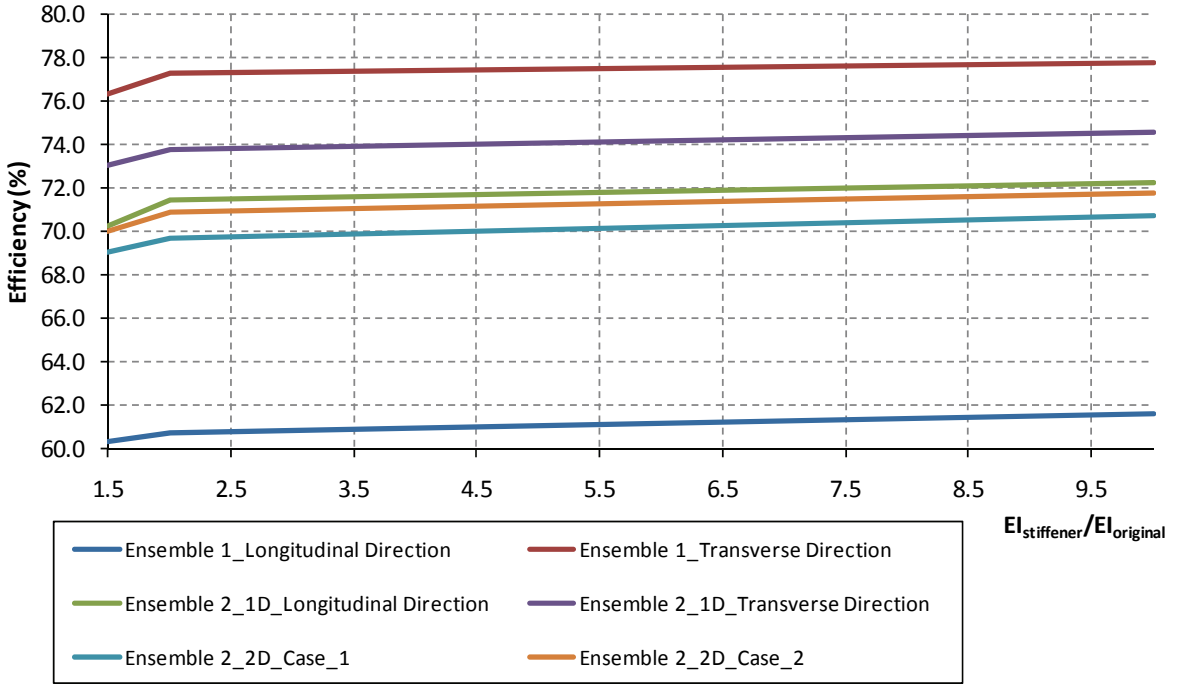

b) Flexural Stiffeners on the Cover Plate of Transformer Tank only in Transverse Direction (Manufacture's Drawings)

Variation of the Efficiency Factor of Adding Flexural Stiffeners on the Cover Plate by Increasing the Stiffness (Section Moment of Area I)

APPENDIX D

COMPARISON OF DESIRED AND ACHIEVED SHAKE TABLE MOTIONS

In this appendix a comparison between response spectra of the achieved motions from the shake table tests and the response spectra of the desired (input) ground motions are presented.

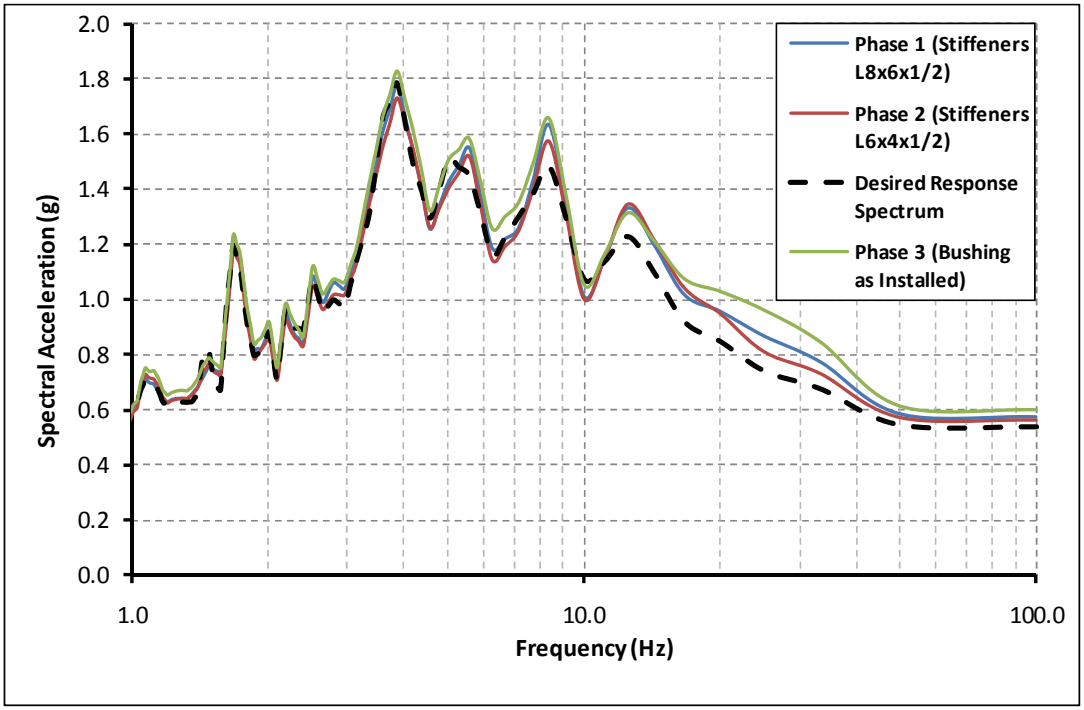

Response Spectra of EQ 1 (EQ. ID. 12011)

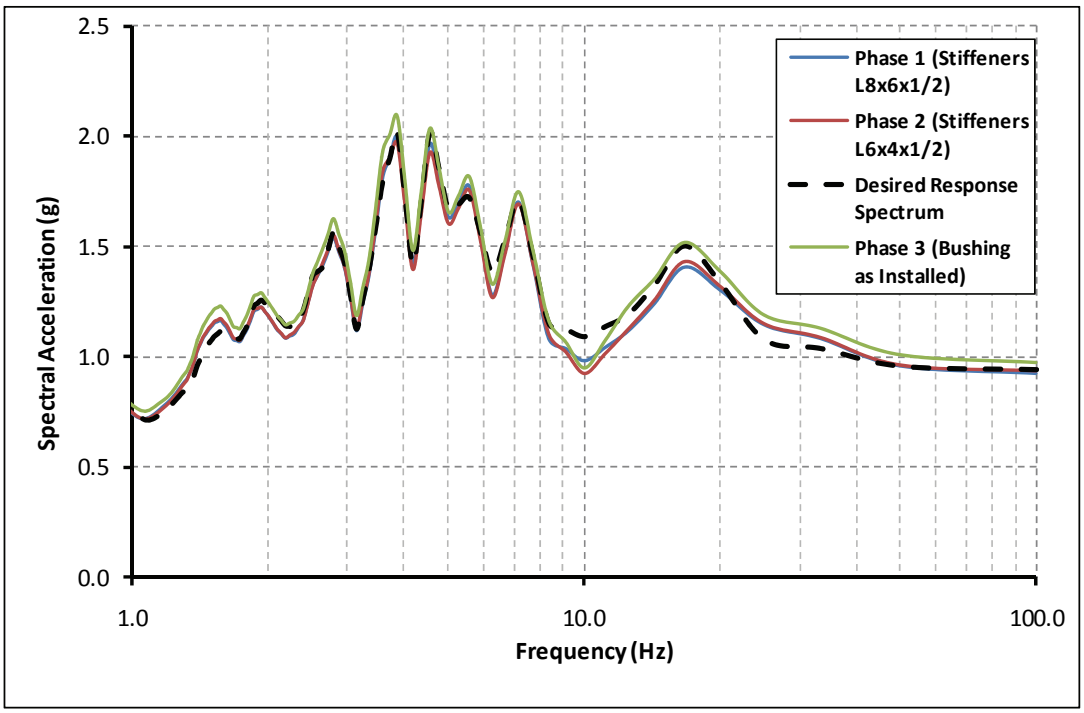

Response Spectra of EQ 2 (EQ. ID. 12041)

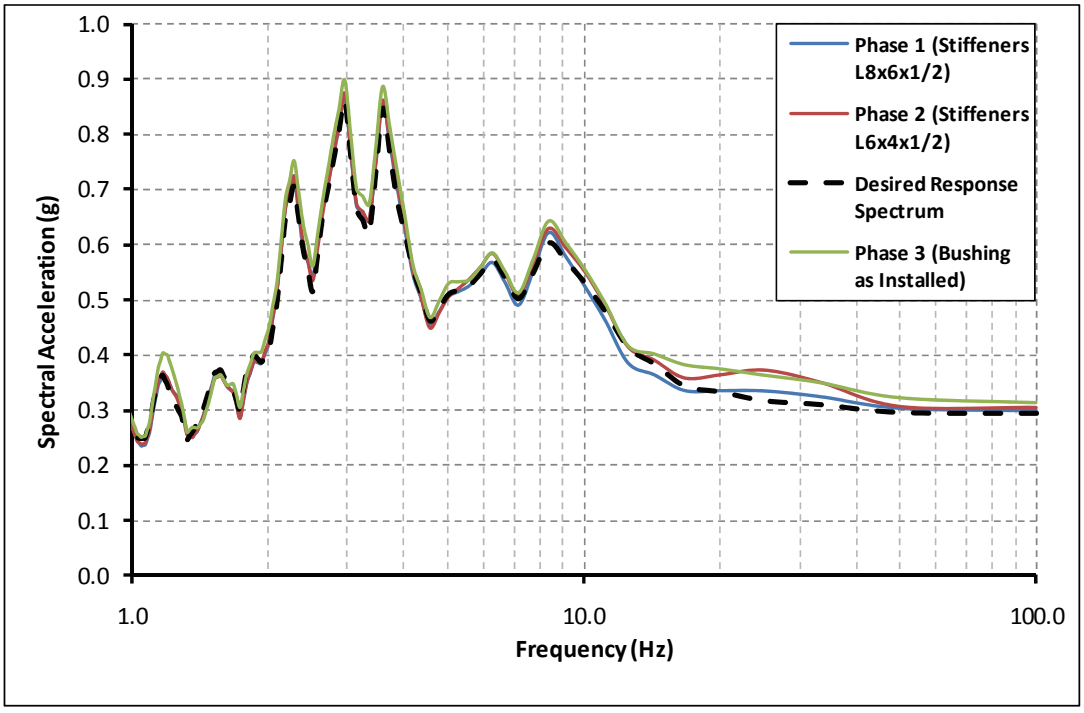

Response Spectra of EQ 3 (EQ. ID. 12072)

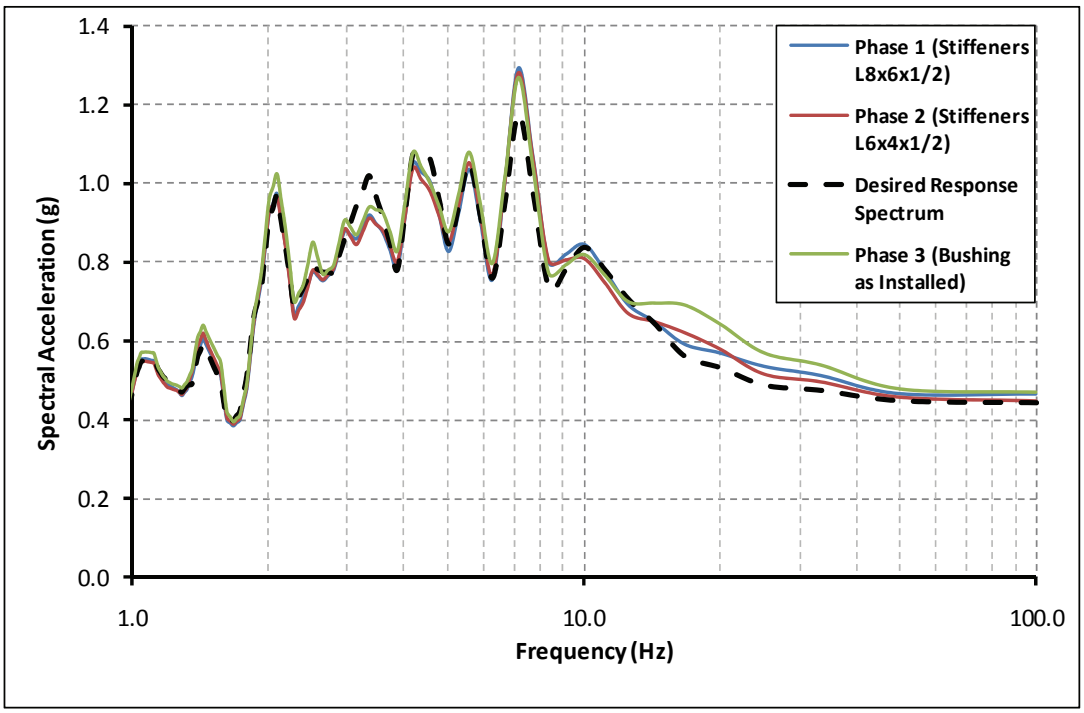

Response Spectra of EQ 4 (EQ. ID. 12092)

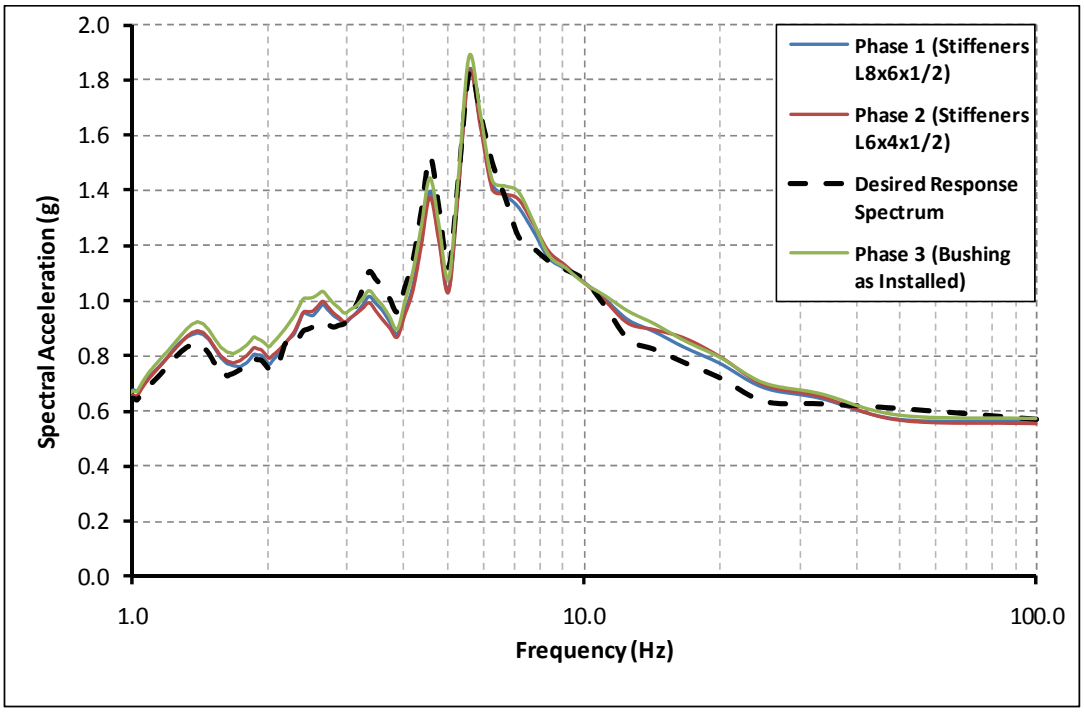

Response Spectra of EQ 5 (EQ. ID. 12132)

MCEER Technical Reports

MCEER publishes technical reports on a variety of subjects written by authors funded through MCEER. These reports are available from both MCEER Publications and the National Technical Information Service (NTIS). Requests for reports should be directed to MCEER Publications, MCEER, University at Buffalo, State University of New York, 133A Ketter Hall, Buffalo, New York 14260. Reports can also be requested through NTIS, P.O. Box 1425, Springfield, Virginia 22151. NTIS accession numbers are shown in parenthesis, if available.

NCEER-87-0001 "First-Year Program in Research, Education and Technology Transfer," 3/5/87, (PB88-134275, A04, MF-A01).

NCEER-87-0002 "Experimental Evaluation of Instantaneous Optimal Algorithms for Structural Control," by R.C. Lin, T.T. Soong and A.M. Reinhorn, 4/20/87, (PB88-134341, A04, MF-A01).

NCEER-87-0003 "Experimentation Using the Earthquake Simulation Facilities at University at Buffalo," by A.M. Reinhorn and R.L. Ketter, to be published.

NCEER-87-0004 "The System Characteristics and Performance of a Shaking Table," by J.S. Hwang, K.C. Chang and G.C. Lee, 6/1/87, (PB88-134259, A03, MF-A01). This report is available only through NTIS (see address given above).

NCEER-87-0005 "A Finite Element Formulation for Nonlinear Viscoplastic Material Using a Q Model," by O. Gyebi and G. Dasgupta, 11/2/87, (PB88-213764, A08, MF-A01).

NCEER-87-0006 "Symbolic Manipulation Program (SMP) - Algebraic Codes for Two and Three Dimensional Finite Element Formulations," by X. Lee and G. Dasgupta, 11/9/87, (PB88-218522, A05, MF-A01).

NCEER-87-0007 "Instantaneous Optimal Control Laws for Tall Buildings Under Seismic Excitations," by J.N. Yang, A. Akbarpour and P. Ghaemmaghami, 6/10/87, (PB88-134333, A06, MF-A01). This report is only available through NTIS (see address given above).

NCEER-87-0008 "IDARC: Inelastic Damage Analysis of Reinforced Concrete Frame - Shear-Wall Structures," by Y.J. Park, A.M. Reinhorn and S.K. Kunnath, 7/20/87, (PB88-134325, A09, MF-A01). This report is only available through NTIS (see address given above).

NCEER-87-0009 "Liquefaction Potential for New York State: A Preliminary Report on Sites in Manhattan and Buffalo," by M. Budhu, V. Vijayakumar, R.F. Giese and L. Baumgras, 8/31/87, (PB88-163704, A03, MF-A01). This report is available only through NTIS (see address given above).

NCEER-87-0010 "Vertical and Torsional Vibration of Foundations in Inhomogeneous Media," by A.S. Veletsos and K.W. Dotson, 6/1/87, (PB88-134291, A03, MF-A01). This report is only available through NTIS (see address given above).

NCEER-87-0011 "Seismic Probabilistic Risk Assessment and Seismic Margins Studies for Nuclear Power Plants," by Howard H.M. Hwang, 6/15/87, (PB88-134267, A03, MF-A01). This report is only available through NTIS (see address given above).

NCEER-87-0012 "Parametric Studies of Frequency Response of Secondary Systems Under Ground-Acceleration Excitations," by Y. Yong and Y.K. Lin, 6/10/87, (PB88-134309, A03, MF-A01). This report is only available through NTIS (see address given above).

NCEER-87-0013 "Frequency Response of Secondary Systems Under Seismic Excitation," by J.A. HoLung, J. Cai and Y.K. Lin, 7/31/87, (PB88-134317, A05, MF-A01). This report is only available through NTIS (see address given above).

NCEER-87-0014 "Modelling Earthquake Ground Motions in Seismically Active Regions Using Parametric Time Series Methods," by G.W. Ellis and A.S. Cakmak, 8/25/87, (PB88-134283, A08, MF-A01). This report is only available through NTIS (see address given above).

NCEER-87-0015 "Detection and Assessment of Seismic Structural Damage," by E. DiPasquale and A.S. Cakmak, 8/25/87, (PB88-163712, A05, MF-A01). This report is only available through NTIS (see address given above).

NCEER-87-0016 "Pipeline Experiment at Parkfield, California," by J. Isenberg and E. Richardson, 9/15/87, (PB88-163720, A03, MF-A01). This report is available only through NTIS (see address given above).

NCEER-87-0017 "Digital Simulation of Seismic Ground Motion," by M. Shinozuka, G. Deodatis and T. Harada, 8/31/87, (PB88-155197, A04, MF-A01). This report is available only through NTIS (see address given above).

NCEER-87-0018 "Practical Considerations for Structural Control: System Uncertainty, System Time Delay and Truncation of Small Control Forces," J.N. Yang and A. Akbarpour, 8/10/87, (PB88-163738, A08, MF-A01). This report is only available through NTIS (see address given above).

NCEER-87-0019 "Modal Analysis of Nonclassically Damped Structural Systems Using Canonical Transformation," by J.N. Yang, S. Sarkani and F.X. Long, 9/27/87, (PB88-187851, A04, MF-A01).

NCEER-87-0020 "A Nonstationary Solution in Random Vibration Theory," by J.R. Red-Horse and P.D. Spanos, 11/3/87, (PB88-163746, A03, MF-A01).

NCEER-87-0021 "Horizontal Impedances for Radially Inhomogeneous Viscoelastic Soil Layers," by A.S. Veletsos and K.W. Dotson, 10/15/87, (PB88-150859, A04, MF-A01).

NCEER-87-0022 "Seismic Damage Assessment of Reinforced Concrete Members," by Y.S. Chung, C. Meyer and M. Shinozuka, 10/9/87, (PB88-150867, A05, MF-A01). This report is available only through NTIS (see address given above).

NCEER-87-0023 "Active Structural Control in Civil Engineering," by T.T. Soong, 11/11/87, (PB88-187778, A03, MF-A01).

NCEER-87-0024 "Vertical and Torsional Impedances for Radially Inhomogeneous Viscoelastic Soil Layers," by K.W. Dotson and A.S. Veletsos, 12/87, (PB88-187786, A03, MF-A01).

NCEER-87-0025 "Proceedings from the Symposium on Seismic Hazards, Ground Motions, Soil-Liquefaction and Engineering Practice in Eastern North America," October 20-22, 1987, edited by K.H. Jacob, 12/87, (PB88-188115, A23, MF-A01). This report is available only through NTIS (see address given above).

NCEER-87-0026 "Report on the Whittier-Narrows, California, Earthquake of October 1, 1987," by J. Pantelic and A. Reinhorn, 11/87, (PB88-187752, A03, MF-A01). This report is available only through NTIS (see address given above).

NCEER-87-0027 "Design of a Modular Program for Transient Nonlinear Analysis of Large 3-D Building Structures," by S. Srivastav and J.F. Abel, 12/30/87, (PB88-187950, A05, MF-A01). This report is only available through NTIS (see address given above).

NCEER-87-0028 "Second-Year Program in Research, Education and Technology Transfer," 3/8/88, (PB88-219480, A04, MF-A01).

NCEER-88-0001 "Workshop on Seismic Computer Analysis and Design of Buildings With Interactive Graphics," by W. McGuire, J.F. Abel and C.H. Conley, 1/18/88, (PB88-187760, A03, MF-A01). This report is only available through NTIS (see address given above).

NCEER-88-0002 "Optimal Control of Nonlinear Flexible Structures," by J.N. Yang, F.X. Long and D. Wong, 1/22/88, (PB88-213772, A06, MF-A01).

NCEER-88-0003 "Substructuring Techniques in the Time Domain for Primary-Secondary Structural Systems," by G.D. Manolis and G. Juhn, 2/10/88, (PB88-213780, A04, MF-A01).

NCEER-88-0004 "Iterative Seismic Analysis of Primary-Secondary Systems," by A. Singhal, L.D. Lutes and P.D. Spanos, 2/23/88, (PB88-213798, A04, MF-A01).

NCEER-88-0005 "Stochastic Finite Element Expansion for Random Media," by P.D. Spanos and R. Ghanem, 3/14/88, (PB88-213806, A03, MF-A01).

NCEER-88-0006 "Combining Structural Optimization and Structural Control," by F.Y. Cheng and C.P. Pantelides, 1/10/88, (PB88-213814, A05, MF-A01).

NCEER-88-0007 "Seismic Performance Assessment of Code-Designed Structures," by H.H-M. Hwang, J-W. Jaw and H-J. Shau, 3/20/88, (PB88-219423, A04, MF-A01). This report is only available through NTIS (see address given above).

NCEER-88-0008 "Reliability Analysis of Code-Designed Structures Under Natural Hazards," by H.H-M. Hwang, H. Ushiba and M. Shinozuka, 2/29/88, (PB88-229471, A07, MF-A01). This report is only available through NTIS (see address given above).

NCEER-88-0009 "Seismic Fragility Analysis of Shear Wall Structures," by J-W Jaw and H.H-M. Hwang, 4/30/88, (PB89-102867, A04, MF-A01).

NCEER-88-0010 "Base Isolation of a Multi-Story Building Under a Harmonic Ground Motion - A Comparison of Performances of Various Systems," by F-G Fan, G. Ahmadi and I.G. Tadjbakhsh, 5/18/88, (PB89-122238, A06, MF-A01). This report is only available through NTIS (see address given above).

NCEER-88-0011 "Seismic Floor Response Spectra for a Combined System by Green's Functions," by F.M. Lavelle, L.A. Bergman and P.D. Spanos, 5/1/88, (PB89-102875, A03, MF-A01).

NCEER-88-0012 "A New Solution Technique for Randomly Excited Hysteretic Structures," by G.Q. Cai and Y.K. Lin, 5/16/88, (PB89-102883, A03, MF-A01).

NCEER-88-0013 "A Study of Radiation Damping and Soil-Structure Interaction Effects in the Centrifuge," by K. Weissman, supervised by J.H. Prevost, 5/24/88, (PB89-144703, A06, MF-A01).

NCEER-88-0014 "Parameter Identification and Implementation of a Kinematic Plasticity Model for Frictional Soils," by J.H. Prevost and D.V. Griffiths, to be published.

NCEER-88-0015 "Two- and Three- Dimensional Dynamic Finite Element Analyses of the Long Valley Dam," by D.V. Griffiths and J.H. Prevost, 6/17/88, (PB89-144711, A04, MF-A01).

NCEER-88-0016 "Damage Assessment of Reinforced Concrete Structures in Eastern United States," by A.M. Reinhorn, M.J. Seidel, S.K. Kunnath and Y.J. Park, 6/15/88, (PB89-122220, A04, MF-A01). This report is only available through NTIS (see address given above).

NCEER-88-0017 "Dynamic Compliance of Vertically Loaded Strip Foundations in Multilayered Viscoelastic Soils," by S. Ahmad and A.S.M. Israil, 6/17/88, (PB89-102891, A04, MF-A01).

NCEER-88-0018 "An Experimental Study of Seismic Structural Response With Added Viscoelastic Dampers," by R.C. Lin, Z. Liang, T.T. Soong and R.H. Zhang, 6/30/88, (PB89-122212, A05, MF-A01). This report is available only through NTIS (see address given above).

NCEER-88-0019 "Experimental Investigation of Primary - Secondary System Interaction," by G.D. Manolis, G. Juhn and A.M. Reinhorn, 5/27/88, (PB89-122204, A04, MF-A01).

NCEER-88-0020 "A Response Spectrum Approach For Analysis of Nonclassically Damped Structures," by J.N. Yang, S. Sarkani and F.X. Long, 4/22/88, (PB89-102909, A04, MF-A01).

NCEER-88-0021 "Seismic Interaction of Structures and Soils: Stochastic Approach," by A.S. Veletsos and A.M. Prasad, 7/21/88, (PB89-122196, A04, MF-A01). This report is only available through NTIS (see address given above).

NCEER-88-0022 "Identification of the Serviceability Limit State and Detection of Seismic Structural Damage," by E. DiPasquale and A.S. Cakmak, 6/15/88, (PB89-122188, A05, MF-A01). This report is available only through NTIS (see address given above).

NCEER-88-0023 "Multi-Hazard Risk Analysis: Case of a Simple Offshore Structure," by B.K. Bhartia and E.H. Vanmarcke, 7/21/88, (PB89-145213, A05, MF-A01).

NCEER-88-0024 "Automated Seismic Design of Reinforced Concrete Buildings," by Y.S. Chung, C. Meyer and M. Shinozuka, 7/5/88, (PB89-122170, A06, MF-A01). This report is available only through NTIS (see address given above).

NCEER-88-0025 "Experimental Study of Active Control of MDOF Structures Under Seismic Excitations," by L.L. Chung, R.C. Lin, T.T. Soong and A.M. Reinhorn, 7/10/88, (PB89-122600, A04, MF-A01).

NCEER-88-0026 "Earthquake Simulation Tests of a Low-Rise Metal Structure," by J.S. Hwang, K.C. Chang, G.C. Lee and R.L. Ketter, 8/1/88, (PB89-102917, A04, MF-A01).

NCEER-88-0027 "Systems Study of Urban Response and Reconstruction Due to Catastrophic Earthquakes," by F. Kozin and H.K. Zhou, 9/22/88, (PB90-162348, A04, MF-A01).

NCEER-88-0028 "Seismic Fragility Analysis of Plane Frame Structures," by H.H-M. Hwang and Y.K. Low, 7/31/88, (PB89-131445, A06, MF-A01).

NCEER-88-0029 "Response Analysis of Stochastic Structures," by A. Kardara, C. Bucher and M. Shinozuka, 9/22/88, (PB89-174429, A04, MF-A01).

NCEER-88-0030 "Nonnormal Accelerations Due to Yielding in a Primary Structure," by D.C.K. Chen and L.D. Lutes, 9/19/88, (PB89-131437, A04, MF-A01).

NCEER-88-0031 "Design Approaches for Soil-Structure Interaction," by A.S. Veletsos, A.M. Prasad and Y. Tang, 12/30/88, (PB89-174437, A03, MF-A01). This report is available only through NTIS (see address given above).

NCEER-88-0032 "A Re-evaluation of Design Spectra for Seismic Damage Control," by C.J. Turkstra and A.G. Tallin, 11/7/88, (PB89-145221, A05, MF-A01).

NCEER-88-0033 "The Behavior and Design of Noncontact Lap Splices Subjected to Repeated Inelastic Tensile Loading," by V.E. Sagan, P. Gergely and R.N. White, 12/8/88, (PB89-163737, A08, MF-A01).

NCEER-88-0034 "Seismic Response of Pile Foundations," by S.M. Mamoon, P.K. Banerjee and S. Ahmad, 11/1/88, (PB89-145239, A04, MF-A01).

NCEER-88-0035 "Modeling of R/C Building Structures With Flexible Floor Diaphragms (IDARC2)," by A.M. Reinhorn, S.K. Kunnath and N. Panahshahi, 9/7/88, (PB89-207153, A07, MF-A01).

NCEER-88-0036 "Solution of the Dam-Reservoir Interaction Problem Using a Combination of FEM, BEM with Particular Integrals, Modal Analysis, and Substructuring," by C-S. Tsai, G.C. Lee and R.L. Ketter, 12/31/88, (PB89-207146, A04, MF-A01).

NCEER-88-0037 "Optimal Placement of Actuators for Structural Control," by F.Y. Cheng and C.P. Pantelides, 8/15/88, (PB89-162846, A05, MF-A01).

NCEER-88-0038 "Teflon Bearings in Aseismic Base Isolation: Experimental Studies and Mathematical Modeling," by A. Mokha, M.C. Constantinou and A.M. Reinhorn, 12/5/88, (PB89-218457, A10, MF-A01). This report is available only through NTIS (see address given above).

NCEER-88-0039 "Seismic Behavior of Flat Slab High-Rise Buildings in the New York City Area," by P. Weidlinger and M. Ettouney, 10/15/88, (PB90-145681, A04, MF-A01).

NCEER-88-0040 "Evaluation of the Earthquake Resistance of Existing Buildings in New York City," by P. Weidlinger and M. Ettouney, 10/15/88, to be published.

NCEER-88-0041 "Small-Scale Modeling Techniques for Reinforced Concrete Structures Subjected to Seismic Loads," by W. Kim, A. El-Attar and R.N. White, 11/22/88, (PB89-189625, A05, MF-A01).

NCEER-88-0042 "Modeling Strong Ground Motion from Multiple Event Earthquakes," by G.W. Ellis and A.S. Cakmak, 10/15/88, (PB89-174445, A03, MF-A01).

NCEER-88-0043 "Nonstationary Models of Seismic Ground Acceleration," by M. Grigoriu, S.E. Ruiz and E. Rosenblueth, 7/15/88, (PB89-189617, A04, MF-A01).

NCEER-88-0044 "SARCF User's Guide: Seismic Analysis of Reinforced Concrete Frames," by Y.S. Chung, C. Meyer and M. Shinozuka, 11/9/88, (PB89-174452, A08, MF-A01).

NCEER-88-0045 "First Expert Panel Meeting on Disaster Research and Planning," edited by J. Pantelic and J. Stoyle, 9/15/88, (PB89-174460, A05, MF-A01).

NCEER-88-0046 "Preliminary Studies of the Effect of Degrading Infill Walls on the Nonlinear Seismic Response of Steel Frames," by C.Z. Chrysostomou, P. Gergely and J.F. Abel, 12/19/88, (PB89-208383, A05, MF-A01).

NCEER-88-0047 "Reinforced Concrete Frame Component Testing Facility - Design, Construction, Instrumentation and Operation," by S.P. Pessiki, C. Conley, T. Bond, P. Gergely and R.N. White, 12/16/88, (PB89-174478, A04, MF-A01).

NCEER-89-0001 "Effects of Protective Cushion and Soil Compliancy on the Response of Equipment Within a Seismically Excited Building," by J.A. HoLung, 2/16/89, (PB89-207179, A04, MF-A01).

NCEER-89-0002 "Statistical Evaluation of Response Modification Factors for Reinforced Concrete Structures," by H.H-M. Hwang and J-W. Jaw, 2/17/89, (PB89-207187, A05, MF-A01).

NCEER-89-0003 "Hysteretic Columns Under Random Excitation," by G-Q. Cai and Y.K. Lin, 1/9/89, (PB89-196513, A03, MF-A01).

NCEER-89-0004 "Experimental Study of `Elephant Foot Bulge' Instability of Thin-Walled Metal Tanks," by Z-H. Jia and R.L. Ketter, 2/22/89, (PB89-207195, A03, MF-A01).

NCEER-89-0005 "Experiment on Performance of Buried Pipelines Across San Andreas Fault," by J. Isenberg, E. Richardson and T.D. O'Rourke, 3/10/89, (PB89-218440, A04, MF-A01). This report is available only through NTIS (see address given above).

NCEER-89-0006 "A Knowledge-Based Approach to Structural Design of Earthquake-Resistant Buildings," by M. Subramani, P. Gergely, C.H. Conley, J.F. Abel and A.H. Zaghw, 1/15/89, (PB89-218465, A06, MF-A01).

NCEER-89-0007 "Liquefaction Hazards and Their Effects on Buried Pipelines," by T.D. O'Rourke and P.A. Lane, 2/1/89, (PB89-218481, A09, MF-A01).

NCEER-89-0008 "Fundamentals of System Identification in Structural Dynamics," by H. Imai, C-B. Yun, O. Maruyama and M. Shinozuka, 1/26/89, (PB89-207211, A04, MF-A01).

NCEER-89-0009 "Effects of the 1985 Michoacan Earthquake on Water Systems and Other Buried Lifelines in Mexico," by A.G. Ayala and M.J. O'Rourke, 3/8/89, (PB89-207229, A06, MF-A01).

NCEER-89-R010 "NCEER Bibliography of Earthquake Education Materials," by K.E.K. Ross, Second Revision, 9/1/89, (PB90-125352, A05, MF-A01). This report is replaced by NCEER-92-0018.

NCEER-89-0011 "Inelastic Three-Dimensional Response Analysis of Reinforced Concrete Building Structures (IDARC-3D), Part I - Modeling," by S.K. Kunnath and A.M. Reinhorn, 4/17/89, (PB90-114612, A07, MF-A01). This report is available only through NTIS (see address given above).

NCEER-89-0012 "Recommended Modifications to ATC-14," by C.D. Poland and J.O. Malley, 4/12/89, (PB90-108648, A15, MF-A01).

NCEER-89-0013 "Repair and Strengthening of Beam-to-Column Connections Subjected to Earthquake Loading," by M. Corazao and A.J. Durrani, 2/28/89, (PB90-109885, A06, MF-A01).

NCEER-89-0014 "Program EXKAL2 for Identification of Structural Dynamic Systems," by O. Maruyama, C-B. Yun, M. Hoshiya and M. Shinozuka, 5/19/89, (PB90-109877, A09, MF-A01).

NCEER-89-0015 "Response of Frames With Bolted Semi-Rigid Connections, Part I - Experimental Study and Analytical Predictions," by P.J. DiCorso, A.M. Reinhorn, J.R. Dickerson, J.B. Radziminski and W.L. Harper, 6/1/89, to be published.

NCEER-89-0016 "ARMA Monte Carlo Simulation in Probabilistic Structural Analysis," by P.D. Spanos and M.P. Mignolet, 7/10/89, (PB90-109893, A03, MF-A01).

NCEER-89-P017 "Preliminary Proceedings from the Conference on Disaster Preparedness - The Place of Earthquake Education in Our Schools," Edited by K.E.K. Ross, 6/23/89, (PB90-108606, A03, MF-A01).

NCEER-89-0017 "Proceedings from the Conference on Disaster Preparedness - The Place of Earthquake Education in Our Schools," Edited by K.E.K. Ross, 12/31/89, (PB90-207895, A012, MF-A02). This report is available only through NTIS (see address given above).

NCEER-89-0018 "Multidimensional Models of Hysteretic Material Behavior for Vibration Analysis of Shape Memory Energy Absorbing Devices, by E.J. Graesser and F.A. Cozzarelli, 6/7/89, (PB90-164146, A04, MF-A01).

NCEER-89-0019 "Nonlinear Dynamic Analysis of Three-Dimensional Base Isolated Structures (3D-BASIS)," by S. Nagarajaiah, A.M. Reinhorn and M.C. Constantinou, 8/3/89, (PB90-161936, A06, MF-A01). This report has been replaced by NCEER-93-0011.

NCEER-89-0020 "Structural Control Considering Time-Rate of Control Forces and Control Rate Constraints," by F.Y. Cheng and C.P. Pantelides, 8/3/89, (PB90-120445, A04, MF-A01).

NCEER-89-0021 "Subsurface Conditions of Memphis and Shelby County," by K.W. Ng, T-S. Chang and H-H.M. Hwang, 7/26/89, (PB90-120437, A03, MF-A01).

NCEER-89-0022 "Seismic Wave Propagation Effects on Straight Jointed Buried Pipelines," by K. Elhmadi and M.J. O'Rourke, 8/24/89, (PB90-162322, A10, MF-A02).

NCEER-89-0023 "Workshop on Serviceability Analysis of Water Delivery Systems," edited by M. Grigoriu, 3/6/89, (PB90-127424, A03, MF-A01).

NCEER-89-0024 "Shaking Table Study of a 1/5 Scale Steel Frame Composed of Tapered Members," by K.C. Chang, J.S. Hwang and G.C. Lee, 9/18/89, (PB90-160169, A04, MF-A01).

NCEER-89-0025 "DYNA1D: A Computer Program for Nonlinear Seismic Site Response Analysis - Technical Documentation," by Jean H. Prevost, 9/14/89, (PB90-161944, A07, MF-A01). This report is available only through NTIS (see address given above).

NCEER-89-0026 "1:4 Scale Model Studies of Active Tendon Systems and Active Mass Dampers for Aseismic Protection," by A.M. Reinhorn, T.T. Soong, R.C. Lin, Y.P. Yang, Y. Fukao, H. Abe and M. Nakai, 9/15/89, (PB90-173246, A10, MF-A02). This report is available only through NTIS (see address given above).

NCEER-89-0027 "Scattering of Waves by Inclusions in a Nonhomogeneous Elastic Half Space Solved by Boundary Element Methods," by P.K. Hadley, A. Askar and A.S. Cakmak, 6/15/89, (PB90-145699, A07, MF-A01).

NCEER-89-0028 "Statistical Evaluation of Deflection Amplification Factors for Reinforced Concrete Structures," by H.H.M. Hwang, J-W. Jaw and A.L. Ch'ng, 8/31/89, (PB90-164633, A05, MF-A01).

NCEER-89-0029 "Bedrock Accelerations in Memphis Area Due to Large New Madrid Earthquakes," by H.H.M. Hwang, C.H.S. Chen and G. Yu, 11/7/89, (PB90-162330, A04, MF-A01).

NCEER-89-0030 "Seismic Behavior and Response Sensitivity of Secondary Structural Systems," by Y.Q. Chen and T.T. Soong, 10/23/89, (PB90-164658, A08, MF-A01).

NCEER-89-0031 "Random Vibration and Reliability Analysis of Primary-Secondary Structural Systems," by Y. Ibrahim, M. Grigoriu and T.T. Soong, 11/10/89, (PB90-161951, A04, MF-A01).

NCEER-89-0032 "Proceedings from the Second U.S. - Japan Workshop on Liquefaction, Large Ground Deformation and Their Effects on Lifelines, September 26-29, 1989," Edited by T.D. O'Rourke and M. Hamada, 12/1/89, (PB90-209388, A22, MF-A03).

NCEER-89-0033 "Deterministic Model for Seismic Damage Evaluation of Reinforced Concrete Structures," by J.M. Bracci, A.M. Reinhorn, J.B. Mander and S.K. Kunnath, 9/27/89, (PB91-108803, A06, MF-A01).

NCEER-89-0034 "On the Relation Between Local and Global Damage Indices," by E. DiPasquale and A.S. Cakmak, 8/15/89, (PB90-173865, A05, MF-A01).

NCEER-89-0035 "Cyclic Undrained Behavior of Nonplastic and Low Plasticity Silts," by A.J. Walker and H.E. Stewart, 7/26/89, (PB90-183518, A10, MF-A01).

NCEER-89-0036 "Liquefaction Potential of Surficial Deposits in the City of Buffalo, New York," by M. Budhu, R. Giese and L. Baumgrass, 1/17/89, (PB90-208455, A04, MF-A01).

NCEER-89-0037 "A Deterministic Assessment of Effects of Ground Motion Incoherence," by A.S. Veletsos and Y. Tang, 7/15/89, (PB90-164294, A03, MF-A01).

NCEER-89-0038 "Workshop on Ground Motion Parameters for Seismic Hazard Mapping," July 17-18, 1989, edited by R.V. Whitman, 12/1/89, (PB90-173923, A04, MF-A01).

NCEER-89-0039 "Seismic Effects on Elevated Transit Lines of the New York City Transit Authority," by C.J. Costantino, C.A. Miller and E. Heymsfield, 12/26/89, (PB90-207887, A06, MF-A01).

NCEER-89-0040 "Centrifugal Modeling of Dynamic Soil-Structure Interaction," by K. Weissman, Supervised by J.H. Prevost, 5/10/89, (PB90-207879, A07, MF-A01).

NCEER-89-0041 "Linearized Identification of Buildings With Cores for Seismic Vulnerability Assessment," by I-K. Ho and A.E. Aktan, 11/1/89, (PB90-251943, A07, MF-A01).

NCEER-90-0001 "Geotechnical and Lifeline Aspects of the October 17, 1989 Loma Prieta Earthquake in San Francisco," by T.D. O'Rourke, H.E. Stewart, F.T. Blackburn and T.S. Dickerman, 1/90, (PB90-208596, A05, MF-A01).

NCEER-90-0002 "Nonnormal Secondary Response Due to Yielding in a Primary Structure," by D.C.K. Chen and L.D. Lutes, 2/28/90, (PB90-251976, A07, MF-A01).

NCEER-90-0003 "Earthquake Education Materials for Grades K-12," by K.E.K. Ross, 4/16/90, (PB91-251984, A05, MF-A05). This report has been replaced by NCEER-92-0018.

NCEER-90-0004 "Catalog of Strong Motion Stations in Eastern North America," by R.W. Busby, 4/3/90, (PB90-251984, A05, MF-A01).

NCEER-90-0005 "NCEER Strong-Motion Data Base: A User Manual for the GeoBase Release (Version 1.0 for the Sun3)," by P. Friberg and K. Jacob, 3/31/90 (PB90-258062, A04, MF-A01).

NCEER-90-0006 "Seismic Hazard Along a Crude Oil Pipeline in the Event of an 1811-1812 Type New Madrid Earthquake," by H.H.M. Hwang and C-H.S. Chen, 4/16/90, (PB90-258054, A04, MF-A01).

NCEER-90-0007 "Site-Specific Response Spectra for Memphis Sheahan Pumping Station," by H.H.M. Hwang and C.S. Lee, 5/15/90, (PB91-108811, A05, MF-A01).

NCEER-90-0008 "Pilot Study on Seismic Vulnerability of Crude Oil Transmission Systems," by T. Ariman, R. Dobry, M. Grigoriu, F. Kozin, M. O'Rourke, T. O'Rourke and M. Shinozuka, 5/25/90, (PB91-108837, A06, MF-A01).

NCEER-90-0009 "A Program to Generate Site Dependent Time Histories: EQGEN," by G.W. Ellis, M. Srinivasan and A.S. Cakmak, 1/30/90, (PB91-108829, A04, MF-A01).

NCEER-90-0010 "Active Isolation for Seismic Protection of Operating Rooms," by M.E. Talbott, Supervised by M. Shinozuka, 6/8/9, (PB91-110205, A05, MF-A01).

NCEER-90-0011 "Program LINEARID for Identification of Linear Structural Dynamic Systems," by C-B. Yun and M. Shinozuka, 6/25/90, (PB91-110312, A08, MF-A01).

NCEER-90-0012 "Two-Dimensional Two-Phase Elasto-Plastic Seismic Response of Earth Dams," by A.N. Yiagos, Supervised by J.H. Prevost, 6/20/90, (PB91-110197, A13, MF-A02).

NCEER-90-0013 "Secondary Systems in Base-Isolated Structures: Experimental Investigation, Stochastic Response and Stochastic Sensitivity," by G.D. Manolis, G. Juhn, M.C. Constantinou and A.M. Reinhorn, 7/1/90, (PB91-110320, A08, MF-A01).

NCEER-90-0014 "Seismic Behavior of Lightly-Reinforced Concrete Column and Beam-Column Joint Details," by S.P. Pessiki, C.H. Conley, P. Gergely and R.N. White, 8/22/90, (PB91-108795, A11, MF-A02).

NCEER-90-0015 "Two Hybrid Control Systems for Building Structures Under Strong Earthquakes," by J.N. Yang and A. Danielians, 6/29/90, (PB91-125393, A04, MF-A01).

NCEER-90-0016 "Instantaneous Optimal Control with Acceleration and Velocity Feedback," by J.N. Yang and Z. Li, 6/29/90, (PB91-125401, A03, MF-A01).

NCEER-90-0017 "Reconnaissance Report on the Northern Iran Earthquake of June 21, 1990," by M. Mehrain, 10/4/90, (PB91-125377, A03, MF-A01).

NCEER-90-0018 "Evaluation of Liquefaction Potential in Memphis and Shelby County," by T.S. Chang, P.S. Tang, C.S. Lee and H. Hwang, 8/10/90, (PB91-125427, A09, MF-A01).

NCEER-90-0019 "Experimental and Analytical Study of a Combined Sliding Disc Bearing and Helical Steel Spring Isolation System," by M.C. Constantinou, A.S. Mokha and A.M. Reinhorn, 10/4/90, (PB91-125385, A06, MF-A01). This report is available only through NTIS (see address given above).

NCEER-90-0020 "Experimental Study and Analytical Prediction of Earthquake Response of a Sliding Isolation System with a Spherical Surface," by A.S. Mokha, M.C. Constantinou and A.M. Reinhorn, 10/11/90, (PB91-125419, A05, MF-A01).

NCEER-90-0021 "Dynamic Interaction Factors for Floating Pile Groups," by G. Gazetas, K. Fan, A. Kaynia and E. Kausel, 9/10/90, (PB91-170381, A05, MF-A01).

NCEER-90-0022 "Evaluation of Seismic Damage Indices for Reinforced Concrete Structures," by S. Rodriguez-Gomez and A.S. Cakmak, 9/30/90, PB91-171322, A06, MF-A01).

NCEER-90-0023 "Study of Site Response at a Selected Memphis Site," by H. Desai, S. Ahmad, E.S. Gazetas and M.R. Oh, 10/11/90, (PB91-196857, A03, MF-A01).

NCEER-90-0024 "A User's Guide to Strongmo: Version 1.0 of NCEER's Strong-Motion Data Access Tool for PCs and Terminals," by P.A. Friberg and C.A.T. Susch, 11/15/90, (PB91-171272, A03, MF-A01).

NCEER-90-0025 "A Three-Dimensional Analytical Study of Spatial Variability of Seismic Ground Motions," by L-L. Hong and A.H.-S. Ang, 10/30/90, (PB91-170399, A09, MF-A01).

NCEER-90-0026 "MUMOID User's Guide - A Program for the Identification of Modal Parameters," by S. Rodriguez-Gomez and E. DiPasquale, 9/30/90, (PB91-171298, A04, MF-A01).

NCEER-90-0027 "SARCF-II User's Guide - Seismic Analysis of Reinforced Concrete Frames," by S. Rodriguez-Gomez, Y.S. Chung and C. Meyer, 9/30/90, (PB91-171280, A05, MF-A01).

NCEER-90-0028 "Viscous Dampers: Testing, Modeling and Application in Vibration and Seismic Isolation," by N. Makris and M.C. Constantinou, 12/20/90 (PB91-190561, A06, MF-A01).

NCEER-90-0029 "Soil Effects on Earthquake Ground Motions in the Memphis Area," by H. Hwang, C.S. Lee, K.W. Ng and T.S. Chang, 8/2/90, (PB91-190751, A05, MF-A01).

NCEER-91-0001 "Proceedings from the Third Japan-U.S. Workshop on Earthquake Resistant Design of Lifeline Facilities and Countermeasures for Soil Liquefaction, December 17-19, 1990," edited by T.D. O'Rourke and M. Hamada, 2/1/91, (PB91-179259, A99, MF-A04).

NCEER-91-0002 "Physical Space Solutions of Non-Proportionally Damped Systems," by M. Tong, Z. Liang and G.C. Lee, 1/15/91, (PB91-179242, A04, MF-A01).

NCEER-91-0003 "Seismic Response of Single Piles and Pile Groups," by K. Fan and G. Gazetas, 1/10/91, (PB92-174994, A04, MF-A01).

NCEER-91-0004 "Damping of Structures: Part 1 - Theory of Complex Damping," by Z. Liang and G. Lee, 10/10/91, (PB92-197235, A12, MF-A03).

NCEER-91-0005 "3D-BASIS - Nonlinear Dynamic Analysis of Three Dimensional Base Isolated Structures: Part II," by S. Nagarajaiah, A.M. Reinhorn and M.C. Constantinou, 2/28/91, (PB91-190553, A07, MF-A01). This report has been replaced by NCEER-93-0011.

NCEER-91-0006 "A Multidimensional Hysteretic Model for Plasticity Deforming Metals in Energy Absorbing Devices," by E.J. Graesser and F.A. Cozzarelli, 4/9/91, (PB92-108364, A04, MF-A01).

NCEER-91-0007 "A Framework for Customizable Knowledge-Based Expert Systems with an Application to a KBES for Evaluating the Seismic Resistance of Existing Buildings," by E.G. Ibarra-Anaya and S.J. Fenves, 4/9/91, (PB91-210930, A08, MF-A01).

NCEER-91-0008 "Nonlinear Analysis of Steel Frames with Semi-Rigid Connections Using the Capacity Spectrum Method," by G.G. Deierlein, S-H. Hsieh, Y-J. Shen and J.F. Abel, 7/2/91, (PB92-113828, A05, MF-A01).

NCEER-91-0009 "Earthquake Education Materials for Grades K-12," by K.E.K. Ross, 4/30/91, (PB91-212142, A06, MF-A01). This report has been replaced by NCEER-92-0018.

NCEER-91-0010 "Phase Wave Velocities and Displacement Phase Differences in a Harmonically Oscillating Pile," by N. Makris and G. Gazetas, 7/8/91, (PB92-108356, A04, MF-A01).

NCEER-91-0011 "Dynamic Characteristics of a Full-Size Five-Story Steel Structure and a 2/5 Scale Model," by K.C. Chang, G.C. Yao, G.C. Lee, D.S. Hao and Y.C. Yeh," 7/2/91, (PB93-116648, A06, MF-A02).

NCEER-91-0012 "Seismic Response of a 2/5 Scale Steel Structure with Added Viscoelastic Dampers," by K.C. Chang, T.T. Soong, S-T. Oh and M.L. Lai, 5/17/91, (PB92-110816, A05, MF-A01).

NCEER-91-0013 "Earthquake Response of Retaining Walls; Full-Scale Testing and Computational Modeling," by S. Alampalli and A-W.M. Elgamal, 6/20/91, to be published.

NCEER-91-0014 "3D-BASIS-M: Nonlinear Dynamic Analysis of Multiple Building Base Isolated Structures," by P.C. Tsopelas, S. Nagarajaiah, M.C. Constantinou and A.M. Reinhorn, 5/28/91, (PB92-113885, A09, MF-A02).

NCEER-91-0015 "Evaluation of SEAOC Design Requirements for Sliding Isolated Structures," by D. Theodossiou and M.C. Constantinou, 6/10/91, (PB92-114602, A11, MF-A03).

NCEER-91-0016 "Closed-Loop Modal Testing of a 27-Story Reinforced Concrete Flat Plate-Core Building," by H.R. Somaprasad, T. Toksoy, H. Yoshiyuki and A.E. Aktan, 7/15/91, (PB92-129980, A07, MF-A02).

NCEER-91-0017 "Shake Table Test of a 1/6 Scale Two-Story Lightly Reinforced Concrete Building," by A.G. El-Attar, R.N. White and P. Gergely, 2/28/91, (PB92-222447, A06, MF-A02).

NCEER-91-0018 "Shake Table Test of a 1/8 Scale Three-Story Lightly Reinforced Concrete Building," by A.G. El-Attar, R.N. White and P. Gergely, 2/28/91, (PB93-116630, A08, MF-A02).

NCEER-91-0019 "Transfer Functions for Rigid Rectangular Foundations," by A.S. Veletsos, A.M. Prasad and W.H. Wu, 7/31/91, to be published.

NCEER-91-0020 "Hybrid Control of Seismic-Excited Nonlinear and Inelastic Structural Systems," by J.N. Yang, Z. Li and A. Danielians, 8/1/91, (PB92-143171, A06, MF-A02).

NCEER-91-0021 "The NCEER-91 Earthquake Catalog: Improved Intensity-Based Magnitudes and Recurrence Relations for U.S. Earthquakes East of New Madrid," by L. Seeber and J.G. Armbruster, 8/28/91, (PB92-176742, A06, MF-A02).

NCEER-91-0022 "Proceedings from the Implementation of Earthquake Planning and Education in Schools: The Need for Change - The Roles of the Changemakers," by K.E.K. Ross and F. Winslow, 7/23/91, (PB92-129998, A12, MF-A03).

NCEER-91-0023 "A Study of Reliability-Based Criteria for Seismic Design of Reinforced Concrete Frame Buildings," by H.H.M. Hwang and H-M. Hsu, 8/10/91, (PB92-140235, A09, MF-A02).

NCEER-91-0024 "Experimental Verification of a Number of Structural System Identification Algorithms," by R.G. Ghanem, H. Gavin and M. Shinozuka, 9/18/91, (PB92-176577, A18, MF-A04).

NCEER-91-0025 "Probabilistic Evaluation of Liquefaction Potential," by H.H.M. Hwang and C.S. Lee," 11/25/91, (PB92-143429, A05, MF-A01).

NCEER-91-0026 "Instantaneous Optimal Control for Linear, Nonlinear and Hysteretic Structures - Stable Controllers," by J.N. Yang and Z. Li, 11/15/91, (PB92-163807, A04, MF-A01).

NCEER-91-0027 "Experimental and Theoretical Study of a Sliding Isolation System for Bridges," by M.C. Constantinou, A. Kartoum, A.M. Reinhorn and P. Bradford, 11/15/91, (PB92-176973, A10, MF-A03).

NCEER-92-0001 "Case Studies of Liquefaction and Lifeline Performance During Past Earthquakes, Volume 1: Japanese Case Studies," Edited by M. Hamada and T. O'Rourke, 2/17/92, (PB92-197243, A18, MF-A04).

NCEER-92-0002 "Case Studies of Liquefaction and Lifeline Performance During Past Earthquakes, Volume 2: United States Case Studies," Edited by T. O'Rourke and M. Hamada, 2/17/92, (PB92-197250, A20, MF-A04).

NCEER-92-0003 "Issues in Earthquake Education," Edited by K. Ross, 2/3/92, (PB92-222389, A07, MF-A02).

NCEER-92-0004 "Proceedings from the First U.S. - Japan Workshop on Earthquake Protective Systems for Bridges," Edited by I.G. Buckle, 2/4/92, (PB94-142239, A99, MF-A06).

NCEER-92-0005 "Seismic Ground Motion from a Haskell-Type Source in a Multiple-Layered Half-Space," A.P. Theoharis, G. Deodatis and M. Shinozuka, 1/2/92, to be published.

NCEER-92-0006 "Proceedings from the Site Effects Workshop," Edited by R. Whitman, 2/29/92, (PB92-197201, A04, MF-A01).

NCEER-92-0007 "Engineering Evaluation of Permanent Ground Deformations Due to Seismically-Induced Liquefaction," by M.H. Baziar, R. Dobry and A-W.M. Elgamal, 3/24/92, (PB92-222421, A13, MF-A03).

NCEER-92-0008 "A Procedure for the Seismic Evaluation of Buildings in the Central and Eastern United States," by C.D. Poland and J.O. Malley, 4/2/92, (PB92-222439, A20, MF-A04).

NCEER-92-0009 "Experimental and Analytical Study of a Hybrid Isolation System Using Friction Controllable Sliding Bearings," by M.Q. Feng, S. Fujii and M. Shinozuka, 5/15/92, (PB93-150282, A06, MF-A02).

NCEER-92-0010 "Seismic Resistance of Slab-Column Connections in Existing Non-Ductile Flat-Plate Buildings," by A.J. Durrani and Y. Du, 5/18/92, (PB93-116812, A06, MF-A02).

NCEER-92-0011 "The Hysteretic and Dynamic Behavior of Brick Masonry Walls Upgraded by Ferrocement Coatings Under Cyclic Loading and Strong Simulated Ground Motion," by H. Lee and S.P. Prawel, 5/11/92, to be published.

NCEER-92-0012 "Study of Wire Rope Systems for Seismic Protection of Equipment in Buildings," by G.F. Demetriades, M.C. Constantinou and A.M. Reinhorn, 5/20/92, (PB93-116655, A08, MF-A02).

NCEER-92-0013 "Shape Memory Structural Dampers: Material Properties, Design and Seismic Testing," by P.R. Witting and F.A. Cozzarelli, 5/26/92, (PB93-116663, A05, MF-A01).

NCEER-92-0014 "Longitudinal Permanent Ground Deformation Effects on Buried Continuous Pipelines," by M.J. O'Rourke, and C. Nordberg, 6/15/92, (PB93-116671, A08, MF-A02).

NCEER-92-0015 "A Simulation Method for Stationary Gaussian Random Functions Based on the Sampling Theorem," by M. Grigoriu and S. Balopoulou, 6/11/92, (PB93-127496, A05, MF-A01).

NCEER-92-0016 "Gravity-Load-Designed Reinforced Concrete Buildings: Seismic Evaluation of Existing Construction and Detailing Strategies for Improved Seismic Resistance," by G.W. Hoffmann, S.K. Kunnath, A.M. Reinhorn and J.B. Mander, 7/15/92, (PB94-142007, A08, MF-A02).

NCEER-92-0017 "Observations on Water System and Pipeline Performance in the Limón Area of Costa Rica Due to the April 22, 1991 Earthquake," by M. O'Rourke and D. Ballantyne, 6/30/92, (PB93-126811, A06, MF-A02).

NCEER-92-0018 "Fourth Edition of Earthquake Education Materials for Grades K-12," Edited by K.E.K. Ross, 8/10/92, (PB93-114023, A07, MF-A02).

NCEER-92-0019 "Proceedings from the Fourth Japan-U.S. Workshop on Earthquake Resistant Design of Lifeline Facilities and Countermeasures for Soil Liquefaction," Edited by M. Hamada and T.D. O'Rourke, 8/12/92, (PB93-163939, A99, MF-E11).

NCEER-92-0020 "Active Bracing System: A Full Scale Implementation of Active Control," by A.M. Reinhorn, T.T. Soong, R.C. Lin, M.A. Riley, Y.P. Wang, S. Aizawa and M. Higashino, 8/14/92, (PB93-127512, A06, MF-A02).

NCEER-92-0021 "Empirical Analysis of Horizontal Ground Displacement Generated by Liquefaction-Induced Lateral Spreads," by S.F. Bartlett and T.L. Youd, 8/17/92, (PB93-188241, A06, MF-A02).

NCEER-92-0022 "IDARC Version 3.0: Inelastic Damage Analysis of Reinforced Concrete Structures," by S.K. Kunnath, A.M. Reinhorn and R.F. Lobo, 8/31/92, (PB93-227502, A07, MF-A02).

NCEER-92-0023 "A Semi-Empirical Analysis of Strong-Motion Peaks in Terms of Seismic Source, Propagation Path and Local Site Conditions, by M. Kamiyama, M.J. O'Rourke and R. Flores-Berrones, 9/9/92, (PB93-150266, A08, MF-A02).

NCEER-92-0024 "Seismic Behavior of Reinforced Concrete Frame Structures with Nonductile Details, Part I: Summary of Experimental Findings of Full Scale Beam-Column Joint Tests," by A. Beres, R.N. White and P. Gergely, 9/30/92, (PB93-227783, A05, MF-A01).

NCEER-92-0025 "Experimental Results of Repaired and Retrofitted Beam-Column Joint Tests in Lightly Reinforced Concrete Frame Buildings," by A. Beres, S. El-Borgi, R.N. White and P. Gergely, 10/29/92, (PB93-227791, A05, MF-A01).

NCEER-92-0026 "A Generalization of Optimal Control Theory: Linear and Nonlinear Structures," by J.N. Yang, Z. Li and S. Vongchavalitkul, 11/2/92, (PB93-188621, A05, MF-A01).

NCEER-92-0027 "Seismic Resistance of Reinforced Concrete Frame Structures Designed Only for Gravity Loads: Part I - Design and Properties of a One-Third Scale Model Structure," by J.M. Bracci, A.M. Reinhorn and J.B. Mander, 12/1/92, (PB94-104502, A08, MF-A02).

NCEER-92-0028 "Seismic Resistance of Reinforced Concrete Frame Structures Designed Only for Gravity Loads: Part II - Experimental Performance of Subassemblages," by L.E. Aycardi, J.B. Mander and A.M. Reinhorn, 12/1/92, (PB94-104510, A08, MF-A02).

NCEER-92-0029 "Seismic Resistance of Reinforced Concrete Frame Structures Designed Only for Gravity Loads: Part III - Experimental Performance and Analytical Study of a Structural Model," by J.M. Bracci, A.M. Reinhorn and J.B. Mander, 12/1/92, (PB93-227528, A09, MF-A01).

NCEER-92-0030 "Evaluation of Seismic Retrofit of Reinforced Concrete Frame Structures: Part I - Experimental Performance of Retrofitted Subassemblages," by D. Choudhuri, J.B. Mander and A.M. Reinhorn, 12/8/92, (PB93-198307, A07, MF-A02).

NCEER-92-0031 "Evaluation of Seismic Retrofit of Reinforced Concrete Frame Structures: Part II - Experimental Performance and Analytical Study of a Retrofitted Structural Model," by J.M. Bracci, A.M. Reinhorn and J.B. Mander, 12/8/92, (PB93-198315, A09, MF-A03).

NCEER-92-0032 "Experimental and Analytical Investigation of Seismic Response of Structures with Supplemental Fluid Viscous Dampers," by M.C. Constantinou and M.D. Symans, 12/21/92, (PB93-191435, A10, MF-A03). This report is available only through NTIS (see address given above).

NCEER-92-0033 "Reconnaissance Report on the Cairo, Egypt Earthquake of October 12, 1992," by M. Khater, 12/23/92, (PB93-188621, A03, MF-A01).

NCEER-92-0034 "Low-Level Dynamic Characteristics of Four Tall Flat-Plate Buildings in New York City," by H. Gavin, S. Yuan, J. Grossman, E. Pekelis and K. Jacob, 12/28/92, (PB93-188217, A07, MF-A02).

NCEER-93-0001 "An Experimental Study on the Seismic Performance of Brick-Infilled Steel Frames With and Without Retrofit," by J.B. Mander, B. Nair, K. Wojtkowski and J. Ma, 1/29/93, (PB93-227510, A07, MF-A02).

NCEER-93-0002 "Social Accounting for Disaster Preparedness and Recovery Planning," by S. Cole, E. Pantoja and V. Razak, 2/22/93, (PB94-142114, A12, MF-A03).

NCEER-93-0003 "Assessment of 1991 NEHRP Provisions for Nonstructural Components and Recommended Revisions," by T.T. Soong, G. Chen, Z. Wu, R-H. Zhang and M. Grigoriu, 3/1/93, (PB93-188639, A06, MF-A02).

NCEER-93-0004 "Evaluation of Static and Response Spectrum Analysis Procedures of SEAOC/UBC for Seismic Isolated Structures," by C.W. Winters and M.C. Constantinou, 3/23/93, (PB93-198299, A10, MF-A03).

NCEER-93-0005 "Earthquakes in the Northeast - Are We Ignoring the Hazard? A Workshop on Earthquake Science and Safety for Educators," edited by K.E.K. Ross, 4/2/93, (PB94-103066, A09, MF-A02).

NCEER-93-0006 "Inelastic Response of Reinforced Concrete Structures with Viscoelastic Braces," by R.F. Lobo, J.M. Bracci, K.L. Shen, A.M. Reinhorn and T.T. Soong, 4/5/93, (PB93-227486, A05, MF-A02).

NCEER-93-0007 "Seismic Testing of Installation Methods for Computers and Data Processing Equipment," by K. Kosar, T.T. Soong, K.L. Shen, J.A. HoLung and Y.K. Lin, 4/12/93, (PB93-198299, A07, MF-A02).

NCEER-93-0008 "Retrofit of Reinforced Concrete Frames Using Added Dampers," by A. Reinhorn, M. Constantinou and C. Li, to be published.

NCEER-93-0009 "Seismic Behavior and Design Guidelines for Steel Frame Structures with Added Viscoelastic Dampers," by K.C. Chang, M.L. Lai, T.T. Soong, D.S. Hao and Y.C. Yeh, 5/1/93, (PB94-141959, A07, MF-A02).

NCEER-93-0010 "Seismic Performance of Shear-Critical Reinforced Concrete Bridge Piers," by J.B. Mander, S.M. Waheed, M.T.A. Chaudhary and S.S. Chen, 5/12/93, (PB93-227494, A08, MF-A02).

NCEER-93-0011 "3D-BASIS-TABS: Computer Program for Nonlinear Dynamic Analysis of Three Dimensional Base Isolated Structures," by S. Nagarajaiah, C. Li, A.M. Reinhorn and M.C. Constantinou, 8/2/93, (PB94-141819, A09, MF-A02).

NCEER-93-0012 "Effects of Hydrocarbon Spills from an Oil Pipeline Break on Ground Water," by O.J. Helweg and H.H.M. Hwang, 8/3/93, (PB94-141942, A06, MF-A02).

NCEER-93-0013 "Simplified Procedures for Seismic Design of Nonstructural Components and Assessment of Current Code Provisions," by M.P. Singh, L.E. Suarez, E.E. Matheu and G.O. Maldonado, 8/4/93, (PB94-141827, A09, MF-A02).

NCEER-93-0014 "An Energy Approach to Seismic Analysis and Design of Secondary Systems," by G. Chen and T.T. Soong, 8/6/93, (PB94-142767, A11, MF-A03).

NCEER-93-0015 "Proceedings from School Sites: Becoming Prepared for Earthquakes - Commemorating the Third Anniversary of the Loma Prieta Earthquake," Edited by F.E. Winslow and K.E.K. Ross, 8/16/93, (PB94-154275, A16, MF-A02).

NCEER-93-0016 "Reconnaissance Report of Damage to Historic Monuments in Cairo, Egypt Following the October 12, 1992 Dahshur Earthquake," by D. Sykora, D. Look, G. Croci, E. Karaesmen and E. Karaesmen, 8/19/93, (PB94-142221, A08, MF-A02).

NCEER-93-0017 "The Island of Guam Earthquake of August 8, 1993," by S.W. Swan and S.K. Harris, 9/30/93, (PB94-141843, A04, MF-A01).

NCEER-93-0018 "Engineering Aspects of the October 12, 1992 Egyptian Earthquake," by A.W. Elgamal, M. Amer, K. Adalier and A. Abul-Fadl, 10/7/93, (PB94-141983, A05, MF-A01).

NCEER-93-0019 "Development of an Earthquake Motion Simulator and its Application in Dynamic Centrifuge Testing," by I. Krstelj, Supervised by J.H. Prevost, 10/23/93, (PB94-181773, A-10, MF-A03).

NCEER-93-0020 "NCEER-Taisei Corporation Research Program on Sliding Seismic Isolation Systems for Bridges: Experimental and Analytical Study of a Friction Pendulum System (FPS)," by M.C. Constantinou, P. Tsopelas, Y-S. Kim and S. Okamoto, 11/1/93, (PB94-142775, A08, MF-A02).

NCEER-93-0021 "Finite Element Modeling of Elastomeric Seismic Isolation Bearings," by L.J. Billings, Supervised by R. Shepherd, 11/8/93, to be published.

NCEER-93-0022 "Seismic Vulnerability of Equipment in Critical Facilities: Life-Safety and Operational Consequences," by K. Porter, G.S. Johnson, M.M. Zadeh, C. Scawthorn and S. Eder, 11/24/93, (PB94-181765, A16, MF-A03).

NCEER-93-0023 "Hokkaido Nansei-oki, Japan Earthquake of July 12, 1993, by P.I. Yanev and C.R. Scawthorn, 12/23/93, (PB94-181500, A07, MF-A01).

NCEER-94-0001 "An Evaluation of Seismic Serviceability of Water Supply Networks with Application to the San Francisco Auxiliary Water Supply System," by I. Markov, Supervised by M. Grigoriu and T. O'Rourke, 1/21/94, (PB94-204013, A07, MF-A02).

NCEER-94-0002 "NCEER-Taisei Corporation Research Program on Sliding Seismic Isolation Systems for Bridges: Experimental and Analytical Study of Systems Consisting of Sliding Bearings, Rubber Restoring Force Devices and Fluid Dampers," Volumes I and II, by P. Tsopelas, S. Okamoto, M.C. Constantinou, D. Ozaki and S. Fujii, 2/4/94, (PB94-181740, A09, MF-A02 and PB94-181757, A12, MF-A03).

NCEER-94-0003 "A Markov Model for Local and Global Damage Indices in Seismic Analysis," by S. Rahman and M. Grigoriu, 2/18/94, (PB94-206000, A12, MF-A03).

NCEER-94-0004 "Proceedings from the NCEER Workshop on Seismic Response of Masonry Infills," edited by D.P. Abrams, 3/1/94, (PB94-180783, A07, MF-A02).

NCEER-94-0005 "The Northridge, California Earthquake of January 17, 1994: General Reconnaissance Report," edited by J.D. Goltz, 3/11/94, (PB94-193943, A10, MF-A03).

NCEER-94-0006 "Seismic Energy Based Fatigue Damage Analysis of Bridge Columns: Part I - Evaluation of Seismic Capacity," by G.A. Chang and J.B. Mander, 3/14/94, (PB94-219185, A11, MF-A03).

NCEER-94-0007 "Seismic Isolation of Multi-Story Frame Structures Using Spherical Sliding Isolation Systems," by T.M. Al-Hussaini, V.A. Zayas and M.C. Constantinou, 3/17/94, (PB94-193745, A09, MF-A02).

NCEER-94-0008 "The Northridge, California Earthquake of January 17, 1994: Performance of Highway Bridges," edited by I.G. Buckle, 3/24/94, (PB94-193851, A06, MF-A02).

NCEER-94-0009 "Proceedings of the Third U.S.-Japan Workshop on Earthquake Protective Systems for Bridges," edited by I.G. Buckle and I. Friedland, 3/31/94, (PB94-195815, A99, MF-A06).

NCEER-94-0010 "3D-BASIS-ME: Computer Program for Nonlinear Dynamic Analysis of Seismically Isolated Single and Multiple Structures and Liquid Storage Tanks," by P.C. Tsopelas, M.C. Constantinou and A.M. Reinhorn, 4/12/94, (PB94-204922, A09, MF-A02).

NCEER-94-0011 "The Northridge, California Earthquake of January 17, 1994: Performance of Gas Transmission Pipelines," by T.D. O'Rourke and M.C. Palmer, 5/16/94, (PB94-204989, A05, MF-A01).

NCEER-94-0012 "Feasibility Study of Replacement Procedures and Earthquake Performance Related to Gas Transmission Pipelines," by T.D. O'Rourke and M.C. Palmer, 5/25/94, (PB94-206638, A09, MF-A02).

NCEER-94-0013 "Seismic Energy Based Fatigue Damage Analysis of Bridge Columns: Part II - Evaluation of Seismic Demand," by G.A. Chang and J.B. Mander, 6/1/94, (PB95-18106, A08, MF-A02).

NCEER-94-0014 "NCEER-Taisei Corporation Research Program on Sliding Seismic Isolation Systems for Bridges: Experimental and Analytical Study of a System Consisting of Sliding Bearings and Fluid Restoring Force/Damping Devices," by P. Tsopelas and M.C. Constantinou, 6/13/94, (PB94-219144, A10, MF-A03).

NCEER-94-0015 "Generation of Hazard-Consistent Fragility Curves for Seismic Loss Estimation Studies," by H. Hwang and J-R. Huo, 6/14/94, (PB95-181996, A09, MF-A02).

NCEER-94-0016 "Seismic Study of Building Frames with Added Energy-Absorbing Devices," by W.S. Pong, C.S. Tsai and G.C. Lee, 6/20/94, (PB94-219136, A10, A03).

NCEER-94-0017 "Sliding Mode Control for Seismic-Excited Linear and Nonlinear Civil Engineering Structures," by J. Yang, J. Wu, A. Agrawal and Z. Li, 6/21/94, (PB95-138483, A06, MF-A02).

NCEER-94-0018 "3D-BASIS-TABS Version 2.0: Computer Program for Nonlinear Dynamic Analysis of Three Dimensional Base Isolated Structures," by A.M. Reinhorn, S. Nagarajaiah, M.C. Constantinou, P. Tsopelas and R. Li, 6/22/94, (PB95-182176, A08, MF-A02).

NCEER-94-0019 "Proceedings of the International Workshop on Civil Infrastructure Systems: Application of Intelligent Systems and Advanced Materials on Bridge Systems," Edited by G.C. Lee and K.C. Chang, 7/18/94, (PB95-252474, A20, MF-A04).

NCEER-94-0020 "Study of Seismic Isolation Systems for Computer Floors," by V. Lambrou and M.C. Constantinou, 7/19/94, (PB95-138533, A10, MF-A03).

NCEER-94-0021 "Proceedings of the U.S.-Italian Workshop on Guidelines for Seismic Evaluation and Rehabilitation of Unreinforced Masonry Buildings," Edited by D.P. Abrams and G.M. Calvi, 7/20/94, (PB95-138749, A13, MF-A03).

NCEER-94-0022 "NCEER-Taisei Corporation Research Program on Sliding Seismic Isolation Systems for Bridges: Experimental and Analytical Study of a System Consisting of Lubricated PTFE Sliding Bearings and Mild Steel Dampers," by P. Tsopelas and M.C. Constantinou, 7/22/94, (PB95-182184, A08, MF-A02).

NCEER-94-0023 “Development of Reliability-Based Design Criteria for Buildings Under Seismic Load,” by Y.K. Wen, H. Hwang and M. Shinozuka, 8/1/94, (PB95-211934, A08, MF-A02).

NCEER-94-0024 “Experimental Verification of Acceleration Feedback Control Strategies for an Active Tendon System,” by S.J. Dyke, B.F. Spencer, Jr., P. Quast, M.K. Sain, D.C. Kaspari, Jr. and T.T. Soong, 8/29/94, (PB95-212320, A05, MF-A01).

NCEER-94-0025 “Seismic Retrofitting Manual for Highway Bridges,” Edited by I.G. Buckle and I.F. Friedland, published by the Federal Highway Administration (PB95-212676, A15, MF-A03).

NCEER-94-0026 “Proceedings from the Fifth U.S.-Japan Workshop on Earthquake Resistant Design of Lifeline Facilities and Countermeasures Against Soil Liquefaction,” Edited by T.D. O’Rourke and M. Hamada, 11/7/94, (PB95-220802, A99, MF-E08).

NCEER-95-0001 "Experimental and Analytical Investigation of Seismic Retrofit of Structures with Supplemental Damping: Part 1 - Fluid Viscous Damping Devices," by A.M. Reinhorn, C. Li and M.C. Constantinou, 1/3/95, (PB95-266599, A09, MF-A02).

NCEER-95-0002 "Experimental and Analytical Study of Low-Cycle Fatigue Behavior of Semi-Rigid Top-And-Seat Angle Connections," by G. Pekcan, J.B. Mander and S.S. Chen, 1/5/95, (PB95-220042, A07, MF-A02).

NCEER-95-0003 "NCEER-ATC Joint Study on Fragility of Buildings," by T. Anagnos, C. Rojahn and A.S. Kiremidjian, 1/20/95, (PB95-220026, A06, MF-A02).

NCEER-95-0004 "Nonlinear Control Algorithms for Peak Response Reduction," by Z. Wu, T.T. Soong, V. Gattulli and R.C. Lin, 2/16/95, (PB95-220349, A05, MF-A01).

NCEER-95-0005 "Pipeline Replacement Feasibility Study: A Methodology for Minimizing Seismic and Corrosion Risks to Underground Natural Gas Pipelines," by R.T. Eguchi, H.A. Seligson and D.G. Honegger, 3/2/95, (PB95-252326, A06, MF-A02).

NCEER-95-0006 "Evaluation of Seismic Performance of an 11-Story Frame Building During the 1994 Northridge Earthquake," by F. Naeim, R. DiSulio, K. Benuska, A. Reinhorn and C. Li, to be published.

NCEER-95-0007 "Prioritization of Bridges for Seismic Retrofitting," by N. Basöz and A.S. Kiremidjian, 4/24/95, (PB95-252300, A08, MF-A02).

NCEER-95-0008 "Method for Developing Motion Damage Relationships for Reinforced Concrete Frames," by A. Singhal and A.S. Kiremidjian, 5/11/95, (PB95-266607, A06, MF-A02).

NCEER-95-0009 "Experimental and Analytical Investigation of Seismic Retrofit of Structures with Supplemental Damping: Part II - Friction Devices," by C. Li and A.M. Reinhorn, 7/6/95, (PB96-128087, A11, MF-A03).

NCEER-95-0010 "Experimental Performance and Analytical Study of a Non-Ductile Reinforced Concrete Frame Structure Retrofitted with Elastomeric Spring Dampers," by G. Pekcan, J.B. Mander and S.S. Chen, 7/14/95, (PB96-137161, A08, MF-A02).

NCEER-95-0011 "Development and Experimental Study of Semi-Active Fluid Damping Devices for Seismic Protection of Structures," by M.D. Symans and M.C. Constantinou, 8/3/95, (PB96-136940, A23, MF-A04).

NCEER-95-0012 "Real-Time Structural Parameter Modification (RSPM): Development of Innervated Structures," by Z. Liang, M. Tong and G.C. Lee, 4/11/95, (PB96-137153, A06, MF-A01).

NCEER-95-0013 "Experimental and Analytical Investigation of Seismic Retrofit of Structures with Supplemental Damping: Part III - Viscous Damping Walls," by A.M. Reinhorn and C. Li, 10/1/95, (PB96-176409, A11, MF-A03).

NCEER-95-0014 "Seismic Fragility Analysis of Equipment and Structures in a Memphis Electric Substation," by J-R. Huo and H.H.M. Hwang, 8/10/95, (PB96-128087, A09, MF-A02).

NCEER-95-0015 "The Hanshin-Awaji Earthquake of January 17, 1995: Performance of Lifelines," Edited by M. Shinozuka, 11/3/95, (PB96-176383, A15, MF-A03).

NCEER-95-0016 "Highway Culvert Performance During Earthquakes," by T.L. Youd and C.J. Beckman, available as NCEER-96-0015.

NCEER-95-0017 "The Hanshin-Awaji Earthquake of January 17, 1995: Performance of Highway Bridges," Edited by I.G. Buckle, 12/1/95, to be published.

NCEER-95-0018 "Modeling of Masonry Infill Panels for Structural Analysis," by A.M. Reinhorn, A. Madan, R.E. Valles, Y. Reichmann and J.B. Mander, 12/8/95, (PB97-110886, MF-A01, A06).

NCEER-95-0019 "Optimal Polynomial Control for Linear and Nonlinear Structures," by A.K. Agrawal and J.N. Yang, 12/11/95, (PB96-168737, A07, MF-A02).

NCEER-95-0020 "Retrofit of Non-Ductile Reinforced Concrete Frames Using Friction Dampers," by R.S. Rao, P. Gergely and R.N. White, 12/22/95, (PB97-133508, A10, MF-A02).

NCEER-95-0021 "Parametric Results for Seismic Response of Pile-Supported Bridge Bents," by G. Mylonakis, A. Nikolaou and G. Gazetas, 12/22/95, (PB97-100242, A12, MF-A03).

NCEER-95-0022 "Kinematic Bending Moments in Seismically Stressed Piles," by A. Nikolaou, G. Mylonakis and G. Gazetas, 12/23/95, (PB97-113914, MF-A03, A13).

NCEER-96-0001 "Dynamic Response of Unreinforced Masonry Buildings with Flexible Diaphragms," by A.C. Costley and D.P. Abrams," 10/10/96, (PB97-133573, MF-A03, A15).

NCEER-96-0002 "State of the Art Review: Foundations and Retaining Structures," by I. Po Lam, to be published.

NCEER-96-0003 "Ductility of Rectangular Reinforced Concrete Bridge Columns with Moderate Confinement," by N. Wehbe, M. Saiidi, D. Sanders and B. Douglas, 11/7/96, (PB97-133557, A06, MF-A02).

NCEER-96-0004 "Proceedings of the Long-Span Bridge Seismic Research Workshop," edited by I.G. Buckle and I.M. Friedland, to be published.

NCEER-96-0005 "Establish Representative Pier Types for Comprehensive Study: Eastern United States," by J. Kulicki and Z. Prucz, 5/28/96, (PB98-119217, A07, MF-A02).

NCEER-96-0006 "Establish Representative Pier Types for Comprehensive Study: Western United States," by R. Imbsen, R.A. Schamber and T.A. Osterkamp, 5/28/96, (PB98-118607, A07, MF-A02).

NCEER-96-0007 "Nonlinear Control Techniques for Dynamical Systems with Uncertain Parameters," by R.G. Ghanem and M.I. Bujakov, 5/27/96, (PB97-100259, A17, MF-A03).

NCEER-96-0008 "Seismic Evaluation of a 30-Year Old Non-Ductile Highway Bridge Pier and Its Retrofit," by J.B. Mander, B. Mahmoodzadegan, S. Bhadra and S.S. Chen, 5/31/96, (PB97-110902, MF-A03, A10).

NCEER-96-0009 "Seismic Performance of a Model Reinforced Concrete Bridge Pier Before and After Retrofit," by J.B. Mander, J.H. Kim and C.A. Ligozio, 5/31/96, (PB97-110910, MF-A02, A10).

NCEER-96-0010 "IDARC2D Version 4.0: A Computer Program for the Inelastic Damage Analysis of Buildings," by R.E. Valles, A.M. Reinhorn, S.K. Kunnath, C. Li and A. Madan, 6/3/96, (PB97-100234, A17, MF-A03).

NCEER-96-0011 "Estimation of the Economic Impact of Multiple Lifeline Disruption: Memphis Light, Gas and Water Division Case Study," by S.E. Chang, H.A. Seligson and R.T. Eguchi, 8/16/96, (PB97-133490, A11, MF-A03).

NCEER-96-0012 "Proceedings from the Sixth Japan-U.S. Workshop on Earthquake Resistant Design of Lifeline Facilities and Countermeasures Against Soil Liquefaction, Edited by M. Hamada and T. O'Rourke, 9/11/96, (PB97-133581, A99, MF-A06).

NCEER-96-0013 "Chemical Hazards, Mitigation and Preparedness in Areas of High Seismic Risk: A Methodology for Estimating the Risk of Post-Earthquake Hazardous Materials Release," by H.A. Seligson, R.T. Eguchi, K.J. Tierney and K. Richmond, 11/7/96, (PB97-133565, MF-A02, A08).

NCEER-96-0014 "Response of Steel Bridge Bearings to Reversed Cyclic Loading," by J.B. Mander, D-K. Kim, S.S. Chen and G.J. Premus, 11/13/96, (PB97-140735, A12, MF-A03).

NCEER-96-0015 "Highway Culvert Performance During Past Earthquakes," by T.L. Youd and C.J. Beckman, 11/25/96, (PB97-133532, A06, MF-A01).

NCEER-97-0001 "Evaluation, Prevention and Mitigation of Pounding Effects in Building Structures," by R.E. Valles and A.M. Reinhorn, 2/20/97, (PB97-159552, A14, MF-A03).

NCEER-97-0002 "Seismic Design Criteria for Bridges and Other Highway Structures," by C. Rojahn, R. Mayes, D.G. Anderson, J. Clark, J.H. Hom, R.V. Nutt and M.J. O'Rourke, 4/30/97, (PB97-194658, A06, MF-A03).

NCEER-97-0003 “Proceedings of the U.S.-Italian Workshop on Seismic Evaluation and Retrofit,” Edited by D.P. Abrams and G.M. Calvi, 3/19/97, (PB97-194666, A13, MF-A03).

NCEER-97-0004 "Investigation of Seismic Response of Buildings with Linear and Nonlinear Fluid Viscous Dampers," by A.A. Seleemah and M.C. Constantinou, 5/21/97, (PB98-109002, A15, MF-A03).

NCEER-97-0005 "Proceedings of the Workshop on Earthquake Engineering Frontiers in Transportation Facilities," edited by G.C. Lee and I.M. Friedland, 8/29/97, (PB98-128911, A25, MR-A04).

NCEER-97-0006 "Cumulative Seismic Damage of Reinforced Concrete Bridge Piers," by S.K. Kunnath, A. El-Bahy, A. Taylor and W. Stone, 9/2/97, (PB98-108814, A11, MF-A03).

NCEER-97-0007 "Structural Details to Accommodate Seismic Movements of Highway Bridges and Retaining Walls," by R.A. Imbsen, R.A. Schamber, E. Thorkildsen, A. Kartoum, B.T. Martin, T.N. Rosser and J.M. Kulicki, 9/3/97, (PB98-108996, A09, MF-A02).

NCEER-97-0008 "A Method for Earthquake Motion-Damage Relationships with Application to Reinforced Concrete Frames," by A. Singhal and A.S. Kiremidjian, 9/10/97, (PB98-108988, A13, MF-A03).

NCEER-97-0009 "Seismic Analysis and Design of Bridge Abutments Considering Sliding and Rotation," by K. Fishman and R. Richards, Jr., 9/15/97, (PB98-108897, A06, MF-A02).

NCEER-97-0010 "Proceedings of the FHWA/NCEER Workshop on the National Representation of Seismic Ground Motion for New and Existing Highway Facilities," edited by I.M. Friedland, M.S. Power and R.L. Mayes, 9/22/97, (PB98-128903, A21, MF-A04).

NCEER-97-0011 "Seismic Analysis for Design or Retrofit of Gravity Bridge Abutments," by K.L. Fishman, R. Richards, Jr. and R.C. Divito, 10/2/97, (PB98-128937, A08, MF-A02).

NCEER-97-0012 "Evaluation of Simplified Methods of Analysis for Yielding Structures," by P. Tsopelas, M.C. Constantinou, C.A. Kircher and A.S. Whittaker, 10/31/97, (PB98-128929, A10, MF-A03).

NCEER-97-0013 "Seismic Design of Bridge Columns Based on Control and Repairability of Damage," by C-T. Cheng and J.B. Mander, 12/8/97, (PB98-144249, A11, MF-A03).

NCEER-97-0014 "Seismic Resistance of Bridge Piers Based on Damage Avoidance Design," by J.B. Mander and C-T. Cheng, 12/10/97, (PB98-144223, A09, MF-A02).

NCEER-97-0015 “Seismic Response of Nominally Symmetric Systems with Strength Uncertainty,” by S. Balopoulou and M. Grigoriu, 12/23/97, (PB98-153422, A11, MF-A03).

NCEER-97-0016 “Evaluation of Seismic Retrofit Methods for Reinforced Concrete Bridge Columns,” by T.J. Wipf, F.W. Klaiber and F.M. Russo, 12/28/97, (PB98-144215, A12, MF-A03).

NCEER-97-0017 “Seismic Fragility of Existing Conventional Reinforced Concrete Highway Bridges,” by C.L. Mullen and A.S. Cakmak, 12/30/97, (PB98-153406, A08, MF-A02).

NCEER-97-0018 “Loss Asssessment of Memphis Buildings,” edited by D.P. Abrams and M. Shinozuka, 12/31/97, (PB98-144231, A13, MF-A03).

NCEER-97-0019 “Seismic Evaluation of Frames with Infill Walls Using Quasi-static Experiments,” by K.M. Mosalam, R.N. White and P. Gergely, 12/31/97, (PB98-153455, A07, MF-A02).

NCEER-97-0020 “Seismic Evaluation of Frames with Infill Walls Using Pseudo-dynamic Experiments,” by K.M. Mosalam, R.N. White and P. Gergely, 12/31/97, (PB98-153430, A07, MF-A02).

NCEER-97-0021 “Computational Strategies for Frames with Infill Walls: Discrete and Smeared Crack Analyses and Seismic Fragility,” by K.M. Mosalam, R.N. White and P. Gergely, 12/31/97, (PB98-153414, A10, MF-A02).

NCEER-97-0022 "Proceedings of the NCEER Workshop on Evaluation of Liquefaction Resistance of Soils," edited by T.L. Youd and I.M. Idriss, 12/31/97, (PB98-155617, A15, MF-A03).

MCEER-98-0001 "Extraction of Nonlinear Hysteretic Properties of Seismically Isolated Bridges from Quick-Release Field Tests," by Q. Chen, B.M. Douglas, E.M. Maragakis and I.G. Buckle, 5/26/98, (PB99-118838, A06, MF-A01).

MCEER-98-0002 "Methodologies for Evaluating the Importance of Highway Bridges," by A. Thomas, S. Eshenaur and J. Kulicki, 5/29/98, (PB99-118846, A10, MF-A02).

MCEER-98-0003 "Capacity Design of Bridge Piers and the Analysis of Overstrength," by J.B. Mander, A. Dutta and P. Goel, 6/1/98, (PB99-118853, A09, MF-A02).

MCEER-98-0004 "Evaluation of Bridge Damage Data from the Loma Prieta and Northridge, California Earthquakes," by N. Basoz and A. Kiremidjian, 6/2/98, (PB99-118861, A15, MF-A03).

MCEER-98-0005 "Screening Guide for Rapid Assessment of Liquefaction Hazard at Highway Bridge Sites," by T. L. Youd, 6/16/98, (PB99-118879, A06, not available on microfiche).

MCEER-98-0006 "Structural Steel and Steel/Concrete Interface Details for Bridges," by P. Ritchie, N. Kauhl and J. Kulicki, 7/13/98, (PB99-118945, A06, MF-A01).

MCEER-98-0007 "Capacity Design and Fatigue Analysis of Confined Concrete Columns," by A. Dutta and J.B. Mander, 7/14/98, (PB99-118960, A14, MF-A03).

MCEER-98-0008 "Proceedings of the Workshop on Performance Criteria for Telecommunication Services Under Earthquake Conditions," edited by A.J. Schiff, 7/15/98, (PB99-118952, A08, MF-A02).

MCEER-98-0009 "Fatigue Analysis of Unconfined Concrete Columns," by J.B. Mander, A. Dutta and J.H. Kim, 9/12/98, (PB99-123655, A10, MF-A02).

MCEER-98-0010 "Centrifuge Modeling of Cyclic Lateral Response of Pile-Cap Systems and Seat-Type Abutments in Dry Sands," by A.D. Gadre and R. Dobry, 10/2/98, (PB99-123606, A13, MF-A03).

MCEER-98-0011 "IDARC-BRIDGE: A Computational Platform for Seismic Damage Assessment of Bridge Structures," by A.M. Reinhorn, V. Simeonov, G. Mylonakis and Y. Reichman, 10/2/98, (PB99-162919, A15, MF-A03).

MCEER-98-0012 "Experimental Investigation of the Dynamic Response of Two Bridges Before and After Retrofitting with Elastomeric Bearings," by D.A. Wendichansky, S.S. Chen and J.B. Mander, 10/2/98, (PB99-162927, A15, MF-A03).

MCEER-98-0013 "Design Procedures for Hinge Restrainers and Hinge Sear Width for Multiple-Frame Bridges," by R. Des Roches and G.L. Fenves, 11/3/98, (PB99-140477, A13, MF-A03).

MCEER-98-0014 "Response Modification Factors for Seismically Isolated Bridges," by M.C. Constantinou and J.K. Quarshie, 11/3/98, (PB99-140485, A14, MF-A03).

MCEER-98-0015 "Proceedings of the U.S.-Italy Workshop on Seismic Protective Systems for Bridges," edited by I.M. Friedland and M.C. Constantinou, 11/3/98, (PB2000-101711, A22, MF-A04).

MCEER-98-0016 "Appropriate Seismic Reliability for Critical Equipment Systems: Recommendations Based on Regional Analysis of Financial and Life Loss," by K. Porter, C. Scawthorn, C. Taylor and N. Blais, 11/10/98, (PB99-157265, A08, MF-A02).

MCEER-98-0017 "Proceedings of the U.S. Japan Joint Seminar on Civil Infrastructure Systems Research," edited by M. Shinozuka and A. Rose, 11/12/98, (PB99-156713, A16, MF-A03).

MCEER-98-0018 "Modeling of Pile Footings and Drilled Shafts for Seismic Design," by I. PoLam, M. Kapuskar and D. Chaudhuri, 12/21/98, (PB99-157257, A09, MF-A02).

MCEER-99-0001 "Seismic Evaluation of a Masonry Infilled Reinforced Concrete Frame by Pseudodynamic Testing," by S.G. Buonopane and R.N. White, 2/16/99, (PB99-162851, A09, MF-A02).

MCEER-99-0002 "Response History Analysis of Structures with Seismic Isolation and Energy Dissipation Systems: Verification Examples for Program SAP2000," by J. Scheller and M.C. Constantinou, 2/22/99, (PB99-162869, A08, MF-A02).

MCEER-99-0003 "Experimental Study on the Seismic Design and Retrofit of Bridge Columns Including Axial Load Effects," by A. Dutta, T. Kokorina and J.B. Mander, 2/22/99, (PB99-162877, A09, MF-A02).

MCEER-99-0004 "Experimental Study of Bridge Elastomeric and Other Isolation and Energy Dissipation Systems with Emphasis on Uplift Prevention and High Velocity Near-source Seismic Excitation," by A. Kasalanati and M. C. Constantinou, 2/26/99, (PB99-162885, A12, MF-A03).

MCEER-99-0005 "Truss Modeling of Reinforced Concrete Shear-flexure Behavior," by J.H. Kim and J.B. Mander, 3/8/99, (PB99-163693, A12, MF-A03).

MCEER-99-0006 "Experimental Investigation and Computational Modeling of Seismic Response of a 1:4 Scale Model Steel Structure with a Load Balancing Supplemental Damping System," by G. Pekcan, J.B. Mander and S.S. Chen, 4/2/99, (PB99-162893, A11, MF-A03).

MCEER-99-0007 "Effect of Vertical Ground Motions on the Structural Response of Highway Bridges," by M.R. Button, C.J. Cronin and R.L. Mayes, 4/10/99, (PB2000-101411, A10, MF-A03).

MCEER-99-0008 "Seismic Reliability Assessment of Critical Facilities: A Handbook, Supporting Documentation, and Model Code Provisions," by G.S. Johnson, R.E. Sheppard, M.D. Quilici, S.J. Eder and C.R. Scawthorn, 4/12/99, (PB2000-101701, A18, MF-A04).

MCEER-99-0009 "Impact Assessment of Selected MCEER Highway Project Research on the Seismic Design of Highway Structures," by C. Rojahn, R. Mayes, D.G. Anderson, J.H. Clark, D'Appolonia Engineering, S. Gloyd and R.V. Nutt, 4/14/99, (PB99-162901, A10, MF-A02).

MCEER-99-0010 "Site Factors and Site Categories in Seismic Codes," by R. Dobry, R. Ramos and M.S. Power, 7/19/99, (PB2000-101705, A08, MF-A02).

MCEER-99-0011 "Restrainer Design Procedures for Multi-Span Simply-Supported Bridges," by M.J. Randall, M. Saiidi, E. Maragakis and T. Isakovic, 7/20/99, (PB2000-101702, A10, MF-A02).

MCEER-99-0012 "Property Modification Factors for Seismic Isolation Bearings," by M.C. Constantinou, P. Tsopelas, A. Kasalanati and E. Wolff, 7/20/99, (PB2000-103387, A11, MF-A03).

MCEER-99-0013 "Critical Seismic Issues for Existing Steel Bridges," by P. Ritchie, N. Kauhl and J. Kulicki, 7/20/99, (PB2000-101697, A09, MF-A02).

MCEER-99-0014 "Nonstructural Damage Database," by A. Kao, T.T. Soong and A. Vender, 7/24/99, (PB2000-101407, A06, MF-A01).

MCEER-99-0015 "Guide to Remedial Measures for Liquefaction Mitigation at Existing Highway Bridge Sites," by H.G. Cooke and J. K. Mitchell, 7/26/99, (PB2000-101703, A11, MF-A03).

MCEER-99-0016 "Proceedings of the MCEER Workshop on Ground Motion Methodologies for the Eastern United States," edited by N. Abrahamson and A. Becker, 8/11/99, (PB2000-103385, A07, MF-A02).

MCEER-99-0017 "Quindío, Colombia Earthquake of January 25, 1999: Reconnaissance Report," by A.P. Asfura and P.J. Flores, 10/4/99, (PB2000-106893, A06, MF-A01).

MCEER-99-0018 "Hysteretic Models for Cyclic Behavior of Deteriorating Inelastic Structures," by M.V. Sivaselvan and A.M. Reinhorn, 11/5/99, (PB2000-103386, A08, MF-A02).

MCEER-99-0019 "Proceedings of the 7th U.S.- Japan Workshop on Earthquake Resistant Design of Lifeline Facilities and Countermeasures Against Soil Liquefaction," edited by T.D. O'Rourke, J.P. Bardet and M. Hamada, 11/19/99, (PB2000-103354, A99, MF-A06).

MCEER-99-0020 "Development of Measurement Capability for Micro-Vibration Evaluations with Application to Chip Fabrication Facilities," by G.C. Lee, Z. Liang, J.W. Song, J.D. Shen and W.C. Liu, 12/1/99, (PB2000-105993, A08, MF-A02).

MCEER-99-0021 "Design and Retrofit Methodology for Building Structures with Supplemental Energy Dissipating Systems," by G. Pekcan, J.B. Mander and S.S. Chen, 12/31/99, (PB2000-105994, A11, MF-A03).

MCEER-00-0001 "The Marmara, Turkey Earthquake of August 17, 1999: Reconnaissance Report," edited by C. Scawthorn; with major contributions by M. Bruneau, R. Eguchi, T. Holzer, G. Johnson, J. Mander, J. Mitchell, W. Mitchell, A. Papageorgiou, C. Scaethorn, and G. Webb, 3/23/00, (PB2000-106200, A11, MF-A03).

MCEER-00-0002 "Proceedings of the MCEER Workshop for Seismic Hazard Mitigation of Health Care Facilities," edited by G.C. Lee, M. Ettouney, M. Grigoriu, J. Hauer and J. Nigg, 3/29/00, (PB2000-106892, A08, MF-A02).

MCEER-00-0003 "The Chi-Chi, Taiwan Earthquake of September 21, 1999: Reconnaissance Report," edited by G.C. Lee and C.H. Loh, with major contributions by G.C. Lee, M. Bruneau, I.G. Buckle, S.E. Chang, P.J. Flores, T.D. O'Rourke, M. Shinozuka, T.T. Soong, C-H. Loh, K-C. Chang, Z-J. Chen, J-S. Hwang, M-L. Lin, G-Y. Liu, K-C. Tsai, G.C. Yao and C-L. Yen, 4/30/00, (PB2001-100980, A10, MF-A02).

MCEER-00-0004 "Seismic Retrofit of End-Sway Frames of Steel Deck-Truss Bridges with a Supplemental Tendon System: Experimental and Analytical Investigation," by G. Pekcan, J.B. Mander and S.S. Chen, 7/1/00, (PB2001-100982, A10, MF-A02).

MCEER-00-0005 "Sliding Fragility of Unrestrained Equipment in Critical Facilities," by W.H. Chong and T.T. Soong, 7/5/00, (PB2001-100983, A08, MF-A02).

MCEER-00-0006 "Seismic Response of Reinforced Concrete Bridge Pier Walls in the Weak Direction," by N. Abo-Shadi, M. Saiidi and D. Sanders, 7/17/00, (PB2001-100981, A17, MF-A03).

MCEER-00-0007 "Low-Cycle Fatigue Behavior of Longitudinal Reinforcement in Reinforced Concrete Bridge Columns," by J. Brown and S.K. Kunnath, 7/23/00, (PB2001-104392, A08, MF-A02).

MCEER-00-0008 "Soil Structure Interaction of Bridges for Seismic Analysis," I. PoLam and H. Law, 9/25/00, (PB2001-105397, A08, MF-A02).

MCEER-00-0009 "Proceedings of the First MCEER Workshop on Mitigation of Earthquake Disaster by Advanced Technologies (MEDAT-1), edited by M. Shinozuka, D.J. Inman and T.D. O'Rourke, 11/10/00, (PB2001-105399, A14, MF-A03).

MCEER-00-0010 "Development and Evaluation of Simplified Procedures for Analysis and Design of Buildings with Passive Energy Dissipation Systems, Revision 01," by O.M. Ramirez, M.C. Constantinou, C.A. Kircher, A.S. Whittaker, M.W. Johnson, J.D. Gomez and C. Chrysostomou, 11/16/01, (PB2001-105523, A23, MF-A04).

MCEER-00-0011 "Dynamic Soil-Foundation-Structure Interaction Analyses of Large Caissons," by C-Y. Chang, C-M. Mok, Z-L. Wang, R. Settgast, F. Waggoner, M.A. Ketchum, H.M. Gonnermann and C-C. Chin, 12/30/00, (PB2001-104373, A07, MF-A02).

MCEER-00-0012 "Experimental Evaluation of Seismic Performance of Bridge Restrainers," by A.G. Vlassis, E.M. Maragakis and M. Saiid Saiidi, 12/30/00, (PB2001-104354, A09, MF-A02).

MCEER-00-0013 "Effect of Spatial Variation of Ground Motion on Highway Structures," by M. Shinozuka, V. Saxena and G. Deodatis, 12/31/00, (PB2001-108755, A13, MF-A03).

MCEER-00-0014 "A Risk-Based Methodology for Assessing the Seismic Performance of Highway Systems," by S.D. Werner, C.E. Taylor, J.E. Moore, II, J.S. Walton and S. Cho, 12/31/00, (PB2001-108756, A14, MF-A03).

MCEER-01-0001 "Experimental Investigation of P-Delta Effects to Collapse During Earthquakes," by D. Vian and M. Bruneau, 6/25/01, (PB2002-100534, A17, MF-A03).

MCEER-01-0002 "Proceedings of the Second MCEER Workshop on Mitigation of Earthquake Disaster by Advanced Technologies (MEDAT-2)," edited by M. Bruneau and D.J. Inman, 7/23/01, (PB2002-100434, A16, MF-A03).

MCEER-01-0003 "Sensitivity Analysis of Dynamic Systems Subjected to Seismic Loads," by C. Roth and M. Grigoriu, 9/18/01, (PB2003-100884, A12, MF-A03).

MCEER-01-0004 "Overcoming Obstacles to Implementing Earthquake Hazard Mitigation Policies: Stage 1 Report," by D.J. Alesch and W.J. Petak, 12/17/01, (PB2002-107949, A07, MF-A02).

MCEER-01-0005 "Updating Real-Time Earthquake Loss Estimates: Methods, Problems and Insights," by C.E. Taylor, S.E. Chang and R.T. Eguchi, 12/17/01, (PB2002-107948, A05, MF-A01).

MCEER-01-0006 "Experimental Investigation and Retrofit of Steel Pile Foundations and Pile Bents Under Cyclic Lateral Loadings," by A. Shama, J. Mander, B. Blabac and S. Chen, 12/31/01, (PB2002-107950, A13, MF-A03).

MCEER-02-0001 "Assessment of Performance of Bolu Viaduct in the 1999 Duzce Earthquake in Turkey" by P.C. Roussis, M.C. Constantinou, M. Erdik, E. Durukal and M. Dicleli, 5/8/02, (PB2003-100883, A08, MF-A02).

MCEER-02-0002 "Seismic Behavior of Rail Counterweight Systems of Elevators in Buildings," by M.P. Singh, Rildova and L.E. Suarez, 5/27/02. (PB2003-100882, A11, MF-A03).

MCEER-02-0003 "Development of Analysis and Design Procedures for Spread Footings," by G. Mylonakis, G. Gazetas, S. Nikolaou and A. Chauncey, 10/02/02, (PB2004-101636, A13, MF-A03, CD-A13).

MCEER-02-0004 "Bare-Earth Algorithms for Use with SAR and LIDAR Digital Elevation Models," by C.K. Huyck, R.T. Eguchi and B. Houshmand, 10/16/02, (PB2004-101637, A07, CD-A07).

MCEER-02-0005 "Review of Energy Dissipation of Compression Members in Concentrically Braced Frames," by K.Lee and M. Bruneau, 10/18/02, (PB2004-101638, A10, CD-A10).

MCEER-03-0001 "Experimental Investigation of Light-Gauge Steel Plate Shear Walls for the Seismic Retrofit of Buildings" by J. Berman and M. Bruneau, 5/2/03, (PB2004-101622, A10, MF-A03, CD-A10).

MCEER-03-0002 "Statistical Analysis of Fragility Curves," by M. Shinozuka, M.Q. Feng, H. Kim, T. Uzawa and T. Ueda, 6/16/03, (PB2004-101849, A09, CD-A09).

MCEER-03-0003 "Proceedings of the Eighth U.S.-Japan Workshop on Earthquake Resistant Design f Lifeline Facilities and Countermeasures Against Liquefaction," edited by M. Hamada, J.P. Bardet and T.D. O'Rourke, 6/30/03, (PB2004-104386, A99, CD-A99).

MCEER-03-0004 "Proceedings of the PRC-US Workshop on Seismic Analysis and Design of Special Bridges," edited by L.C. Fan and G.C. Lee, 7/15/03, (PB2004-104387, A14, CD-A14).

MCEER-03-0005 "Urban Disaster Recovery: A Framework and Simulation Model," by S.B. Miles and S.E. Chang, 7/25/03, (PB2004-104388, A07, CD-A07).

MCEER-03-0006 "Behavior of Underground Piping Joints Due to Static and Dynamic Loading," by R.D. Meis, M. Maragakis and R. Siddharthan, 11/17/03, (PB2005-102194, A13, MF-A03, CD-A00).

MCEER-04-0001 "Experimental Study of Seismic Isolation Systems with Emphasis on Secondary System Response and Verification of Accuracy of Dynamic Response History Analysis Methods," by E. Wolff and M. Constantinou, 1/16/04 (PB2005-102195, A99, MF-E08, CD-A00).

MCEER-04-0002 "Tension, Compression and Cyclic Testing of Engineered Cementitious Composite Materials," by K. Kesner and S.L. Billington, 3/1/04, (PB2005-102196, A08, CD-A08).

MCEER-04-0003 "Cyclic Testing of Braces Laterally Restrained by Steel Studs to Enhance Performance During Earthquakes," by O.C. Celik, J.W. Berman and M. Bruneau, 3/16/04, (PB2005-102197, A13, MF-A03, CD-A00).

MCEER-04-0004 "Methodologies for Post Earthquake Building Damage Detection Using SAR and Optical Remote Sensing: Application to the August 17, 1999 Marmara, Turkey Earthquake," by C.K. Huyck, B.J. Adams, S. Cho, R.T. Eguchi, B. Mansouri and B. Houshmand, 6/15/04, (PB2005-104888, A10, CD-A00).

MCEER-04-0005 "Nonlinear Structural Analysis Towards Collapse Simulation: A Dynamical Systems Approach," by M.V. Sivaselvan and A.M. Reinhorn, 6/16/04, (PB2005-104889, A11, MF-A03, CD-A00).

MCEER-04-0006 "Proceedings of the Second PRC-US Workshop on Seismic Analysis and Design of Special Bridges," edited by G.C. Lee and L.C. Fan, 6/25/04, (PB2005-104890, A16, CD-A00).

MCEER-04-0007 "Seismic Vulnerability Evaluation of Axially Loaded Steel Built-up Laced Members," by K. Lee and M. Bruneau, 6/30/04, (PB2005-104891, A16, CD-A00).

MCEER-04-0008 "Evaluation of Accuracy of Simplified Methods of Analysis and Design of Buildings with Damping Systems for Near-Fault and for Soft-Soil Seismic Motions," by E.A. Pavlou and M.C. Constantinou, 8/16/04, (PB2005-104892, A08, MF-A02, CD-A00).

MCEER-04-0009 "Assessment of Geotechnical Issues in Acute Care Facilities in California," by M. Lew, T.D. O'Rourke, R. Dobry and M. Koch, 9/15/04, (PB2005-104893, A08, CD-A00).

MCEER-04-0010 "Scissor-Jack-Damper Energy Dissipation System," by A.N. Sigaher-Boyle and M.C. Constantinou, 12/1/04 (PB2005-108221).

MCEER-04-0011 "Seismic Retrofit of Bridge Steel Truss Piers Using a Controlled Rocking Approach," by M. Pollino and M. Bruneau, 12/20/04 (PB2006-105795).

MCEER-05-0001 "Experimental and Analytical Studies of Structures Seismically Isolated with an Uplift-Restraint Isolation System," by P.C. Roussis and M.C. Constantinou, 1/10/05 (PB2005-108222).

MCEER-05-0002 "A Versatile Experimentation Model for Study of Structures Near Collapse Applied to Seismic Evaluation of Irregular Structures," by D. Kusumastuti, A.M. Reinhorn and A. Rutenberg, 3/31/05 (PB2006-101523).

MCEER-05-0003 "Proceedings of the Third PRC-US Workshop on Seismic Analysis and Design of Special Bridges," edited by L.C. Fan and G.C. Lee, 4/20/05, (PB2006-105796).

MCEER-05-0004 "Approaches for the Seismic Retrofit of Braced Steel Bridge Piers and Proof-of-Concept Testing of an Eccentrically Braced Frame with Tubular Link," by J.W. Berman and M. Bruneau, 4/21/05 (PB2006-101524).

MCEER-05-0005 "Simulation of Strong Ground Motions for Seismic Fragility Evaluation of Nonstructural Components in Hospitals," by A. Wanitkorkul and A. Filiatrault, 5/26/05 (PB2006-500027).

MCEER-05-0006 "Seismic Safety in California Hospitals: Assessing an Attempt to Accelerate the Replacement or Seismic Retrofit of Older Hospital Facilities," by D.J. Alesch, L.A. Arendt and W.J. Petak, 6/6/05 (PB2006-105794).

MCEER-05-0007 "Development of Seismic Strengthening and Retrofit Strategies for Critical Facilities Using Engineered Cementitious Composite Materials," by K. Kesner and S.L. Billington, 8/29/05 (PB2006-111701).

MCEER-05-0008 "Experimental and Analytical Studies of Base Isolation Systems for Seismic Protection of Power Transformers," by N. Murota, M.Q. Feng and G-Y. Liu, 9/30/05 (PB2006-111702).

MCEER-05-0009 "3D-BASIS-ME-MB: Computer Program for Nonlinear Dynamic Analysis of Seismically Isolated Structures," by P.C. Tsopelas, P.C. Roussis, M.C. Constantinou, R. Buchanan and A.M. Reinhorn, 10/3/05 (PB2006-111703).

MCEER-05-0010 "Steel Plate Shear Walls for Seismic Design and Retrofit of Building Structures," by D. Vian and M. Bruneau, 12/15/05 (PB2006-111704).

MCEER-05-0011 "The Performance-Based Design Paradigm," by M.J. Astrella and A. Whittaker, 12/15/05 (PB2006-111705).

MCEER-06-0001 "Seismic Fragility of Suspended Ceiling Systems," H. Badillo-Almaraz, A.S. Whittaker, A.M. Reinhorn and G.P. Cimellaro, 2/4/06 (PB2006-111706).

MCEER-06-0002 "Multi-Dimensional Fragility of Structures," by G.P. Cimellaro, A.M. Reinhorn and M. Bruneau, 3/1/06 (PB2007-106974, A09, MF-A02, CD A00).

MCEER-06-0003 "Built-Up Shear Links as Energy Dissipators for Seismic Protection of Bridges," by P. Dusicka, A.M. Itani and I.G. Buckle, 3/15/06 (PB2006-111708).

MCEER-06-0004 "Analytical Investigation of the Structural Fuse Concept," by R.E. Vargas and M. Bruneau, 3/16/06 (PB2006-111709).

MCEER-06-0005 "Experimental Investigation of the Structural Fuse Concept," by R.E. Vargas and M. Bruneau, 3/17/06 (PB2006-111710).

MCEER-06-0006 "Further Development of Tubular Eccentrically Braced Frame Links for the Seismic Retrofit of Braced Steel Truss Bridge Piers," by J.W. Berman and M. Bruneau, 3/27/06 (PB2007-105147).

MCEER-06-0007 "REDARS Validation Report," by S. Cho, C.K. Huyck, S. Ghosh and R.T. Eguchi, 8/8/06 (PB2007-106983).

MCEER-06-0008 "Review of Current NDE Technologies for Post-Earthquake Assessment of Retrofitted Bridge Columns," by J.W. Song, Z. Liang and G.C. Lee, 8/21/06 (PB2007-106984).

MCEER-06-0009 "Liquefaction Remediation in Silty Soils Using Dynamic Compaction and Stone Columns," by S. Thevanayagam, G.R. Martin, R. Nashed, T. Shenthan, T. Kanagalingam and N. Ecemis, 8/28/06 (PB2007-106985).

MCEER-06-0010 "Conceptual Design and Experimental Investigation of Polymer Matrix Composite Infill Panels for Seismic Retrofitting," by W. Jung, M. Chiewanichakorn and A.J. Aref, 9/21/06 (PB2007-106986).

MCEER-06-0011 "A Study of the Coupled Horizontal-Vertical Behavior of Elastomeric and Lead-Rubber Seismic Isolation Bearings," by G.P. Warn and A.S. Whittaker, 9/22/06 (PB2007-108679).

MCEER-06-0012 "Proceedings of the Fourth PRC-US Workshop on Seismic Analysis and Design of Special Bridges: Advancing Bridge Technologies in Research, Design, Construction and Preservation," Edited by L.C. Fan, G.C. Lee and L. Ziang, 10/12/06 (PB2007-109042).

MCEER-06-0013 "Cyclic Response and Low Cycle Fatigue Characteristics of Plate Steels," by P. Dusicka, A.M. Itani and I.G. Buckle, 11/1/06 06 (PB2007-106987).

MCEER-06-0014 "Proceedings of the Second US-Taiwan Bridge Engineering Workshop," edited by W.P. Yen, J. Shen, J-Y. Chen and M. Wang, 11/15/06 (PB2008-500041).

MCEER-06-0015 "User Manual and Technical Documentation for the REDARS^{TM} Import Wizard," by S. Cho, S. Ghosh, C.K. Huyck and S.D. Werner, 11/30/06 (PB2007-114766).

MCEER-06-0016 "Hazard Mitigation Strategy and Monitoring Technologies for Urban and Infrastructure Public Buildings: Proceedings of the China-US Workshops," edited by X.Y. Zhou, A.L. Zhang, G.C. Lee and M. Tong, 12/12/06 (PB2008-500018).

MCEER-07-0001 "Static and Kinetic Coefficients of Friction for Rigid Blocks," by C. Kafali, S. Fathali, M. Grigoriu and A.S. Whittaker, 3/20/07 (PB2007-114767).

MCEER-07-0002 "Hazard Mitigation Investment Decision Making: Organizational Response to Legislative Mandate," by L.A. Arendt, D.J. Alesch and W.J. Petak, 4/9/07 (PB2007-114768).

MCEER-07-0003 "Seismic Behavior of Bidirectional-Resistant Ductile End Diaphragms with Unbonded Braces in Straight or Skewed Steel Bridges," by O. Celik and M. Bruneau, 4/11/07 (PB2008-105141).

MCEER-07-0004 "Modeling Pile Behavior in Large Pile Groups Under Lateral Loading," by A.M. Dodds and G.R. Martin, 4/16/07(PB2008-105142).

MCEER-07-0005 "Experimental Investigation of Blast Performance of Seismically Resistant Concrete-Filled Steel Tube Bridge Piers," by S. Fujikura, M. Bruneau and D. Lopez-Garcia, 4/20/07 (PB2008-105143).

MCEER-07-0006 "Seismic Analysis of Conventional and Isolated Liquefied Natural Gas Tanks Using Mechanical Analogs," by I.P. Christovasilis and A.S. Whittaker, 5/1/07.

MCEER-07-0007 "Experimental Seismic Performance Evaluation of Isolation/Restraint Systems for Mechanical Equipment – Part 1: Heavy Equipment Study," by S. Fathali and A. Filiatrault, 6/6/07 (PB2008-105144).

MCEER-07-0008 "Seismic Vulnerability of Timber Bridges and Timber Substructures," by A.A. Sharma, J.B. Mander, I.M. Friedland and D.R. Allicock, 6/7/07 (PB2008-105145).

MCEER-07-0009 "Experimental and Analytical Study of the XY-Friction Pendulum (XY-FP) Bearing for Bridge Applications," by C.C. Marin-Artieda, A.S. Whittaker and M.C. Constantinou, 6/7/07 (PB2008-105191).

MCEER-07-0010 "Proceedings of the PRC-US Earthquake Engineering Forum for Young Researchers," Edited by G.C. Lee and X.Z. Qi, 6/8/07 (PB2008-500058).

MCEER-07-0011 "Design Recommendations for Perforated Steel Plate Shear Walls," by R. Purba and M. Bruneau, 6/18/07, (PB2008-105192).

MCEER-07-0012 "Performance of Seismic Isolation Hardware Under Service and Seismic Loading," by M.C. Constantinou, A.S. Whittaker, Y. Kalpakidis, D.M. Fenz and G.P. Warn, 8/27/07, (PB2008-105193).

MCEER-07-0013 "Experimental Evaluation of the Seismic Performance of Hospital Piping Subassemblies," by E.R. Goodwin, E. Maragakis and A.M. Itani, 9/4/07, (PB2008-105194).

MCEER-07-0014 "A Simulation Model of Urban Disaster Recovery and Resilience: Implementation for the 1994 Northridge Earthquake," by S. Miles and S.E. Chang, 9/7/07, (PB2008-106426).

MCEER-07-0015 "Statistical and Mechanistic Fragility Analysis of Concrete Bridges," by M. Shinozuka, S. Banerjee and S-H. Kim, 9/10/07, (PB2008-106427).

MCEER-07-0016 "Three-Dimensional Modeling of Inelastic Buckling in Frame Structures," by M. Schachter and AM. Reinhorn, 9/13/07, (PB2008-108125).

MCEER-07-0017 "Modeling of Seismic Wave Scattering on Pile Groups and Caissons," by I. Po Lam, H. Law and C.T. Yang, 9/17/07 (PB2008-108150).

MCEER-07-0018 "Bridge Foundations: Modeling Large Pile Groups and Caissons for Seismic Design," by I. Po Lam, H. Law and G.R. Martin (Coordinating Author), 12/1/07 (PB2008-111190).

MCEER-07-0019 "Principles and Performance of Roller Seismic Isolation Bearings for Highway Bridges," by G.C. Lee, Y.C. Ou, Z. Liang, T.C. Niu and J. Song, 12/10/07 (PB2009-110466).

MCEER-07-0020 "Centrifuge Modeling of Permeability and Pinning Reinforcement Effects on Pile Response to Lateral Spreading," by L.L Gonzalez-Lagos, T. Abdoun and R. Dobry, 12/10/07 (PB2008-111191).

MCEER-07-0021 "Damage to the Highway System from the Pisco, Perú Earthquake of August 15, 2007," by J.S. O'Connor, L. Mesa and M. Nykamp, 12/10/07, (PB2008-108126).

MCEER-07-0022 "Experimental Seismic Performance Evaluation of Isolation/Restraint Systems for Mechanical Equipment – Part 2: Light Equipment Study," by S. Fathali and A. Filiatrault, 12/13/07 (PB2008-111192).

MCEER-07-0023 "Fragility Considerations in Highway Bridge Design," by M. Shinozuka, S. Banerjee and S.H. Kim, 12/14/07 (PB2008-111193).

MCEER-07-0024 "Performance Estimates for Seismically Isolated Bridges," by G.P. Warn and A.S. Whittaker, 12/30/07 (PB2008-112230).

MCEER-08-0001 "Seismic Performance of Steel Girder Bridge Superstructures with Conventional Cross Frames," by L.P. Carden, A.M. Itani and I.G. Buckle, 1/7/08, (PB2008-112231).

MCEER-08-0002 "Seismic Performance of Steel Girder Bridge Superstructures with Ductile End Cross Frames with Seismic Isolators," by L.P. Carden, A.M. Itani and I.G. Buckle, 1/7/08 (PB2008-112232).

MCEER-08-0003 "Analytical and Experimental Investigation of a Controlled Rocking Approach for Seismic Protection of Bridge Steel Truss Piers," by M. Pollino and M. Bruneau, 1/21/08 (PB2008-112233).

MCEER-08-0004 "Linking Lifeline Infrastructure Performance and Community Disaster Resilience: Models and Multi-Stakeholder Processes," by S.E. Chang, C. Pasion, K. Tatebe and R. Ahmad, 3/3/08 (PB2008-112234).

MCEER-08-0005 "Modal Analysis of Generally Damped Linear Structures Subjected to Seismic Excitations," by J. Song, Y-L. Chu, Z. Liang and G.C. Lee, 3/4/08 (PB2009-102311).

MCEER-08-0006 "System Performance Under Multi-Hazard Environments," by C. Kafali and M. Grigoriu, 3/4/08 (PB2008-112235).

MCEER-08-0007 "Mechanical Behavior of Multi-Spherical Sliding Bearings," by D.M. Fenz and M.C. Constantinou, 3/6/08 (PB2008-112236).

MCEER-08-0008 "Post-Earthquake Restoration of the Los Angeles Water Supply System," by T.H.P. Tabucchi and R.A. Davidson, 3/7/08 (PB2008-112237).

MCEER-08-0009 "Fragility Analysis of Water Supply Systems," by A. Jacobson and M. Grigoriu, 3/10/08 (PB2009-105545).

MCEER-08-0010 "Experimental Investigation of Full-Scale Two-Story Steel Plate Shear Walls with Reduced Beam Section Connections," by B. Qu, M. Bruneau, C-H. Lin and K-C. Tsai, 3/17/08 (PB2009-106368).

MCEER-08-0011 "Seismic Evaluation and Rehabilitation of Critical Components of Electrical Power Systems," S. Ersoy, B. Feizi, A. Ashrafi and M. Ala Saadeghvaziri, 3/17/08 (PB2009-105546).

MCEER-08-0012 "Seismic Behavior and Design of Boundary Frame Members of Steel Plate Shear Walls," by B. Qu and M. Bruneau, 4/26/08 . (PB2009-106744).

MCEER-08-0013 "Development and Appraisal of a Numerical Cyclic Loading Protocol for Quantifying Building System Performance," by A. Filiatrault, A. Wanitkorkul and M. Constantinou, 4/27/08 (PB2009-107906).

MCEER-08-0014 "Structural and Nonstructural Earthquake Design: The Challenge of Integrating Specialty Areas in Designing Complex, Critical Facilities," by W.J. Petak and D.J. Alesch, 4/30/08 (PB2009-107907).

MCEER-08-0015 "Seismic Performance Evaluation of Water Systems," by Y. Wang and T.D. O'Rourke, 5/5/08 (PB2009-107908).

MCEER-08-0016 "Seismic Response Modeling of Water Supply Systems," by P. Shi and T.D. O'Rourke, 5/5/08 (PB2009-107910).

MCEER-08-0017 "Numerical and Experimental Studies of Self-Centering Post-Tensioned Steel Frames," by D. Wang and A. Filiatrault, 5/12/08 (PB2009-110479).

MCEER-08-0018 "Development, Implementation and Verification of Dynamic Analysis Models for Multi-Spherical Sliding Bearings," by D.M. Fenz and M.C. Constantinou, 8/15/08 (PB2009-107911).

MCEER-08-0019 "Performance Assessment of Conventional and Base Isolated Nuclear Power Plants for Earthquake Blast Loadings," by Y.N. Huang, A.S. Whittaker and N. Luco, 10/28/08 (PB2009-107912).

MCEER-08-0020 "Remote Sensing for Resilient Multi-Hazard Disaster Response – Volume I: Introduction to Damage Assessment Methodologies," by B.J. Adams and R.T. Eguchi, 11/17/08 (PB2010-102695).

MCEER-08-0021 "Remote Sensing for Resilient Multi-Hazard Disaster Response – Volume II: Counting the Number of Collapsed Buildings Using an Object-Oriented Analysis: Case Study of the 2003 Bam Earthquake," by L. Gusella, C.K. Huyck and B.J. Adams, 11/17/08 (PB2010-100925).

MCEER-08-0022 "Remote Sensing for Resilient Multi-Hazard Disaster Response – Volume III: Multi-Sensor Image Fusion Techniques for Robust Neighborhood-Scale Urban Damage Assessment," by B.J. Adams and A. McMillan, 11/17/08 (PB2010-100926).

MCEER-08-0023 "Remote Sensing for Resilient Multi-Hazard Disaster Response – Volume IV: A Study of Multi-Temporal and Multi-Resolution SAR Imagery for Post-Katrina Flood Monitoring in New Orleans," by A. McMillan, J.G. Morley, B.J. Adams and S. Chesworth, 11/17/08 (PB2010-100927).

MCEER-08-0024 "Remote Sensing for Resilient Multi-Hazard Disaster Response – Volume V: Integration of Remote Sensing Imagery and VIEWS^{TM} Field Data for Post-Hurricane Charley Building Damage Assessment," by J.A. Womble, K. Mehta and B.J. Adams, 11/17/08 (PB2009-115532).

MCEER-08-0025 "Building Inventory Compilation for Disaster Management: Application of Remote Sensing and Statistical Modeling," by P. Sarabandi, A.S. Kiremidjian, R.T. Eguchi and B. J. Adams, 11/20/08 (PB2009-110484).

MCEER-08-0026 "New Experimental Capabilities and Loading Protocols for Seismic Qualification and Fragility Assessment of Nonstructural Systems," by R. Retamales, G. Mosqueda, A. Filiatrault and A. Reinhorn, 11/24/08 (PB2009-110485).

MCEER-08-0027 "Effects of Heating and Load History on the Behavior of Lead-Rubber Bearings," by I.V. Kalpakidis and M.C. Constantinou, 12/1/08 (PB2009-115533).

MCEER-08-0028 "Experimental and Analytical Investigation of Blast Performance of Seismically Resistant Bridge Piers," by S.Fujikura and M. Bruneau, 12/8/08 (PB2009-115534).

MCEER-08-0029 "Evolutionary Methodology for Aseismic Decision Support," by Y. Hu and G. Dargush, 12/15/08.

MCEER-08-0030 "Development of a Steel Plate Shear Wall Bridge Pier System Conceived from a Multi-Hazard Perspective," by D. Keller and M. Bruneau, 12/19/08 (PB2010-102696).

MCEER-09-0001 "Modal Analysis of Arbitrarily Damped Three-Dimensional Linear Structures Subjected to Seismic Excitations," by Y.L. Chu, J. Song and G.C. Lee, 1/31/09 (PB2010-100922).

MCEER-09-0002 "Air-Blast Effects on Structural Shapes," by G. Ballantyne, A.S. Whittaker, A.J. Aref and G.F. Dargush, 2/2/09 (PB2010-102697).

MCEER-09-0003 "Water Supply Performance During Earthquakes and Extreme Events," by A.L. Bonneau and T.D. O'Rourke, 2/16/09 (PB2010-100923).

MCEER-09-0004 "Generalized Linear (Mixed) Models of Post-Earthquake Ignitions," by R.A. Davidson, 7/20/09 (PB2010-102698).

MCEER-09-0005 "Seismic Testing of a Full-Scale Two-Story Light-Frame Wood Building: NEESWood Benchmark Test," by I.P. Christovasilis, A. Filiatrault and A. Wanitkorkul, 7/22/09 (PB2012-102401).

MCEER-09-0006 "IDARC2D Version 7.0: A Program for the Inelastic Damage Analysis of Structures," by A.M. Reinhorn, H. Roh, M. Sivaselvan, S.K. Kunnath, R.E. Valles, A. Madan, C. Li, R. Lobo and Y.J. Park, 7/28/09 (PB2010-103199).

MCEER-09-0007 "Enhancements to Hospital Resiliency: Improving Emergency Planning for and Response to Hurricanes," by D.B. Hess and L.A. Arendt, 7/30/09 (PB2010-100924).

MCEER-09-0008 "Assessment of Base-Isolated Nuclear Structures for Design and Beyond-Design Basis Earthquake Shaking," by Y.N. Huang, A.S. Whittaker, R.P. Kennedy and R.L. Mayes, 8/20/09 (PB2010-102699).

MCEER-09-0009 "Quantification of Disaster Resilience of Health Care Facilities," by G.P. Cimellaro, C. Fumo, A.M Reinhorn and M. Bruneau, 9/14/09 (PB2010-105384).

MCEER-09-0010 "Performance-Based Assessment and Design of Squat Reinforced Concrete Shear Walls," by C.K. Gulec and A.S. Whittaker, 9/15/09 (PB2010-102700).

MCEER-09-0011 "Proceedings of the Fourth US-Taiwan Bridge Engineering Workshop," edited by W.P. Yen, J.J. Shen, T.M. Lee and R.B. Zheng, 10/27/09 (PB2010-500009).

MCEER-09-0012 "Proceedings of the Special International Workshop on Seismic Connection Details for Segmental Bridge Construction," edited by W. Phillip Yen and George C. Lee, 12/21/09 (PB2012-102402).

MCEER-10-0001 "Direct Displacement Procedure for Performance-Based Seismic Design of Multistory Woodframe Structures," by W. Pang and D. Rosowsky, 4/26/10 (PB2012-102403).

MCEER-10-0002 "Simplified Direct Displacement Design of Six-Story NEESWood Capstone Building and Pre-Test Seismic Performance Assessment," by W. Pang, D. Rosowsky, J. van de Lindt and S. Pei, 5/28/10 (PB2012-102404).

MCEER-10-0003 "Integration of Seismic Protection Systems in Performance-Based Seismic Design of Woodframed Structures," by J.K. Shinde and M.D. Symans, 6/18/10 (PB2012-102405).

MCEER-10-0004 "Modeling and Seismic Evaluation of Nonstructural Components: Testing Frame for Experimental Evaluation of Suspended Ceiling Systems," by A.M. Reinhorn, K.P. Ryu and G. Maddaloni, 6/30/10 (PB2012-102406).

MCEER-10-0005 "Analytical Development and Experimental Validation of a Structural-Fuse Bridge Pier Concept," by S. El-Bahey and M. Bruneau, 10/1/10 (PB2012-102407).

MCEER-10-0006 "A Framework for Defining and Measuring Resilience at the Community Scale: The PEOPLES Resilience Framework," by C.S. Renschler, A.E. Frazier, L.A. Arendt, G.P. Cimellaro, A.M. Reinhorn and M. Bruneau, 10/8/10 (PB2012-102408).

MCEER-10-0007 "Impact of Horizontal Boundary Elements Design on Seismic Behavior of Steel Plate Shear Walls," by R. Purba and M. Bruneau, 11/14/10 (PB2012-102409).

MCEER-10-0008 "Seismic Testing of a Full-Scale Mid-Rise Building: The NEESWood Capstone Test," by S. Pei, J.W. van de Lindt, S.E. Pryor, H. Shimizu, H. Isoda and D.R. Rammer, 12/1/10 (PB2012-102410).

MCEER-10-0009 "Modeling the Effects of Detonations of High Explosives to Inform Blast-Resistant Design," by P. Sherkar, A.S. Whittaker and A.J. Aref, 12/1/10 (PB2012-102411).

MCEER-10-0010 "L'Aquila Earthquake of April 6, 2009 in Italy: Rebuilding a Resilient City to Withstand Multiple Hazards," by G.P. Cimellaro, I.P. Christovasilis, A.M. Reinhorn, A. De Stefano and T. Kirova, 12/29/10.

MCEER-11-0001 "Numerical and Experimental Investigation of the Seismic Response of Light-Frame Wood Structures," by I.P. Christovasilis and A. Filiatrault, 8/8/11 (PB2012-102412).

MCEER-11-0002 "Seismic Design and Analysis of a Precast Segmental Concrete Bridge Model," by M. Anagnostopoulou, A. Filiatrault and A. Aref, 9/15/11.

MCEER-11-0003 'Proceedings of the Workshop on Improving Earthquake Response of Substation Equipment," Edited by A.M. Reinhorn, 9/19/11 (PB2012-102413).

MCEER-11-0004 "LRFD-Based Analysis and Design Procedures for Bridge Bearings and Seismic Isolators," by M.C. Constantinou, I. Kalpakidis, A. Filiatrault and R.A. Ecker Lay, 9/26/11.

MCEER-11-0005 "Experimental Seismic Evaluation, Model Parameterization, and Effects of Cold-Formed Steel-Framed Gypsum Partition Walls on the Seismic Performance of an Essential Facility," by R. Davies, R. Retamales, G. Mosqueda and A. Filiatrault, 10/12/11.

MCEER-11-0006 "Modeling and Seismic Performance Evaluation of High Voltage Transformers and Bushings," by A.M. Reinhorn, K. Oikonomou, H. Roh, A. Schiff and L. Kempner, Jr., 10/3/11.

MCEER-11-0007 "Extreme Load Combinations: A Survey of State Bridge Engineers," by G.C. Lee, Z. Liang, J.J. Shen and J.S. O'Connor, 10/14/11.

MCEER-12-0001 "Simplified Analysis Procedures in Support of Performance Based Seismic Design," by Y.N. Huang and A.S. Whittaker.

MCEER-12-0002 "Seismic Protection of Electrical Transformer Bushing Systems by Stiffening Techniques," by M. Koliou, A. Filiatrault, A.M. Reinhorn and N. Oliveto, 6/1/12.

ISSN 1520-295X